12-2011

An Early Warning Monitoring System for CNC Spindle Bearing Failure

Andrew Werner
Clemson University, awerner@g.clemson.edu

AN EARLY WARNING MONITORING SYSTEM FOR CNC SPINDLE BEARING
FAILURE

A Thesis
Presented to
the Graduate School of
Clemson University

In Partial Fulfillment
of the Requirements for the Degree
Master of Science
Mechanical Engineering

by
Andrew F. Werner
December 2011

Accepted by:
Dr. Gregory Mocko, Committee Chair
Dr. Laine Mears
Dr. Ardalan Vahidi

ABSTRACT

Equipment employed in a manufacturing environment must be able to operate as long as possible having as little downtime as possible. Therefore, maintenance is crucial in order to allow for the equipment to perform its designated tasks without failure, especially on critical systems. In a CNC machine, if the spindle fails, the machine is useless. Having the ability to detect spindle degradation to the point where a replacement spindle installation can be planned, via condition monitoring, is invaluable to a manufacturer who utilizes these types of machines.

An early warning monitoring system for CNC spindle bearing failure has been developed to be utilized directly on a CNC machine's controller employing an open architecture structure. The main system uses an ultrasonic sensor as its primary sensing component and provides a singular value as to the spindle condition. The system allows for both real time data recording as well as provides a trending history for the machine. Additionally, the system allows for the data to be seen remotely via the internet. Accessory devices can be added to perform an in-depth bearing failure analysis. The total system (including accessories) costs just under $2,400, allowing for a very effective system at a very low price. A few thousand dollars towards a predictive and preventive maintenance monitoring solution can prevent tens-of-thousands of dollars in lost production and unnecessary maintenance costs if the system is utilized as intended.

System performance was tested to investigate sensor measurement applicability. Spindle speed was found to have an effect on the sensor's output, however excessive vibration did not. Therefore, the same spindle speed must be used each time a

measurement is taken. Measurements while the machine is cutting can be performed, however, a test mode is recommended for the most accurate results. The amount of variation for an in-process reading was found to be lower for a harder material (ie: steel vs. aluminum), for the same spindle speed and depth of cut. The system was tested to see if it could detect the various stages of bearing failure. It was unable to detect a plastic/resin bearing cage degradation failure until it was too late as the failure was too quiet to detect.

DEDICATION

To my parents…

And how they have supported my goals and dreams throughout my life and have allowed me to grow into the man I am today.

ACKNOWLEDGMENTS

Dr. Mears, for his guidance, support, and understanding of what all a graduate student goes through during his time of study.

Parikshit "Perry" Mehta, for mentoring me and showing me the ropes of what graduate work is all about.

Okuma America Corporation, for giving me the chance to work with them, for them, and provide the basis for the thesis work presented here.

Ron Sanders and Frank Gonzalez of Okuma, for their help and dedication to what I was trying to accomplish.

Adrian Messer and Mark Goodman from UE Systems Inc., for their support with the ultrasonic sensor hardware.

Everybody else I could not mention here.

TABLE OF CONTENTS

Table of Contents (Continued)

Table of Contents (Continued)

LIST OF TABLES

LIST OF FIGURES

List of Figures (Continued)

Figure   Page

List of Figures (Continued)

Figure   Page

List of Figures (Continued)

List of Figures (Continued)

Figure   Page

CHAPTER 1: INTRODUCTION AND MOTIVATION

This thesis details the development of a spindle monitoring system for a computer numerical control (CNC) machine as well as investigates the system's performance and its ability to detect a spindle problem. The focus of this work was to develop a system that would monitor a CNC machine's spindle health and provide feedback as to when maintenance will be necessary. Having the ability to detect spindle degradation to the point where a replacement spindle installation can be planned is invaluable to a manufacturer who utilizes these machines. Machine downtime, due to spindle issues, can be eliminated and maintenance costs reduced by employing such a system. At the same time, a machine's productivity and efficiency can be increased.

Several questions needed to be answered before the system could be developed. Currently, no CNC tool manufacturer provides such a system for their machines. Tool manufacturers do provide service options, such as calibrations, maintenance plans, and vibration analysis for benchmarking [1]; however there is no on-board system that is available as a possible stock option. Therefore, how can existing condition-based maintenance (CBM) techniques be combined with an open architecture structure to create a CBM system that provides the necessary information needed for spindle monitoring and be able to be utilized on the machine control? Fundamental investigations of maintenance theory, existing commercialized monitoring systems, devices and sensors those systems employed, spindle monitoring techniques, and various communication architectures were performed in order to effectively realize such a system.

What separates this system from the other spindle monitoring systems currently on the market today is that it is integrated into the machine control through the use of an open architecture system, needing no additional or secondary computer system. It also allows for an early detection of spindle bearing problems through the use of ultrasonic sensing technology, being able to detect problems before the traditional vibration based methods. The data collected can be accessed through the controller and can be seen remotely, preventing a machine service representative from physically going to the machine location to investigate a possible spindle problem. The system is the first of its kind in the world of machine tool manufacturers and will hopefully lay a foundation for the future of maintenance in the machine tool industry.

However, before this system can put into the field, it needed to be tested and its performance understood in a research and development environment. Sensor performance was the main item investigated as there are numerous conditions the system could be exposed to. The work in this thesis was aimed to answer questions such as does spindle speed affect the sensor output?, does spindle vibration have any effect on the sensor output?, can a spindle measurement be accurately taken while a cutting operation is being performed?, and finally, can the system detect the various stages of bearing failure?

This thesis has been divided into eleven chapters, as shown in Figure 1. Chapters 2 – 6 provide the necessary background information for the work presented in Chapters 7 – 10. After the preliminary introduction of Chapter 1, the need for a maintenance strategy is explained in Chapter 2 as well as a brief description of existing maintenance

strategies currently being employed in the manufacturing today. Chapter 3 details the importance of a condition monitoring in maintenance practices as well as current methods being used. Chapter 4 provides a description of open architecture systems and how these systems allow for application customization. Chapter 5 discusses both the general design requirements for a CBM system as well as customer specific requirements for the spindle monitoring system. Chapter 6 allows for the reader to become familiar with the current sensors and techniques used in spindle monitoring today.

The system that has been developed to monitor CNC spindle bearing and allow for appropriate maintenance planning to be coordinated has been detailed in Chapter 7. The performance of the system is then investigated in Chapter 8 to see how the system can be improved. However, improving the system does not mean that it will actually work the way it was intended. Therefore, a spindle bearing failure test was performed to see if the system could detect a true bearing failure, in Chapter 9. Chapter 10 summarizes the main conclusions found in Chapters 8 and 9. These conclusions allow for the monitoring system to become more reliable. Finally, other work recommended for system and knowledge enhancement is discussed in Chapter 11.
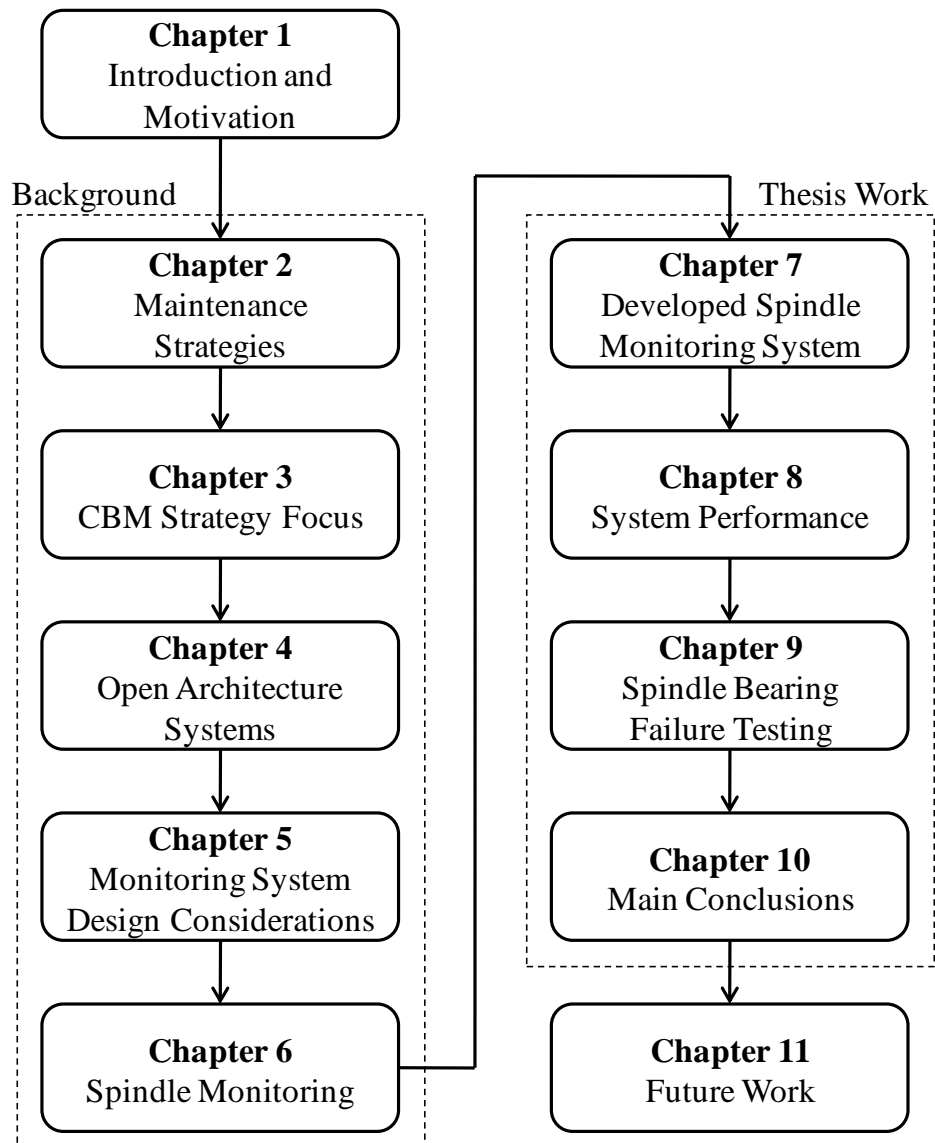
Figure 1: Thesis Outline.

CHAPTER 2: MAINTENANCE STRATEGIES

2.1 <u>A Need for a Maintenance Strategy</u>

To be competitive in today's manufacturing market, a company not only has to have a superior product, but also a superior process which is capable of producing that product. Machine upkeep is a crucial component to ensuring manufacturing machines are capable of carrying out their designed functions. Without routine maintenance, machine components can have excessive degradation resulting a reduced life cycle. This degradation, and possible failure, not only damages and degrades other components within the machine, but can also cause quality defects in the product(s) the machine is responsible for producing. An unexpected machine component failure can render the machine unusable, costing a company thousands of dollars at the same time. The cost associated with this downtime is dependent on how long the machine is down and the criticality of the machine in the overall manufacturing process. For example, if a critical process machine were to have a component failure, a plant could be shut down until the component has been replaced. If the component is not in the plant's spare parts inventory, the shutdown time could be as long as or longer than the time required to receive the component as the lead time can be very long.

This maintenance cost (rather lack thereof) can represent between fifteen to forty percent of the total consumer good price. More importantly, from a manufacturing cost perspective, improperly performed maintenance and/or unnecessary maintenance accounts for one-third of all maintenance costs [2]. Therefore, ineffective maintenance strategies can have a drastic impact on the competitiveness of a company. These

ineffective strategies can be attributed to three major problems facing many manufacturing plants [3]:

- Inability to pre-schedule or pre-plan maintenance work

- Inability to reduce spare part inventory costs

- Inability to eliminate unplanned downtime by avoiding catastrophic failures

A maintenance strategy known as total productive maintenance (TPM) provides a comprehensive solution to eliminate these costly maintenance issues. It takes a variety of different strategies and effectively combines these methods into a solution that is applicable for almost every application.

2.2 Existing Maintenance Strategies

Before TPM is introduced any further, it is essential to understand the common maintenance practices that exist today, being utilized in manufacturing today, and how these practices impact the organization. This will allow for the reader to recognize the need for TPM and understand its importance.

2.2.1 Run to Failure

Run to failure maintenance is a reactive maintenance strategy in which repair work is performed on a piece of machinery after an equipment failure or stoppage has occurred [2], [4]. This type of strategy is also known as breakdown maintenance [4]. It leads to a low productivity environment where "fire-fighting," also know as reactive maintenance, is imminent. Machines are continuously breaking down, leading to higher

associated costs in spare parts inventory, overtime labor, and machine downtime, while at the same time causing lower production availability.

The hidden issue with having a spare parts inventory is that plant floor space is required for storage of the parts or the organization has to rely on equipment vendors for the delivery of the parts [2]. If storing items within the plant, maintenance on these spare parts may need to be performed in order to maintain the integrity of the components or else they can become degraded (such as rotating a motor shaft a quarter turn every three months to prevent bearing sag). However, these types of tasks are probably neglected as well. Therefore, when a new motor (with bearing sag) is replaced, it is already damaged from the beginning of its service life. If a plant relies on vendors, the vendors need to provide immediate delivery. This can incur high expedited delivery costs.

A run to failure strategy is not really a maintenance strategy at all. Maintenance is defined as the upkeep of property or equipment [5]. By employing a run to failure strategy, equipment upkeep is either not performed or is neglected, therefore eventually leading to the equipment breaking down. The typical saying in this culture is "if it ain't broke, don't fix it" [2].

2.2.2 Autonomous Maintenance

Autonomous maintenance is a maintenance strategy that is centered around the personnel or operators using a piece of equipment [6], as a part of the TPM strategy [7], [8]. It has two goals: 1) promote the development of operator knowledge of the machine(s) they are working with and 2) create a set of "normal" conditions, where any

7

departure from normal can be easily identified [8]. In a lean manufacturing environment, the second goal is accomplished by employing 5-S, a lean principle [7].

The majority of autonomous maintenance performed is tasks checking for items such as component wear, looseness, abnormal vibrations, or lack of lubrication. This allows for the operators to take on machine ownership and make them feel empowered. This strategy relies heavily on the operator's skill to detect abnormal conditions and does not necessarily mean that they should perform the maintenance themselves, but rather bring known issues to the attention of personnel who should be investigating the possible problems [8].

2.2.3 Preventive Maintenance

Preventive maintenance is a time-based component replacement maintenance program that assigns maintenance tasks based on the number of hours the component or machine has been in operation [2]. These tasks, known as PM's, are scheduled activities to check machine and component conditions for deterioration or to replace critical items before they fail. The mean-time-to-failure (MTTF) statistic is used when trying to determine if and when a component will fail [2]. This metric is also referred to as the mean-time-between-failures (MTBF) [9]. Tires are a good example of this concept. They are rated based on their MTTF. A 50,000 mile tire should, in theory, last 50,000 miles before it fails or needs to be replaced.

A model representative of a component's life with respect to its failure rate can be seen in Figure 2. This particular model is known as the "bathtub curve" and provides a good general concept for the lifetime of machine components.
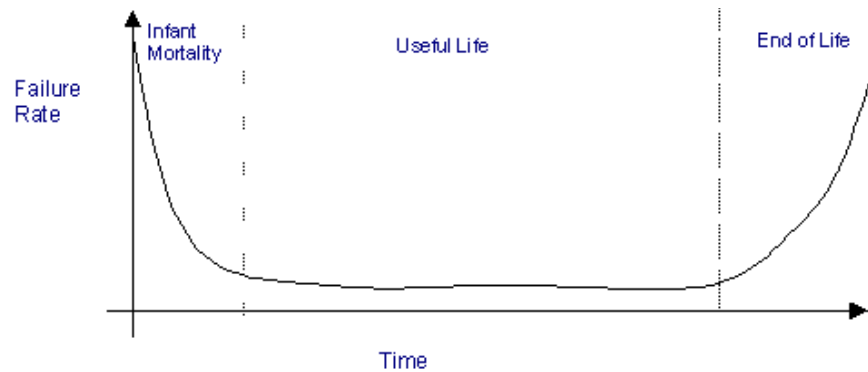
Figure 2: A Bathtub Curve [10].

As indicated on the curve, components have a high rate of failure, known as the "infant mortality", at the beginning of their life. This type of failure is usually due to manufacturing defects and causes a component to fail prematurely. As the lifetime of a component progresses out of its infant mortality period, it enters its normal operation mode. This time period is known as the equipment's "useful life". Its failure rate is somewhat constant; as the component was designed operate properly for its given application. As time continues, and the component starts to show signs of age and wear, it enters its "end of life" phase [10], [11], [12]. This is the time when the catastrophic failures start to take place.

The main goal of the MTTF statistic is to define the service life of a component before this catastrophic failure occurs. Ideally, components will be replaced before they fail during the "end of life" failure period. However, there are two drawbacks with this strategy, although it is better than no maintenance strategy at all (ie: run to failure). A component could fail prematurely (before its MTTF), therefore causing the organization to revert back to a reactive maintenance mode. On the other side of the spectrum, a component could be replaced prematurely as well, meaning it is taken out of service but it

9

still has available life left. Both scenarios have an increase in associated costs for the component itself and labor to replace it. Therefore, employing only a preventive maintenance strategy will not completely eliminate breakdowns [7].

2.2.4 Predictive Maintenance

Predictive maintenance, often referred to as condition-based maintenance (CBM) [13], is a maintenance strategy that uses a combination of predictive monitoring tools to determine the condition of equipment. These tools range from thermal imaging and ultrasonics to vibration monitoring and oil analysis. Utilization of these tools provides a better understanding of components' health, therefore allowing a better prediction of when failure will occur. Mathematical and physical models have also been developed to aid in this prediction based on the past and current circumstances. Due to this ability to now predict a failure, maintenance can be scheduled on an "as needed" basis rather than being based on specific MTTF intervals [2]. This strategy helps to maximize a component's life cycle while reducing the maintenance costs associated with its replacement. Machine uptime is also increased as maintenance work can be scheduled and planned to be performed when the machine is not being utilized. The relationship between maintenance costs and reliability with respect to how much component life remains is represented graphically in Figure 3.
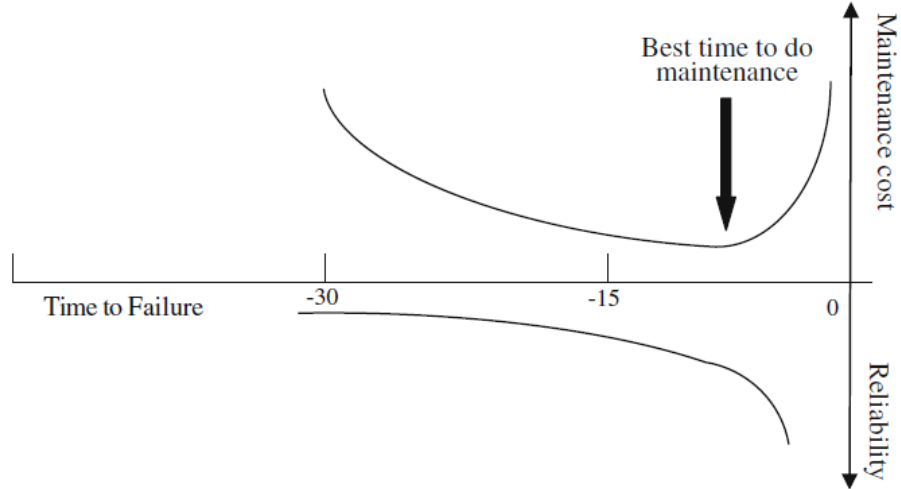
Figure 3: **Relationship Between Maintenance Costs and Component Reliability [14].**

The tire analogy discussed in the Preventive Maintenance section, can be applicable here as well. Monitoring the condition of the tread wear allows for a better determination as to when it is time to replace the tires. This maximizes the life of the tires as well as prevents a catastrophic failure, such as a blow-out or an accident due to loss of traction from occurring.

2.2.5 Reliability Centered Maintenance

Reliability centered maintenance (RCM) provides a structured and logical process that identifies the maintenance requirements of a piece of equipment [13]. The main objective of this strategy is to focus on the most important functions of the equipment, eliminating or reducing unnecessary maintenance tasks. This helps to reduce the overall maintenance costs and to optimize the PM program for the equipment [15].

RCM allows for the identification of the functions the equipment was designed to perform and the associated failures with each function. Understanding the causes and

11

effects for each failure through the utilization of tools such as the failure mode and effects analysis (FMEA) allows for the equipment's inherent reliability to be realized [13]. It is important to note that RCM should not be used as a substitute for poor build quality, improper maintenance practices, or bad mechanical designs [15]. It only ensures the proper maintenance is being performed on the components most at risk for failure.

2.2.6 Corrective Maintenance

Corrective maintenance is a means of improving a piece of equipment while performing maintenance on it for an identified issue [13], [16]. This improvement helps to eliminate the chance of another failure occurring while increasing the equipment's reliability [17]. Improvements, such as design changes, aid in providing more maintenance-free equipment. These equipment improvements and design changes are useful for future generations of the equipment, allowing for the new equipment to perform better than their predecessors as the "bugs" have been fixed [13].

2.2.7 Total Productive Maintenance

Each of the maintenance strategies discussed prior to now have their own advantages and can be used individually or together. However, in order to have maximum maintenance benefits, all of these strategies should be included in an overall maintenance program that is comprehensive in nature. This will allow for an almost complete minimization of costs, increased product quality, and decreased amounts of stress and headaches put on the employees. TPM is a maintenance strategy that allows for these items to be realized.

Introduced in Japan in 1971, TPM is a system designed to achieve zero breakdowns while at the same time achieving a process that produces zero defects. In its formal definition, TPM is productive maintenance carried out on equipment by all employees, on a company-wide basis, through small group activities [7]. In essence, TPM is an all inclusive maintenance program/system that adds value to plant processes by preventing breakdowns. It is comprised of five maintenance improvement elements known as the "Five Pillars." These pillars are [18]:

- Elimination of the "six big losses"

- Preventive Maintenance

- Autonomous Maintenance

- Training

- Maintenance Prevention

The "six big losses" cause the hindrance in equipment efficiency and can be categorized into three subgroups: downtime, speed losses, and defects. The hierarchy is can be seen in Figure 4, with the "six big losses" itemized in the figure [7].

Downtime	Speed Losses	Defects
Equipment Failure from Breakdowns	Idling and Minor Stoppages	Process Defects
Setup and Adjustment	Reduced Speed	Reduced Machine Yield
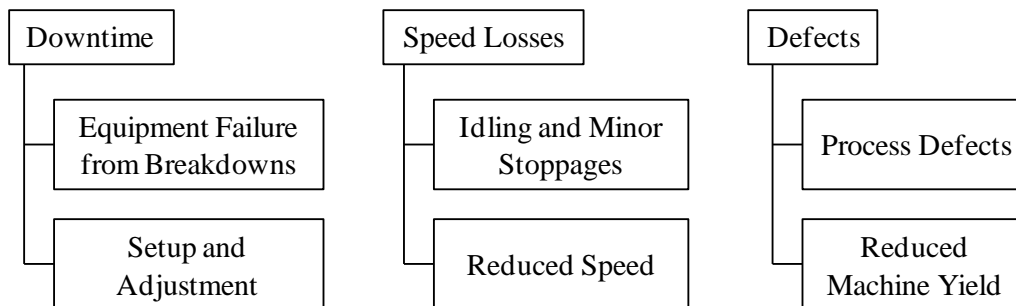
Figure 4: The "Six Big Losses" Hierarchy.

By eliminating these six losses, the overall equipment effectiveness (OEE) of the machine can be dramatically improved. In many cases, simple and easy tasks can be

performed, such as cleaning or re-alignment, to help improve OEE. OEE is the driving metric upon which TPM uses to assess how well the system is performing. OEE takes the "six big losses" into account while looking at machine availability, performance, and rate of quality products. An improvement in one metric provides an improved OEE, as given by [7]:

$$OEE = \text{Availability x Performancy Efficiency x Rate of Quality Products} \qquad (1)$$

Where:

$$\text{Availability} = \frac{\text{Operation Time}}{\text{LoadingTime}} = \frac{\text{Loading Time - Downtime}}{\text{Loading Time}} \qquad (2)$$

$$\text{Performance Efficiency} = \frac{\text{Ideal Cycle Time}}{\text{Operating Time / Total Parts Produced}} \qquad (3)$$

$$\text{Rate of Quality Products} = \frac{\text{Number of Good Parts Produced}}{\text{Total Parts Produced}} \qquad (4)$$

Implementing a TPM strategy allows for the bathtub curve, shown in Figure 2, to be modified to the bathtub curve shown in Figure 5. The rate of breakdowns or failures during the equipment's infant mortality is reduced by preventive engineering and early equipment management. Providing adequate maintenance helps to extend the useful life of the equipment during its wear-out period. However, most importantly, TPM allows for the occurrence of breakdowns during a machine's useful life to be theoretically reduced to zero.
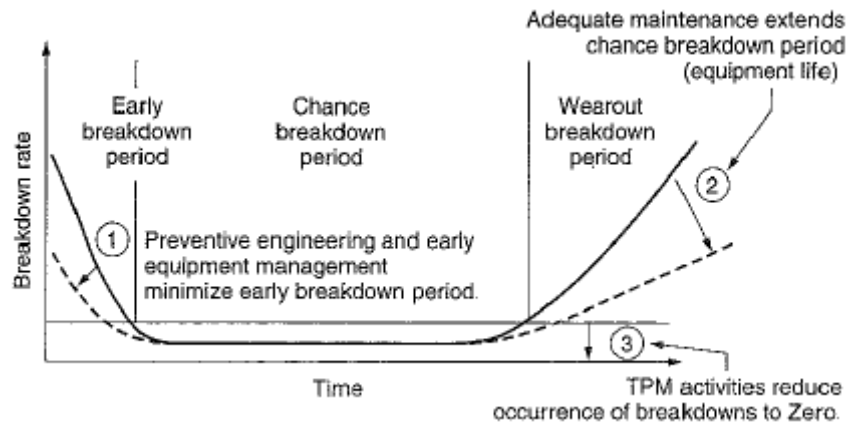
Figure 5: Bathtub Curve with TPM Activities [8].

2.3 Maintenance Strategy Summary

  To summarize all of the maintenance strategies discussed, Figure 6 has been created to show a mapping of how each maintenance strategy is either coinciding or separated from the others. While TPM includes many of the strategies, all of them should be included where applicable. For example, note that the run to failure strategy is included in the overall "Best Maintenance Strategy." This is due to the fact that in some applications, it may make sense to perform maintenance after a failure has already occurred, where it is not cost preventive, such as an o-ring in a low pressure air regulator. However, a run to failure strategy should not be the predominant strategy by any means. In addition, certain strategies should be used only when and where it makes sense and the benefits supersede the costs.
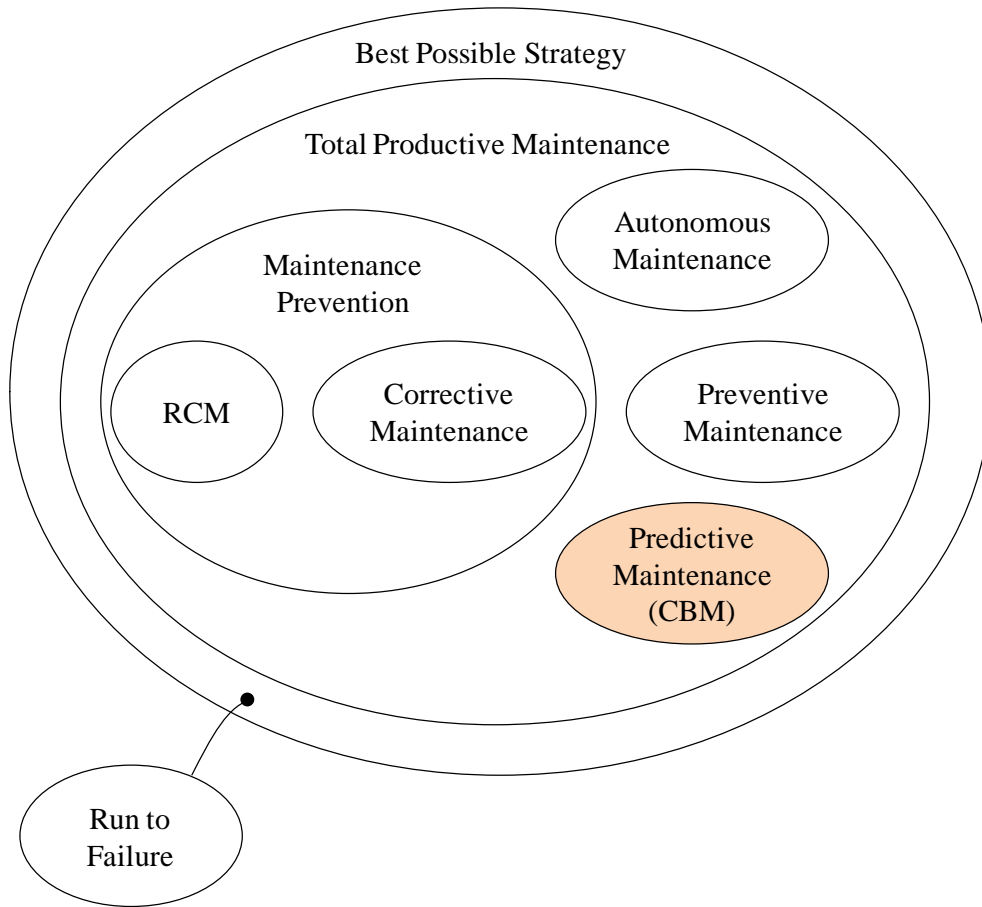
Figure 6: A Mapping of Maintenance Strategies.

CHAPTER 3: MOTIVATION TO FOCUS ON THE CBM STRATEGY

As stated in Chapter 1, the work completed for this thesis focuses on a CBM system for a CNC machine. The ability to implement a CBM program effectively with in a manufacturing organization provides many advantages:

- Lower maintenance costs

- Fewer machine failures

- Less repair downtime

- Reduced inventory of repair parts

- Longer machine life

- Increased production

- Improved operator safety [2]

- Advance warning of failures

- Reduced equipment life-cycle cost

- Advancement of current fielded systems and better future maintenance methods [19]

While the numerous advantages more than make up for the disadvantages of a CBM program, the disadvantages are still important to note. They are:

- Increase in diagnostic equipment costs

- Increased personnel training costs

- Potential savings not seen by management [12]

A computerized CBM system from a machine's original equipment manufacturers' (OEM) perspective allows for maintenance to be built into the machine which provides many benefits. The machine owner can be knowledgeable about the condition of their machine and be alerted that the machine will need maintenance soon. This also aids the OEM as it provides them with better information so they can keep the proper spare parts in stock.

A system such as this can also lead to a better understanding of the product's operation in the field. This better understanding benefits both future machine designs as well as the OEM's service department for machines currently in operation. This allows for both the corrective maintenance and maintenance prevention strategies to be employed as well as CBM, adding to the system's capability and effectiveness.

3.1 Implementation of a CBM Strategy

CBM can be completed by utilizing hand-held devices, where an employee physically checks specified components on a machine(s) or it can be performed via a data acquisition and signal processing system. Depending on each facility's situation, it may not be optimal or impossible to have a human perform CBM checks. This can be due to the location of the components needing to be checked, sheer volume of checks, or a limited timeframe provided to complete the checks, among other issues. This is where a computerized data acquisition system may be of more value to an organization. However, data collection can overwhelm databases and cause difficulty for the individuals reviewing the data to extract the information they need. Therefore, the goal of

a computerized monitoring system should be to gather important and useful data that is easily managed and will benefit a plant's organizations, employees, and customers [20].

3.2 <u>System Components in a Computerized Monitoring System</u>

A typical computerized monitoring system usually consists of four main components: sensors, a microprocessor or data acquisition system (DAQ), a host computer, and software program(s) [2]. The sensors would allow for signals to be acquired via the DAQ. These signals would then be sent to the host computer and be processed through its designed software program(s). The software programs should allow for the machine health and its conditions to be determined as well as providing prognostics to help decide maintenance actions [21]. Technological advances have allowed these type systems to be much more flexible. Signal processing can be performed on a host computer [2], as well as by a central server [22]. The use of a central server allows for multiple parties to view data on the same network or over the internet. Data can even be transmitted to the DAQ components via wireless sensors [21], [23], [24], [25]. A system schematic including many of these components discussed is shown in Figure 7.
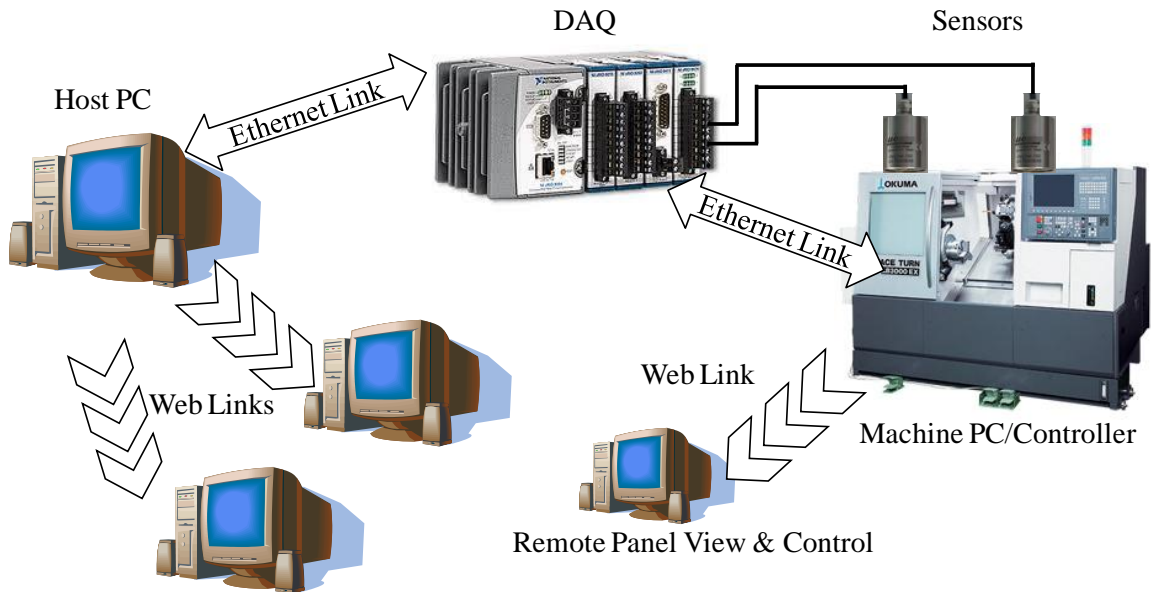
Figure 7: A Typical CBM System Architecture.

The system previously described can be extended to multiple machines as well, as shown in Figure 8. Individual machines are at the bottom-most level, containing either an individual CBM system for each machine or a central server to monitor all machines at once. Both of the approaches have their own advantages and disadvantages. Separate systems for machines induce greater hardware costs; however they ensure reliability of the total connected system should one of the CBM systems fail. This inherent redundancy allows for monitoring of the other machines to continue despite one system failing.
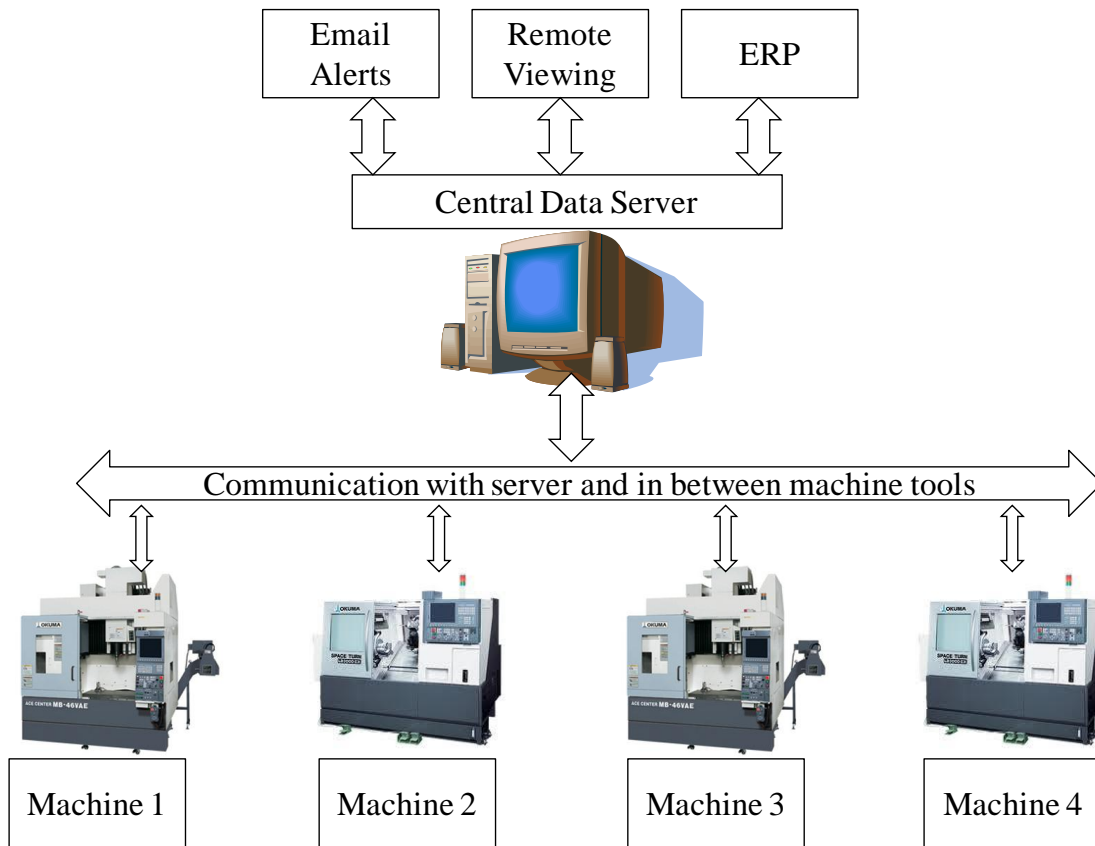
Figure 8: **CBM System Extension to Multiple Machine Environments with Integration of other Features.**

Other features can be added to the system in this configuration as well. If a prescribed limit is exceeded for a machine, emails can be automatically generated and sent to the necessary people. They can use a remote viewing application to get current process information about the machine and decide what action is needed. At the same time of the email generation, an enterprise resource planning (ERP) system could place an order for the spare part required, if none are on hand at the facility, as well as schedule the maintenance work on the machine, with approval from the engineers.

3.3 <u>Methodologies Behind Existing Monitoring Systems</u>

3.3.1 Hardware

There are a variety of techniques currently being employed today to help monitor equipment conditions and aid in maintenance planning and execution. All CBM systems are of two basic configurations, compact (all-in-one) or modular [23]. An example of the hardware used for each system can be seen in Figure 9 and Figure 10 respectively. The advantage of an all-in-one system is that only one unit is needed, however the unit may be limited by the different types of inputs it can receive, thus limiting the types of sensors that can be used. The advantage of having a modular system allows for a variety of multiple sensors to be utilized, but may have a higher cost associated with it as each module needs to be purchased separately.

Figure 9: Example of Possible Compact Monitoring System Hardware [26].

a) Base Chassis   b) Module

Figure 10: Example of Modular Monitoring System Hardware [27], [28].

A variety of sensors are currently being utilized in commercial maintenance monitoring systems today. The use of the sensors would be dependent on the parameter of interest. They are [23], [29]:

- Power

- Torque

- Strain

- Force

- Acoustic Emission

- Vibration

- Ultrasound

- Cameras

- Lasers

- Temperature

- Pressure

Once the physical system hardware has been decided on, it all comes down to the signal processing of the data acquired and software programming. This is where the monitoring system can become unique in its applications.

3.3.2 Diagnostics

A monitoring system can be one that is diagnostic in nature, where the system can detect and isolate faults and failures [19]. Sometimes referred to as an intelligent predictive decision support system (IPDSS), it diagnoses the faults based on rules, cases, models or a combination of the three. A rule based system would be set up to flag certain conditions, such as prescribed limits, and alert users of possible faults that can occur [30], [31], [32]. In the area of tool monitoring, items such as how the part signature changes with respect to time, wear estimation, and breakage detection via a reference pattern are employed [23]. A breakage detection example can be seen in Figure 11.
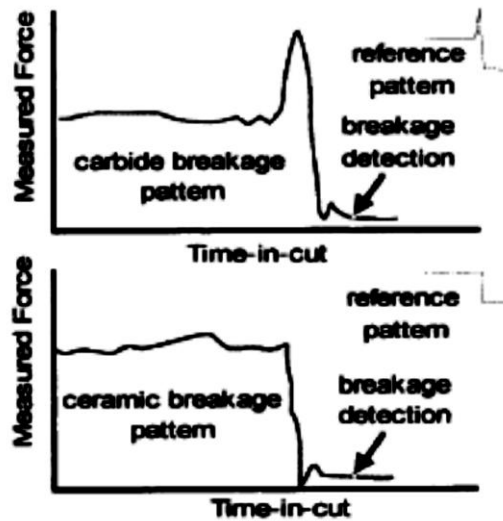
Figure 11: Tool Breakage Detection through Pattern Recognition [33], [34].

Case based systems use historical records via a case library with the past faults for the machine to gauge which faults may occur. The system does this by selecting a stored record that is most similar to the current conditions. Model based systems use a mathematical neural network to provide logical methods and reasoning to compare current conditions with what the models say they should be, given the various system

24

inputs involved [30], [31], [32]. Neural networks successfully overcome traditional statistical techniques due to their ability to learn a time series with non-linear features and thus are commonly used in forecasting [35]. As an example, to show the power of using a neural network, Bansal et al. have created a real time algorithm that is able to predict what the next incoming signal from the DAQ system should be, based on the real time input machining parameters [36]. An example of the calculated response versus the actual response can be seen in Figure 12.
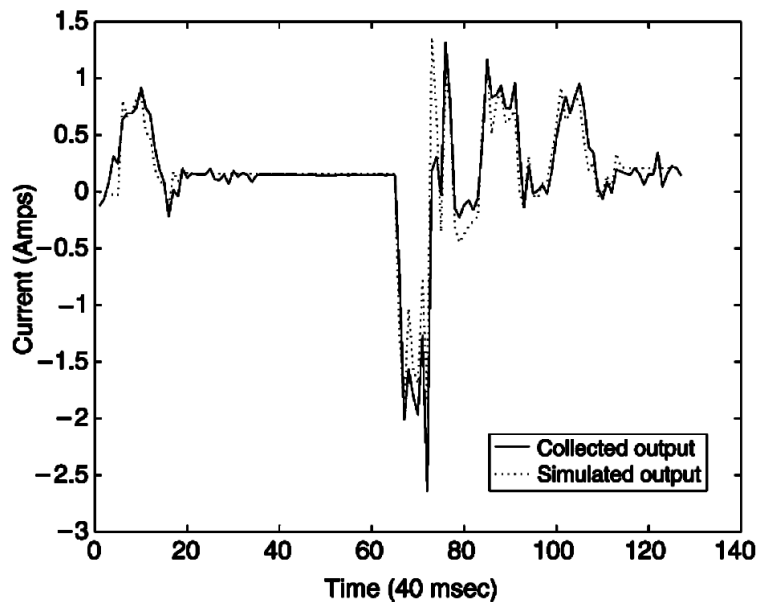
Figure 12: Simulated vs. Real Data from a Production Machine [36].

3.3.3 Prognostics

A monitoring system can also be prognostic, sometimes referred to as prognostics and health management (PHM) [37]. A prognostic system allows for the reliability of a component to be predicted based on the current and historic conditions [19]. Such a system can actually predict the remaining useful life of machine components. It does this

by assessing and then quantifying the amount of degradation that should occur under normal operating conditions. Two approaches are taken to determine the degradation: the physics of failure approach and the data driven approach [37].

3.3.3.1 Physics of Failure Approach

The physics of failure or PoF approach is similar to the model based approach of a neural network system. It takes into account the fundamental processes, such as mechanical, chemical, and electrical processes, to calculate the cumulative damage and remaining life of the component. An FMEA is utilized to help determine this metric [37]. The basic principles and flow of a PoF approach can be seen in Figure 13 and an application of the approach can be seen in Figure 14.
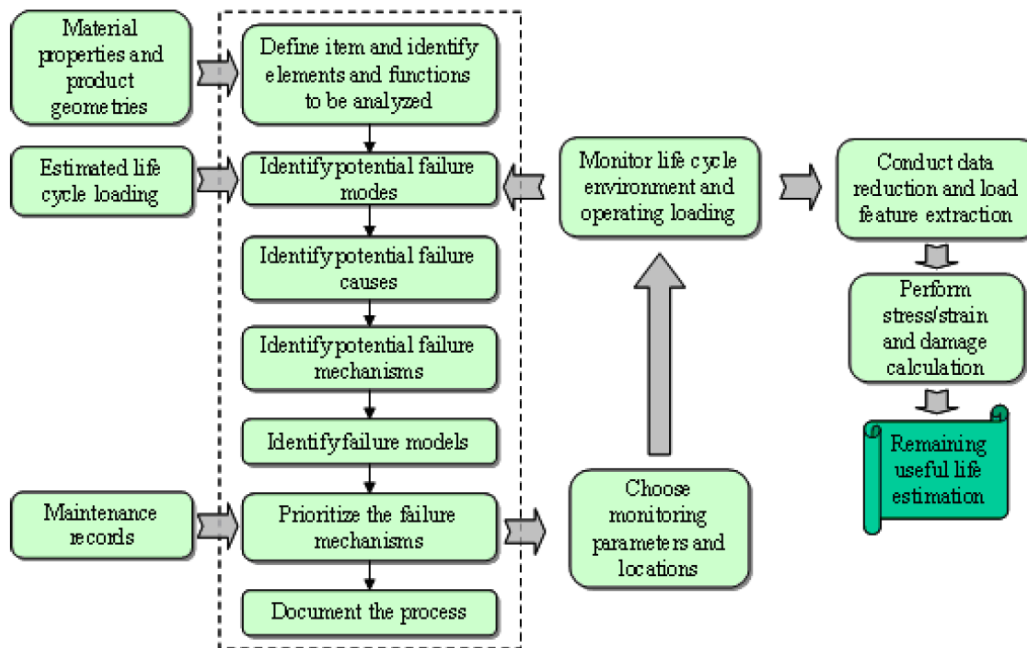
Figure 13: PoF Based Approach [37].
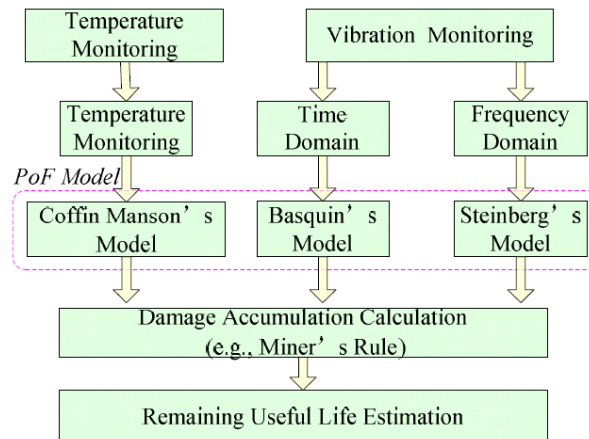
Figure 14: Example of a PoF Approach Employing Physical Modeling for Damage Calculation [37].

3.3.3.2 Data Driven Approach

The data driven approach uses patterns or relationships within the acquired data and processes it. The approach can be subdivided into two categories: machine learning and statistical methods, as shown in Figure 15 [37]. These categories can then be divided further, depending on which method(s) are employed.
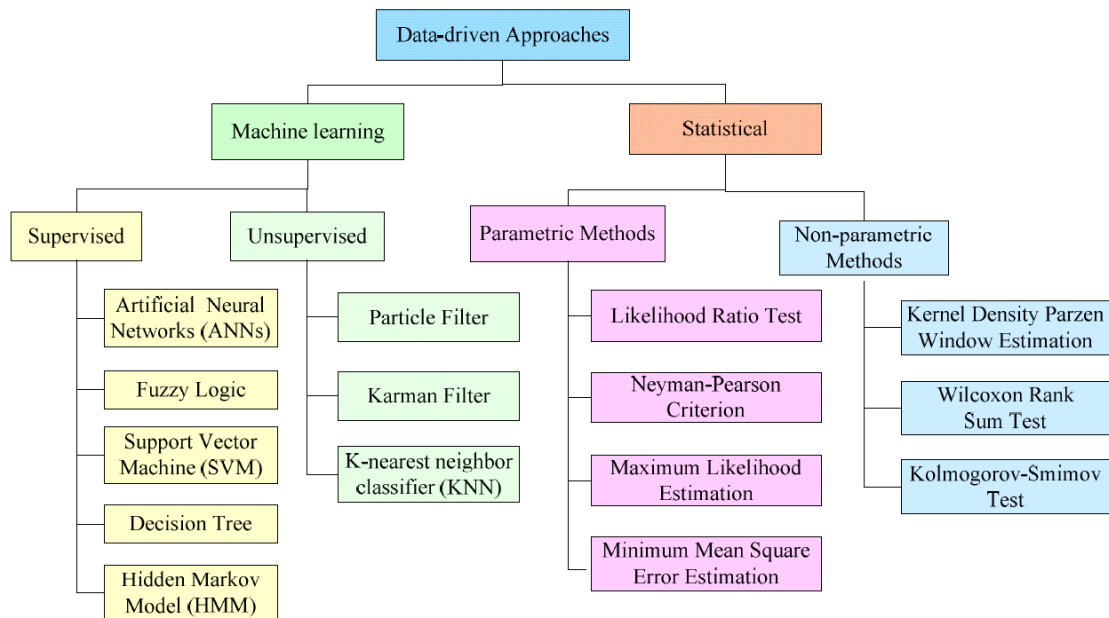
Figure 15: Data Driven Approach [37].

27

3.3.3.3 Hybrid Approach

The two approaches can also be combined to form a hybrid PHM approach. Its process algorithm can be seen in Figure 16. The hybrid approach combines the best of both worlds. The PoF approach is more accurate when trying to determine component life, however a great amount of component information is required and the approach may not be accurate at a system level. The data driven approach is economical and flexible, but it uses no knowledge of the stress being applied to the component and needs a large amount of failure data [37]. By combining both systems, a better PHM system can be achieved.
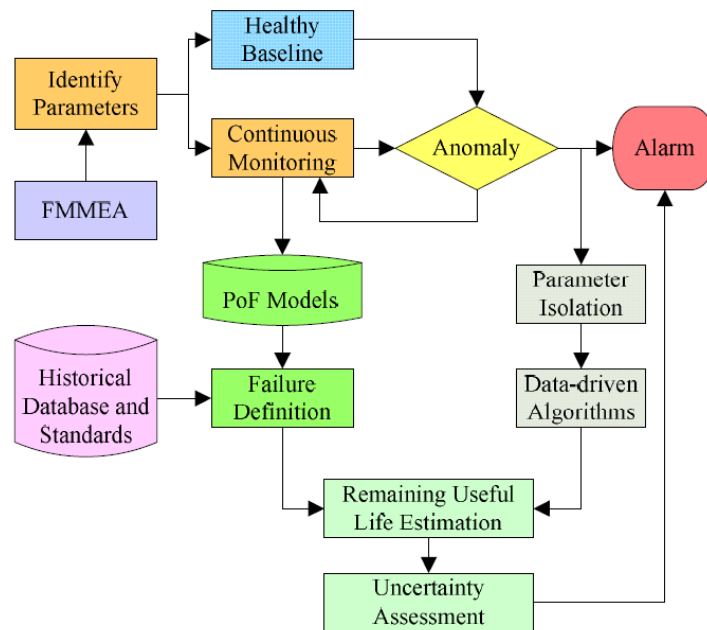
Figure 16: The Hybrid Approach [37].

Table 1 provides a summary of everything discussed in this section for convenience and clarity.

Table 1: Various CBM System Options.

Hardware	Software Programs	Methods
Compact Or Modular	Diagnostic	Rules Cases Models
	Prognostic	Physics of Failure Data Driven Hybrid

3.4 Health Parameters

Health parameters (HP) can also be defined. Martin and Thrope define a "healthy" value for a metric or a health parameter being investigated by dividing the current value for the metric by the "healthy" value [38]. An example for coolant temperature is shown in Equation 5.

$$\text{HP(Coolant Temp)} = \frac{\text{Coolant Temp(Actual)}}{\text{Coolant Temp(Healthy)}} \times 100\% \tag{5}$$

This provides a ratio which can then be converted into a health percentage. The lowest percentage for any health parameter at a particular instant in time for any health parameter would denote the machine's health [38].

3.5 Challenges for Integration of Computer-Based CBM Systems to a Production Environment

While there are computerized CBM systems currently available on the market, such as the Predator system [39], GE's Bently Nevada Continuous On-line Monitoring Systems [40], and InCheck Technologies' InSite remote condition monitoring system [22], the use of these commercial systems is not continuously seen throughout the manufacturing industry. This may be because of a general monitoring system cannot serve the specific need of a particular company or operation.

Academic research is also being carried out to help advance and improve monitoring systems, yet its impact on industry has been limited [41]. This lack of commercial system usage in industry can be attributed to different causes. They are:

- Difficulties with commercial-off-the-shelf (COTS) products integrating properly into machines

- Proprietary interfaces

- Software performance and flexibility issues [21]

- Costs of the sensors and sensor installation

- Insufficient understanding of the benefits a system such as this can provide [41]

Before trying to tackle the sensor costs and lack of benefit understanding, the first three causes can be offset by employing an architecture system that supports both event-based and time-based data processing and reporting. This is the main motivation behind the work covered in this thesis. Utilization of an open architecture system would allow for these issues to be efficiently overcome.

CHAPTER 4: OPEN ARCHITECTURE SYSTEMS

As observed by Matsubara et al. [41], the application of intelligent control techniques in an industrial environment is majorly inhibited because of proprietary controls by machine tool manufacturers. The control algorithms developed by these manufacturers are not made to be altered by engineers who wish to enhance the performance of the machine tool outside the machine tool manufacturing organization. However, with the European initiative for the Open System Architecture for Controls Within Automation Systems (OSACA) in 1992, development of an "open" architecture control system was sought [42]. Open architecture control (OAC) was born from this initiative. OAC provides the possibility to access a machine's internal data as well as have the ability for more user control in a machine's movements.

State of the art open control systems include Sinumerik 840D from Siemens [43], IndraMotion MTX from Bosch [44], and the TwinCat system from Beckhoff [45]. Sinumerik 840D works on the structure of object oriented NC kernel developed in C++. IndraMotion MTX provides users with the possibility of integrating their own jobs built in the C language. TwinCat uses the Microsoft's Visual Basic.NET framework for the programming of their devices.

4.1 OAC on Machine Tools

Various machine tool OEMs are now providing OAC systems with their machines. Okuma, a CNC machine tool OEM, has developed its own OAC machine controller, called the THINC OSP. The OSP is essentially a Windows PC mounted on

the backside of a numerical control (NC) real time controller. With the help of an application programming interface (API), the user can extract some of the machine data and control some of the signals. API applications are written in the Visual Basic.NET framework. Data such as spindle speed, current part program, and current tool selected can be gathered via the API. The API also allows for the feed-rate to be controlled; however, control signals for the spindle motor and turret still remain inaccessible.

Okuma, as well as other companies, are now developing applications for the Okuma OSP. The following application is an example of what the capabilities of these new OAC systems can provide.

Figure 17: Okuma Coolant Monitor – Main Page.

The application, shown in Figure 17, monitors both the machine's coolant concentration and pH from the machine control simultaneously as the machine is operating. It is an interactive CBM program and is flexible to allow for the program to be adjusted based on the specific coolant type the machine tool is using. The application provides both the current health of the coolant, Figure 17, as well as a past history, Figure 18, allowing for any historical patterns to be noticed. The program even has an "events" page that allows the user to know of any changes that have occurred. As an example, Figure 19 shows that at 7:29 am on July 22,2011, both the concentration and pH were at alarm levels.

Figure 18: Okuma Coolant Monitor - History Trending.
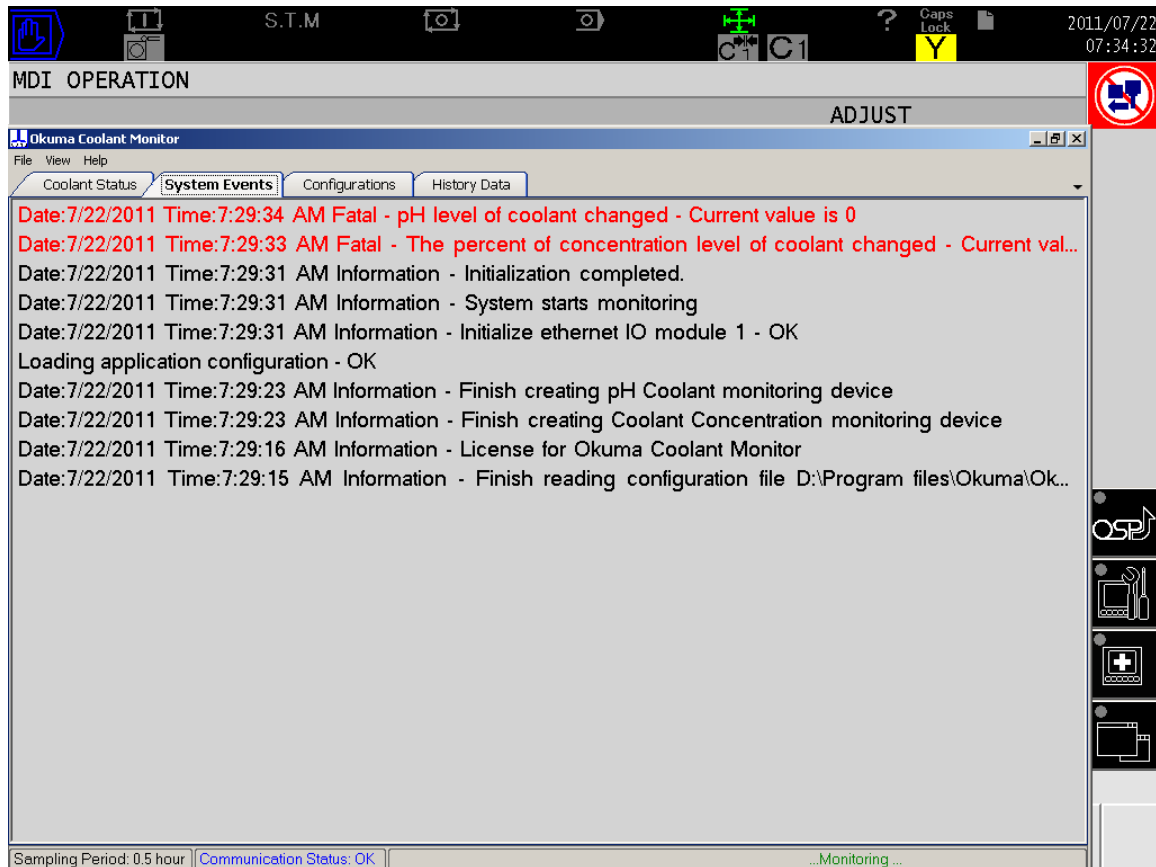
Figure 19: Okuma Coolant Monitor – System Events.

One limitation with this application is that it does not use any of the API features that are provided with the machine. This limits the amount of information that can be passed from the machine to the engineer. For example, if the pH of the coolant increases suddenly, the direct cause may be unknown. However, the API utilization would allow for a part program history to be recovered and may be able to inform the engineer that the pH changes only when Part X is machined, indicating that the parts are dirty entering the machine. Another limitation of not using the API prevents internet remote viewing from taking place as the data is held internally within the application. The API allows for data

to be written to what is known as a *Common Variable* where it can be uploaded to a web server.

4.2 <u>OAC Limitations for a Machine Tool</u>

The current OAC available allows for a many new applications to be created, however the "openness" of the control is still limited to basic functionality, such as discrete event simulations, integrating macros to supply data to spreadsheets, and remote monitoring of production data. Currently, there are limited opportunities in acquiring real time machine data as well as the ability to control machine parameters in real time. The reasons for this include safety and liability issues, intellectual property, and trade secrets of the machine tool OEMs. The advancements taken by Okuma OSP is an indication that more "open" control systems can be expected and will be needed for the OEMs to stay competitive.

CHAPTER 5: MONITORING SYSTEM DESIGN CONSIDERATIONS

5.1 General System Design Requirements

Before designing a monitoring system, it is important to understand what requirements the system should meet in order to deliver its expected performance. The total system must have the following capabilities [2]:

- User friendly software and hardware

- Automated data acquisition

- Automated data management and trending

- Flexibility

- Reliability

- Accuracy

The ideal computerized system should facilitate "single key input to automatically acquire, analyze, alarm, and store all pertinent data" from the equipment. The software program used should be menu driven and prevent the user from deleting or changing stored data accidentally. It is recommended that it should have an automatic report generation feature as well as be able to compare data among similar machines. It should also be able to accept as many different kinds of sensors as possible while still having the ability to be implemented on various machines [2].

Two different types of alarms can be used in allowing unreliable machine conditions to be recognized: static and dynamic [2]. A static alarm would sound if a measurement exceeds or falls below a prescribed value. This would be indicative of a "soft" fault, where the problem develops slowly with time [46]. A dynamic alarm would

be executed if the rate of change in the measurement exceeds specified limits. This type of alarm can greatly enhance a CBM system's diagnostic capability [2]. This alarm would typically take place at the onset of a "hard" fault or catastrophic failure, which is generally unpredictable. However, employing only a dynamic limit alert system does not eliminate the need for monitoring [46]. Both of these alarm types allow for the reduction of the manual effort required in determining when to perform maintenance [2].

The data acquisition and analysis should be performed while the machine is in operation. This allows for faults to be detected during a machining process, rather than during in a separate test routine (where the component may catastrophically fail before the test routine can even be arranged) [38].

5.2 Important Signals to Monitor

Due to a monitoring system needing to deploy additional hardware and software components to an existing machine, the cost of the overall system needs to be justified. Therefore, it is important to monitor critical signals on a machine. To decide what these important signals are, two questions can be asked [38]:

- What are the critical components?

- Which components have a historically high rate of failure?

Critical components can be defined several different ways. A component could be considered critical if it is very expensive or rare. In some instances, the parts may not be made anymore or are extremely hard to acquire. The component could have a long lead time from date of order or it could have a long installation/repair time associated

with it. A component may also be considered critical if its failure causes other components/systems to fail or provides them with the possibility to fail.

For the CBM system discussed in this thesis, spindle health is of interest. This area of the machine was chosen for a variety of reasons, component criticality is the main reason – if the spindle fails, the machine cannot perform its intended function. Another reason is the functional service benefit provided by a machine subsystem such as this. Typically, when a customer contacts a machine tool OEM, a service representative is sent out to the facility, where he/she gathers vibration data, and then has to analyze it before deciding if the spindle needs to be replaced. The monitoring system, detailed in Chapter 7, would eliminate the need for the service representative to go to the machine to collect data. Rather, the data would be presented to him/her through various means (email, webpage, server, remote access into the machine control) and an informed decision can be made without leaving his/her desk.

Another item that should be taken into account when deciding on important signals to monitor is how fast the component conditions can change. This determines the sensors employed and the acquisition rates and data polling frequencies required of the computerized system. During machine operation, some conditions may change slowly (i.e.: fluid temperatures), while others will change suddenly (i.e.: tool and spindle vibrations). The slower changing conditions will have various rates of change among different components [29]. It is important to realize these changes in order to enhance a CBM system's capabilities and to provide the necessary sampling rates.

5.3 Okuma Specific Design Requirements

As the system was developed for Okuma machines, the OEM, Okuma America Corp., had some requirements of their own. A CBM system to monitor spindle condition was to be developed that could be packaged on their CNC machines. It should be able to be run on the THINC control as well as utilize the API to allow for additional data communication features. In order for this to occur, the application needed to be programmed in the Visual Basic.NET (VB.NET) language. The look of the system should be similar to that of the *Okuma Coolant Monitor* system described in Chapter 4. Additionally, the data acquisition devices used needed to be able to communicate with the VB.NET application. The system's target cost was around $2,000.

The only criteria requested for the system is that it be able to accept any third party peripherals and communicate through the I-Gear interface. The I-Gear interface allows for data to be collected from the machine tool, uploaded onto internet servers, and accessed remotely via a webpage. This can be done through a piece of software call the Data Utility Transport (DTU) and allows the machine tool owner as well as the OEM to monitor machine conditions from the cloud.

Initially, the one of the goals for this system was to have the ability to be installed on any Okuma machine, old or new. However, there were some severe limitations in trying to accomplish this on an older control and the solutions were not very practical. The older machines do not have an OAC controller; they are NC only. Therefore, if any Windows applications were to be used on the machine, a separate PC would have to be used and placed inside the machine's electrical cabinet.

The use of this additional computer would be much more challenging. API programming could not be employed as the API is only available on an Okuma type P controller. This computer would have no monitor, keyboard, or mouse attached to it (in the machine) due to the electrical cabinet space requirements. Therefore if files needed to be accessed on the PC, all items would have to be brought to the machine where an electrician would have to open the cabinet (typical plant operations procedure). Another issue arises if there is a total loss of power to the machine, such as turning the main power off. The electrical cabinet would have to be opened up every time the machine was powered down and the separate PC would have to be manually restarted. Due to all of these limitations, the system was to be developed on the newer (type P) control.

CHAPTER 6: SPINDLE MONITORING

A spindle is a cylindrical shaft, supported by bearings, in which its primary function is to rotate. In machining, this rotation allows for items to be machined, via a mill or a lathe. The bearings allow for the shaft to stay in place while this rotating action is occurring. Various rolling element bearing configurations are used to support the shaft and its loads based on different machining applications. An example of a quad set angular contact roller bearing configuration can be seen in the spindle diagram in Figure 20. It is the bearings that are of most interest when monitoring a spindle for problems.
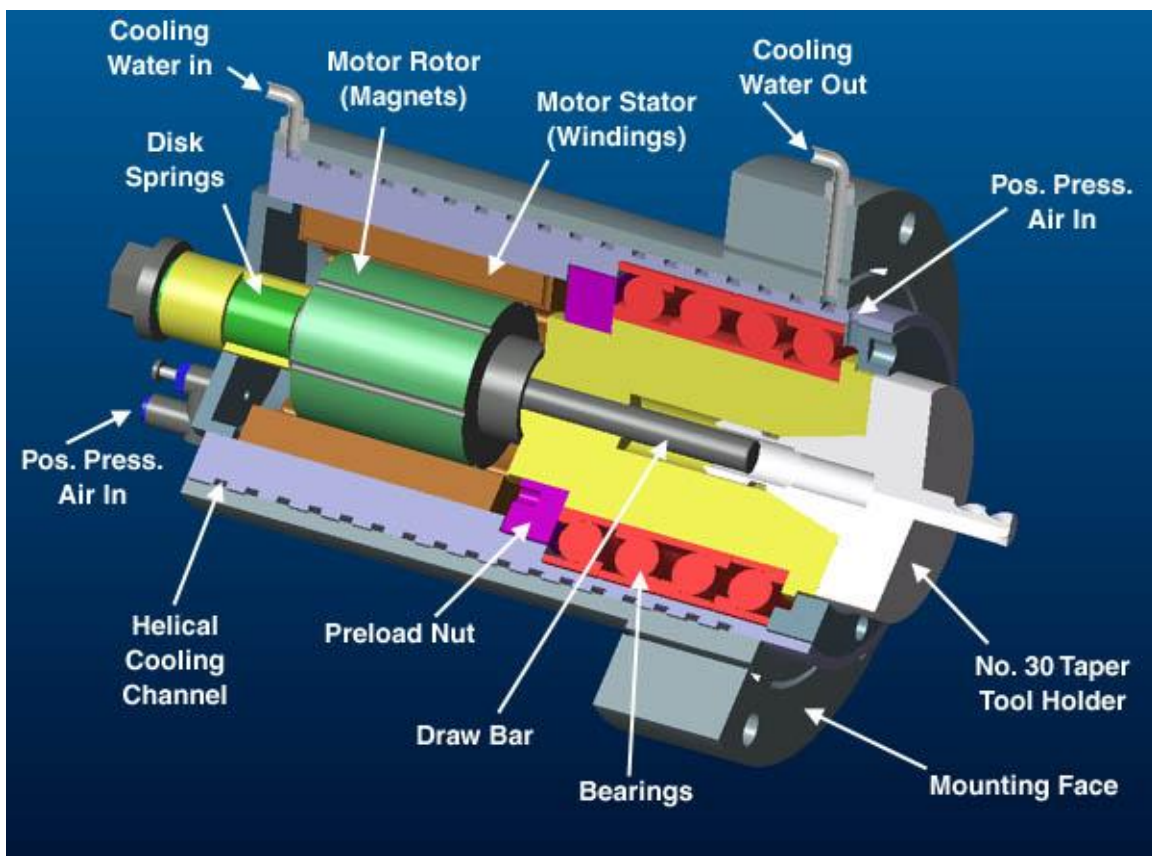
Figure 20: A Cut-Away View of a Spindle [47].

Rolling element bearings are comprised of the rolling elements, an inner race, an outer race, and a cage or retainer to hold the rolling elements. An exploded view can be seen in Figure 21.
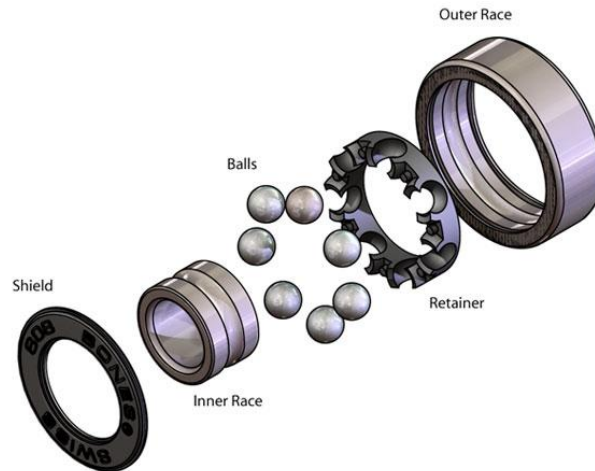
Figure 21: An Exploded View of a Ball Bearing [48].

Vibration in rolling element bearings is inherent when a bearing is in operation. Vibration will occur even if the components of the bearing are geometrically and elastically perfect. This is due to the fact that there are a finite number of mechanical components, within the bearing itself, used to carry a load. For a "perfect" bearing, the source of vibration can be caused by variations in the compliance of the bearing, where compliance is the bearing assembly's total stiffness [49], [50]. For a "non-perfect" bearing, the presence of defects are the cause of the vibration, the main one being waviness (out-of-roundness) of the inner and outer races [50], [51]. Of the two vibration sources, compliance variation and defects, defects are the main item that will cause a significant increase in the vibration level [50].

There are two types of bearing defects, known as either distributed or local [52]. Distributed defects are those that are caused by manufacturing errors such as waviness,

uneven surface roughness, and out-of-round or off-size rolling elements, as well as improper installation and abrasive wear [51].

Local defects are those that include cracking, spalling, and pitting on the rolling surfaces. Spalling is most frequent defect seen in rolling element bearings. This happens when a micro-crack, due to fatigue, occurs below the component surface. The crack then propagates to the surface until a fragment of metal breaks away. The cavity left behind is known as the spall and can occur on both the races of the bearing or the rolling element itself [52].
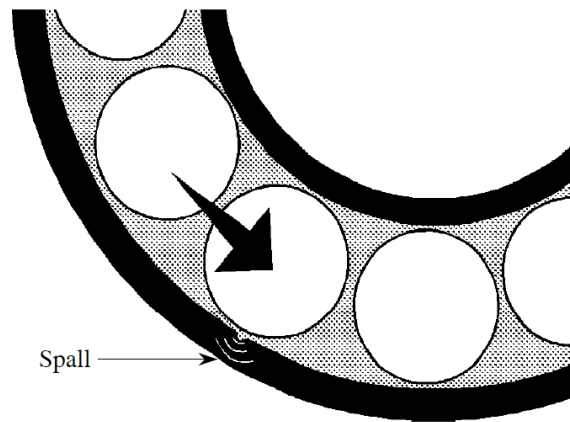
Figure 22: Example of a Bearing Spall Defect [53].

However, in order to verify the true source of the vibration, vibration sensors need to be employed. These sensors are discussed in the next section.

6.1 <u>Vibration Sensors</u>

6.1.1 Non-contact Displacement Transducer [54]

A non-contact displacement transducer, such as a proximity sensor, functions via eddy-current principles. The probe's construction consists of a wire coil mounted in a non-conductive ceramic or plastic. A magnetic field is generated from the tip of the

probe and when the tip is placed close to a conductive material, eddy currents are created. These currents remove energy from the probe, allowing for a change in voltage to be measured. This voltage change can then be related to the change in displacement of the conductive material from the probe. The main limitation with this transducer is that it cannot distinguish between shaft motion and material defects (scratches, dents, conductivity variations). This causes the output to include both shaft vibration as well as material defects, so the response seen is not necessarily the true vibration. This limits the sensor to frequency ranges between 1,000 Hz to 1,500 Hz. Another limitation for this type of transducer is that it only measures relative position and may not indicate a shaft's true movement. True movement can be measured by velocity pickups and accelerometers, both discussed in the next several pages.

| a) | b) |
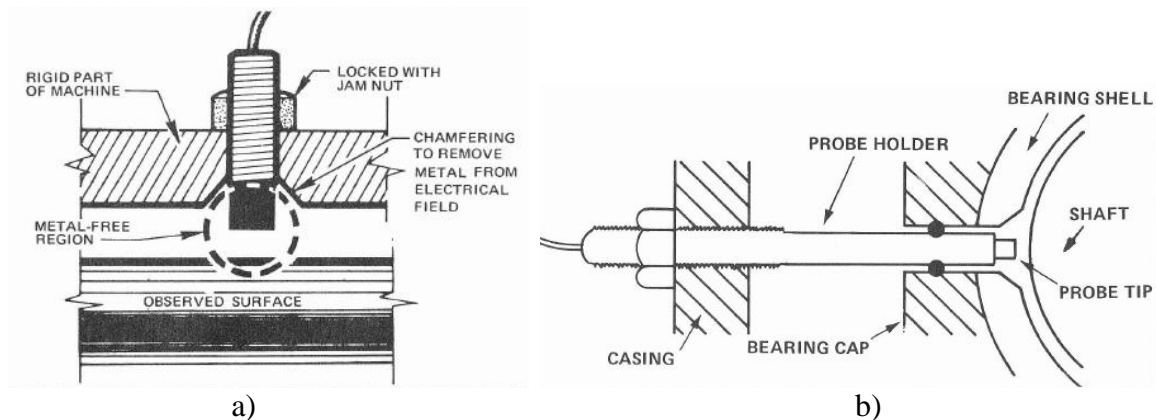
Figure 23: Mounting of a Non-contact Displacement Transducer [54].

6.1.2 Velocity Pickup [54]

A velocity pickup is a cylindrical coil that surrounds a stationary magnet, suspended with springs. A damping fluid between the coil and magnet can be added for various performance applications. When exposed to vibration, the cylindrical coil

vibrates, causing a magnetic flux to come through the coil. This induces a voltage that is proportional to the vibration the sensor is experiencing. As an example, electric guitars use velocity pickups to convert the string vibration into sound through amplification. The main limitation of this transducer is that it is an electromechanical device with moving parts. In aggressive environments, these parts can fail. Thus, these transducers should be used in applications where the frequencies are between 10 Hz to 1,500 Hz.
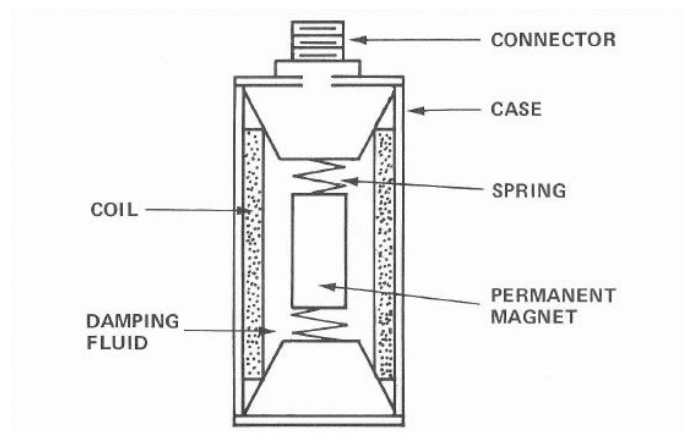
Figure 24: Diagram of a Velocity Pickup [54].

6.1.3 Accelerometer [54]

An accelerometer measures acceleration via its piezoelectric crystal elements. These crystal elements produce electricity when they are stressed by a mass contained inside the sensor. This stress generates a voltage which is proportional to the acceleration the sensor is experiencing. The difference between an accelerometer and a velocity pickup, other than their construction, is that the accelerometer functions based on its natural frequency and therefore can provide a sensing for a wide range of frequencies (less than 1 Hz to greater than 20,000 Hz). This wide range is due to its sensitivity, which can be a limitation as environment conditions, such as temperature, may have an

effect on the signal generated from the sensor. An accelerometer comes in two configurations, compression or shear; with the shear type accelerometer being less affected by thermal radiation than the compression type design.

a) Compression Type Accelerometer   b) Shear Type Accelerometer
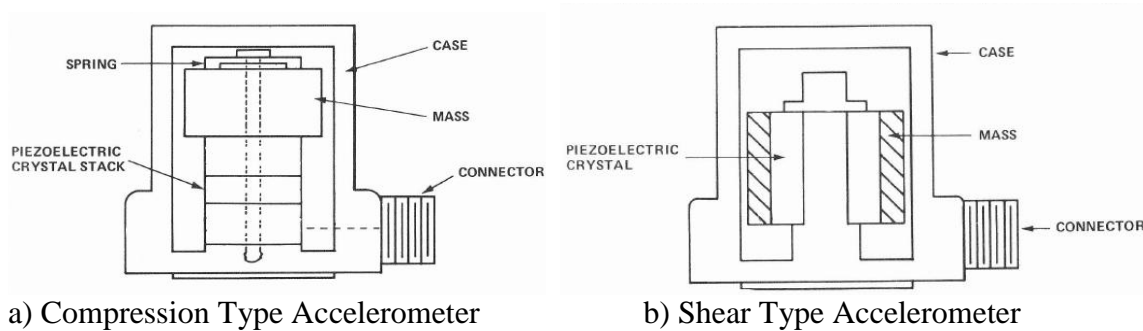
Figure 25: Accelerometer Diagrams [54].

A major problem with accelerometers in vibration analysis is their low signal to noise ratio. This could negatively affect the vibration diagnosis, especially in situations where vibration from other equipment is occurring simultaneously [55].

Table 2 allows for easy comparison as to the ranges of each sensor. As frequency increases, acceleration increases, but displacement decreases. Therefore, for low frequencies (generally at or below the equipment's operating speed) displacement or velocity should be used. However, if the sensor available is an accelerometer, the acceleration can be integrated to find the velocity or displacement.

Table 2: Vibration Sensor Frequency Ranges.

Characteristic	Minimum Frequency Range [Hz]	Maximum Frequency Range [Hz]
Displacement	1,000	1,500
Velocity	10	1,500
Acceleration	< 1	$> 20,000$

Vibration sensors are a good investment, as the information provided is detailed, however, in the case of bearings, the bearing is already in a failure mode if vibration is

occurring. There are other sensors that can be employed to determine bearing condition before there is a vibration problem. These are discussed in the next section.

6.2 Ultrasonic and Acoustic Emission Sensors

Sensors with the ability to detect bearing damage before any noticeable vibration can be detected work on ultrasonic sound frequencies due to acoustic emissions (AE). Ultrasound frequencies are those that are above the human ability to hear, typically greater than 20 kHz. A sensor that is labeled as "ultrasonic" focuses on a frequency range between 20 kHz to 100 kHz. This is not to be confused with an AE sensor, which typically operates in the 100 kHz to 1 MHz frequency range [56].

These sensors measure the amount of ultrasonic noise created when metal degrades. Thus, it is the best tool for discovering the earliest stages of bearing issues. This can be even on the microscopic level where overall vibration is not detectable yet. The technology can be used for many applications, such as [54]:

- Lack of Lubrication

- Bearing Defects

- Cavitation

- Electrical Arching

- And many others

As bearing elements interact with other bearing elements, such as a ball and raceway in a ball bearing, energy, in the form of sound, is released. As a localized defect starts to form, this interaction between bearing components causes a sudden change in the contact stresses at the elements' interface. This causes a short duration pulse to be

47

emitted, which is known as a shock pulse. A piezoelectric transducer with an ultrasonic resonant frequency can be used to identify these pulses. The pulse causes a damped oscillation of the piezoelectric material to resonate at its natural frequency, for which the maximum value of the oscillation is taken [52]. This provides a method for determining bearing condition and is the principle in which the ultrasonic and AE contact sensors are based [57].

6.2.1 Ultrasonic Sensor

The main component of this sensor is a heterodyne circuit that takes an ultrasonic signal, detected by the piezoelectric transducer, and converts it into an audible signal via a demodulator. This audible signal is less than 20 kHz which gives a person the ability to actually listen to a bearing as it turns over. The signal is then sent through a converter to provide a singular RMS value, in decibels, which pertains to the bearing condition [58], [56]. A flowchart of the sensor's inner workings can be seen in Figure 26.
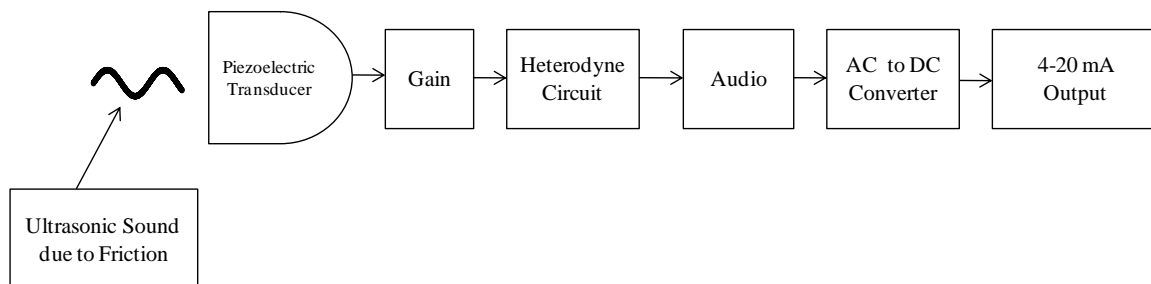
Figure 26: Flowchart for how an Ultrasonic Sensor Works.

This sensor provides many advantages when it comes to spindle monitoring. One of the advantages of this technology, with respect to bearings, is that initial stages of bearing failure can be detected long before a vibration measurement or temperature measurement would detect a problem [59]. The "normal" condition sound signature

starts to change by an increase in sound intensity, therefore causing the measured decibel level to be higher [58]. Another advantage of ultrasound is that is has a high signal to noise ratio for detecting a failure [56], [60] and the sensors work very well on slow speed bearings [58].

The sensor has a unique advantage/disadvantage combination. The measuring point for an ultrasonic contact sensor should be directly on top of the bearing with a minimum number of interfaces between the two components. This is needed due to the short wavelength of the ultrasonic waves having difficulty penetrating more than two mediums [61]. Therefore, sensor placement is limited, especially where space requirements can be an issue. However, using a sensor only being excited by ultrasonic sound allows for the environmental noise and vibrations coming from a machine's other components (fans, pumps, or even another machine) to be filtered out. This allows for the sensor to measure only the bearing sound. The same goes for an AE sensor.

6.2.2 Acoustic Emission Sensor

The phenomenon of AE originates from the creation of a transient elastic wave. This wave is caused by a rapid release of strain energy in solid materials due to mechanical or thermal stresses. The main sources for AE generation come from the creation of or the propagation of cracks caused by plastic deformation of the material [62].

AE sensors use the phenomenon known as ring down counts, the number of times the signal amplitude exceeds the threshold level within a given timeframe, and provides a number value for the bearing condition. As with the "ultrasonic sensors," the advantage

of using an AE sensor over a vibration sensor, such as an accelerometer, is that the AE sensor can detect micro and sub-surface cracks in a material, whereas the vibration sensor can detect the material failure once the crack has already appeared on the material's outer surface [52]. Yoshioka and Fujiwara concluded that AE is superior when compared to vibration in detecting bearing fatigue and ultimately failure [63]. However, one limitation of an AE sensor, as realized by Choudhury and Tandon [62], is that as the size of the bearing defect increases, an AE sensor is unable to provide the additional information needed to clarify the extent of bearing damage.

A figure detailing this sensor's function or construction for this kind of sensor could not be found as this is an emerging technology.

6.3 Spindle Monitoring Measurement and Analysis Methods

As far as the order of the measurement methods is concerned, it makes more sense logically to discuss the way spindle condition is determined through ultrasonics first as these sensors provide the knowledge of a bearing problem before one exists and then follow up with vibration measurements. This is the same procedure that is used in the monitoring system discussed in the next chapter. Therefore, ultrasonics will be discussed first.

6.3.1 Ultrasonic Measurements

Mathew and Alfredson found that if a bearing reading, determined by shock pulses, is within the range of 0-20 dB the bearing is considered to be in a good operating condition, where 0 dB would be considered the baseline. A reading between 20-35 dB shows that the bearing is starting to degrade and a reading between 35-50 dB signifies a

bearing in a bad operating condition. Any measurement over 50 dB would result in a catastrophic failure soon after the 50 dB level is reached [64].

NASA bearing research agrees with these findings. One study performed determined that a bearing defect can provide an ultrasonic level that is 12 to 50 dB higher than the same bearing with no defect for the same fault frequency [65]. Therefore, failure modes based on a decibel level given by an ultrasonic sensor reading can be defined. These levels are used to describe the bearing condition [66]:

Baseline:	0 dB
Lubrication Failure:	8 dB
Beginning Stages of Failure:	16 dB
Catastrophic Failure Eminent:	35 to 50 dB

Where lubrication failure refers to microscopic surface damage to the balls and races and beginning stages of failure refers to macroscopic surface damage. The damage for the latter of the two failure modes is able to be seen with the human eye. To put these dB levels into perspective, a sound multiplication factor can be computed for each level. These have been provided in Table 3. When the bearing is new (with no defects), its normal operating condition provides a multiplication factor of 1 because this is the datum where an increase will be measured from. At 8 dB from baseline, the bearing is producing sound that is 2.5 times louder than its normal operating baseline condition. Once the bearing reaches a catastrophic decibel level, it is producing sound that is 56 to 316 times louder than it was when the bearing was new. For further explanation, more information on decibel scaling can be found in Appendix N.

Table 3: Multiplication Factors based on Decibel Level.

Failure Mode	Decibel Level [dB]	Multiplication Factor
Baseline	0	1x
Lubrication Failure	8	2.5x
Beginning Stages of Failure	16	6.3x
Catastrophic Failure Eminent	35 to 50	56.2x to 316x

Using ultrasonics will not provide the end-all-be-all to condition monitoring, despite their extraordinary capability and early detection of bearing problems. For spindle monitoring, if other items are of interest (ie: not bearings), it is important that vibration be used as well for maximum effectiveness for a condition monitoring program [58].

6.3.2 Vibration Measurements

Vibration is considered one of the best measurements to judge low frequency dynamic conditions such as mechanical looseness, imbalance, misalignment, or excessive bearing wear [53]. It can be measured in one or more of the following directions: horizontal, vertical, or axial. Each direction is represented in Figure 27.
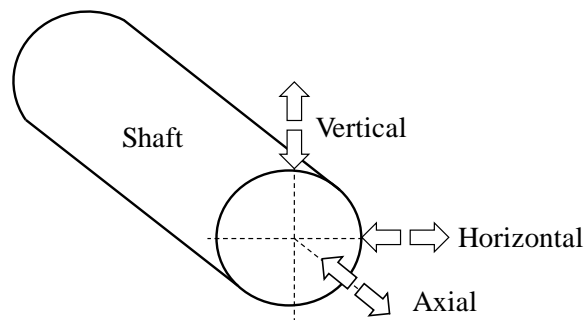
Figure 27: Directions of Movement in which Vibration is Measured.

The horizontal direction typically shows more vibration than the other directions because the machine is more flexible along this axis. The vertical direction tends to show less vibration because the sensor has to overcome gravity. Both the horizontal and

vertical planes would show if the shaft has balance issues as well as bearing problems. The axial direction allows for misalignment or bent shaft problems to be identified [53].

There are a variety of ways to measure vibration with respect to bearing failures. They include overall vibration, frequency spectrum, and envelope detection. Utilization of the frequency spectrum is the most widely used approach for bearing damage detection as well as many other issues, such as imbalance and alignment [56], [53].

6.3.2.1 Overall Vibration

The overall vibration measurement is the total amount of vibration energy measured within a frequency range [53]. It is the simplest monitoring method of all of the vibration measurements [57]. This measurement would be taken and compared to the baseline value of the machine to indicate its current health. This is similar to the rise in decibel level from 0 dB with the ultrasonic sensor.

The best way to visualize this is with a sinusoidal curve, shown in Figure 28. An overall vibration value for the waveform can be calculated several different ways. The average, root mean squared (RMS), or peak value on the positive side of the waveform can be calculated to represent the overall vibration. A peak to peak value can also be used to represent the overall vibration. However, when comparing a measurement to the baseline reading, it is important to ensure the measurements were calculated the same way.
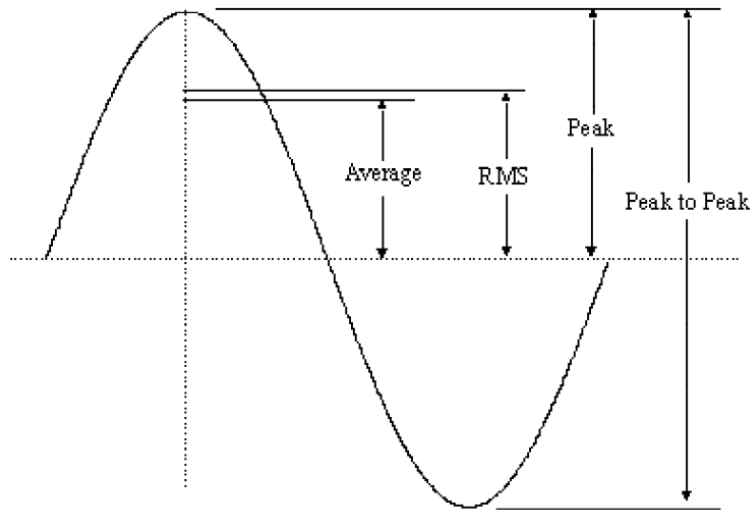
Figure 28: Example of a Vibration Waveform [53].

6.3.2.2 Frequency Spectrum

Frequency analysis is a different method of investigating the vibration. It provides much more information as to what is causing the vibration when compared to the overall vibration method. It works by breaking down a time series waveform and provides the magnitudes of the different frequencies that make up the waveform [53]. A fast Fourier transform (FFT) is used to perform this operation. Figure 29 graphically illustrates the function of an FFT. More information on how the FFT algorithm works can be found in Appendix O.
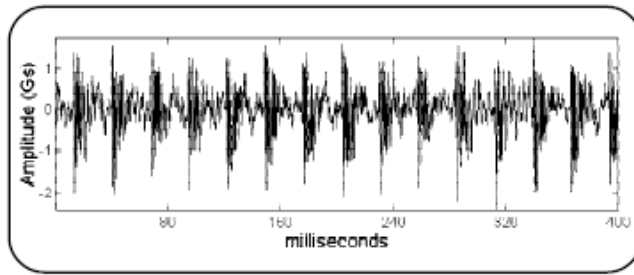
Time Domain
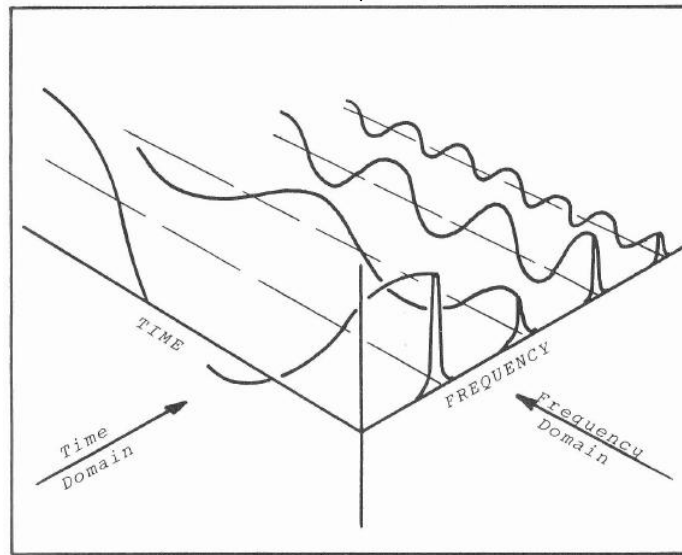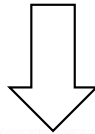
FFT
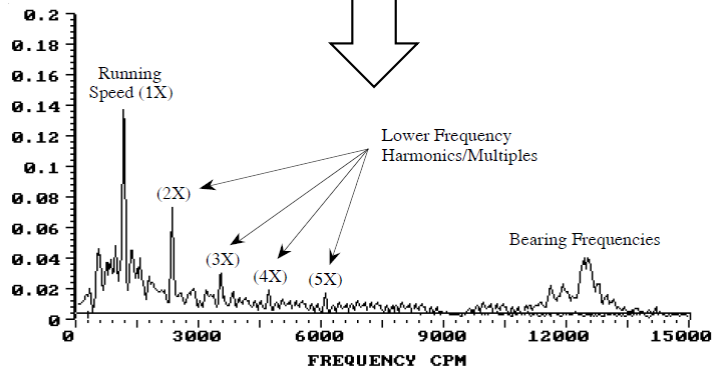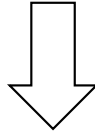
Frequency Domain

Figure 29: FFT Process Illustration (adopted from [53], [54]).

Once the frequency spectrum is obtained, shaft issues such as imbalance, misalignment, or a bent shaft can be determined by the way the spectrum looks at specific frequencies. Bearing problems can also be identified. Each bearing component has its own rotational frequency characteristic and can be seen in the frequency spectrum. A bearing defect increases the vibrational energy associated with that defect, which increases the magnitude of the characteristic frequency [52]. The frequency spectrum allows for a defect to be easily identified, as long as the bearing defect frequencies are known.

The defect frequencies are based on the bearing components' geometry and configuration. All that is needed for these calculations are the rolling element diameter, the number of rolling elements, the pitch diameter, and the contact angle. The rotational speed of the shaft must also be identified as the defect frequencies proportional to the running speed. The typical defect frequency calculations are listed below [53]:

$$FTF = \frac{RPM}{2*60}\left(1 - \frac{B_d}{P_d}\cos\theta\right) \tag{6}$$

$$BPFO = \frac{N*RPM}{2*60}\left(1 - \frac{B_d}{P_d}\cos\theta\right) \tag{7}$$

$$BPF = \frac{N*RPM}{2*60}\left(1 - \left(\frac{B_d}{P_d}\cos\theta\right)^2\right) \tag{8}$$

$$BPFI = \frac{N*RPM}{2*60}\left(1 + \frac{B_d}{P_d}\cos\theta\right) \tag{9}$$
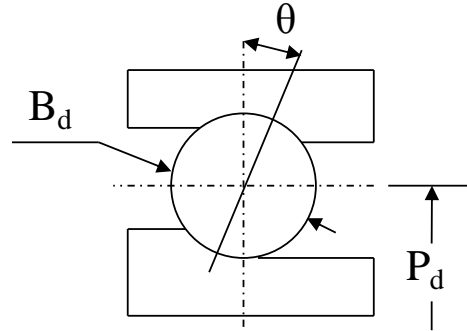
Figure 30: Bearing Dimensions.

Table 4: Bearing Defect Frequency Equation Terms.

Acronym/Parameter	Description
B_d	Ball Diameter
N	Number of Balls
P_d	Pitch Diameter
RPM	Running Speed
θ	Contact Angle
FTF	Fundamental Train Frequency (aka Cage Frequency)
BPFO	Ball Pass Frequency for the Outer Race
BPF	Ball Pass Frequency (aka Ball Spin Frequency)
BPFI	Ball Pass Frequency for the Inner Race

Please note that all of the equations provide the fault frequencies in Hertz as well as θ needs to be in radians. It should also be noted that the calculated values for the bearing fault frequencies may be slightly different as skidding or slipping of the rolling elements may occur [67]. Defects on the inner race are more difficult to detect than those on the outer race, however, defects on the outer race are more easily detectable in comparison to a rolling element defect [55], [56]. It is also important to understand that the amplitude of fault frequency for the good bearing only increases slightly with an increase in rotational speed and does not vary with increasing load. The bad bearing's fault amplitude was found to increase significantly with an increase in the load experienced [65].

6.3.2.3 Enveloping

An enveloping of the frequency spectrum can be performed to allow for the bearing faults to be more easily identified. This technique filters out the low frequencies associated with the rotational vibrations and allows for the enhancement of repetitive defects, such as a spall fracture, to be identified. Sometimes, the vibration signature of these defects gets lost in the overall spectrum because the energy associated with this vibration is so small and is on the same order of magnitude as the structural vibration noise, hence the reason for enveloping [53].

Enveloping is done by using a bandpass filter, centered around the defect frequency. The signal is demodulated by an envelope detector which rectifies and then smoothes the signal. Then the spectrum for the signal is obtained, allowing for the fault frequencies to be identified [57], [68].

At this point, it still may not be clear on how all of this information can be packaged on a CNC machine. More importantly, how can all of this information be made clear to an operator that may not understand the multiple concepts previously discussed? The next chapter addresses how spindle monitoring can be done efficiently, providing even the operator with the knowledge on the condition of the spindle.

CHAPTER 7: DEVELOPED CBM SYSTEM IN DETAIL

7.1 System Overview

The developed CBM system has been designed to be utilized on an Okuma machine with a P-Control. It has been given the name *Okuma Spindle Monitor*. The system is comprised of sensors, data acquisition devices, and interactive software to monitor spindle health. It is a modular, diagnostic, rule based system that has been designed to supply a single quantifiable number for bearing and spindle condition. The sensors are all non-invasive, allowing for the machine's major components to be kept the way they are currently designed. The only items that may need to be modified are the sheet metal covers that surround the spindle.

The software program, composed in the VB.NET framework, allows the user to choose how the monitoring is performed: in a test mode or as an in-process measurement. Regardless of which mode selected, the user will be able to see the machine's current spindle state as well as see the past data on the spindle via history trending. If an issue is indicated, an accessory hardware and software application allows for a "deep dive" to be performed, thus identifying if the issue lies within the spindle or if it is due to some other phenomenon.

The total system cost comes to $2,342.05. However, this cost can be broken up into main hardware and accessory hardware categories. For the main hardware, the system only costs $1,102.58. The additional accessory hardware adds up to an additional $1,239.47 and is discussed in Sections 7.2.3 and 7.2.4.

7.2 <u>Hardware Requirements</u>

7.2.1 Sensors

There were a variety of sensors that had the potential to be utilized within this system however only two of them were selected for practicality reasons: an ultrasonic sensor and an accelerometer. These can be seen in Figure 31. The main sensor of interest to be employed in this system is the Ultra-Trak 750 ultrasonic sensor by UE Systems Inc. As an additional follow up, an IFM Efector accelerometer and vibration module can be used. The main reason that an ultrasonic sensor was selected over the traditional vibration sensors is due to the fact that that ultrasonic technology can detect bearing problems much earlier than vibration and temperature methods [59]. Another advantage of a non-vibration based bearing condition sensor is that nearby vibrations from other equipment on or nearby the machine do not influence the sensor's reading. This is due to the short wavelength of the propagating ultrasonic acoustic waves only traveling several inches before stopping.
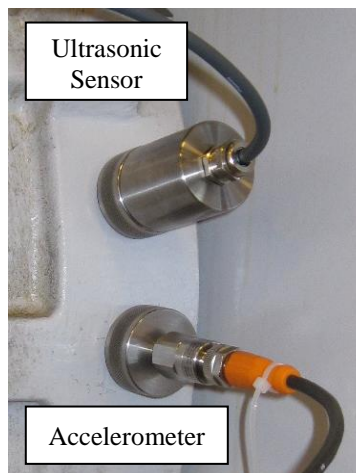
Figure 31: Sensors Employed.

The ultrasonic sensor "listens" to the bearings as it is a transducer that is excited by ultrasonic frequencies (> 20 kHz) produced by the bearing as it rotates. It outputs a 4-20 mA signal that is linearly proportional to a rise of 40 dB above the baseline for the spindle. However, the sensor has a range of $0 - 120$ dB. Figure 32 puts this into perspective for a better understanding. The sensor's sensitivity is adjusted so that the low end of the sensor window is at the baseline for the bearing condition. This adjustment allows the window to be shifted either up or down the decibel range (indicated by the arrows). Once set, the sensor monitors an ultrasonic sound increase of 40 dB from the set baseline.
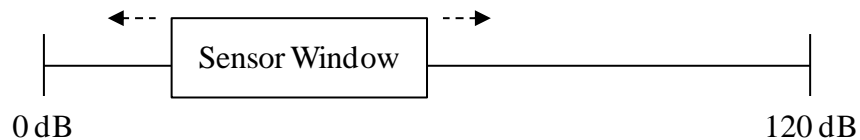
Figure 32: Ultra-Trak 750 Windowing.

Accelerometers were chosen to be used in this system as they provide the maximum benefits for vibration measurements. Attaching a non-contact displacement probe would be too obtrusive, as many design changes would have to be made to the spindle. Velocity pickups for this application where difficult to find, and thus not used. Accelerometers have a wide dynamic range and the signal can be integrated to get velocity, if needed.

The accelerometer used for this system like any typical off-the-shelf accelerometer that can be purchased today, however it can only be used with its respective DAQ device due to its proprietary interfacing. It is responsible for measuring the amount of vibration produced by the spindle and bearing degradation. The particular

accelerometer used is capacitance based and is capable of measuring between ± 25 g's. It is to be used in conjunction with an IFM Efector vibration module, an industrial vibration monitoring system.

7.2.2 Data Acquisition System

Figure 33 shows an overview of the hardware used in the development and testing of this system. It is mainly comprised of a data acquisition programmable logic controller (PLC), a 24 volt power supply, an Ethernet bus hub, as well as the optional IFM Efector vibration module and ultrasonic audio amplifier. A breakdown of each component and its respective cost can be found in Appendix B.
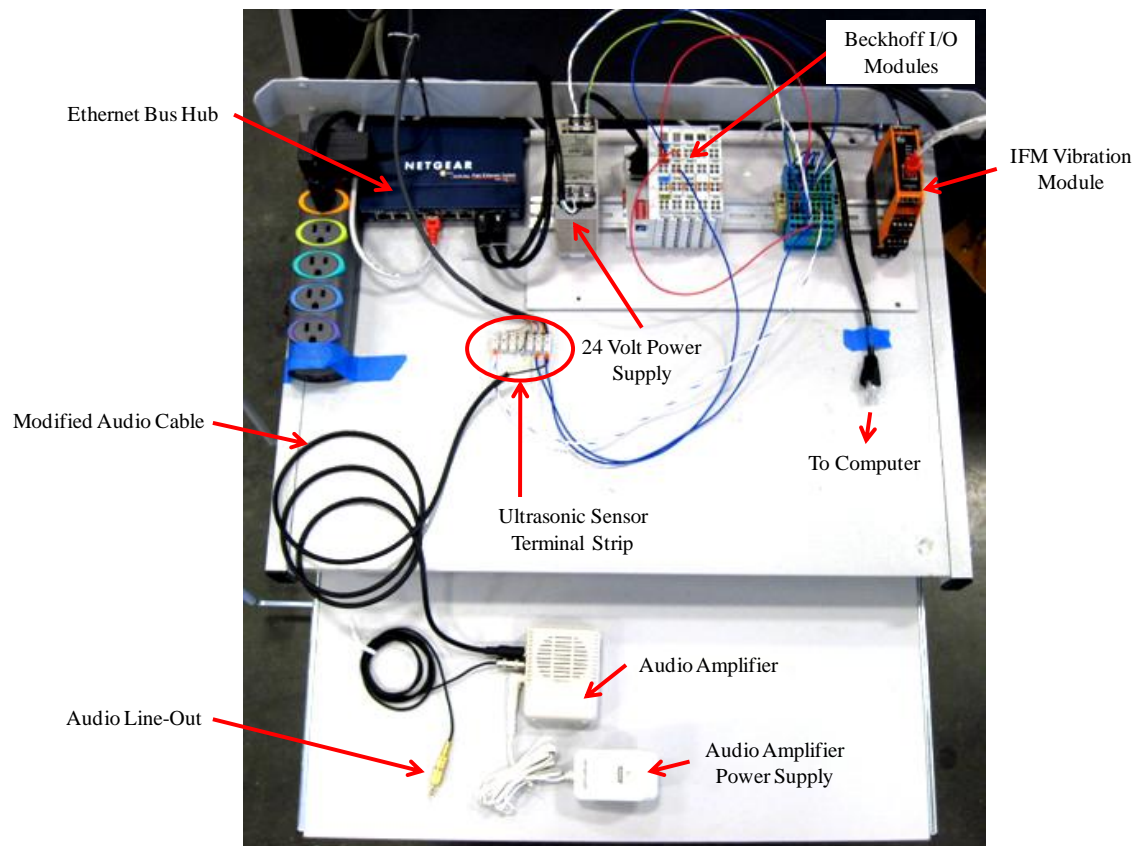
Figure 33: Hardware Layout During System Development.

The PLC is the "brain" of the system, allowing for information to be transferred to a computer for further signal processing. It has modules that can be added on or removed from it, allowing it to be quite versatile. For this application, a Beckhoff BC9050 PLC (non-real time controller) was used. This PLC is part of the TwinCat OAC system discussed in Chapter 4. The additional modules required are the KL3152 (4-20 mA analog current input) and the KL9010 (End Terminal). These can be seen in Figure 34. The KL3152 is a two channel device with a resolution of 16 bits. To help reduce hardware costs, the KL3022 can be used instead as it is the 12 bit version. For the type of data being collected, a 12 bit resolution will be sufficient.

All of the Beckhoff devices are programmed via VB.NET coding to allow for the devices to communicate with the spindle monitor software application. This includes connecting to and accessing the device, the digital to analog conversion, as well as sensor calibration. The data can then be stored once acquired from the PLC. More details on how the data is used are provided in Section 7.5.
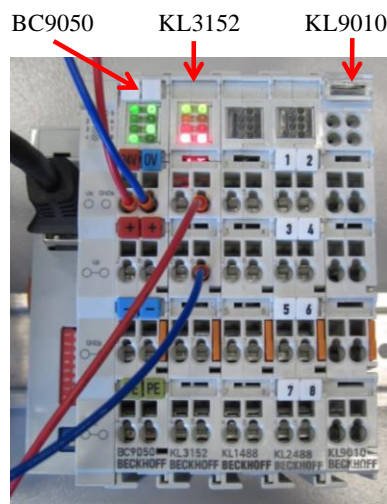
Figure 34: Required Beckhoff Devices.

7.2.3 IFM Efector Vibration Module

The IFM Efector vibration module, allows for vibration to be measured and recorded. The model used was the VSE001 (the newer model is now named VSE002). A close up picture can be seen in Figure 35. The module can support up to four accelerometers and measure acceleration, both RMS and peak levels in g's, as well as an RMS velocity in mm/s. It has a sampling rate of 100 kHz and has an exceptional frequency spectrum display (FFT chart) with zooming capabilities. This will allow for even better pinpointing of the bearing fault frequencies. The device settings are configured and set by accessing its own software program, called Octavis VES003. This software can be run on the machine control as well, as it is a Windows based program.

Figure 35: IFM Efector Vibration Module

7.2.4 Ultra-Trak 750 Accessories

Additional accessories can be added to the Ultra-Trak 750 to help it provide even more information on the bearings. The sensor has an audio output that can be fed into an amplifier and recorded as a sound clip (.WAV) on a computer. A USB sound card can be installed on the machine PC to allow for recordings to take place on the machine control.

The amplifier includes a speaker, which allows for the bearing to be heard. However, in a machine environment, the background noise makes it difficult to hear. Headphones can be used instead and the bearing can be heard in real-time as it is rotating. It is powered via a 9 V AC adapter. All components can be seen in Figure 36.

From Ultra-Trak 750

Amplifier

Power
Supply

To Soundcard
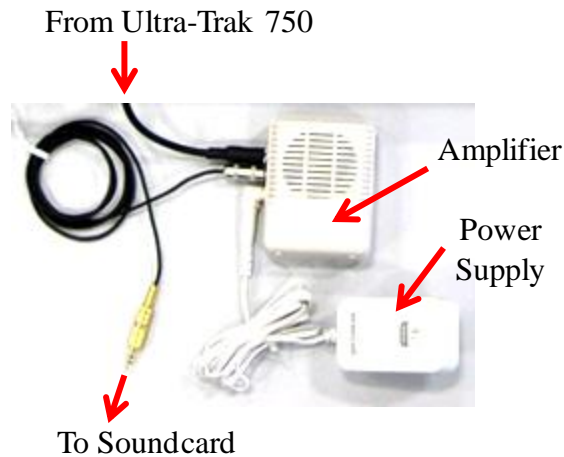
Figure 36: Ultra-Trak 750 Audio Accessories

7.3 Discussion about Open Architecture vs. Closed Architecture Devices

The hardware used in this monitoring system can be broken up into two categories: *Open Source* and *Closed Source*. The *Open Source* devices are those that allow for an open source architecture and software programming to be performed by anyone with a software background. This provides the application developer with complete control of how these devices function. The *Closed Source* devices are those that the developer has no control over device function. Figure 37 provides a system architecture to allow for better device clarification for this monitoring system. The *Closed Source* devices can be removed from the system and the monitoring system will still function the way it was intended, however certain information will not be obtainable.
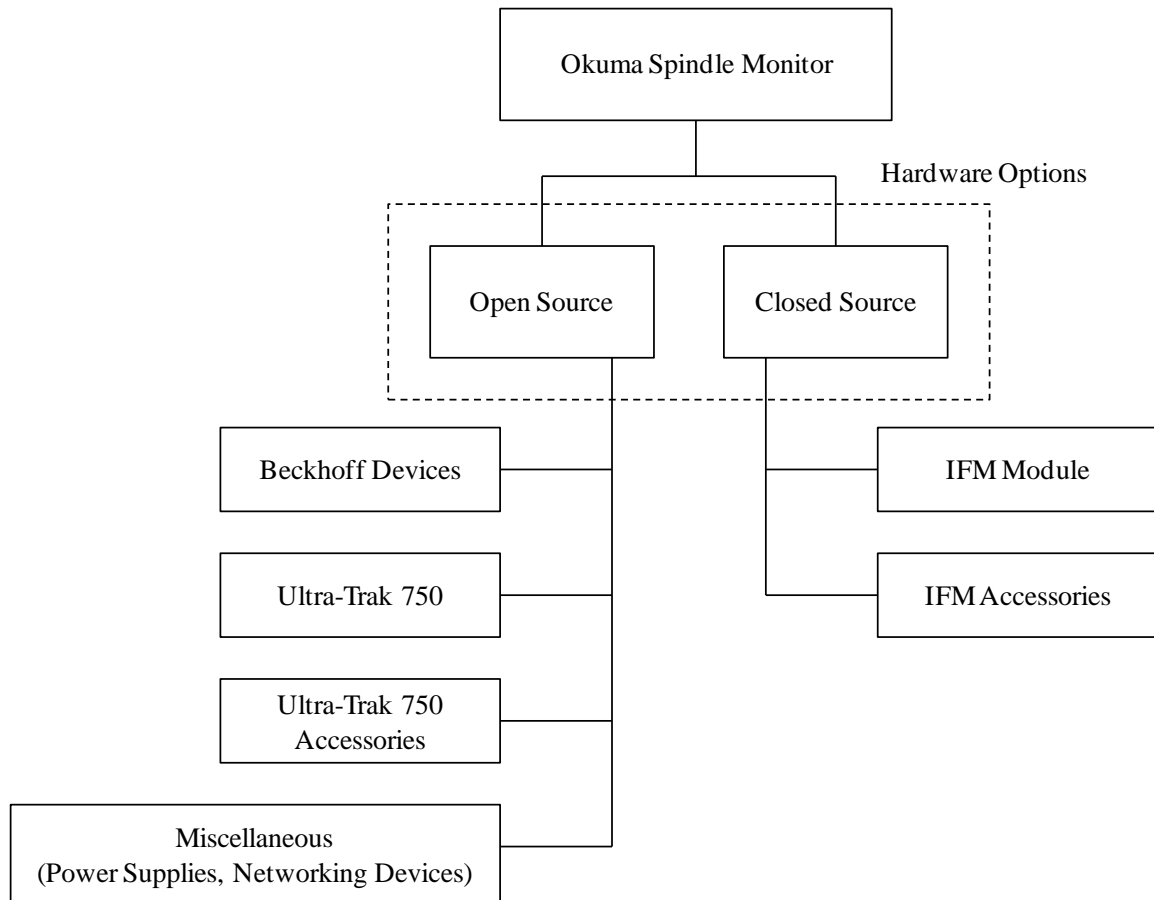
Figure 37: Visual Representation of the Open and Closed Source Hardware the System Employs.

7.3.1 Open Source Devices

The selecting of hardware (and additional software) was researched for roughly two months. In that time, many different options became available. The beauty of using the Beckhoff devices and their OAC system is that they allow for the machine to run multiple applications using the same hardware, with additional input modules being the only item needed to be added to the PLC device. Any sensor with a 4-20 mA output can be employed. This allows for a standard to be created for future predictive and preventive maintenance applications to be used on Okuma machines. As an example, the

Okuma Coolant Monitor system, discussed in Section 4.1, uses the same PLC hardware and software coding. Using the PLC device allows for software to be developed and perform the way a user expects it to, as well as provides the capability of being able to interact with the machine's API.

The ultrasonic sensor(s) are to be used in the Beckhoff data acquisition devices and are intended to be the only sensors required for the necessary information needing to be provided. Rather than trying to re-invent the wheel to create an advanced FFT algorithm for the identification of bearing fault frequencies, it made much more sense to use an available third party device (*Closed Source*). Another reason the use of a *Closed Source* device was utilized in the vibration analysis, is that the Beckhoff PLC and machine control could not handle the data acquisition sampling and calculation rates needed for an FFT frequency spectrum to be produced.

7.3.2 Closed Source Devices

The issue with using a *Closed Source* device, such as the one from IFM, is that it limited the customization and/or functionality of monitoring system that was trying to be developed, hence the reason for an OAC system. In this case, the IFM has an excellent frequency spectrum algorithm that allows the bearing frequencies to be seen very well, however, the data cannot be exported from the program; only a recording of the spectrum can be saved. The other large flaw with this device is that you can only record the overall vibration level at prescribed time intervals. There is no control to tell the unit to record when the machine is executing a certain process (ie: utilize the CNC machine's API). Therefore, one reading may be recorded during a static period and the next one during a

dynamic period (a G00 rapid command for example). These kinds of limitations were found with all of the "vibration" modules on the market today.

Most of the "vibration monitoring systems" currently available would typically be used on equipment that sees the same conditions day-in and day-out, such as a pump or compressor. In a production / machine shop environment, constant conditions may not necessarily be the case for machine tools. Alarm modules can be purchased, but what happens on a CNC machine when a very heavy cut is made and then many light cuts (or vice-versa).

A dilemma is formed: If the vibration alarm is set for the light cut, the heavy cut will set it off. If the vibration alarm is set for the heavy cut, the light cutting may not set it off (even in the event of something going wrong). Therefore, certain conditions must be in place before a measurement can be taken. The Okuma machine API allows for this to be accomplished and is implemented in the software as one of the two recording modes discussed in Section 7.5.

7.4 Sensor Mounting

Two machines were used in the prototyping of this system: an LB4000EX lathe and an MU-500VA (or MB-46VAE) vertical machining center. Sensor placement should allow for the ultrasonic sensor and accelerometer to be as close to the bearings as possible [53]. In addition, special consideration should be taken to ensure that the accelerometer is mounted in the horizontal plane (as indicated in Figure 27 of Chapter 6). Another consideration that needs to be taken into account is the ultrasonic sensor works best if there are only one or two mediums between its transducer and the bearings. All

sensors should be adhered to the spindle with epoxy for permanent mounting [53]. This will prevent the magnetic mounts from breaking free during harsh cutting conditions where the spindle experiences excessive vibration. The magnetic mounts used can be seen in Appendix F.

7.4.1 Lathe Mounting

Figure 38 shows the mounting locations for the LB4000EX. Each oval in Figure 38 indicates the bearing locations for the spindle. The ultrasonic sensor can be mounted on the cover side of the spindle, however the accelerometer will have to be relocated to the opposite side, ensuring that it is mounted in the horizontal plane as close to the bearing as possible. This is due to the accelerometer being too long, preventing the sheet metal panel from being mounted properly.

a) Spindle Front View   b) Spindle Rear View
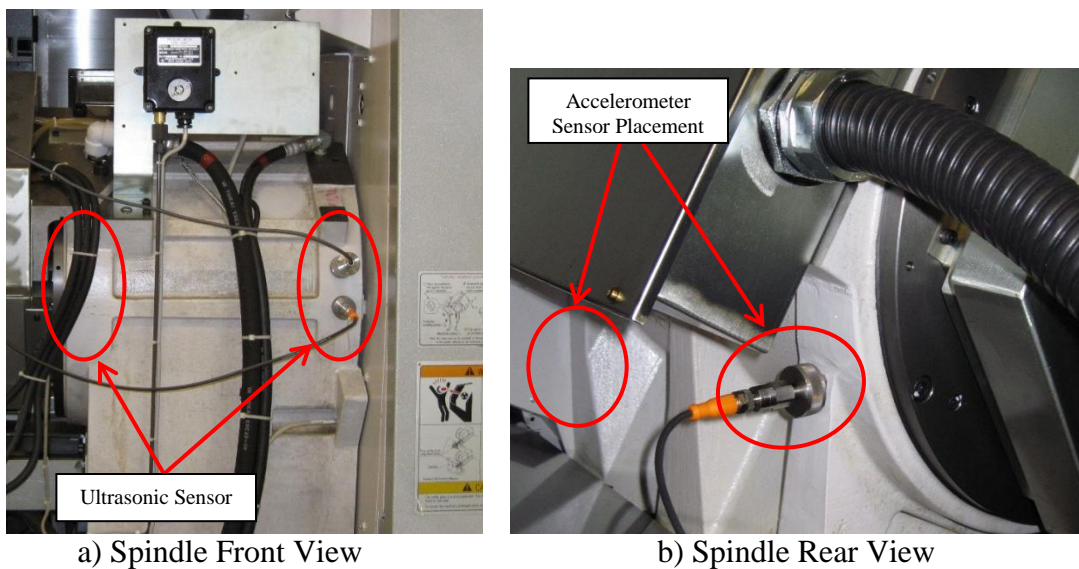
Figure 38: Sensor Placement on the LB4000EX.

On the LB4000EX, IFM accelerometer placement in the horizontal plane is difficult as there is not much room to accommodate the sensor, as shown in Figure 39.
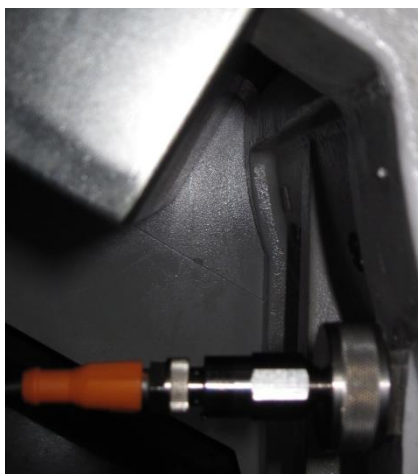
Figure 39: Insufficient Space for Horizontal Accelerometer Mounting on the LB4000EX.

However, one possibility is to mount the accelerometers vertically on the casting, as shown in Figure 40. This will still allow for a good vibration reading to be taken.

Vertical Accelerometer Sensor Placement
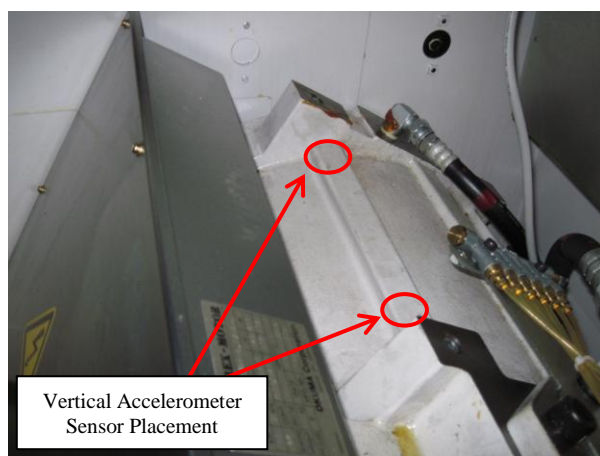
Figure 40: Vertical Accelerometer Mounting Placement on the LB4000EX.

7.4.2 Machining Center Mounting

Placement for the sensors on the machining center is not as easy as there is not much room to work with. This is mainly due to the spindle bearings being located in the nose of the spindle, where the cutting tool is held. To get the best reading, the ultrasonic sensor was mounted on the spindle flange, where the spindle attaches to the z-axis

column assembly. This is shown in Figure 41. Mounting the ultrasonic sensor on the flange provides a good material route straight to the bearings (the ultrasonic sounds can emanate from the bearings and be transferred through only one medium, metal). Placing the sensor on the black spindle cover does not provide as good of a route as it has the spindle chilling fluid behind it (as does the lathe casting).

a) Spindle Front View   b) Spindle Bottom View
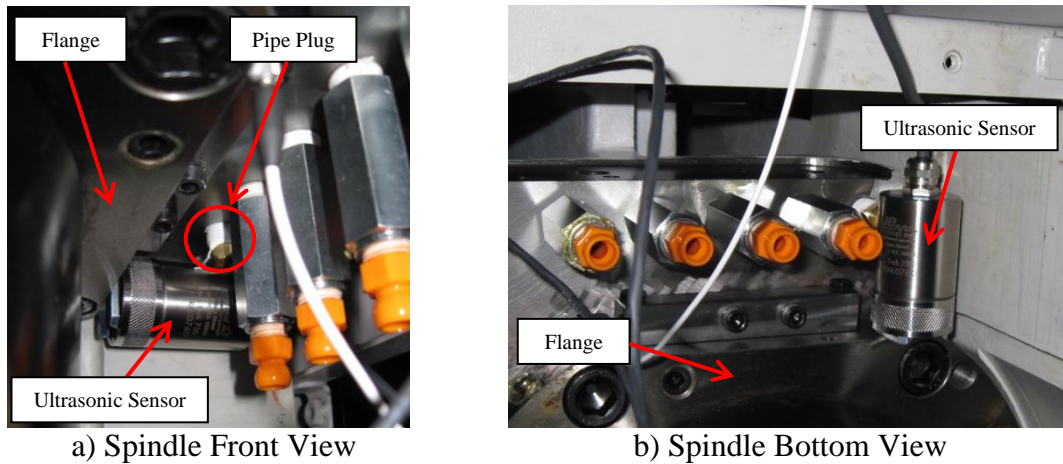
Figure 41: Ultrasonic Sensor Placement on the MU-500VA.

The last coolant nozzle was removed and plugged to ensure the upper ultrasonic sensor had a solid mounting foundation. A pipe plug was put in the nozzle's place to prevent coolant from splashing the sensor. The pipe plug was used as a mock-up piece; however, a set-screw should be used in this hole to allow for the sensor to be mounted higher on the spindle flange, preventing the bottom cover from being modified. This bottom cover is shown in Figure 42.
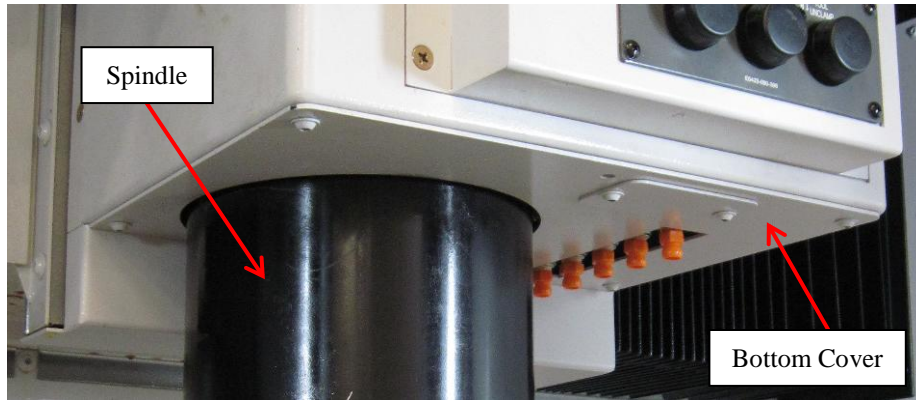
Figure 42: Bottom Cover for the MU-500VA.

If the IFM vibration module is to be used, either another coolant nozzle should be removed and the accelerometer be place on the flange, like the ultrasonic sensor, or it could be fitted in-between the coolant nozzles and mounted on the black spindle cover, as shown in Figure 43. If the latter of the two mounting methods is chosen, the bottom cover will need to sit an additional one inch lower (which would be part of the spindle monitoring options package for the commercial system).
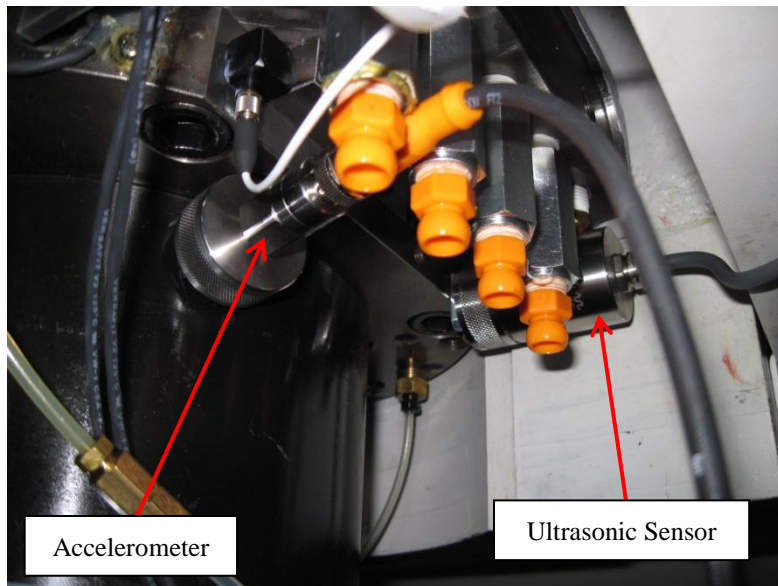
Figure 43: IFM Accelerometer Placement on the MU-500VA.

7.4.3 Mounting Concerns

After investigating all possible sensor placements, without changing the machine's design, a few concerns arise when it comes to mounting. It is suggested that epoxy be used to secure the sensors to the machine, as earlier stated, however, there is major concern with the sensors being dislodged in the event of a spindle crash (especially in a machining center). Further testing should be performed to ensure whether the sensors can survive a crash scenario. This includes being dislodged from the mounting surface as well as having the ability to still function properly.

7.5 Main Application Software

The application developed has been named *Okuma Spindle Monitor*. It was developed using Visual Studio 2010 and coded in the VB.NET language. The application serves two purposes: to provide the current spindle health of the machine as well as provide a health history. The following sections describe how to operate each part of the program.

Before the program is discussed any further, it must be made clear that the program has two distinct recording modes, *Test Mode* and *In Process Mode*. This gives the machine tool owner the ability to select how the measurements are to be performed. There are various advantages and disadvantages for each mode. These can be seen in Figure 44.

```
                    ┌─────────────────────────┐
                    │      Main Program       │
                    │  Okuma Spindle Monitor  │
                    └─────────────────────────┘
                                 │
                        ┌────────────────┐
                        │    Settings    │
                        └────────────────┘
                                 │                    Recording Mode
            ┌ ─ ─ ─ ─ ─ ─ ─ ─ ─ ─ ─ ─ ─ ─ ─ ─ ─ ─ ─ ─ ─ ─ ─ ─ ─ ┐
              ┌────────────────┐      ┌────────────────┐
            │ │   Test Mode    │      │   In Process   │             │
              │  Measurement   │      │  Measurement   │
            └ ─└────────────────┘ ─ ─ └────────────────┘─ ─ ─ ─ ─ ─ ─┘
```

Test Mode Measurement	In Process Measurement
Manual (user dependent)	Automatic (non-user dependent)
No API Utilization	API Utilization
Measurement with no machining	Measurement during machining process
Spindle under no load	Spindle under loading
Low number of variables	High number of variables
Intermittent application use	Continuous running of the application
Reduces production capacity (slightly)	Conserves production capacity

Figure 44: Recording Mode Differences.

The *Test Mode* depends on the user to operate the program, having to physically tell the machine when to take a reading. No machining would take place during this time and the spindle would be rotating under no load. For consistency, a "dummy" tool will need to be used for all readings taken. This method allows for a very low number of variables to be involved when taking this measurement, mainly the only one being the bearing condition. It should also be noted that the machine's API is not use in aiding in the acquisition of data. This mode may not be "ideal" as it relies on a human to take the measurement as well as slowing down the machine's ability to produce product, but it is the recommended method due to the low number of variables involved.

The *In Process Mode* automatically records a measurement while a cut is being performed, therefore not impeding on the machine's production capability. By accessing the API data from the machine, the program can tell if the correct spindle speed has been reached, the correct part program is loaded, as well as the correct tool is doing the cutting. Therefore, no human intervention is required. Due to this, in order for a measurement to take place, the application must be running on the machine control all of the time. This could lower the overall performance of the machine control.

The spindle would be under a considerable amount of load as it would be supporting a machining operation. This leads to a high number of variables to account for the bearing health, such as: workpiece material, tooling, feed rate, depth of cut, spindle speed, and tool wear. Testing, discussed in the next chapter, has shown that the readings are more consistent for a hard material, such as steel.

7.5.1 Spindle Status Tab

The *Spindle Status* tab is the default tab displayed on the form load. It can be seen in Figure 45. It gives the user the current status of the spindle's health by indicating the last decibel value, from the ultrasonic sensor, recorded by the program as well as the date the recording was performed. Indicators (gauges, segment displays, and status boxes) are shown for both the front and rear spindle bearings and are updated accordingly.
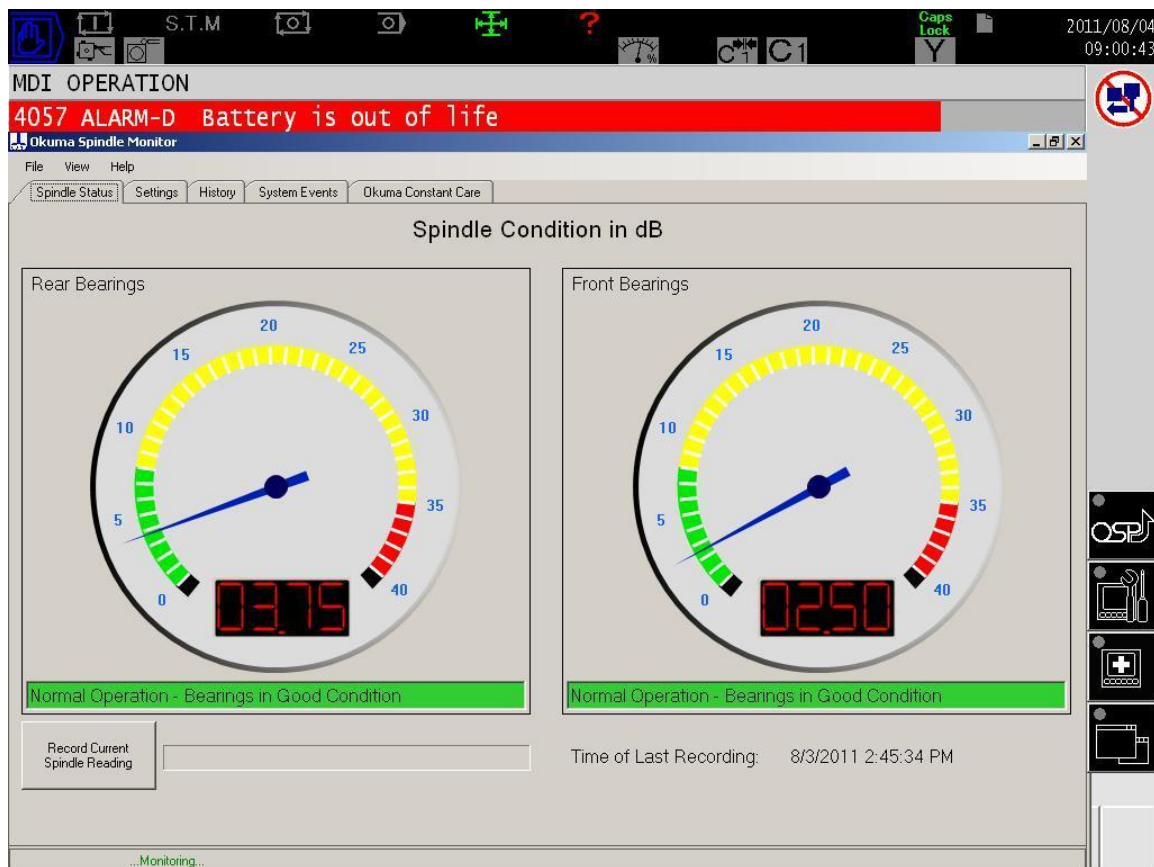
Figure 45: Spindle Status Tab.

7.5.1.1 Test Mode

　　If the program has been set to *Test Mode*, as it has been in Figure 45, the record button and progress bar will be visible. When it comes time for a spindle health recording to be performed, the user will click the record button. A spindle health check is recommended to be done at least once a month if the *Test Mode* is being used. The user will be instructed to set the spindle to the baseline speed (configured in the *Settings*) and then click OK.

Figure 46: Start Spindle Record Message Box.

　　If the speed is not set correctly, this message will appear:

Figure 47: Error Message for Incorrectly set Spindle Speed.

　　This message will continue to pop up when the OK button is pressed if the spindle speed has not been set correctly. The API is utilized here to check that the machine is at the correct spindle speed. This ensures that the same spindle speed is used for all measurements.

　　Once the recording starts, the progress bar will update as well as the gauges' needles flicker to show the current data coming into the program, as shown in Figure 48. This data is stored in an array of 100 entries and then averaged once the 100 values have

been obtained. It is this average value that is saved each time the program is told to perform a measurement. The total time involved is just over 30 seconds.

During and after completion of the measurement, a current status message for the bearings is updated under the gauges. There are 5 different messages, each one for a particular stage of the bearing's life, shown in Figure 49. These values were determined from the ultrasonic sensor manufacturer [66]. Spindle degradation should occur slowly over time, except for when the machine is crashed (slamming spindle into the table). Therefore, the static alarm messages used should suffice.
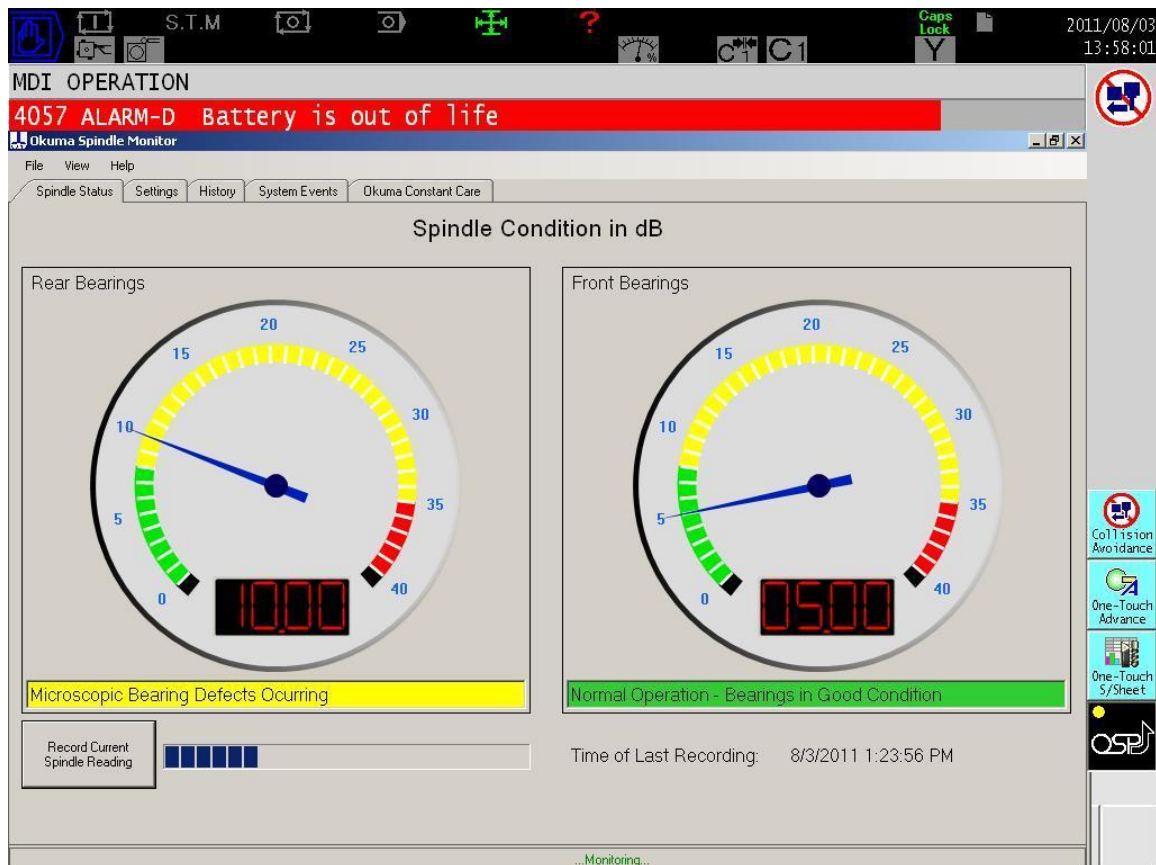
Figure 48: Data Acquisition in Test Mode.

Status Message	dB Value Range
Bearings are quieter than the baseline reading	dB Value < 0
Normal Operation - Bearings in Good Condition	dB Value < 8
Microscopic Bearing Defects Ocurring	$8 \leq$ dB Value < 16
Macroscopic Bearing Defects Ocurring	$16 \leq$ dB Value < 35
Catastrophic Bearing Failure Eminent	$35 \leq$ dB Value

Figure 49: Status Messages Based on Bearing Condition.

The spindles are sealed in both machines. The lathes have grease bearings. Therefore, once the grease no longer exists in the bearing, there is no way to supply additional lubrication. The machining centers have an air-oil lubrication system. They have a constant new supply of lubricating oil injected into the bearings. Due to different machines having different systems, to prevent operator confusion, the choice was made to list the 8 dB failure mode from "lubrication failure" to "microscopic bearing damage." The 16 dB level was also changed from "beginning stages of failure" to "macroscopic bearing damage." This allows for the same terminology to be used for both machines.

Once the data has been recorded and the database updated, the following message box will appear:

Figure 50: Spindle Recording Finished Message in Test Mode.

The label named *Time of Last Recording* in the *Spindle Status* tab is updated to allow the user to easily know when the last measurement was performed.

7.5.1.2 In Process Mode

        If the program is set for an *In Process* measurement, it will take the reading once all parameters (time since last reading, spindle speed, part program, and tool number) are all occurring in unison. The needles on the gauges will move to indicate that the measurement is being taken. However, as stated earlier, the program needs to be running on the machine's PC all of the time in order for a reading to take place.

        Threading was used in order to get the proper sequence of events to happen at the correct times. Threading allows for multiple program loops or processes to run on the computer's central processing unit simultaneously. The flowchart can be seen in Figure 51. All threads run simultaneously every 100 ms. Thread 0 checks to see if enough time has elapsed between the previous measurement taken and the current time. This interval between measurements is set in the *Settings* tab. Thread 1 ensures that the spindle speed is constant (for 2 seconds), the correct part program is loaded, and the correct tool is being used to cut. If Thread 0 and Thread 1 both output a True Boolean expression, then the data recording is allowed to begin. If the one of the three parameters changes in Thread 1 before all of the data has been collected, it the data will be erased and the thread will wait until the next time all three parameters are occurring simultaneously.
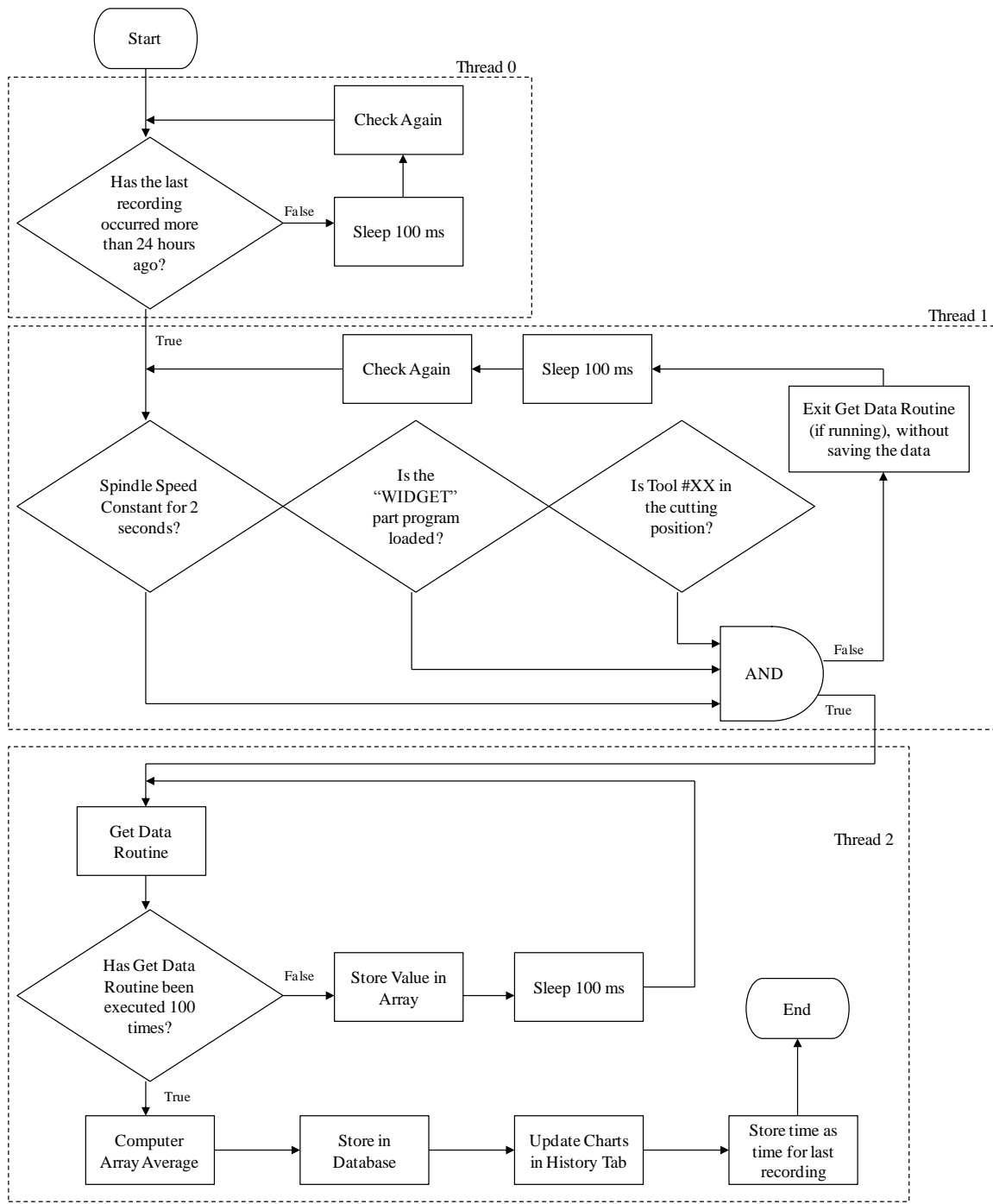
Figure 51: In Process Measurement Flowchart for Threading Execution.

In either measurement mode, if the machine tool owner has the Okuma Constant Care software, which includes the I-Gear DTU, on their machines, they can choose to have the ultrasonic dB values recorded to a common variable on the machine, shown in Figure 52, and have it uploaded on the http://okuma.igearonline.com website. This is done through the *Okuma Constant Care* tab, discussed in Section 7.5.5. This allows for remote viewing of the spindle health to be performed at any time. Figure 53 shows how the dials are updated to reflect the current values written to the machine's *Common Variables*. These web indicators are automatically refreshed every 15 seconds.

Figure 52: Data Values Written to the Common Variables.
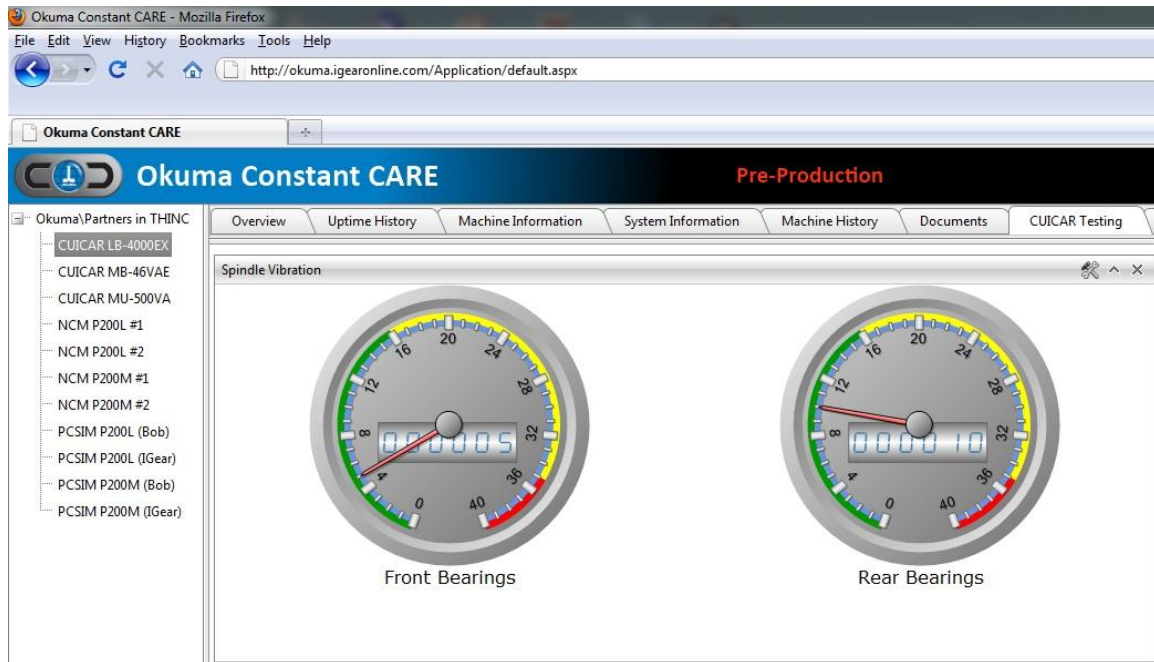
Figure 53: Remote Viewing of Spindle Health via the Internet.

The user of this web interface has the ability to be notified either via email, text, or both in case a prescribed health limit is exceeded. These limits are determined by the user through the Constant Care website. This allows the user to be notified immediately in the event that there is a spindle problem on one of his machines. The application can also be modified to perform this task as well (if need be).

7.5.2 Settings Tab

Figure 54 shows the *Settings* tab. The settings area allows the user to update the gauge ranges (green, yellow, red) based on what they would consider the critical levels to be. By setting the upper limit on a status, the lower limit on the next worse status changes to the same value. The general guidelines set in the Ultra-Trak 750 manual have been included to let the user know how each rise in dB level correlates to the bearings' health [66]. Once the alert thresholds have been set, the user should press the save

button. This will update the dials and save the settings for when the application is shutdown and reopened. The Acquisition Speed is allows for data to be pulled into the program at all times. However, only the gauges are updating. No information is saved.
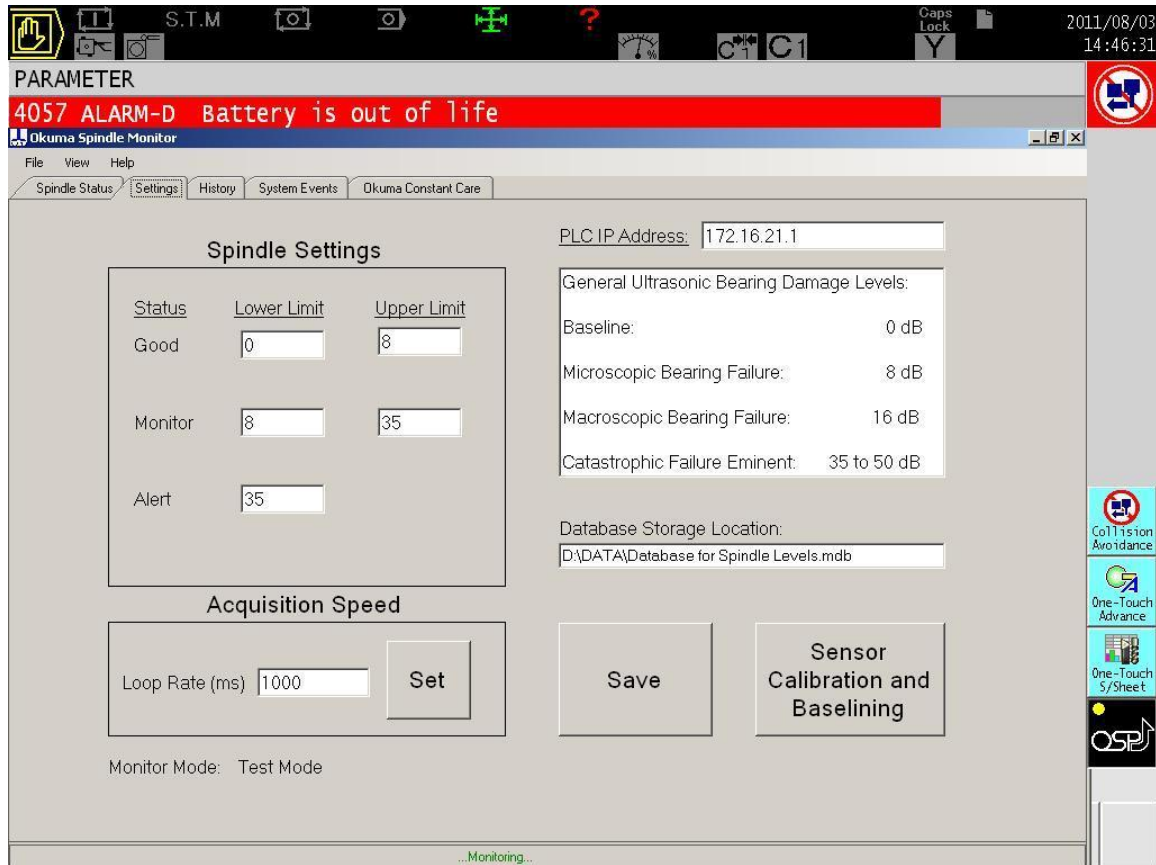
Figure 54: Settings Tab.

The current testing mode is also displayed at the bottom left of the application. To change between modes or to change the calibration settings, the user should click the *Sensor Calibration and Baselining* button. This will bring up the pop up window shown in Figure 55. The user will select a mode and then either the *Test Mode Calibration* window, Figure 56, or the *In Process Mode Calibration* window, Figure 57, will appear. However, once the sensor is adjusted for the baseline (no matter which mode), the

application needs to stay in that mode to perform the readings. The readings will not be the same for each mode. This is due to differing spindle conditions experienced with each mode.
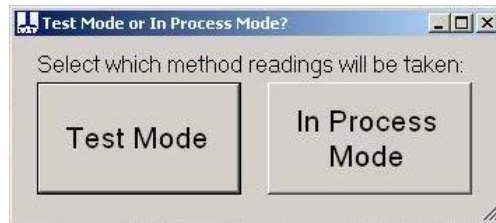
Figure 55: Test Mode or In Process Mode Selection.

If *Test Mode* is chosen, the calibration procedure is listed step by step. The user needs input the spindle speed at which they will be performing the measurements as well as the sensors' milliamp output at that speed. Once completed, the *Set Baseline* button should be clicked. This will save these values and store them in the settings.
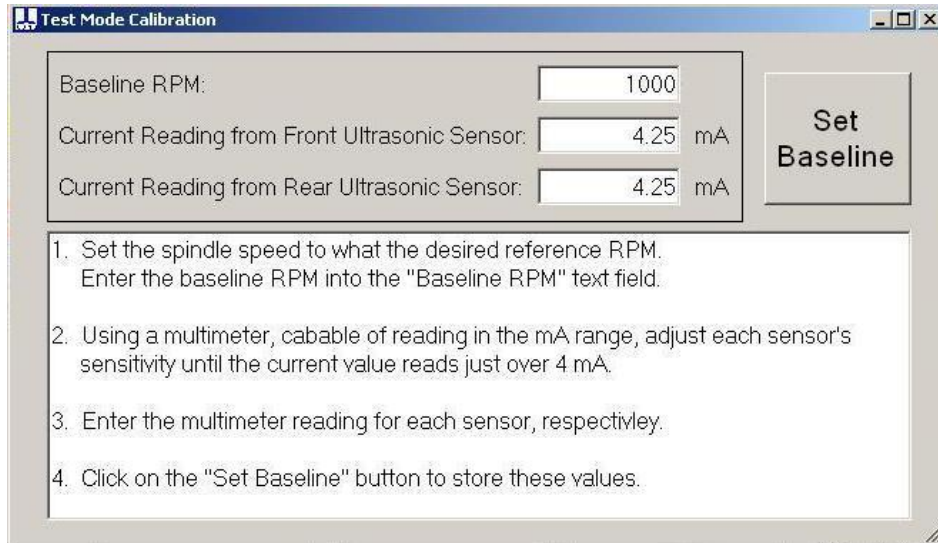
Figure 56: Test Mode Calibration Settings.

If the *In Process Mode* is chosen, the calibration procedure is also given. This procedure will take more time to set up as a part needs to be cut. The user needs to decide what part they want to take the readings on and run a sample part so that the

sensors can be adjusted properly. The user also need to include the program name and the tool number used in the baselining as well as the amount of time to record during the cut and time between recordings.
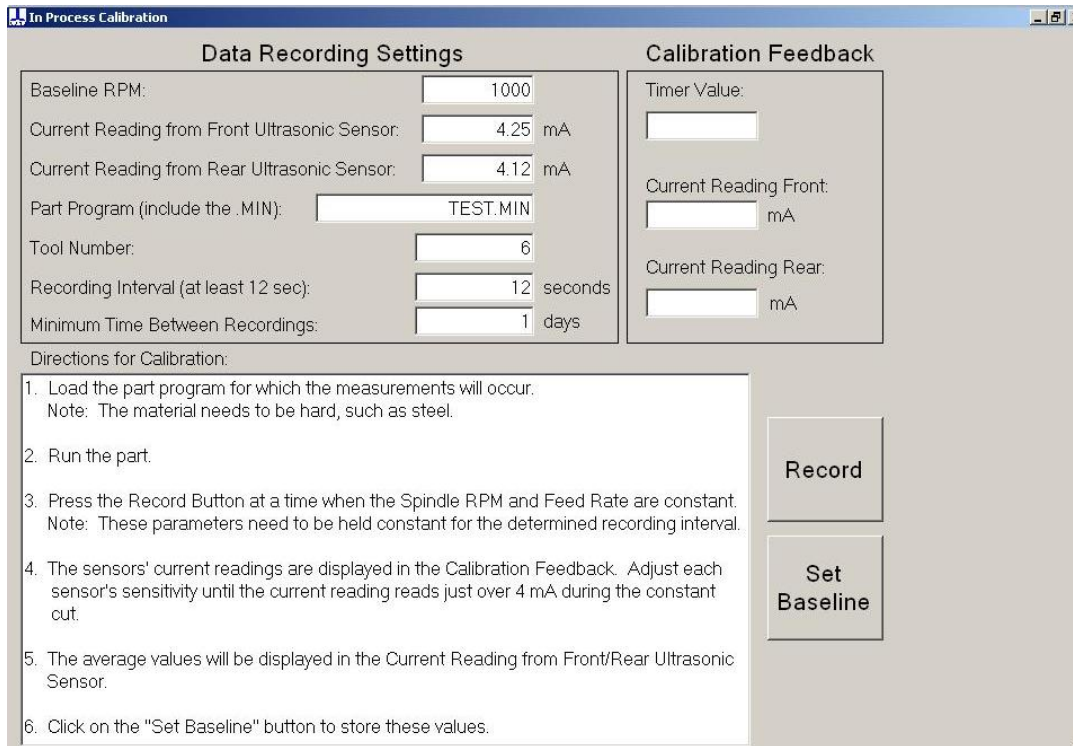
Figure 57: In Process Mode Calibration Settings.

7.5.3 History Tab

The *History* tab allows for the previously recorded data to be viewed. Each time a measurement is taken, the graphs, shown in Figure 58, are updated to reflect that new record. The user has the ability to zoom in manually on each graph by clicking the + symbol on the x-axis scroll. Additionally, DateTimePickers for the exact start and end dates to be zoomed in on has also been included. The x-axis on the charts is scaled with respect to time so that an accurate representation of the time between readings can be seen.

Two buttons have been included to help with the zooming. The first button is the *Display Data* button. This button will display only the data from the dates selected on the DateTimePickers. If the user inputs a start date that occurs after the end date, a message, shown in Figure 59, will pop up to inform the user to re-adjust the dates. If the user selects a start date that is prior to last date of recordings, the message in Figure 60 will be displayed.

The other button, named *Reset Graphs*, allows for all of the data in the database to be displayed. This resets the graphs to the same way they looked when the *History* tab was first selected.

Figure 58: History Tab.

Figure 59: Date Error Message.
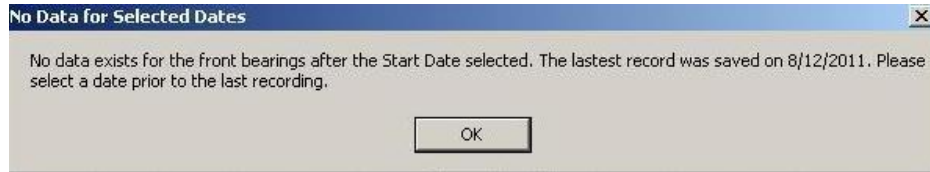
Figure 60: Date Error Message for No Data after Selected Start Date.

7.5.4 Events Tab

This section has been left blank. There is a tab named this in the *Okuma Coolant Monitor*, however, Okuma can decide what they would like to display as an "event" and can modify the program accordingly. An event from a CBM point-of-view would be when the bearing damage level passes into the next elevated state, such as going from no damage to now having microscopic damage. It could be if the difference between the previous value and current value is greater than a certain amount, indicating that the machine was crashed, etc. It could also be something along the line of the system is not getting feedback from the data acquisition system. In any case, the operator can use this tab to see the when (date and time) critical items or events have occurred within the spindle.

7.5.5 Constant Care Tab

As stated earlier, if the customer has Okuma Constant Care installed on the machine, this tab, seen in Figure 61, can be used. All that needs to be done here is that the user just needs to select the common variable location where he/she would like to

store the most recent data value and click the save button. This will save these common variable locations into the program settings. A safety feature has been built into the program to ensure the user picks the appropriate common variable number. If he/she inputs a number greater than the number of common variables the machine allows data to be written, a pop up message, shown in Figure 62, will be displayed.
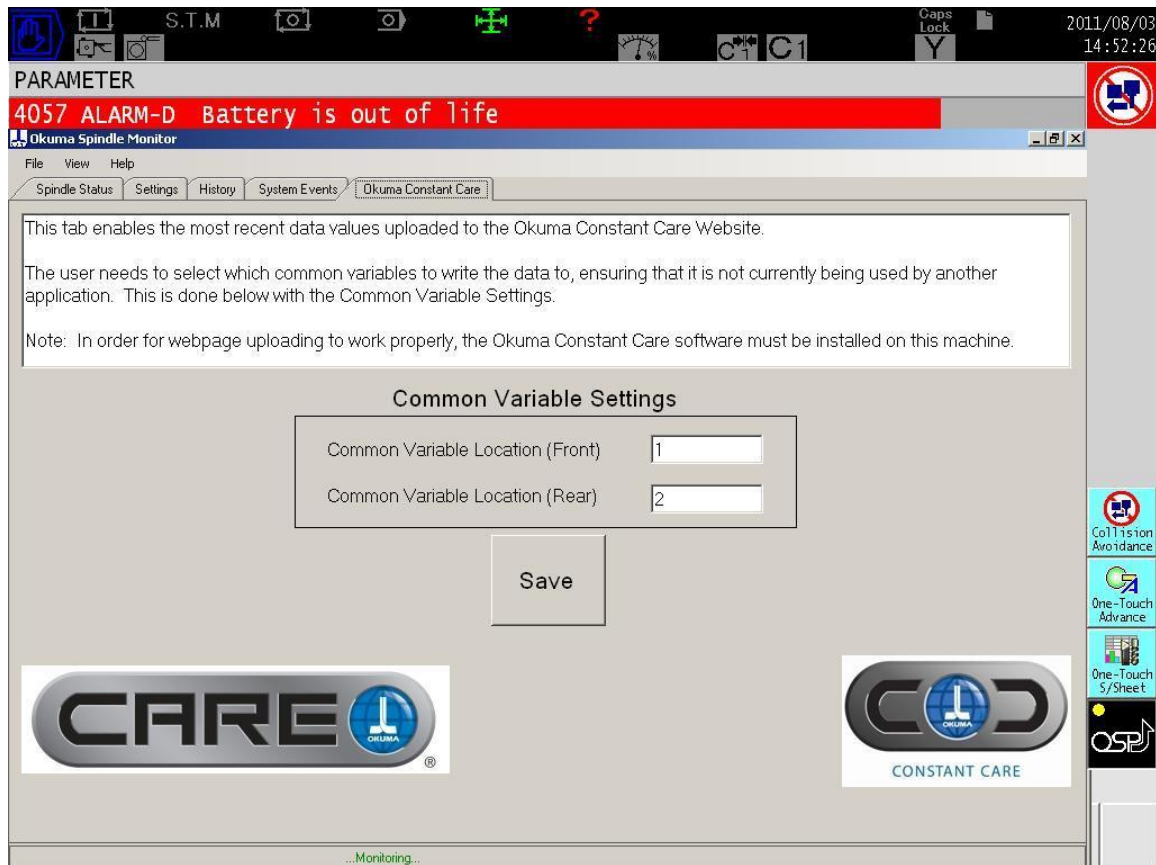
Figure 61: Constant Care Tab.

Figure 62: Common Variable Location Does Not Exist Message.

7.6 <u>Accessory IFM Software</u>

The goal of the *Okuma Spindle Monitor* software is to get a general idea of the bearing condition within a spindle. It provides singular value that is easy to understand and comprehend. If a "deeper dive" is needed, the IFM module can provide more information about the failure modes of the spindle bearings. Using this device provides an effective way to get this information without trying to go through the hassle of developing a secondary/sub system that one can get commercially. This is mainly due to this feature of the system being a bonus or additional option to the main system. If a customer is complaining about vibration in general, the IFM can also provide the information to help determine if the vibration is spindle related or coming from some other source. This is done with the frequency spectrum function of the software.

It should be noted that the IFM vibration system is open productivity and connectivity (OPC) compatible; however the only value provided to the OPC stream is the overall RMS vibration reading. This is not very useful in the application of spindle monitoring, when trying to diagnose the source of the vibration problem.
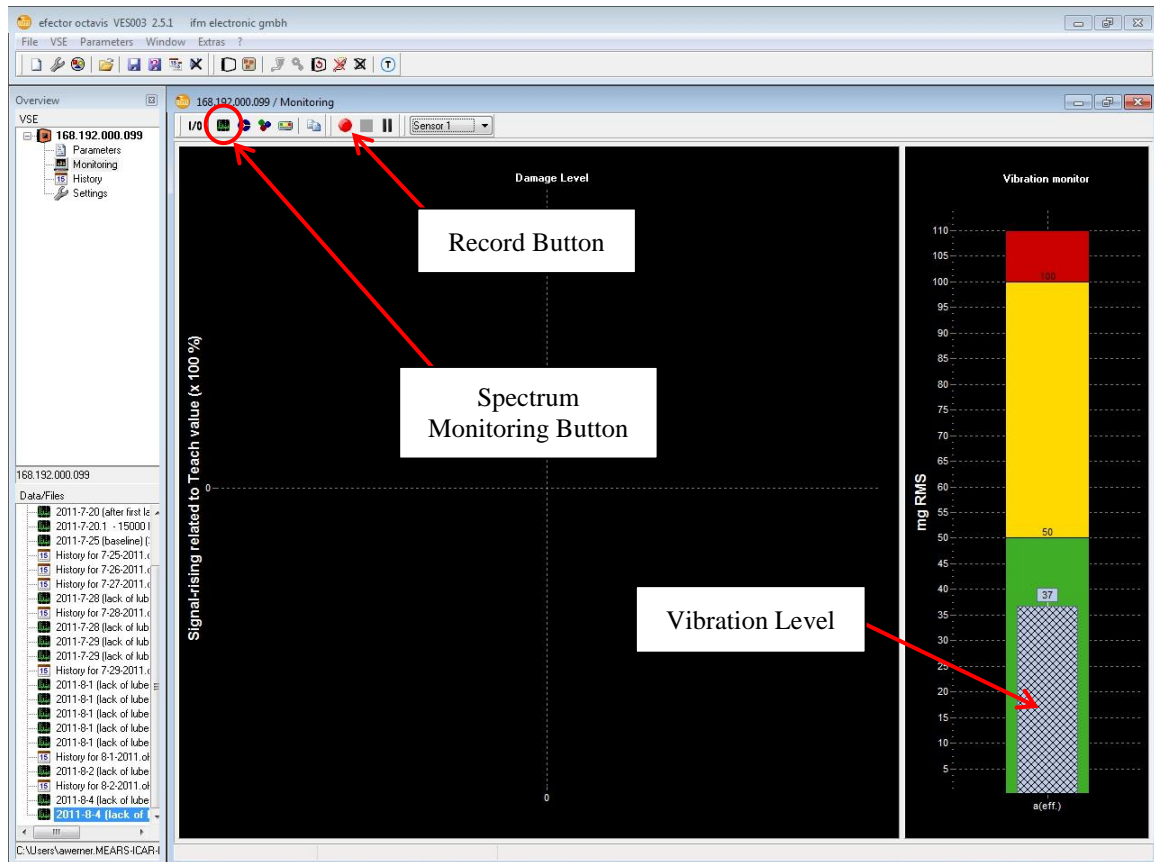
Figure 63: RMS Vibration Screen.

Figure 63 shows the main screen of the IFM software monitoring the overall vibration. By clicking the *Spectrum Monitoring* button, an FFT chart is shown and the values are updated in real time. An example can be seen in Figure 64. The *Record* button can be pressed to get a recording of the FFT. It can be saved as a .ORC file and played back in the IFM software. The nice feature about the recording is that the magnitudes for each frequency are saved and can be seen on playback. This allows the customer to save a recording and send it to Okuma. Using the same software, Okuma can take a look at the file and determine if a bearing problem exists.
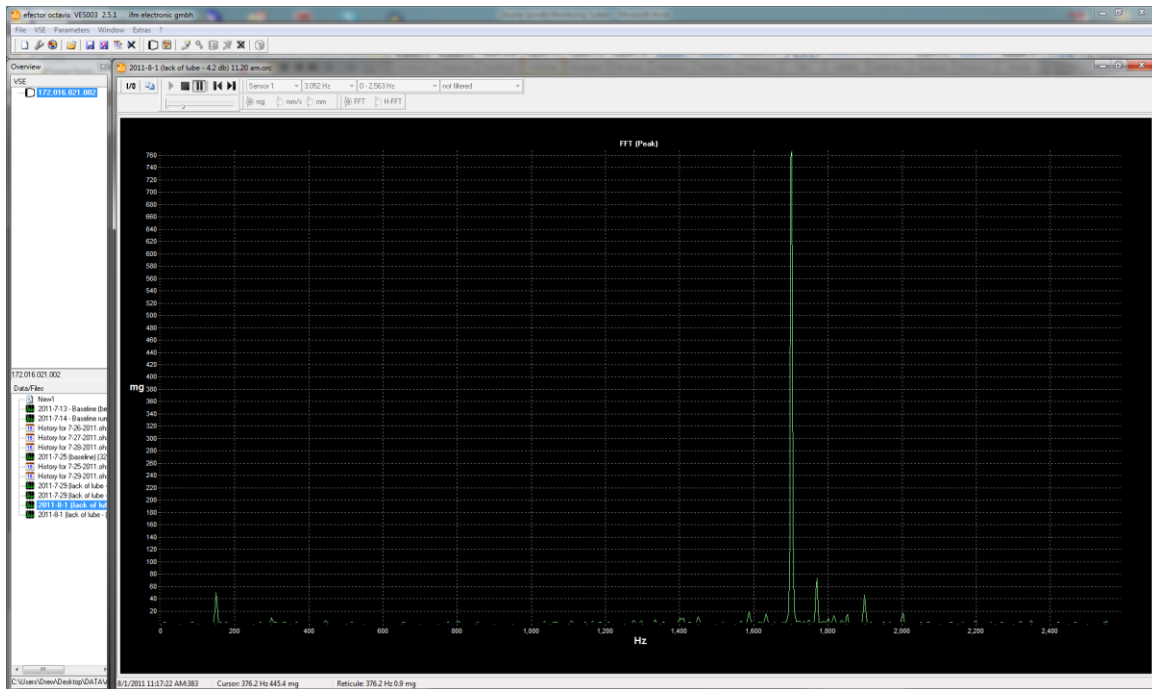
Figure 64: Example of the IFM Frequency Spectrum (FFT) Chart.

One could ask: why does this additional hardware and software cost so much if it only does what was previously described? The answer: it does much more than just provide the RMS and FFT for vibration levels, however, its other functions are not suited for CNC machine applications, such as the automatic RMS recording feature (specified in a time interval only and will not automatically record an FFT spectrum). The unit is not customizable for the functions needed to be performed. Again, this is a limitation in using a *Closed Source* device for such a system.

7.7 Software Usage Summary

In summary, the application developed to be used on the machine control will help the user/engineer to see if the spindle is experiencing bearing problems. This is based on the ultrasonic measurements taken. Depending on how close the measurement

is to the "catastrophic failure eminent level," the machine owner can react accordingly. Having the ability to know that a bearing is entering a failure mode before it actually does through the use of ultrasonic sensing allows for spindle replacement to be planned, rather than become unexpected and requires reactive maintenance to be performed. The flowchart in Figure 65 has been provided to better show the system's process flow and make it easier to understand.

If a further investigation is needed, the IFM software can be used to determine what the bearing issues are (BPFO, BPFI, etc). Through the use of the frequency spectrum, the software can also show if there are other sources of vibration on the machine. This becomes useful if the machine is having tolerance issues. Just because the machine cannot hold tolerance does not mean that the spindle has problems. In any case, the information can be relayed back to Okuma, where they can review it without ever having to leave there office. The system is able to prevent a service call from being needed, saving both parties (OEM and machine tool owner) time and money.
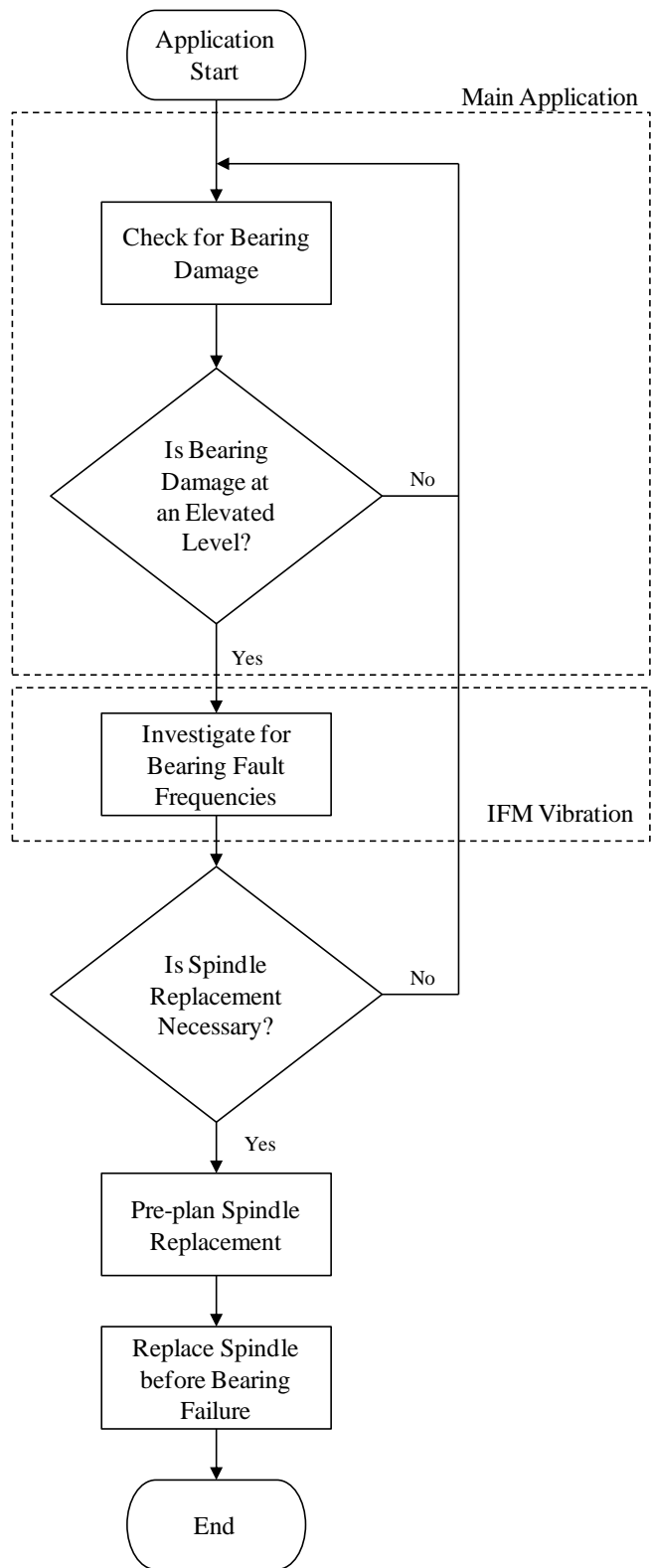
Figure 65: Okuma Spindle Monitor Spindle Replacement Flowchart.

7.8 System Validation

       To ensure that the system was fully functional, an Okuma Machine Simulator was utilized. This allowed for the application to be run on the same computer that a machine would have on it; however there is no machine attached. The validation test setup can be seen in Figure 66. The Beckhoff PLC device was connected directly with the simulator (rather than a bus hub) as this device is the one that communicates with the *Okuma Spindle Monitor* program.

Figure 66: Validation Test Setup on Simulator

A series of tests, such as checking for graphical indicator updates, database updates, and working API program integration were completed on the simulator to ensure the program worked smoothly. This allowed for any programming bugs to be corrected that could not be caught when trying to develop the application on a laptop. After some additional added features and debugging of the program, the program was found to work the way it was designed.

The next validation step was to take the program to an actual machine and test it out under actual conditions. This was performed on an LB3000EX lathe at Okuma's Partners in THINC building, the manufacturer's partner teaming facility. This particular machine was sent to the Interactive Manufacturing Experience (imX) 2011 machine tool show [69] in Las Vegas to debut the developed system. Figure 67, Figure 68, and Figure 69 show the system setup on the machine. To allow for the same data acquisition hardware to employ both the *Okuma Coolant Monitor* as well as the *Okuma Spindle Monitor*, an additional analog current module was added and the software program was modified. This served as a verification that both systems could be run from one PLC.
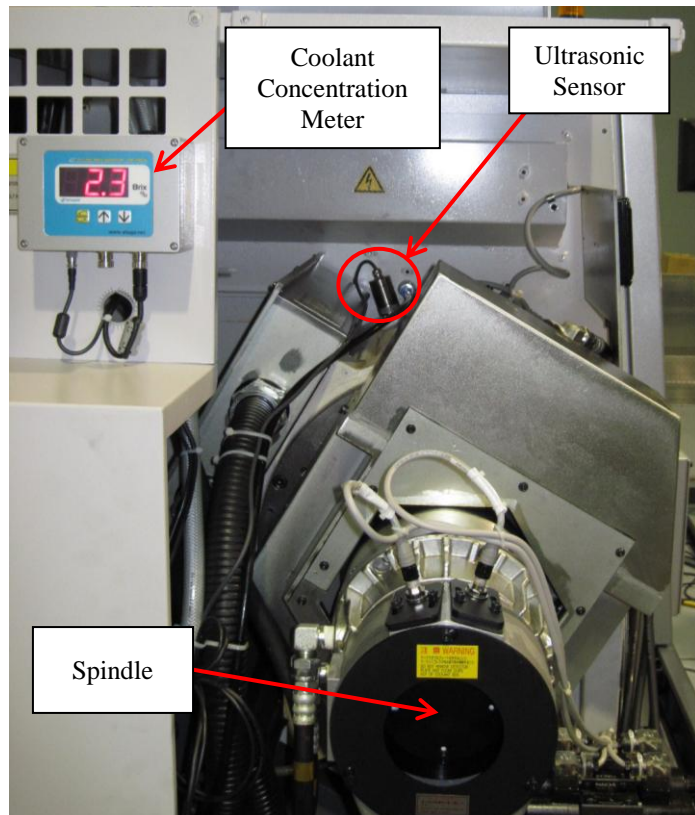
Figure 67: Ultrasonic Sensor Placement.

Figure 68: Software Loaded onto the Machine Control.
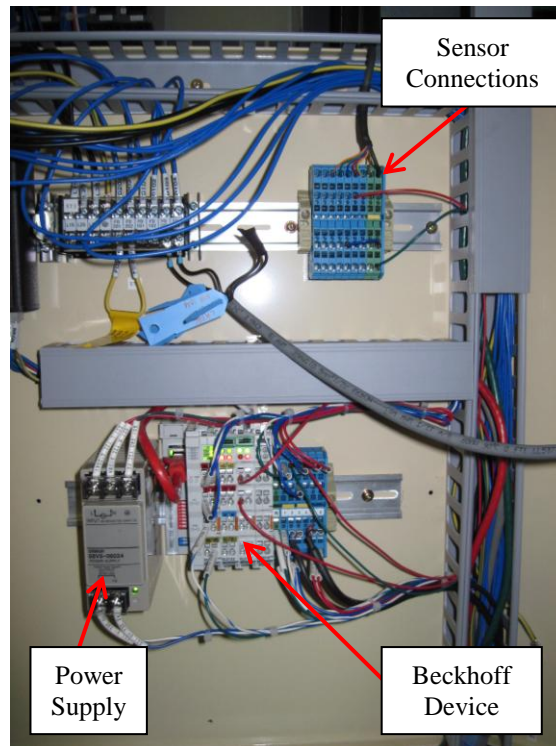
Figure 69: Electrical Connections inside the Electrical Cabinet.

7.9 Additional Possibilities

Additional items can be added into this system to allow for it to provide a better spindle health picture. Access to the spindle temperature system (currently only on Okuma machining centers) via the API would allow for an additional temperature parameter to be collected at the time of data recording. However, it should be noted that the Data API currently does not report this parameter. This would allow for the system to become a multi-parameter one, making the spindle diagnosis more complete.

Spindle load is also another parameter that could be recorded, especially for the in-process measurement mode. Unlike the temperature, this value can be called via the API. These two parameters may become of more value as the system is further developed and enhanced, based on the research findings in the next two chapters.

CHAPTER 8: SYSTEM PERFORMANCE

A system has been created to monitor the spindle as its bearings degrade, as discussed in Chapter 7. A great tool now exists to be used in a CBM strategy on a CNC machine. However, how the system will perform in real world conditions was still unknown. Therefore, research needed to be conducted in order to better understand the system (and sensor) performance.

Research was performed on the Okuma machines located at Clemson University's International Center for Automotive Research (CU-ICAR) in Greenville, South Carolina. The system was initially developed to be used on a lathe; therefore, the same LB4000EX the software prototyping was completed on was used for system testing. Three types of tests were performed: RPM range investigation tests, machining tests, and minimum number of sensor samples test.

8.1 Lathe Test Setup

For the various tests performed on the lathe, the ultrasonic sensor and accelerometer were positioned over the front bearing pair, as shown in Figure 70. Special consideration was taken to ensure the accelerometer was mounted in the horizontal direction. Both sensors where attached with the same type of magnet; however an adapter was created for the ultrasonic sensor to be attached properly. The magnet adapter drawings can be seen in Appendix F.
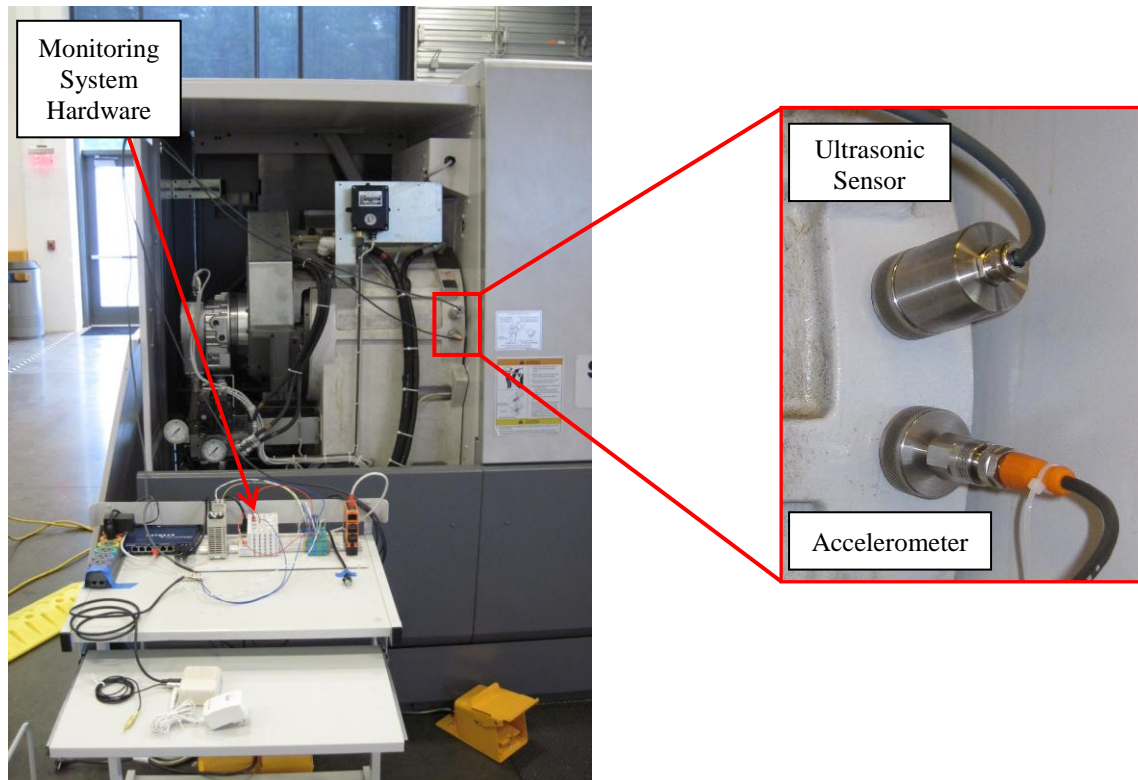
Figure 70: System Setup for the Lathe.

Data was collected using the application developed for the *Okuma Spindle Monitor* system. This would simulate how the data would be relayed back from the machine tool application. The lathe had minimal usage of the spindle prior to these studies being performed. Therefore, the spindle was to be considered in "like-new" condition. The spindle was put through a warm up procedure before any data was recorded. This warm up procedure can be seen in Appendix H. Once the machine reached what was considered to be normal operating conditions, the testing could begin [53].

8.2 <u>RPM Range Investigation – No Load, No Imbalance</u>

The first test completed was to understand how the ultrasonic sensor would react to different spindle speeds under a no load condition. The chuck was placed in the clamped position and was absent of a workpiece. The ultrasonic sensor's sensitivity was adjusted to ensure a baseline at a spindle speed of 1,000 revolutions per minute (RPM) was as close to 0 dB (4 mA) as possible.

Data for spindle speeds between 1,000 to 4,000 RPM, in 100 RPM increments, was recorded over three trials. Trial 1 was taken on one day while Trials 2 and 3 were performed the day after. One thousand data points were sampled with a polling period of 250 ms.

8.2.1 Trial 1

Trial 1 was taken as an initial trial to investigate the ultrasonic sensor performance. It was noticed before the tests that when the spindle was running and the acquisition loop for the data collection was set to a relatively fast polling period, 250 ms in this case, the sensor value fluctuated a bit. Therefore, on this first trial, the sensor's normality and standard deviation were also investigated. A phone call to the sensor manufacturer revealed that a minimum number of data points need to be taken from the sensor in order to get an accurate ultrasonic level. This was later found to be in the range of 60 - 100 data points.
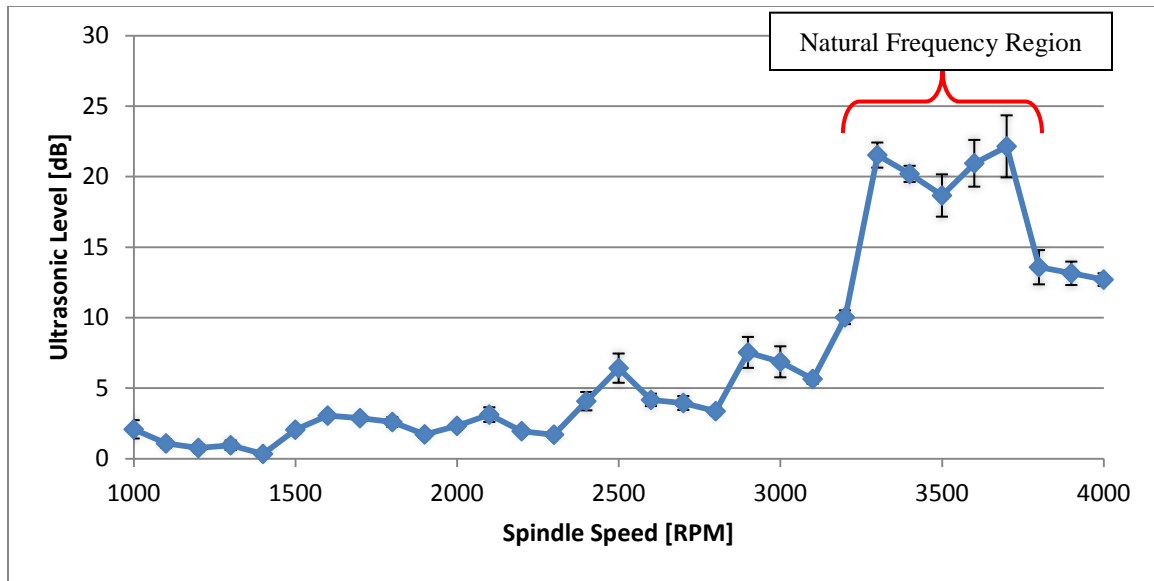
Figure 71: Data for Trial 1 RPM Range Investigation

Figure 71 shows that as the spindle speed increases, the ultrasonic sensor's output stays below 10 dB until 3,200 RPM (76% of the maximum spindle speed). Then, the reading jumps up to around 20 dB, decreasing below 15 dB at 3,800 RPM. The reason for this is thought to be due to the spindle's natural frequency occurring in all Okuma spindles somewhere around 4,000 to 7,000 RPM, as stated by the Okuma spindle experts. This allowed the realization to be made that the spindle bearings' sound output is speed dependent, among other things. Figure 71 shows that the natural frequency for this machine's spindle is somewhere in the 3,300 to 3,700 RPM range. This was verified by looking at the running frequency value from the spindle's FFT spectrum, which will be discussed in Section 8.2.3.

A simple scaling factor calculation, as shown in Appendix N, can be also performed to show that there is some natural frequency resonance occurring. When the spindle is rotating in the area of 3,500 RPM, emitting approximately 20 dB, the sound

level produced by the bearings is around 10 times greater than at 1,000 RPM. This makes sense as the spindle bearings would be much louder at their resonant (natural) frequency when compared to frequencies below or above the natural frequency.

The sensor's output was found to be normally distributed and it had a maximum standard deviation value of 4.40 dB at 3,700 RPM. This frequency was found to have the highest standard deviation in the other two trials as well, being 3.78 and 3.28 dB respectively. This high deviation suggests that 3,700 RPM may be the spindle's true natural frequency.

8.2.2 Trial 2 and Trial 3

The same procedure as Trial 1 was completed for Trial 2 and Trial 3. Figure 72 shows how all three trials compare. All three trials followed the same trend, showing that the measurement is repeatable. Due to the fact that the sensor's highest excitation is in the spindle's natural frequency range, it is suggested that the sensor baseline be set somewhere in this natural frequency range. This should help improve the signal to noise ratio of the sensor when it comes time for the system to take an actual measurement.
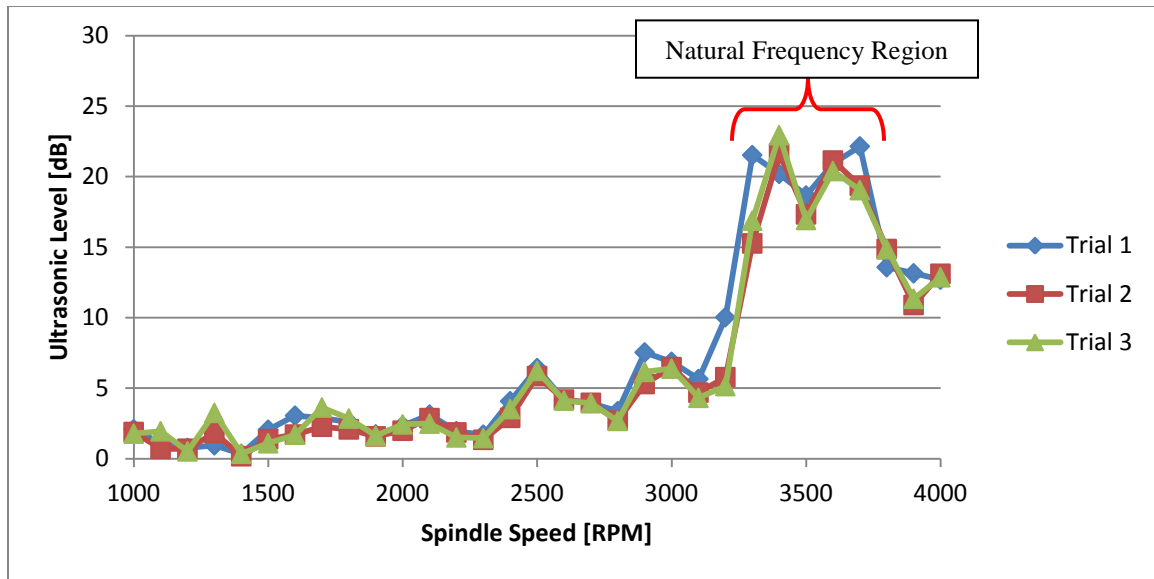
Figure 72: Ultrasonic Levels for Trials 1, 2, and 3 for the LB4000EX.

8.2.3 Natural Frequency Verification

To ensure that the increase in the sensor output in the upper frequency range was indeed due to the spindle's natural frequency, the accelerometer from the IFM module was employed.

The first item that was investigated was to see how the machine's overall RMS vibration value changed. The default RMS reading for acceleration (in mg) was taken, but the discrimination of the readings was too small, causing the readout to say either 10 or 11 mg throughout the whole RPM range tested.

The unit of measure was then switched to a velocity (mm/s) to see if the discrimination could be improved. It was improved, but no conclusion could be gathered as to what was occurring. This can be seen in Figure 73.

104
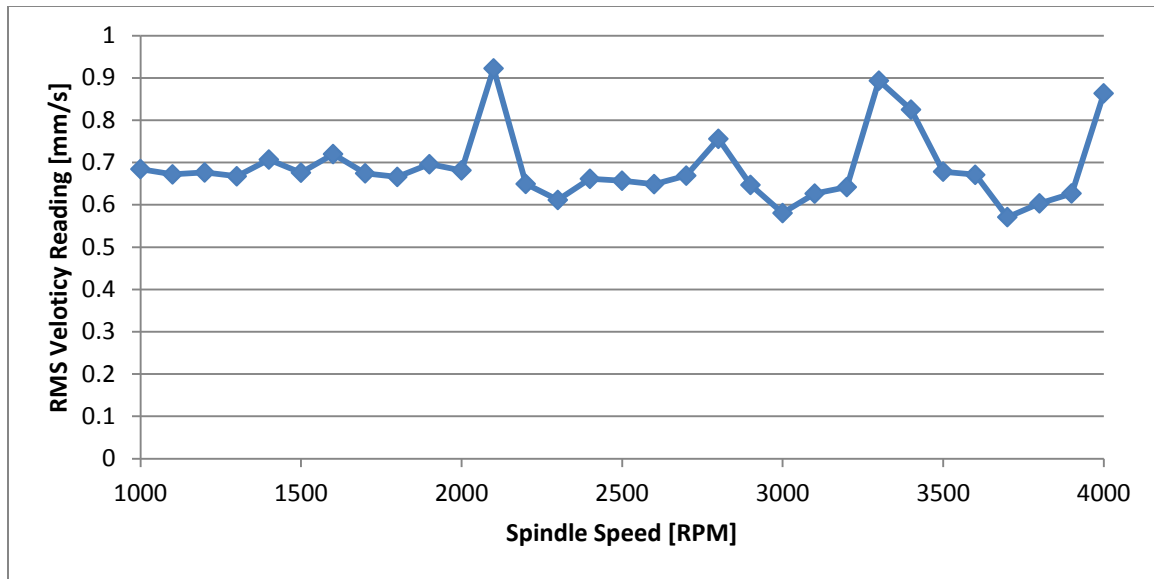
Figure 73: RMS Velocity Measurements.

The next task was to look at the running frequency on the FFT frequency spectrum and see how its value changed. This was done by looking for the magnitude of the spindle speed peak on the FFT chart in the IFM software. Figure 74 shows an example of the appearance of the FFT chart for a spindle speed of 3,700 RPM.
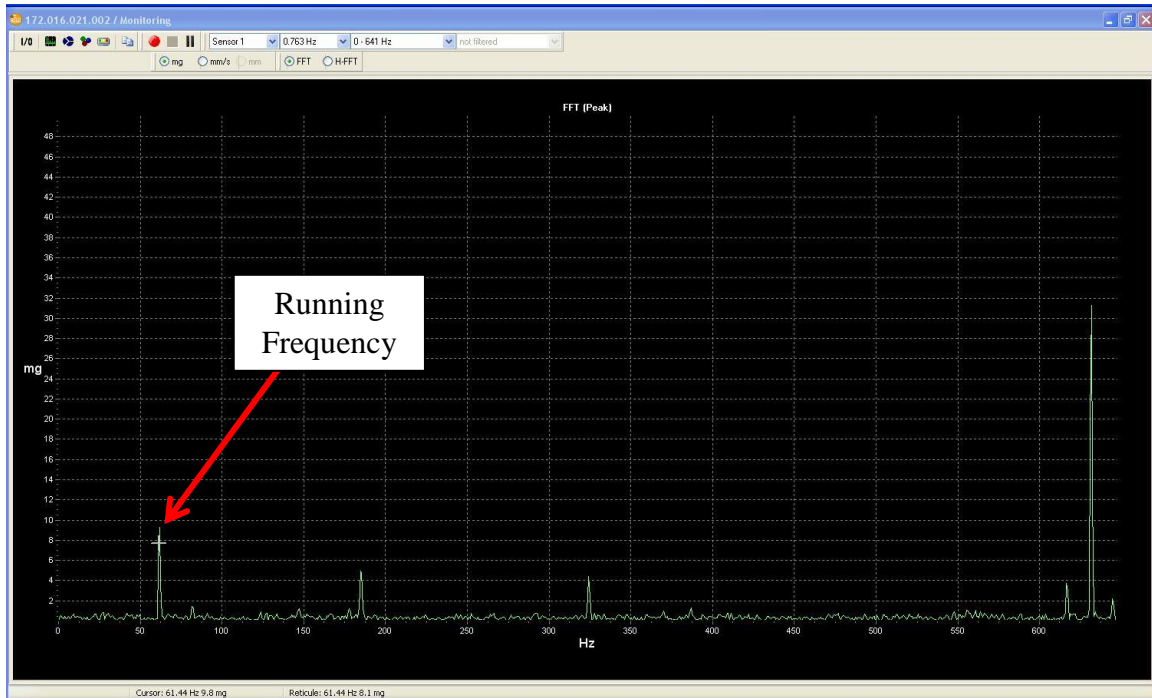
Figure 74: IFM FFT Chart for a Spindle Speed of 3,700 RPM.

The reticule value at a specific frequency was found by moving the mouse along the screen until the correct frequency on the chart was found (for the given running speed of the spindle). This value was given in an acceleration, as can be seen in Figure 75.
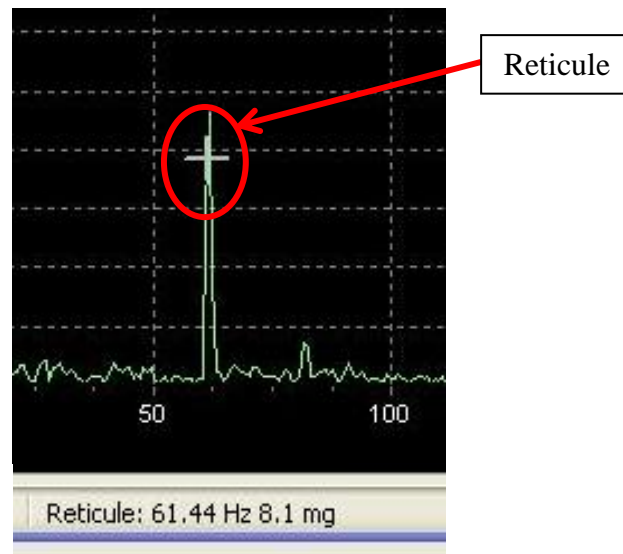
Figure 75: Zoomed-In View for the Running Frequency of 3,700 RPM (61.66 Hz).

This measurement was performed three different times as well, providing the data in Figure 76. Like the ultrasonic measurements, there is an excitation in the 3,300 to 4,000 RPM range, indicating that this is the spindle's natural frequency region. Figure 77 allows for an easy comparison of the ultrasonic readings with the acceleration readings.
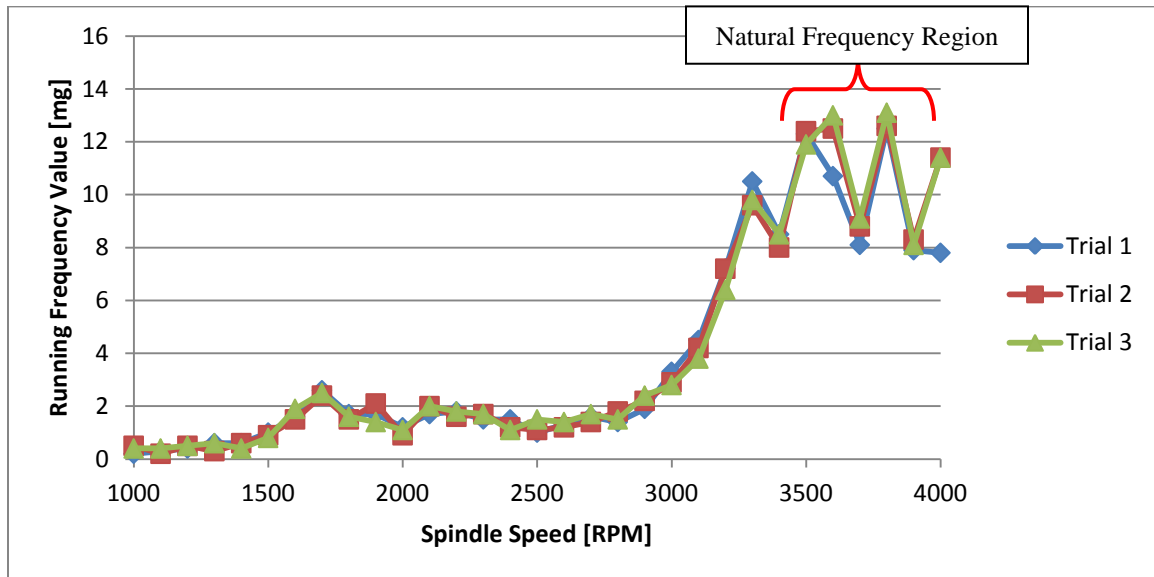
Figure 76: Running Frequency Values from the FFT Chart.
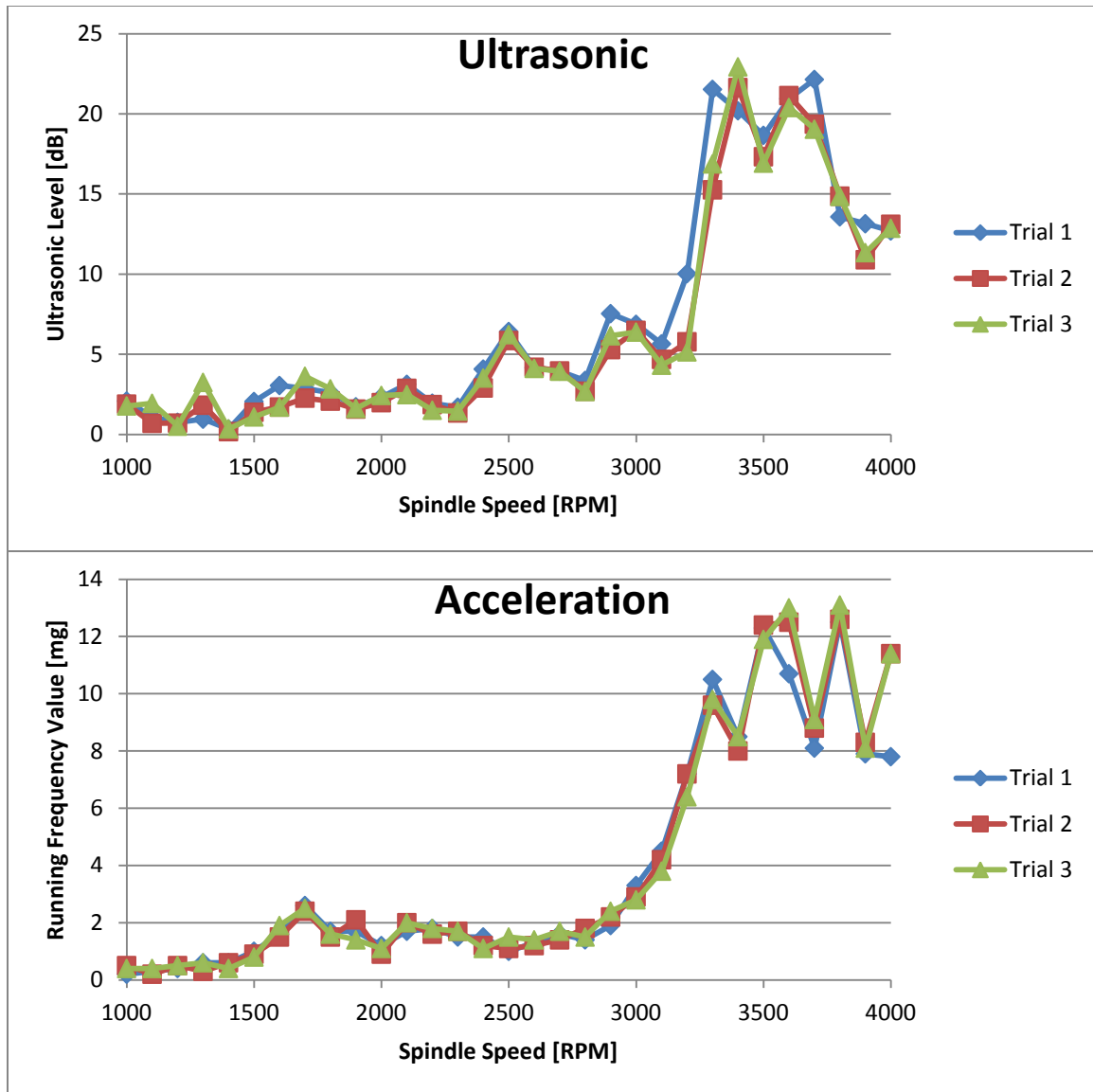
Figure 77: Comparison Between Ultrasonic and Acceleration Readings.

8.3 RPM Range Investigation – No Load, Imbalance

The next test completed was to understand if the ultrasonic sensor would be able to detect stresses put on the bearings due to an imbalance (vibration) condition. The chuck was placed in the clamped position and was absent of a workpiece. The ultrasonic

sensor's sensitivity was not changed from the previous test. This allowed for the baseline reading to be fixed so that it could be used for comparison purposes.

Two different imbalance conditions were tested; 3.5 grams and 21.6 grams. The 3.5 gram mass simulates a small imbalance, while the 21.6 gram mass simulates a large imbalance (ie: noticeable machine vibration). These masses consisted of screws that could be inserted into the machine's chuck, as show in Figure 78b.

a) Masses Used for Imbalance   b) Large Mass in Chuck
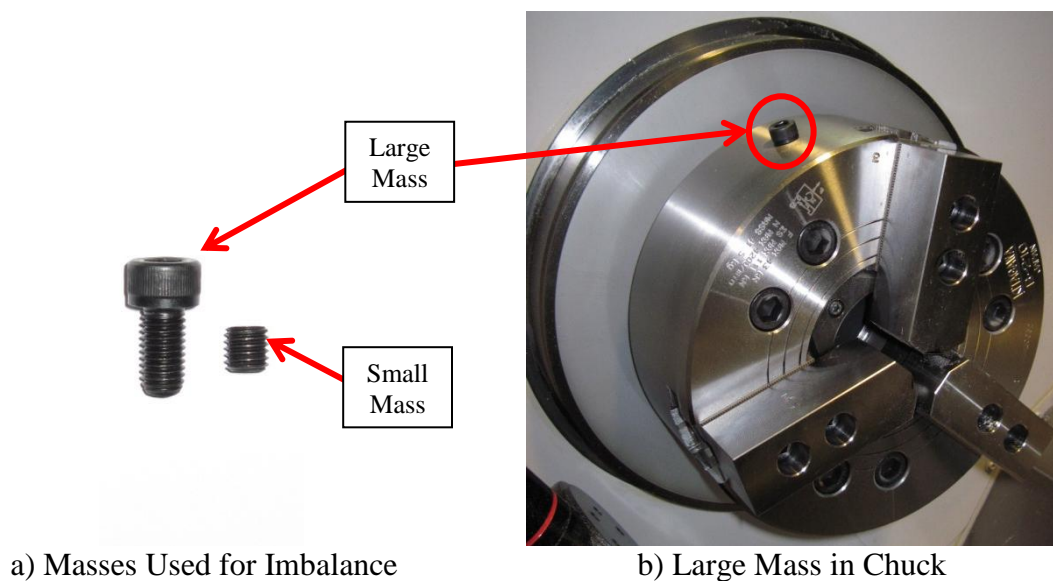
Figure 78: Imbalance Condition Applied to the Chuck.

Data for spindle speeds between 1,000 to 4,000 RPM, in 100 RPM increments, was recorded. Again, one thousand data points were sampled with a polling period of 250 ms. One trial was performed with the small mass and two trials were performed for the large mass.

8.3.1 Small Mass Imbalance

Figure 79 shows how the average for Trials 1, 2, and 3 from the *RPM Range Investigation – No Load, No Imbalance* test compares with the readings collected with

the small mass imbalance. It can be seen that readings are quite similar; therefore indicating that the small mass used to induce vibration has no effect on the ultrasonic reading.
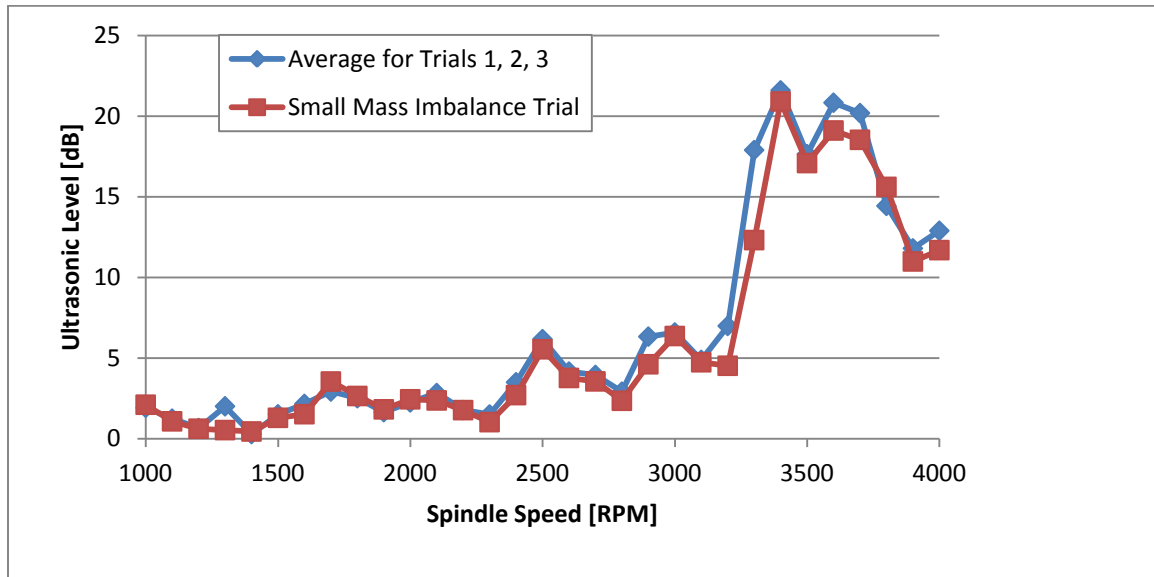
Figure 79: Comparison Between the Average of Trials 1, 2, and 3 and the Small Mass Trial.

8.3.2 Large Mass Imbalance

Two trials were run for the large mass. This was done to see if there was any variation in the readings between Trial 1 and Trial 2 for the large mass imbalance, as the large mass was over six times larger than the small mass. Figure 80 shows similar results for the large mass as Figure 79 did for the small mass. Therefore, it can be concluded that the ultrasonic sensor is not able to detect imbalance conditions. This makes sense as the sensor is intended to be used for bearing condition identification, not vibration. However, as stated earlier, the spindle was in a "like-new" condition. It would be interesting to see if inducing a vibration condition on a worn spindle will cause the imbalance readings to differ from the non-imbalance ones.
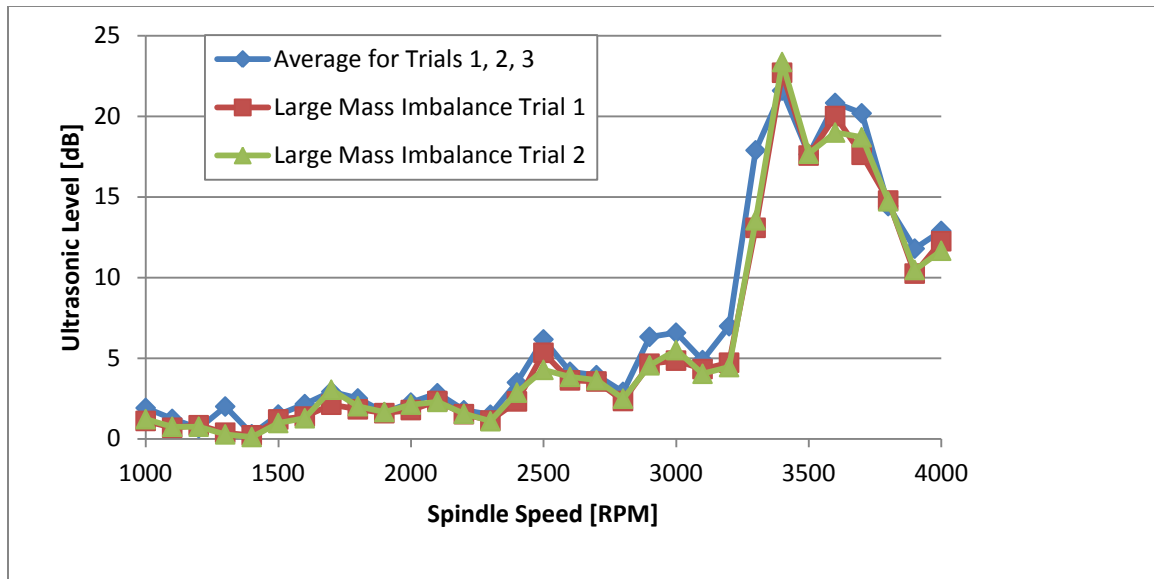
Figure 80: Comparison Between the Average of Trials 1, 2, and 3 and the Large Mass Trials.

8.4 RPM Range Investigation Retest – No Load, No Imbalance

After the imbalance tests were completed, a final test of no load and no imbalance was run to see if the excessive vibration caused by the masses caused an increase from the baseline readings (ie: any noticeable bearing damage after Trials 1, 2, and 3). Figure 81 shows that the average of the three readings before and the one reading after the vibration testing are in similar locations with the same general curve shape. Therefore, it can be said that the testing did not cause an increase in bearing damage. This is good because the spindles are designed to handle eccentric parts that could cause a spindle imbalance at times.
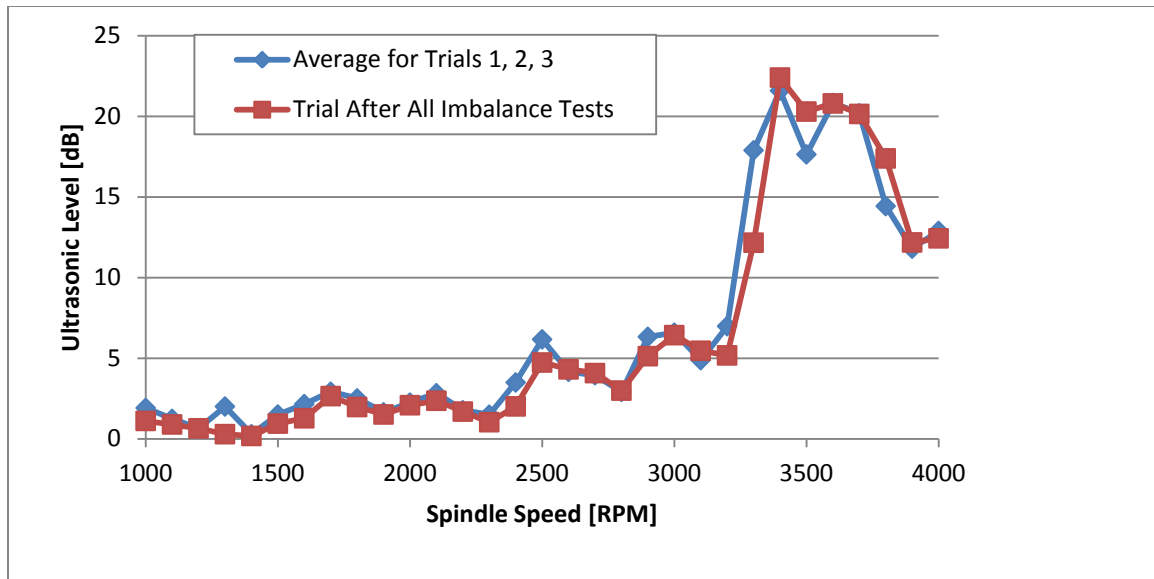
Figure 81: Comparison Between the Average of Trials 1, 2, and 3 and Retest Trial.

8.5 Sensor Sampling Investigation

A sensor sampling investigation was performed in order to find the minimum of samples needed for an accurate ultrasonic average value to be determined. Data averaging needed to be performed as the sensor has some variation in its RMS analog to digital conversion, as described previously in Section 8.2.1. This would then minimize the amount of time and number of data points required for the sensor data recording, which then can be implemented into the developed CBM system.

Five hundred samples from the ultrasonic sensor, with the lathe spindle rotating at 1,000 RPM, were collected at a polling period of 200 ms. These samples were then subgrouped and the average calculated to see the variance. Figure 82 shows how the amount of variation per subgroup average decreases with an increase in the number samples within each subgroup.
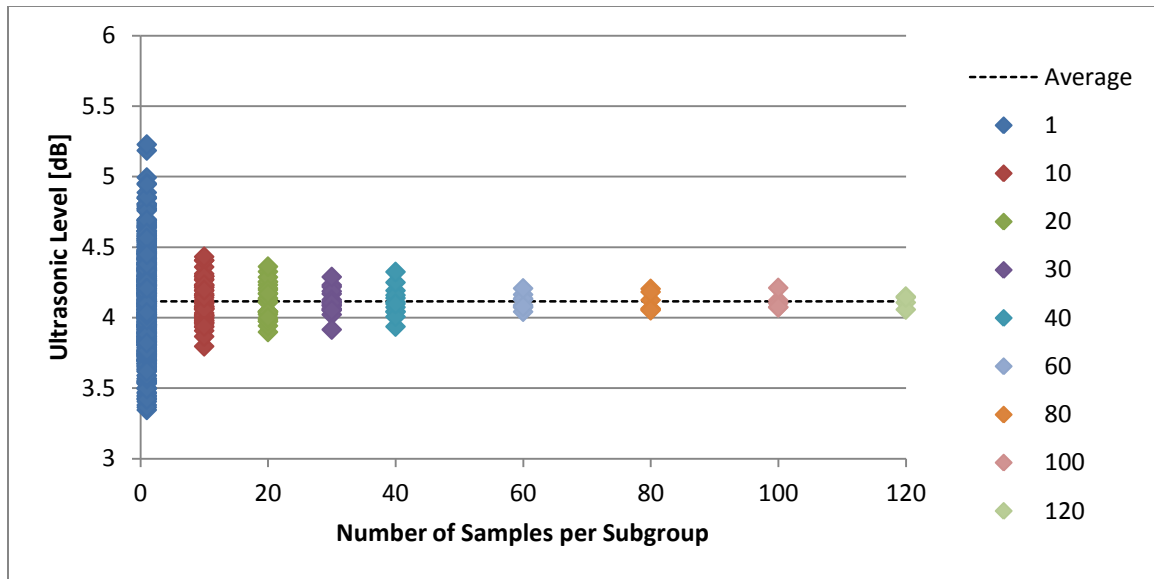
Figure 82: Subgroup Sample Size Convergence.

Based on the data spread in Figure 82, it appears that once the subgroup sample size reaches 60, the amount of variation is small and all subgroup averages are close to that of the population average. Figure 83 shows the standard deviation for the various subgroup sizes. Once the subgroup size reaches 60 samples, the standard deviation becomes approximately 0.05 dB. This value, coupled with the way the data is reflected in Figure 82, allows for the proper number of samples per ultrasonic reading to be found. Ultrasonic sensor averages including 60 samples or greater should be sufficient for an accurate determination of the spindle condition.
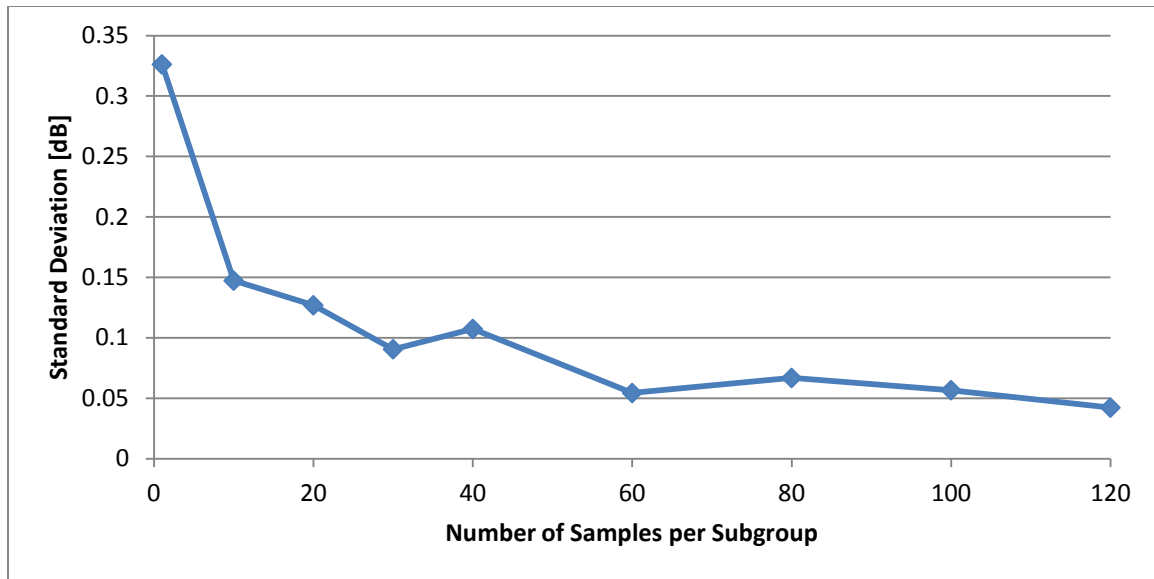
Figure 83: Standard Deviation for Subgrouping.

8.6 Machining Testing

One of the requirements for the *Okuma Spindle Monitor* application was to monitor the spindle and be able to provide a health status for the spindle at all times (machining or otherwise) (if possible). As the previous tests showed, the sensor output changes with spindle speed. The sensor's output during a machining cycle needed to be investigated as well to determine if an in-process monitoring method can be performed accurately.

Two materials were selected for the machining tests. These were 6061 Aluminum and Cold Roll - C-1018 Steel. The reason for investigating two different materials was to see if the sensor's output differed between the two. This allowed for a comparison to be made between a soft material versus a hard material, as many different materials are machined in industry. These metal blanks were three inches long and two inches in diameter.

A part program was created, in Appendix J, and ran for both materials. The spindle speed was held at a constant 2,000 RPM with a constant feed rate of 0.0005 inches/revolution. The depth of cut (DOC) was the parameter that varied, ranging from 0.025 to 0.100 inches, in increments of 0.025. A constant depth of cut was held for an entire machining pass. A Sandvik CNMG 12 04 08-PM 4225 cutting insert was used to do the metal cutting. Table 5 allows for the testing parameters to be seen more easily.

Table 5: Machining Test Parameters.

Material	Dimensions	Spindle Speed	Feed Rate	Depth of Cut
Aluminum (6061)	3 in. long 2 in. diameter	2000 RPM	0.0005 in/rev	0.025 in. 0.050 in. 0.075 in. 0.100 in.
Steel (Cold Rolled C-1018)				

The test specimen was divided up into four sections, as indicated in Figure 84. This was done due to the ultrasonic sensor needing a sample of data to be taken before an average ultrasonic reading could be computed. This would also simulate how the spindle monitoring system would function during a cutting process as well as what kind of data it would provide. Each section length was identical, 0.35 inches in length. Table 6 shows the spanning distance for each section number identified.
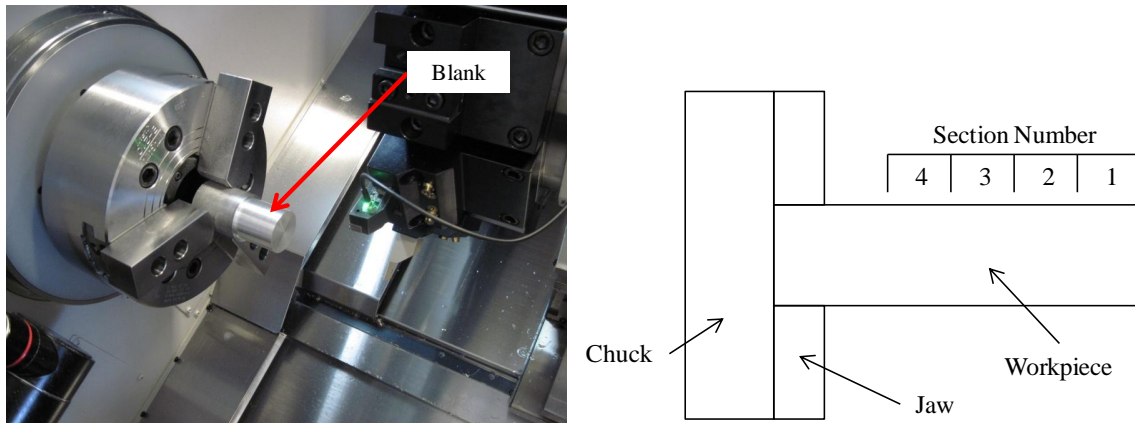
Figure 84: Specimen Configuration.

Table 6: Specimen Section Number and its Respective Distance.

Section Number	Spanning Distance
1	0 – 0.35 in.
2	0.35 – 0.70 in.
3	0.70 – 1.05 in.
4	1.05 in – 1.40 in.

Data was once again acquired with the Spindle Monitoring hardware and software. However, for these tests, only 100 data points were sampled with a polling period of 200 ms for each section of the part. This allowed for "cutting curves" to be constructed based on the cutting distance on the part. The "cutting curves" for each specimen can be seen in Appendix K.

A total of five specimens for each material were cut. The order of cut was an alternating sequence, shown in Table 7. This allowed for any changes in the ultrasonic reading to be seen between materials via the baseline reading (DOC = 0 in). The baseline reading was recorded before each part was machined. This allowed for a reference point to be established before the material processing had occurred.

Table 7: Order of Specimen Cutting.

Sequence	Material	Specimen Number
1	Aluminum	1, 2, 3
2	Steel	1, 2, 3
3	Aluminum	4, 5
4	Steel	4, 5

Figure 85 shows a comparison between the Aluminum Specimen 1 and Steel Specimen 1. This provides a good example as to the clear distinction between the two materials. The aluminum specimens had consistently higher ultrasonic readings than the steel specimens as well as had much more variation between the DOC curves. This is somewhat counter intuitive as one would think that a harder metal would cause the readings to be higher due to a greater amount of thrust force needed.

a) Aluminum Specimen 1   b) Steel Specimen 1
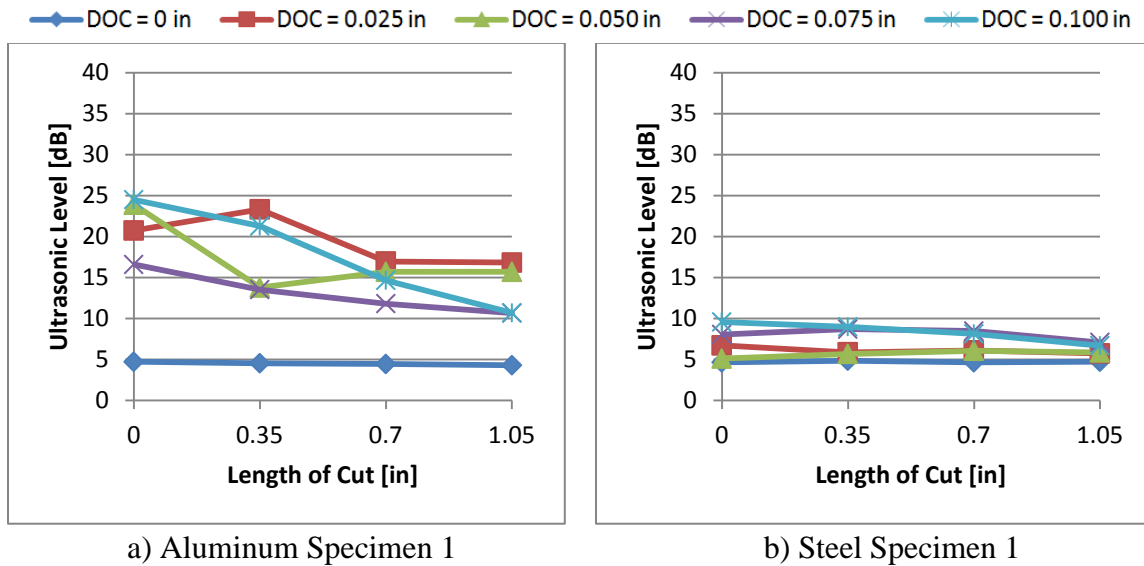
Figure 85: Comparison Between an Aluminum and Steel Specimen.

It was observed in the steel specimens that the ultrasonic readings tend to converge to 6 dB (2 dB above baseline, equivalent to 1.4 times in magnitude) at the end of the cut for all DOC curves. In the aluminum, the DOC curves tend to decrease as the

length of cut increases, however, the curves do not converge towards a single value like the steel and are much high on the dB scale. The likely reason for this convergence and decrease in dB level is due to a lower variability in the cut. As the tool moves closer to the chuck, the deflection of the specimen, caused by the normal force, is reduced.

Another comparison can be performed by investigating a single DOC for all five specimens for both materials. This provides the ability to determine which material is more consistent for an in-process monitoring cut. Steel was found to have a more consistent reading for every depth of cut taken on all five specimens. As an example, Figure 86 shows the DOC for 0.050 inches between both aluminum and steel for all five respective specimens. Due to this finding, it is recommended that a steel part or a relatively hard material be used to perform the in-process measurement. A baseline reference should be taken at some point in the part program, where, if possible, a constant depth of cut with a constant feed rate is taken for at least 12 seconds (with a polling period of 200 ms). This will provide the 60 samples needed for an accurate reading.

a) Aluminum   b) Steel
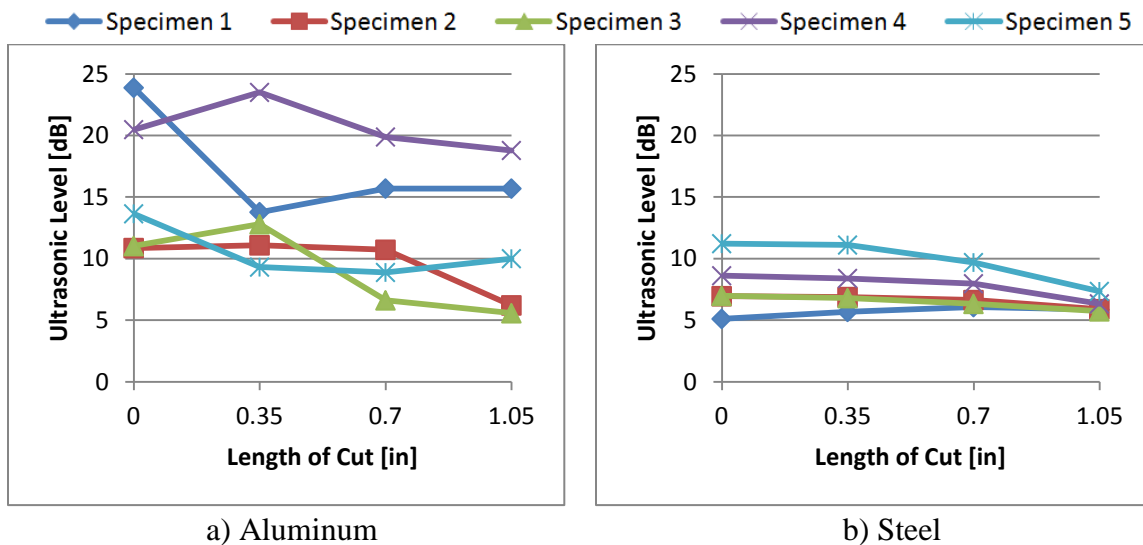
Figure 86: Aluminum and Steel Specimens with a DOC of 0.050 in.

It should be noted that due to the amount of heat generated by the machining process of steel, coolant was used during steel specimen machining. Coolant was not used in the aluminum specimen machining. This could be a possibility as to why the readings in the aluminum vary much more, despite the fact that steel is a much harder material. The coolant allowed for the tool/chip interface to be lubricated, therefore reducing the amount of friction at the interface. The ultrasonic sensor used is friction based, therefore this reduction in friction generated by the machining could be the cause for the more stable readings seen.

Another possible reason as to why the readings for aluminum are much higher is tool chatter. While machining the aluminum specimens, chatter was much more predominant that it was with the steel. It was also noticed that the sensor reading jumped significantly for each high chatter shrill. A reason for the chatter could be due the spindle speed and feed rate not being appropriate for cutting aluminum, but was used so an equal comparison between the two materials could be made.

It was noticed that the ultrasonic bearing readings for the steel specimens increase as each successive specimen was machined. Figure 86b shows an example of this indication. This was the general trend seen for all of the DOCs in the steel specimens. The reason for this could be due to the tooling starting to wear and lose its cutting edge. If this is the case, the in-process measurements for spindle bearing condition may become even less accurate as the tooling starts to degrade.

The last item investigated in this machining study was to see if alternating the type material cut, as in Table 7, caused any significant or noticeable degradation to the

119

bearing condition. This was done by looking at the baseline readings (DOC = 0 in) before each part was machined. All baseline readings can be seen in Figure 87.

a) Aluminum   b) Steel
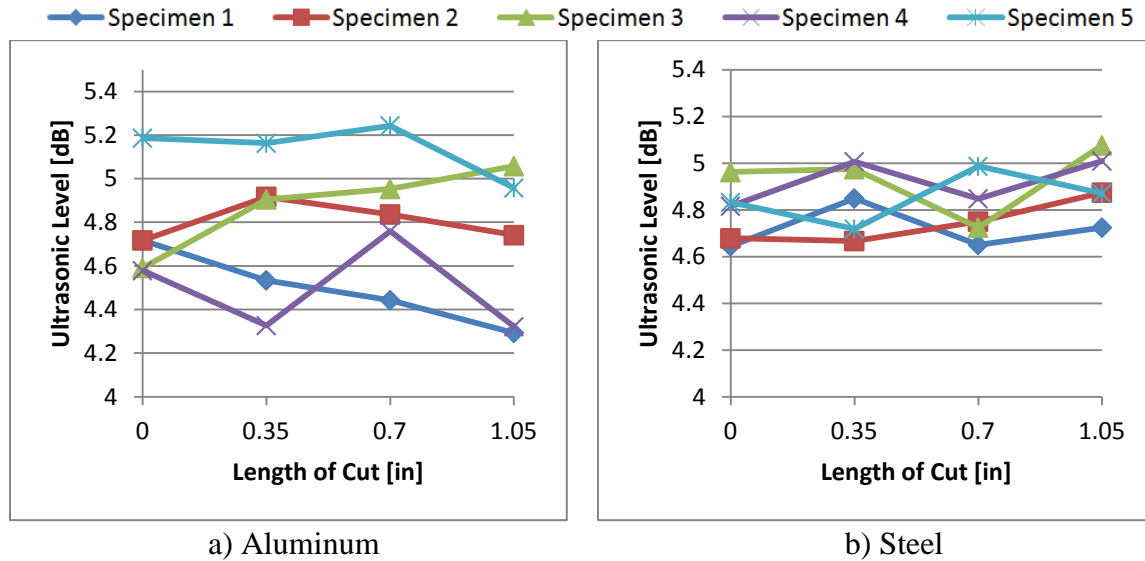
Figure 87: Aluminum and Steel Baseline Readings Before Machining Specimens (DOC = 0 in).

All of the readings were taking under the same set of conditions. The fact that there are no considerable increases between the material sequences ensures that the alternation of the different metals did not have an effect on the ultrasonic baseline. This was determined by studying Specimens 4 and 5 for both materials. Both are within the range of Specimens 1, 2, and 3. Therefore, the bearing condition can be assumed to be the same for both before and after the machining tests were performed.

CHAPTER 9: SPINDLE BEARING FAILURE TESTING

In Chapter 7, a monitoring system for detecting CNC spindle bearing failure was laid out. In Chapter 8, performance testing of that system was completed to show what the kind of data the system would feedback to the user. One question still remains: Can the system actually detect a spindle bearing failure? Many of the articles cited in the background sections of this thesis describe/perform testing under/in laboratory settings, where the bearing is really the only mechanical item in the system [55], [56], [57], [62], [63], [64]. It is important to test the bearings in real life applications to ensure the results still apply. An experiment was performed to find out and endured until a bearing failure had occurred. The findings are discussed in this chapter.

The experiment was designed to investigate a variety of parameters (temperature, ultrasound, and vibration) in order to better understand how these three measurements coincide in the event that there is a spindle bearing problem. Another method for bearing analysis, other than ultrasonic and vibration, uses the bearing temperature to determine health [54]. In the event of a catastrophic failure, there may not be much vibration at the time of failure if the failure is from friction generation. Hence, all three parameters were investigated.

The machine's original spindle was removed from the machine and a brand new rebuilt spindle was installed for testing purposes. This ensured that the bearings were in a very good condition and had no damage to start with as the machine's original spindle had an unknown number of machining hours already on it. Many of the specifications for this test can be found in Appendix L. It was ensured for all mill testing that the spindle

had been put through the warm up cycle as indicated on the side of the machine (4,000 RPM for 10 minutes, then 9,000 RPM for 10 minutes). A 15,000 RPM MB-46 spindle type was chosen to perform the destructive tests. This is the spindle type that is most commonly seen as needing replacement in the field. This is due to fact that this spindle type is the most common spindle used in an Okuma machine. Therefore, the MU-500VA vertical machining center was used, as it was available at the time. The order of testing was chosen in such a way so that many different spindle conditions could be simulated, with each condition allowing for more damage to occur than the previous one. The order of the planned tests and test descriptions can also be found in Appendix L. Only the first two tests, establishing a baseline and lack of lubrication, were able to be performed as one of the bearings failed during the lack of lubrication test.

9.1 Mill Test Setup

A variety of sensors were used to monitor the spindle as the bearings became more and more degraded throughout the testing. A combination of ultrasonic sensors, temperature probes, and accelerometers were used. A schematic of the spindle has been provided, in Figure 88, to show relative the bearing locations in the spindle as well as the sensor positions to measure the bearings. All sensing items can be seen in Figure 89. Figure 90 shows the thermocouples used in measuring the bearing temperatures and how they were inserted through the nose of the spindle. The lower spindle cover was removed in order to gain access to these holes. Each temperature probe examined the temperature at its respective bearing's outer race (i.e.: temperature T1 is for bearing B1).
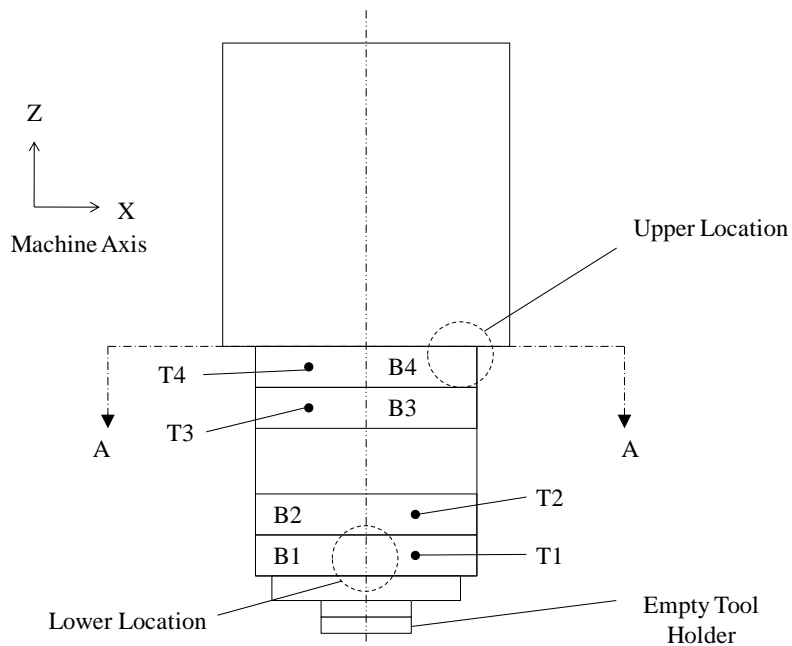
Figure 88: Front View Schematic of the Spindle.
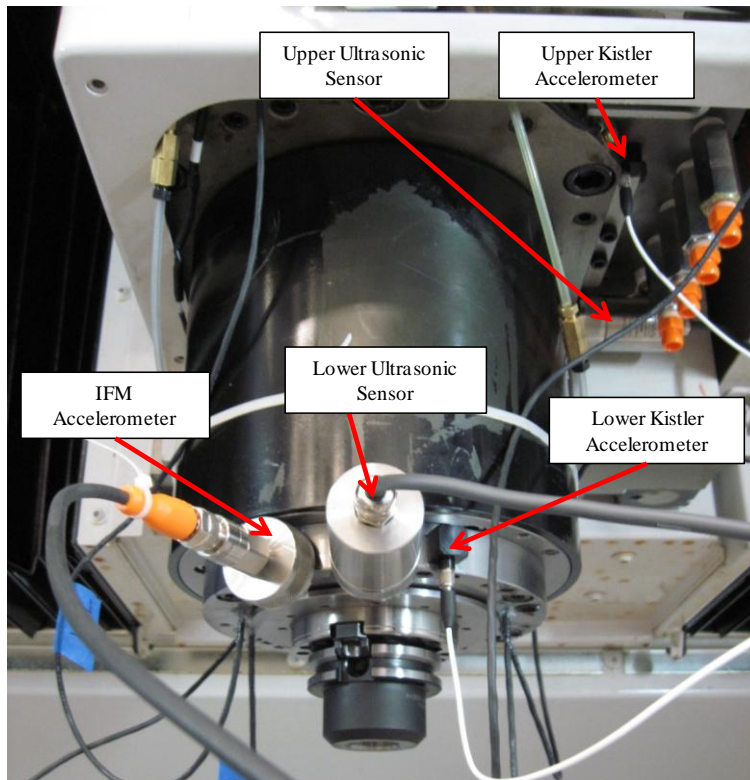
Figure 89: Sensors Used in Spindle Testing.
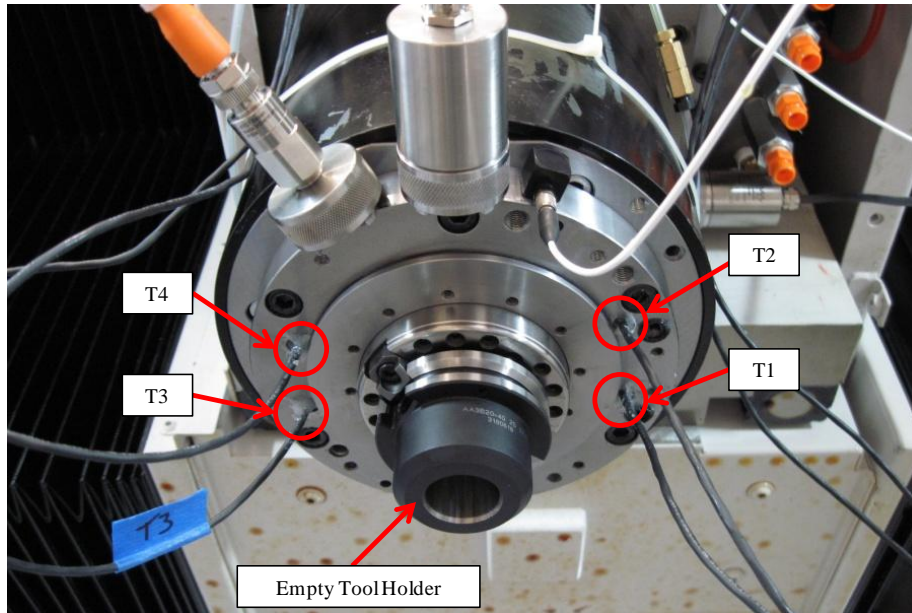
Figure 90: Bearing Temperature Probe Locations.

Figure 91 shows the data acquisition setup. All electrical components were set up inside an electrical cabinet and placed next to the machine. All data recording was performed on the desktop PC, next to the electrical cabinet.
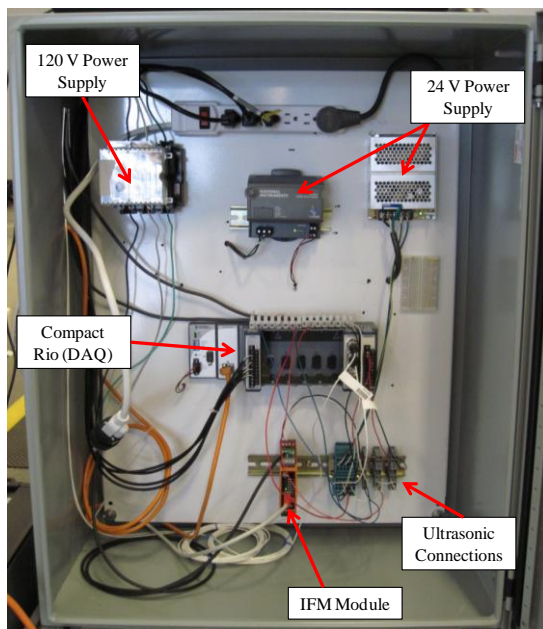
a) Electrical Cabinet Components   b) Total Recording System

Figure 91: Recording System.

A front panel display was created in LabVIEW on this host computer so that the data recording could be performed and monitored more easily. It can be seen in Figure 92, with all of its components labeled. Data was recorded into a spreadsheet at a rate of one data point every 10 seconds. This was due to having an ultrasonic value average outputted every 10 seconds. The average value included 100 samples of data. The polling period of 10 seconds also allowed for the spreadsheet to not become overwhelming when trying to analyze and graph the data after each test.
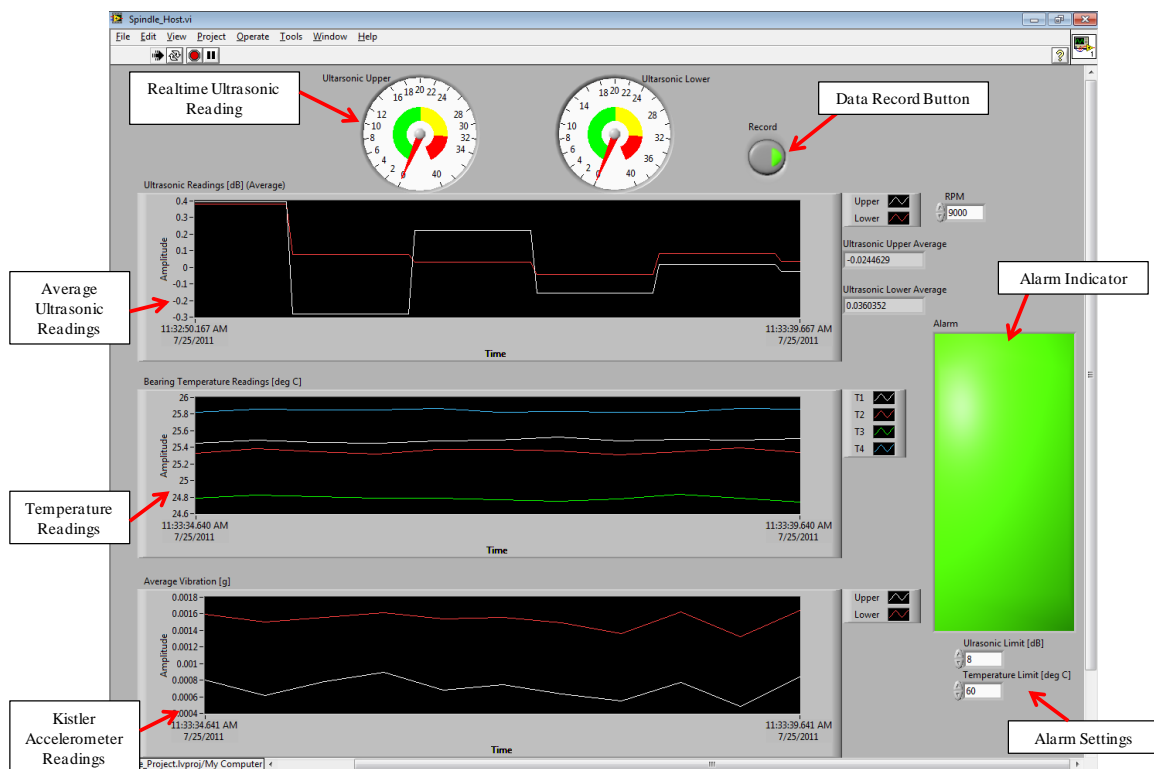
Figure 92: LabVIEW Front Panel for Data Recording.

Before commencing the spindle bearing destructive tests, the natural frequency of the spindle was found. This provided the running speed for which the spindle was ran during the destructive tests. The same procedure was taken for these test as was completed on the lathe (no load, no imbalance), however the RPM range investigated was

from 2,000 to 12,000, in increments of 1,000 RPM. An empty tool holder was clamped into the spindle, as the spindle will not run without a tool holder. The same empty tool holder was used for the spindle bearing destructive tests as well.

Figure 93 shows the ultrasonic sensor placement for this natural frequency test while Figure 94 shows the collected data. The sensor was placed on the spindle so that it was positioned perpendicular to the machine's X-axis. This is the same location where an Okuma service representative would place a vibration sensor.
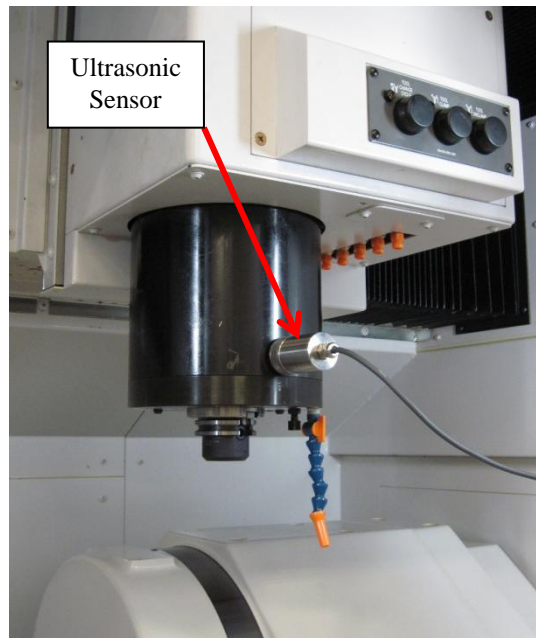
Figure 93: Ultrasonic Sensor Placement for Mill RPM Range Investigation.
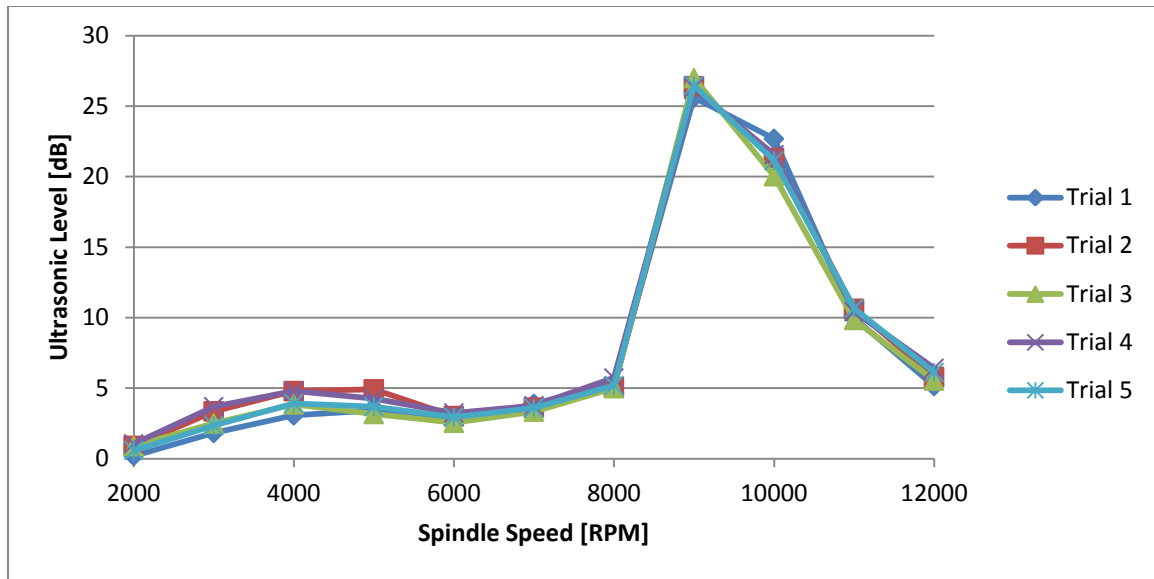
Figure 94: Ultrasonic Levels for Trials 1-5 on the MU-500VA.

The results show that there is a peak in the ultrasonic level at 9,000 RPM (60% of the maximum spindle speed), thus providing the spindle speed at which the destructive tests will be performed. The shape of the curve is similar to one found on the lathe tested in Chapter 8. The ultrasonic readings start out low, and then have a sudden increase in decibel level. For this particular test spindle, this was between 8,000 and 9,000 RPM. After this peak value at 9,000 RPM, the decibel level decreases to become substantially lower.

The readings indicate that when the spindle is rotating in the area of 9,000 RPM, the 27 dB sound level produced by the bearings is around 22.4 times greater than that at 2,000 RPM. The thinking here was that the bearings are stressed most at the 9,000 RPM, as they are the loudest at this speed. This speed would allow for the bearing degradation to be accelerated, thus decreasing the total time needed to see results. This is good as the

accelerated life test had the possibility to run for months (even with incurring damage to the bearings).

For the results discussed, bearing health was based on a decibel level given by the ultrasonic sensor readings. The same levels discussed in Chapter 6 were used [66]:

Baseline:	0 dB
Lubrication Failure (Initial Microscopic Damage):	8 dB
Beginning Stages of Failure (Initial Macroscopic Damage):	16 dB
Catastrophic Failure Eminent:	35 to 50 dB

9.2 <u>Test A: Establishing a Baseline</u>

The first test that needed to occur before any destructive tests were performed was that a baseline needed to be established. The baseline allows the original spindle conditions to be known, therefore providing a datum to determine how much damage has occurred from its original (new) state. The spindle had been "run-in" for 6-8 hours at the Okuma facility and had another 10-12 hours of run-in once installed into the machine. The spindle was in an unloaded state during this run-in period. The goal was to "break in" the bearings and bring them to their normal operating condition state. There were some initial issues with the slinger plate (also known as a "labyrinth") causing false readings due to the vertical orientation of the spindle. It was removed to provide an accurate reading.
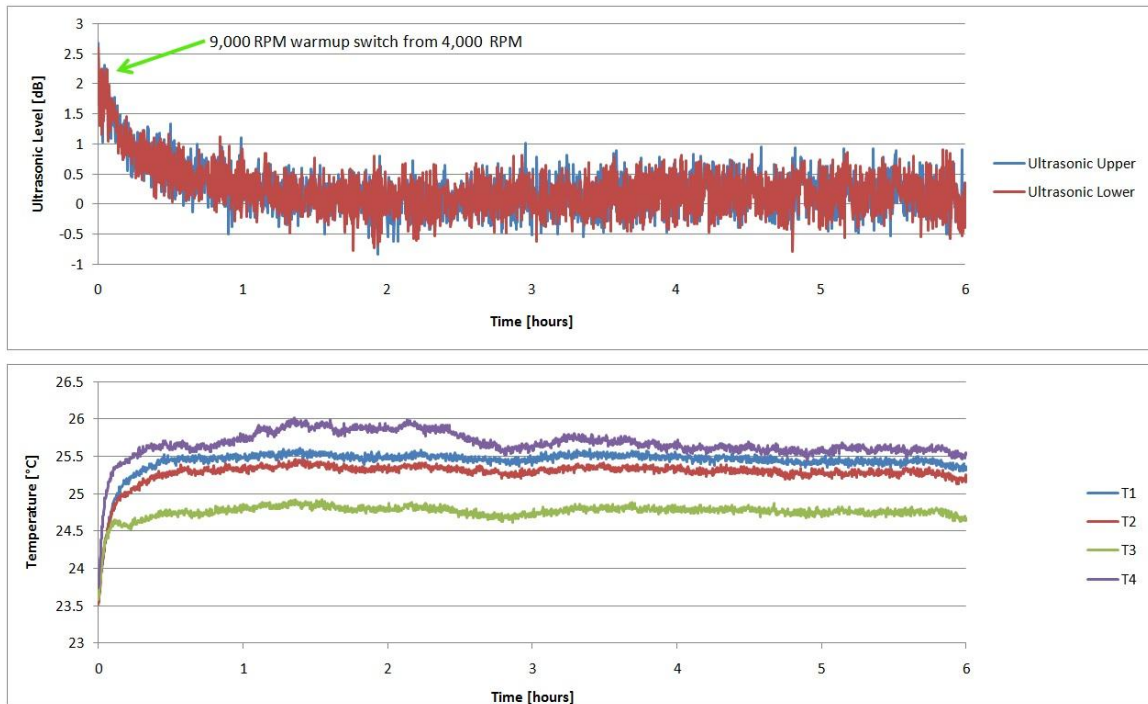
Figure 95: Baseline Readings.

Figure 95 shows the measurements taken during the baseline procedure. The machine was in normal operation with no load on the spindle. As one would expect, the bearing temperatures increase and reach a steady state condition, in the range of 25°C for all four bearings. However, it appears that the bearings' temperature steady states do not occur until about thirty minutes after the RPM was changed to 9,000. In addition, the ultrasonic values do not settle out until more than an hour after the RPM change. It is interesting that the bearings are loudest at startup, by about 2.5 dB. This validates the recommendation that spindle measurements should be taken once the machine has been warmed up [53]. The IFM overall RMS vibration reading was constant at 32 mg throughout this test.

A frequency spectrum, with magnitudes given in mg, was also obtained so that the magnitude of the bearing fault frequencies could be tracked as the damage levels increased. Based on the bearing fault frequency equations provided in Chapter 6, the indicators for bearing defects at 9,000 RPM are listed in Table 8.

Table 8: Bearing Fault Frequencies for 9,000 RPM (150 Hz).

Bearing Defect/Indicator	Frequency [Hz]
Fundamental Train Frequency (aka Pass Frequency Cage/Outer)	68.00
Pass Frequency Cage/Inner	82.00
Running Frequency	150.00
Ball Spin (Rotating) Frequency	757.86
Ball Passing Frequency Against Outer Race	1,700.06
Ball Pass Frequency (aka Ball Defect Frequency)	1,858.68
Ball Passing Frequency Against Inner Race	2,049.94

The baseline FFT chart is shown in Figure 96. The bearing fault frequencies have been labeled where appropriate. From the FFT chart, it appeared that the spindle may have had a bearing issue due to the large magnitude for the ball passing frequency against the outer race. The running frequency was 37 mg while the BPFO was 348 mg, over 9 times higher. The usual case is that the running frequency is the dominant peak. However, only one of the main fault frequencies is present. Typically, once another fault frequency starts to increase in magnitude, then there is a definite bearing problem.

The results were compared with the FFT signature from the machine's original spindle. The same response was seen on that spindle as well. Therefore, the elevated BPFO fault frequency seen here was considered to be an inherent signature in these spindle types. Nonetheless, the 348 mg BPFO was considered to be the baseline

magnitude for the test spindle and an increase from this value was carefully monitored. More information on the phenomenon of why the BPFO was so large can be found in Appendix M.
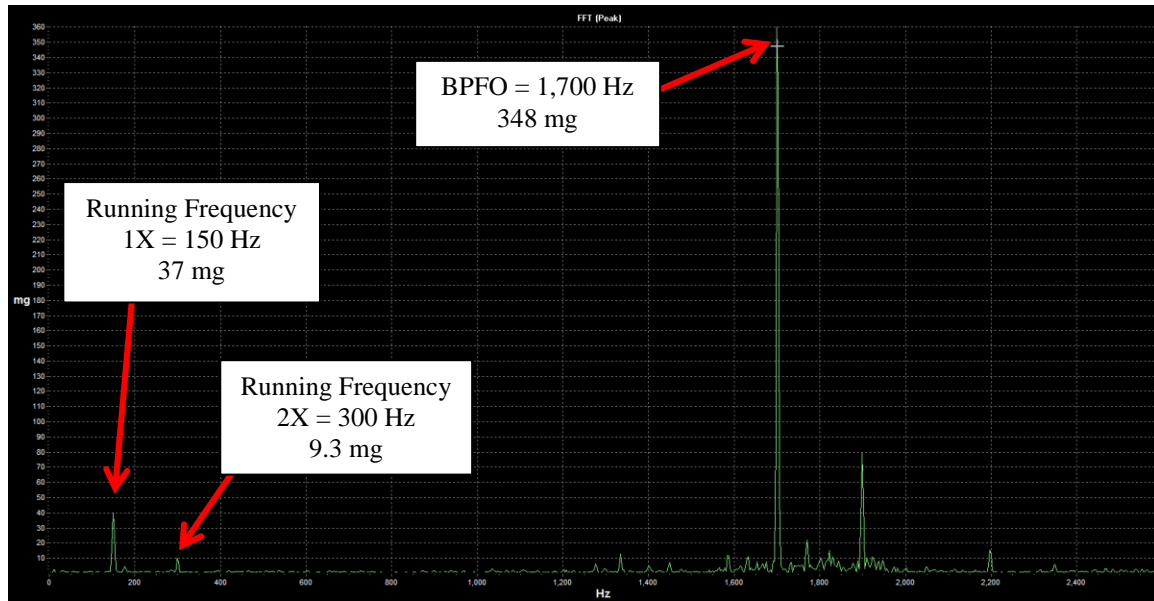
Figure 96: Baseline Frequency Spectrum.

9.3 <u>Test B: Improper or Lack of Lubrication</u>

The next test performed allowed for a lack of lubrication condition to be established. The goal of this test was to see if an increase to the 8 dB from baseline (indicating lack of lubrication) could be suppressed back to 0 dB when lubrication is resupplied. This has been shown to work on grease bearings [58], but it was unknown at the time if the same phenomenon for oil bearings would occur. Sometimes, the bearing's air-oil mixing block gets clogged and needs to be replaced. If the block gets clogged, the bearings are starved of lubrication and inevitably fail. This testing helped to simulate that event.

In order to simulate no oil being delivered through the air-oil system, a secondary mixing block, supplying only air, was used. Air always runs through the mixing block while the spindle is in use, regardless if the oil reservoir is empty. The machine will not run with if the main air supply has low or no pressure.

When it came time to starve the bearings of lubrication, the fittings from the machine housing were attached to the secondary housing. Each lube line for their respective bearing was labeled to ensure mixing consistency. Figure 97 allows for both housings to be seen. The air pressure into the secondary housing block was kept at a constant 26.5 psi, the same pressure as what the primary block would receive during normal machine operation.
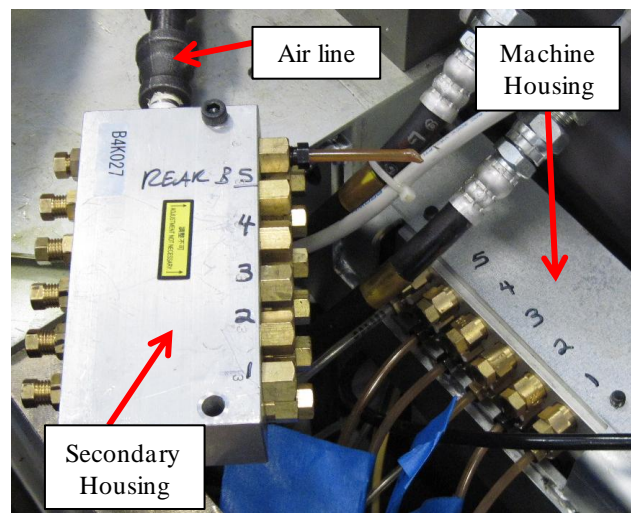
Figure 97: Air-Oil Mixing Blocks.

Unfortunately, the spindle had to be monitored at all times during this portion of the testing to ensure that the bearings did not burn up as there is no way to stop the spindle via the API. Therefore, this test could not be run indefinitely. Hence, the testing could only be performed in 7 to 8 hour intervals.

9.3.1 Trial 1 – No Load Condition

Initially, the spindle was run for more than 40 hours with no oil being injected into the bearings and no change was seen for any of the measurements. The air supply was turned on and off during this time to see if the air would assist or hinder the oil evaporation process off the bearing surfaces. It did not seem to matter for the ultrasonic readings, however, when the air was turned on, the bearing temperatures for B3 and B4 spiked, then returned back to their steady states. This can be seen in the temperature graph in Figure 98.

To help expedite the process, as well as simulate a spindle cooling problem, the spindle cooling unit was turned off. The spindle cooling unit helps to regulate the spindle temperature by first cooling the lower bearings, then the spindle motor, and finally, the rear thrust bearing before running through a refrigeration cycle. The cooling unit was set for ambient temperature (by default) at 22.3°C, keeping the bearings at a constant 25-26°C during spindle operation.

The spindle cooling unit was powered off while the spindle was rotating under no load. There was an immediate increase in both the ultrasonic and temperature measurements, as indicated by Figure 98, and no increase in the overall vibration reading. Fifty minutes into the test, at around a 4 dB reading from the ultrasonic sensor, the machine threw an alarm and automatically turned off the spindle. It appears that the machine's temperature safety feature allows for a 12°C difference above ambient temperature before it will shut off. The temperature profiles for T1 – T4 were in the same order as the bearing configuration (as expected), with the highest temperature at

machine shutdown was B4 at 36.5°C, while B1 had the lowest at 33.3°C. At least in this case, the machine was able to prevent further bearing damage from occurring.
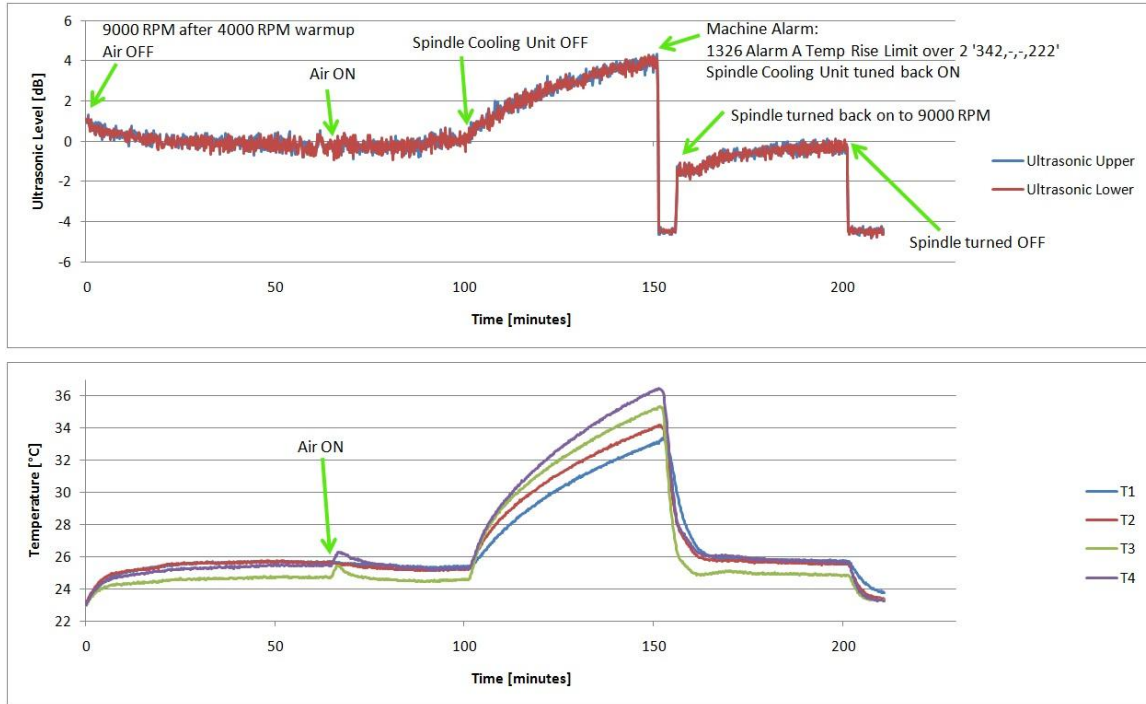
Figure 98: Lack of Lubrication – Trial 1 – Thermal Compensation ON.

It just so happened that a frequency spectrum chart was saved right before the alarm. It can be seen in Figure 99. There was no change in the overall vibration at this point; it was still at 32 mg. However there were changes in the frequency spectrum. The magnitude of the running frequency did not change considerably, however the BPFO bearing fault increased by 298 mg to 646 mg. This is quite a considerable jump with supposedly no microscopic damage occurring in the bearing yet based on the ultrasonic measurement. This was another reason why it was thought the bearings were initially damaged, even though that was not the case.
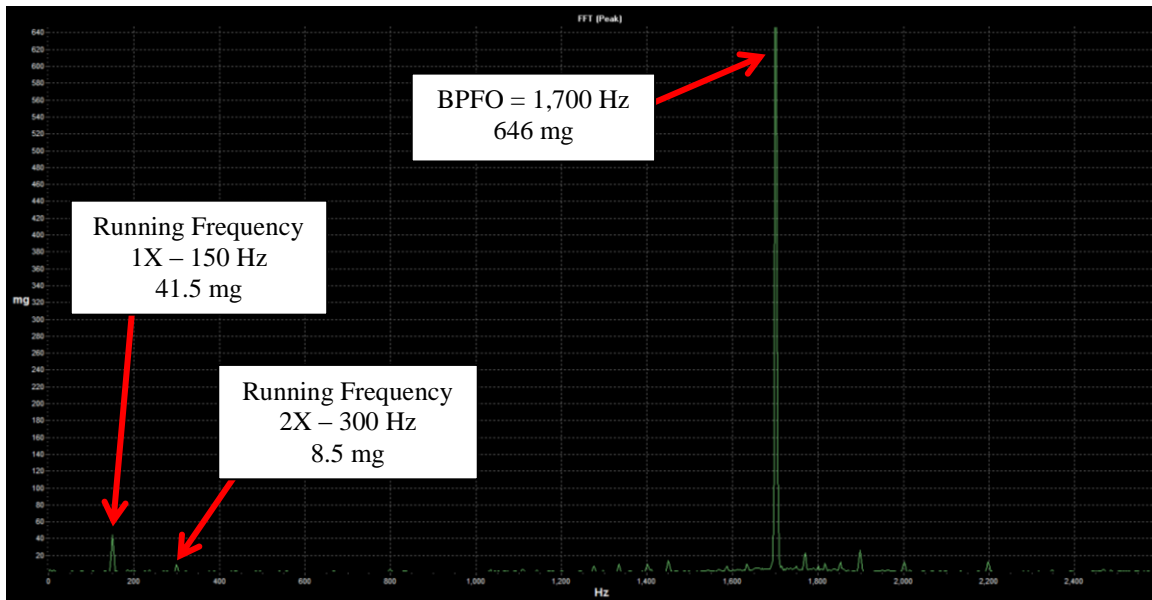
Figure 99: Frequency Spectrum at a 4 dB Reading.

After the alarm was generated, the machine was given a few minutes to cool back down before it was started back up to see if there was any permanent damage done to the bearings. The ultrasonic reading was used to determine this. It turned out that the bearings were about 1.5 dB quieter (0.84 times or 16% quieter) than the baseline reading at the time of this spindle startup. This is also shown in Figure 98. Therefore, the amount of friction in the bearings was reduced until the machine was able to achieve its baseline reading again. This same phenomenon was also seen when performing the RPM Range Investigation for this mill spindle. Figure 98 shows the ultrasonic level eventually returns back to 0 dB. The bearing temperatures had almost returned back to their steady state temperatures before the spindle cooling unit was turned off. The next time the machine was started, the ultrasonic levels read 0 dB, therefore indicating that no damage had occurred.

The frequency spectrum also validated that no significant damage had occurred. Once the machine was allowed to cool down, the BPFO magnitude returned to its baseline value of about 350 mg for the same 9,000 RPM running speed. Therefore, the realization was made that the increase in the BPFO magnitude was due to the thermal growth in the bearings, which allowed for the bearings to have more "play" in them due to greater radial clearances. This allowed them to exhibit more vibration at the BPFO frequency.

9.3.2 Trial 2 – No Load Condition

To prevent the thermal compensation system from generating an alarm, it was turned off and another lack of lubrication trial was run. As shown in Figure 100, once the cooling unit was turned off, there was another rise in both the ultrasonic and temperature readings. However, once the ultrasonic level reached 4 dB about an hour later, it started to decrease until it stabilized at 2 dB. During this decrease in decibel level, the temperature was still increasing but its rate of change was getting slower. It is speculated that due to the bearing's ceramic elements being so hard, the bearing is able to exhibit some self-healing properties by smoothing out any small race imperfections previously caused from the lack of spindle cooling.

An FFT reading was recorded at the point where a maximum 4.2 dB was read, shown in Figure 101. The running frequency had no change, however the BPFO was even higher than that of the previous lack of lubrication test, reaching 794 mg (a 148 mg increase).

As soon as the spindle cooling unit is turn back on, there is a sharp increase in the ultrasonic level from 2 to 3 dB followed by a sharp decrease in the ultrasonic level to about -2.5 dB. The increase may be due to the thermal shock initially given to the bearings to start their cool-down process. The quietness of the bearing after cool-down may also be due to the bearing's self-healing capabilities, as the ultrasonic reading dropped below -2 dB.
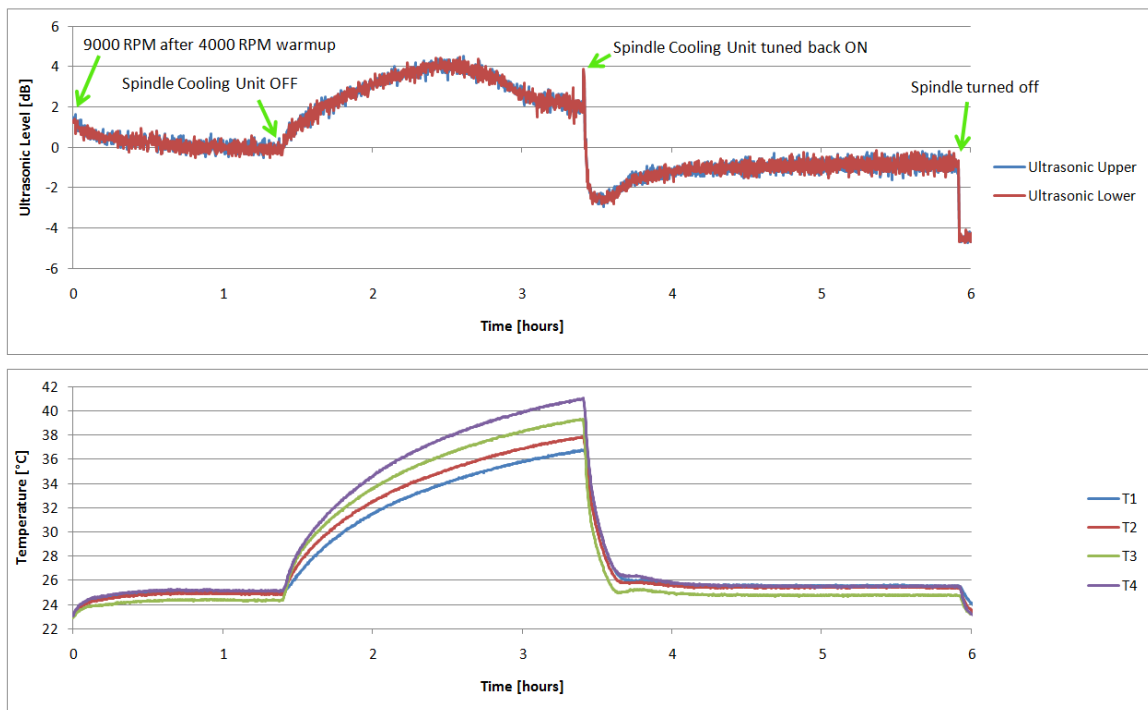
Figure 100: Lack of Lubrication – Trial 2 – Thermal Compensation OFF.

Figure 101: Frequency Spectrum at the 4.2 max dB Reading.

After the cool-down, it was noticed that the bearing temperatures did not reach their previous steady state values from before the spindle cooling unit was turned off. This may have something to do with the ultrasonic reading not going back to 0 dB or vise versa. A verification check was performed to see if the dB level would go back to 0 dB like it did in the previous test. The readings did go back to 0 dB the following day, after the machine was warmed up.

9.3.3 Trial 3 – No Load Condition

The same test as Trial 1 and 2 was performed; however, the cooling unit was left off for a longer period of time (5 hours) to try to get the bearings up to 60°C. This is the point where the damage due to heat can start to occur in the bearings, according to the bearing manufacturer. Reaching 60°C was unable to be accomplished running in an unloaded state, as indicated in Figure 102.
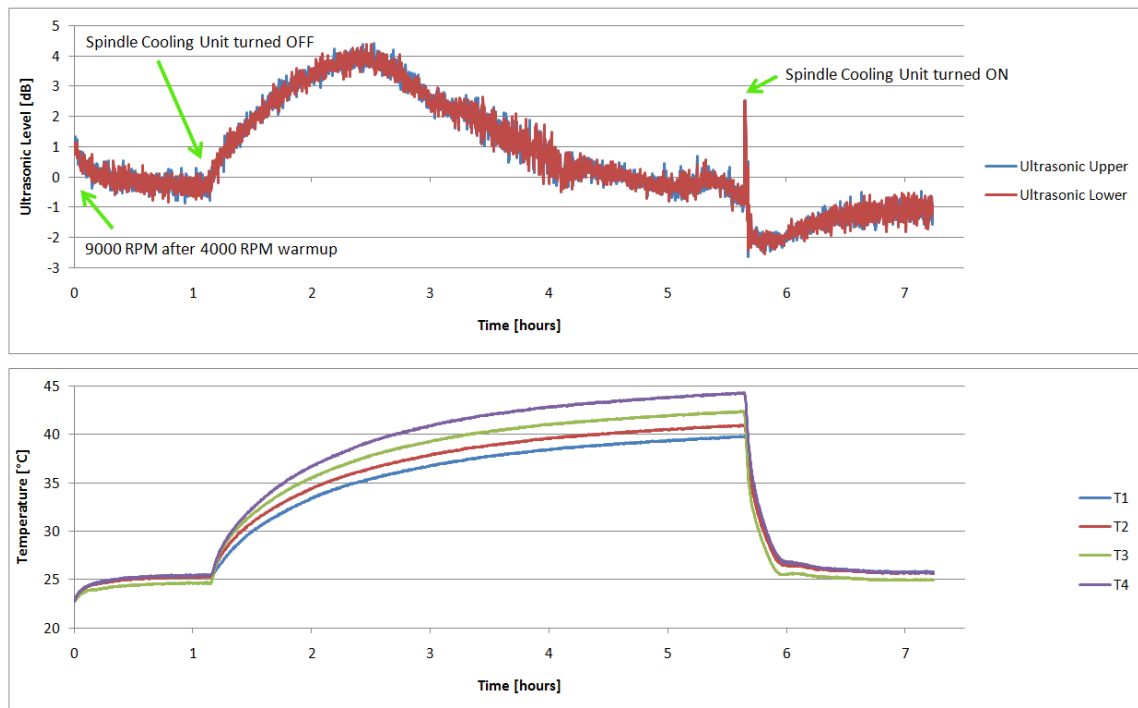
Figure 102: Lack of Lubrication – Trial 3 – Thermal Compensation OFF.

There seems to be a definite relationship between the maximum ultrasonic level reached (4 dB) and the temperature. It can be seen that both the ultrasonic level and the temperature are immediately affected by the spindle cooling unit being turned off. The temperature for B4 reached 38°C at the maximum ultrasonic level for this trial as well as the previous one. The temperatures appear to be reaching a steady state value due to their reducing rate of change as time progresses.

An increase in vibration at the BPFO was noticed on the beginning of the downside of the ultrasonic "hump" in the curve, reaching as high as 860 mg at this particular frequency around an ultrasonic reading of 3.5 dB.

139

Again, once the cooling unit was turned back on, there was a sharp decrease in the ultrasonic level to a negative dB level. At it did previously in Trial 2, the ultrasonic level approached 0 dB after this decrease.

9.3.4 Trial 4 – No Load Condition

A final trial was performed (before loading was applied to the spindle). In preparation for this test, approximately 3-4 mL of alcohol was injected into each bearing to try to wash the rest of the lubricating oil from the bearings (if any oil films still existed). The spindle was left to run for one hour at 50 RPM to let the alcohol work onto and around the bearing surfaces. Then the test could begin. The results can be seen in Figure 103.
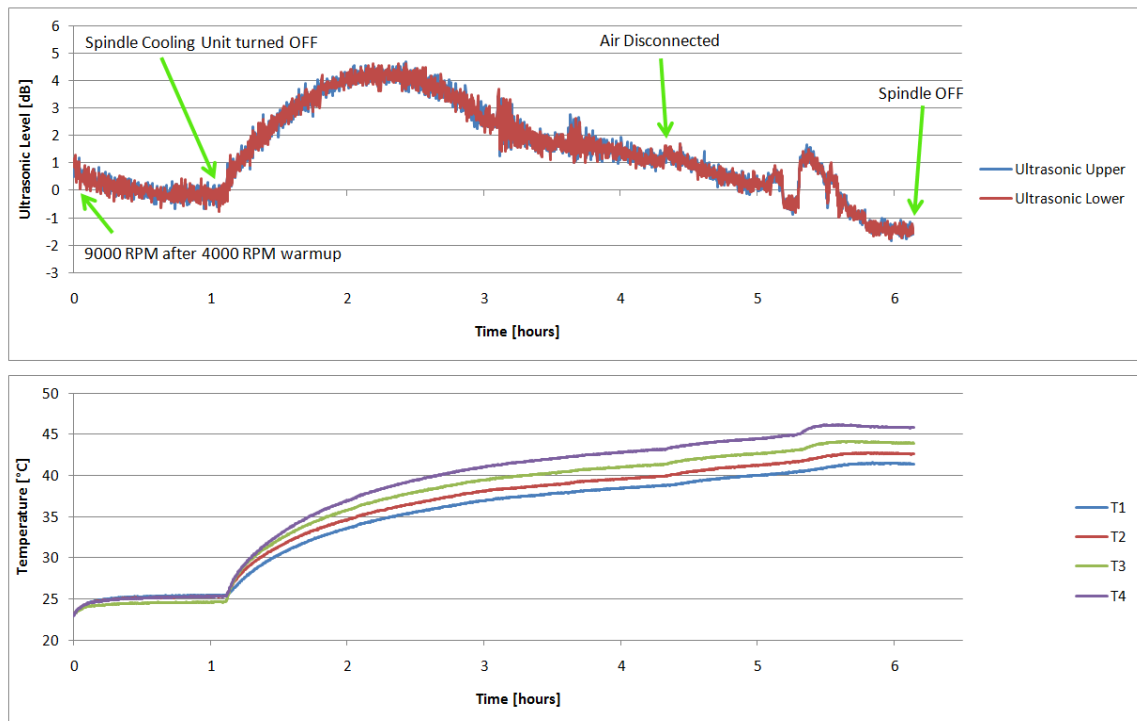
Figure 103: Lack of Lubrication – Trial 4 – Thermal Compensation OFF.

140

The results show that like the previous test, the ultrasonic level reaches 4 dB maximum before the level starts to decrease. It was noticed that a peak BPFO of 845 mg occurred at the same ultrasonic level, 3.5 dB as the last test.

After about three hours from the cooling unit being turned off, the air was disconnected to allow for more heat to be generated as it has somewhat of a convective cooling effect. This allowed the bearing temperatures to increase at a slightly greater rate. At about 5 hours and 15 minutes, the temperature started to increase at a greater rate of change than its previous current rate, seen in Figure 104. The ultrasonic reading also saw a quick rise in value, only to drop back down again. Once it appeared the temperature started to decrease, the test was stopped and the machine turned off.
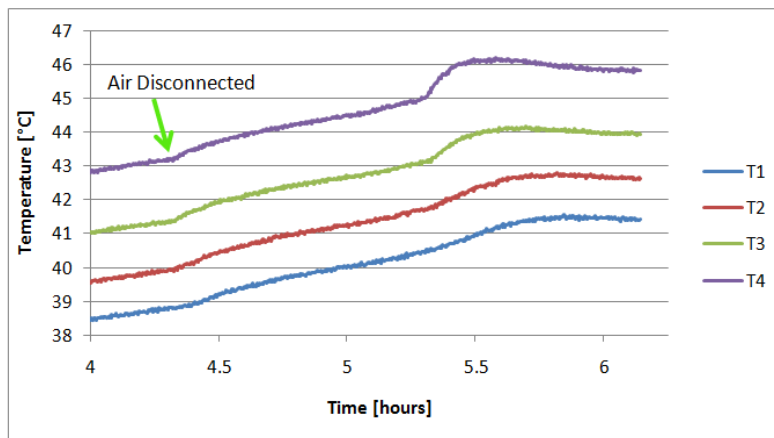
Figure 104: Temperature Close-up for Trial 4.

For comparison purposes, the data collected for the upper ultrasonic sensor in Trials 3 and 4 were overlaid on top of each other and shown in Figure 105. Their shapes are very similar in nature, so the behavior is consistent. The readings also tend to have more variability in between the 3 and 4 hour timeframe as well. It is unknown as to the cause of this.
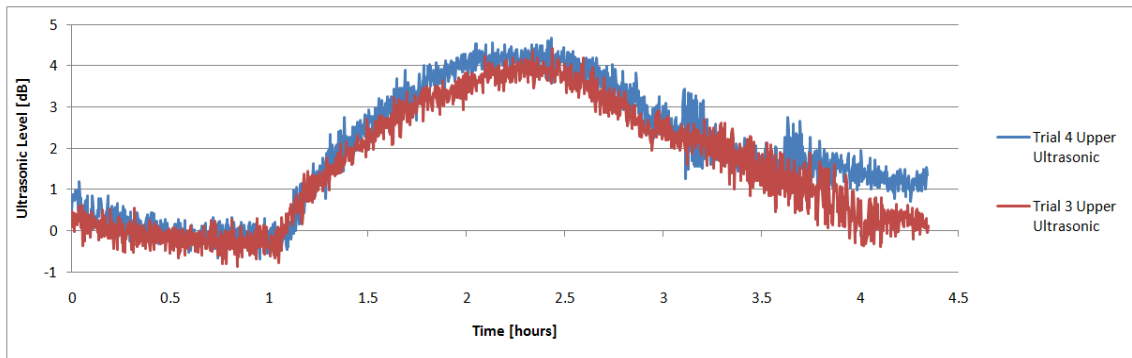
Figure 105: Comparison Between Trial 3 and Trial 4.

9.3.5 Baseline Reading Check

Another set of data was gathered after Trial 4 had occurred and can be seen in Figure 106. Up until this point, it appears that the no damage has been inflicted to the bearings as their dB levels are still at 0 dB. The BPFO was at 351 mg, which can be considered the same as the baseline reading. The temperature is in the same 25°C range as the baseline was as well. With no measureable damage occurring in the bearings, it was concluded that the spindle needed to have an external load applied to it to help the bearings degrade. It is also a possibility that the lubricating oil has not left bearing surfaces at this point, which could be why no changes have been seen.
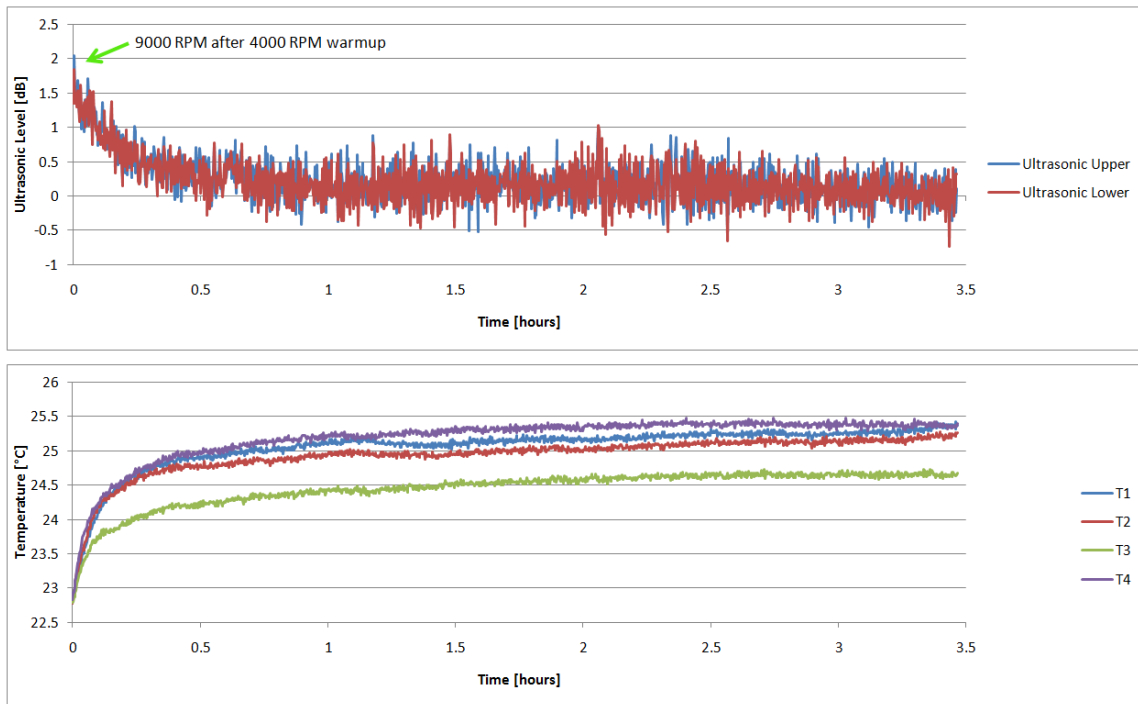
Figure 106: Verification Test to Re-zero the Decibel Level after Trial 4

9.3.6 Trial 5 – Loading Applied

Up until this point, the spindle had about 90 hours of run time for the 9,000 RPM speed, during which the air-oil lubrication system was functioning properly for the first 18 hours. The spindle was run for another 3 hours (75 hours total without lubrication) before loading was applied.

In order to apply loading to the spindle, a fixture was designed and built to perform this task. The fixture consists of a bearing housing, two bearings, a shaft, and a steel ball. Figure 107 shows the internal assembly while Figure 108 shows the entire assembly clamped into the vice on the machine. This fixture allowed for the machine's z-axis to be loaded to the desired level while the spindle was rotating. The tooling used

was another empty tool holder; however it was several inches longer than the tool that was used for all prior mill tests.
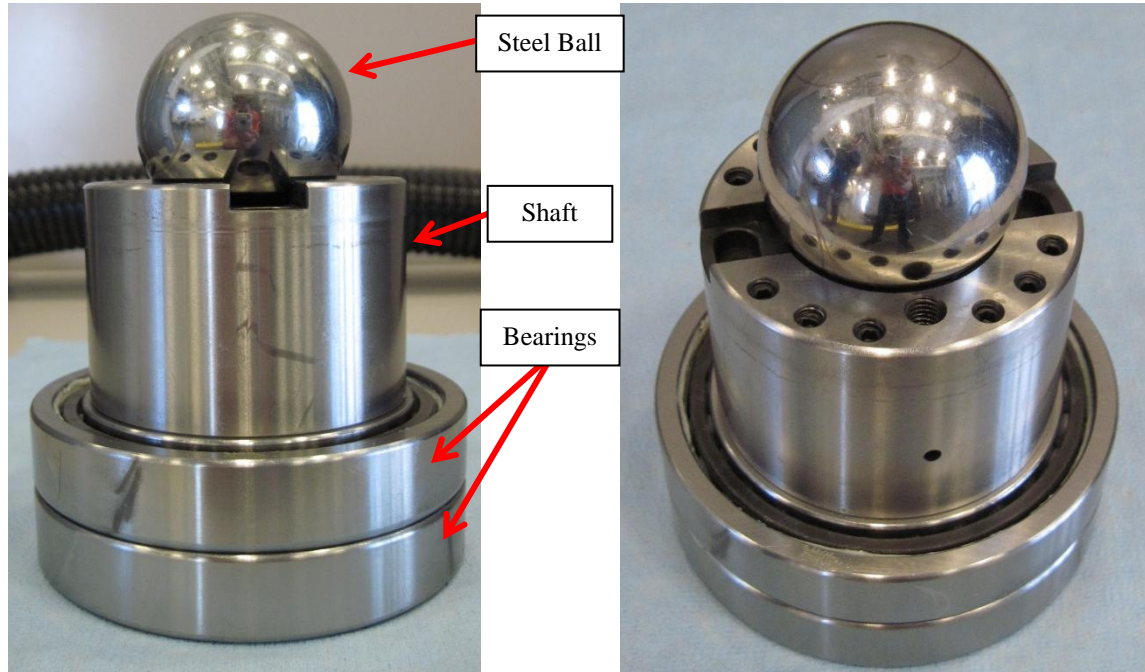
Figure 107: Internal Assembly of Loading Fixture.

The bearings used in the fixture were the same type as the ones in the spindle. However, there were some concerns about these bearings failing due to a lack of lubrication on them as well. Only bearing grease was applied to them, not a constant supply of oil. The bearings did not have any cooling supplied to them either, furthering the concerns. Another concern was that they were pulled out of a used spindle and may affect the vibration reading if damaged, but no resistance could be felt when they were rotated by hand so they were assumed to be in good condition.
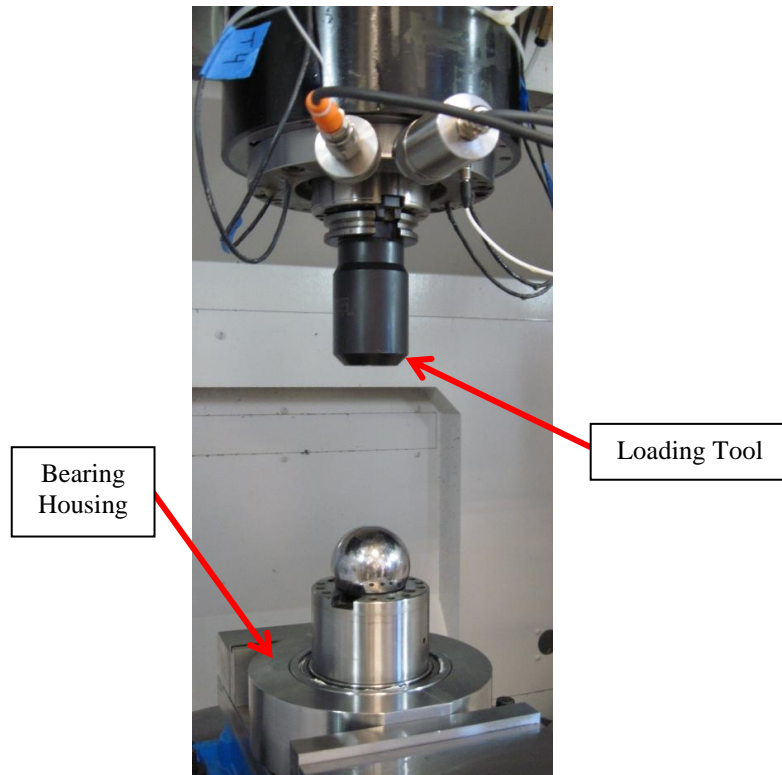
Figure 108: Loading Fixture Clamped into the Machine's Vice.

Only one test with loading was able to be completed before the spindle bearings failed. The events leading up to this failure will now be described, with each part described in detail. Data was somewhat lacking during this test because the failure occurred during the testing of the fixture itself. However, some data was captured.

The overall data capture can be seen in Figure 109. This spindle was run for more than 2 hours before any loading was applied. It was first noticed that the loudness of the bearings seemed to change from the last test by a decrease of 2 dB. This is probably thermal related (building temperature) as the graph shows the ultrasonic reading is steady at -2 dB. It was noticed that the RMS acceleration had also increased from the low 30 mg's to 50 mg. This could be due to the spindle being moved and lowered (cantilevered out along the z-axis) allowing for more side to side travel to occur (very minimal though).

A look at the FFT did show a higher running speed as well, about 55 mg, however the BPFO was still at the normal baseline value (360 mg).
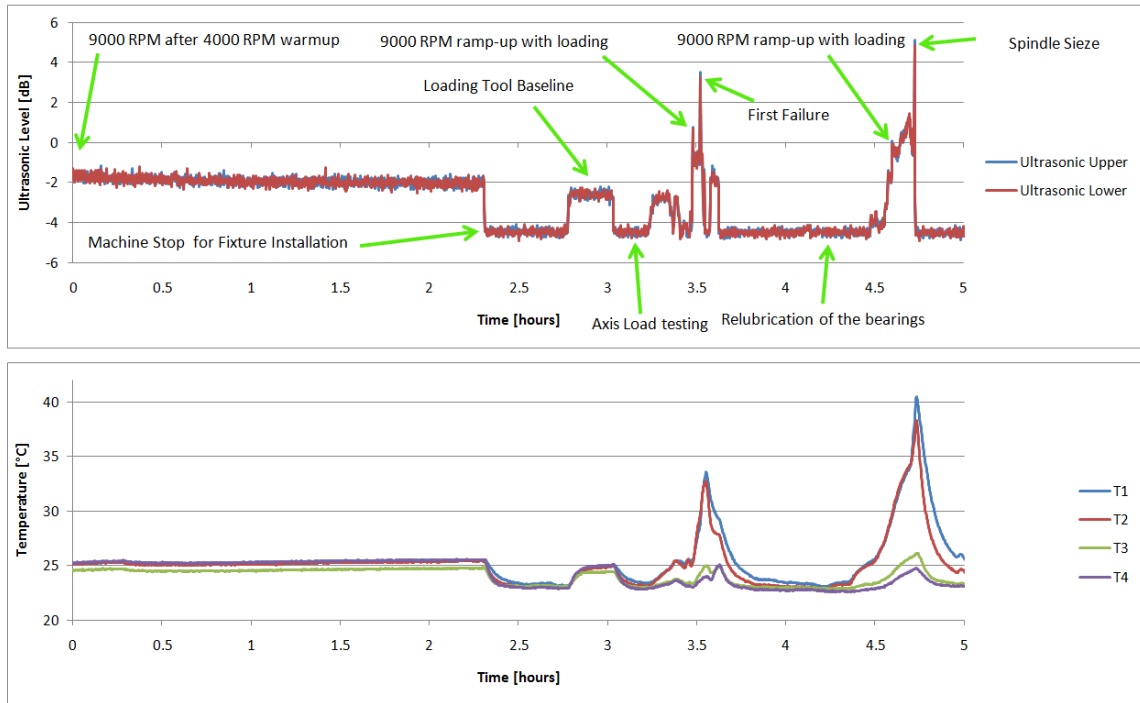
Figure 109: Lack of Lubrication Trial with Loading.

The loading fixture was then installed in the machine and the loading tool in the chuck. A baselining of the loading tool with no load was performed to see how the readings would change. Readings were taken for 12-15 minutes to ensure a steady state condition was reached. The ultrasonic and temperature readings can be seen in Figure 110 where the ultrasonic reading for both sensors was -2.57 dB. Therefore, the loading tool supposedly made the bearings quieter (a minuscule difference from -2 dB). The temperature was the same as the original empty tool holder at 25°C.

The spindle vibration was very different from the previous tool. The RMS overall vibration value was 420 mg, 14 times higher than the empty tool holder's baseline

reading. This amount of vibration was very noticeable standing next to the machine as the floor was vibrating. Some additional vibration can be expected as the tool is more massive (3.38 lbs versus 2.12 for the empty tool holder) and is 2.25 inches longer (therefore providing a larger bending moment on the spindle). The FFT chart, shown in Figure 111, shows the spindle's running frequency to now be 13 times higher than the empty tool holder's running frequency. The running frequency's second harmonic is also higher, by about 4 times. These two items account for the increased overall vibration. The BPFO was in the same range as the empty tool holder's BPFO, it being 309 mg. This shows that the exchange in tooling does not have an effect of this frequency, which it should not.
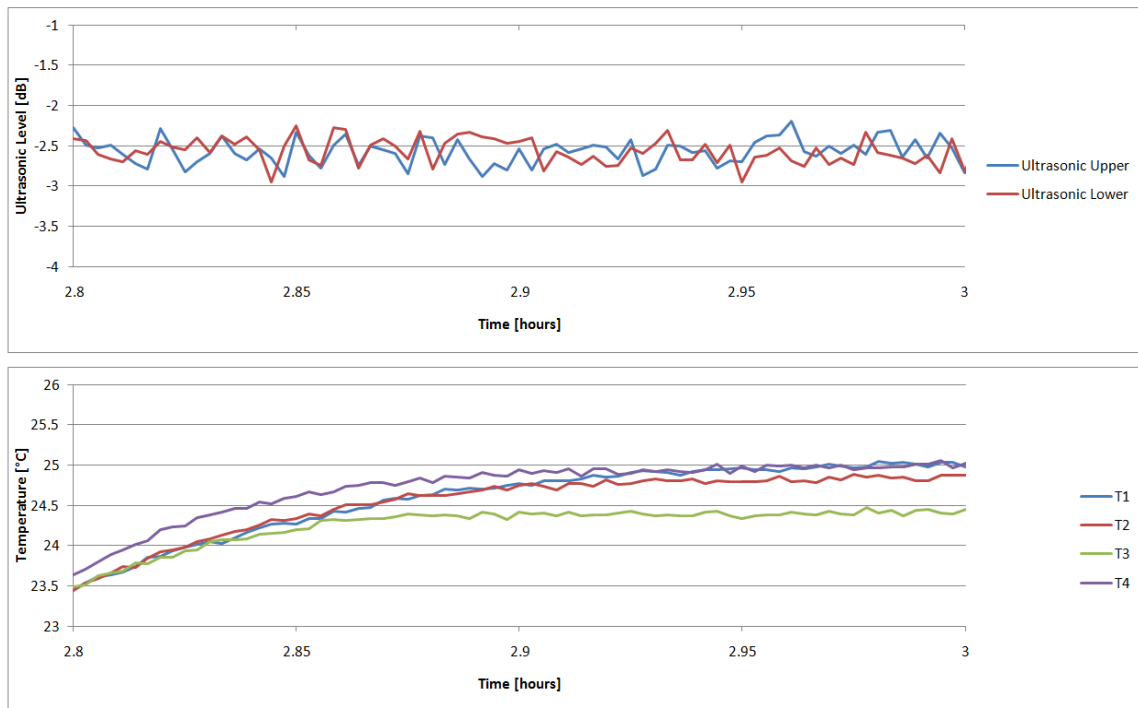
Figure 110: Baseline Readings for the Loading Tool with No Applied Load.
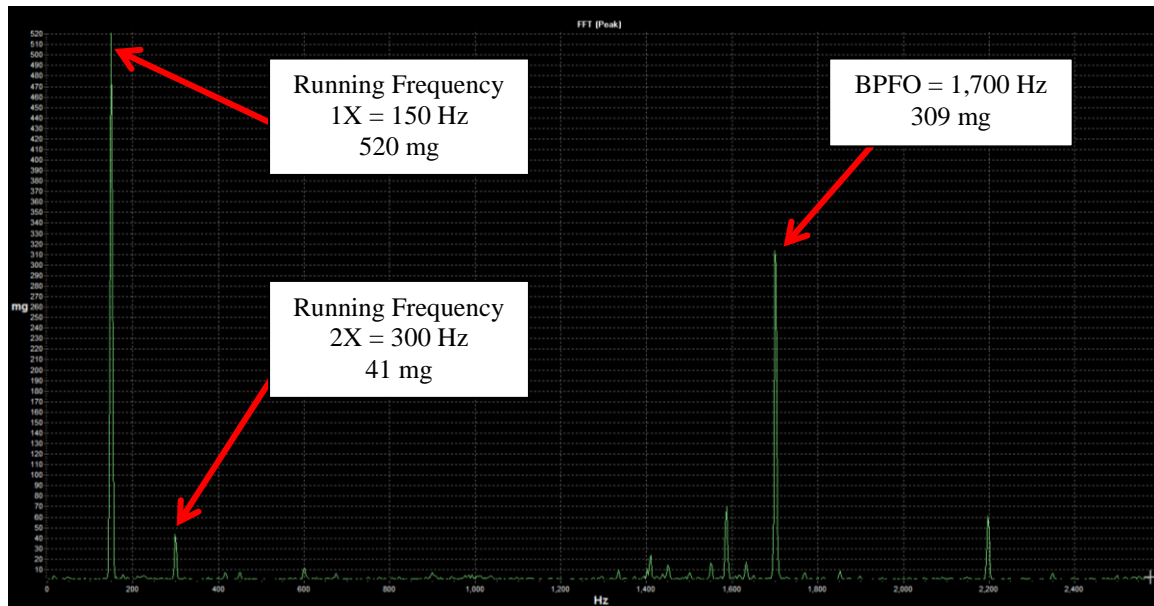
Figure 111: Frequency Spectrum Baseline for Loading Tool

At this point, the spindle load was at 1% and the z-axis load was at -74%. The negative indicates the loading was toward the ground. This is due to the weight of the spindle itself. The z-axis was then loaded to 50%, starting with a very low spindle speed (50 RPM) and working up to 9,000. This can be seen in Figure 112. It is unknown what speeds correlate to the data in the figure before 9,000 RPM. The thermal growth for the bearings in the loading fixture could be seen as the z-axis load increased up to 105% and then remained at that percentage. There was an initial spike in the ultrasonic reading to about 1 dB from the original baseline, as indicated in the figure, which was most likely due to the spindle changing speeds. The ultrasonic level then decreased to -1 dB and remained at this level for about 2 minutes. The spindle was only running for 2.5 minutes before there was a sharp jump in the ultrasonic reading to 3.5 dB. At this point, there was a screeching sound coming from the machine. At the same time, the FFT chart became saturated, having many spikes over the whole frequency range. The spectrum was

148

updated a second later and the BPFO had dropped to 52 mg. At the time of the sound, the spindle load was at 20%. The machine was run for a few more seconds and then stopped.

The fixture was checked to see if its bearings were burning up (as indicated by the screeching sound [70]). It was warm, as was the spindle, but not too terribly hot. The temperature readings for the spindle bearings indicate that the temperature for the lower-most bearing, B1, only reached a maximum of 33.5°C. This maximum temperature occurred after the machine was stopped. The temperature is delayed because the probes are mounted in a sub-casting that surrounds the bearings. However, this 33.5°C temperature did not occur until 2 minutes after the screeching sound was heard and the rate of change was fairly constant and not that drastic.

Notice how the temperatures for B1 and B2 are much higher than B3 and B4. This is due to the loading experienced by the lower two bearings. These lower two bearings are the ones that take the load during machining; therefore they would experience the same phenomenon in the real world.
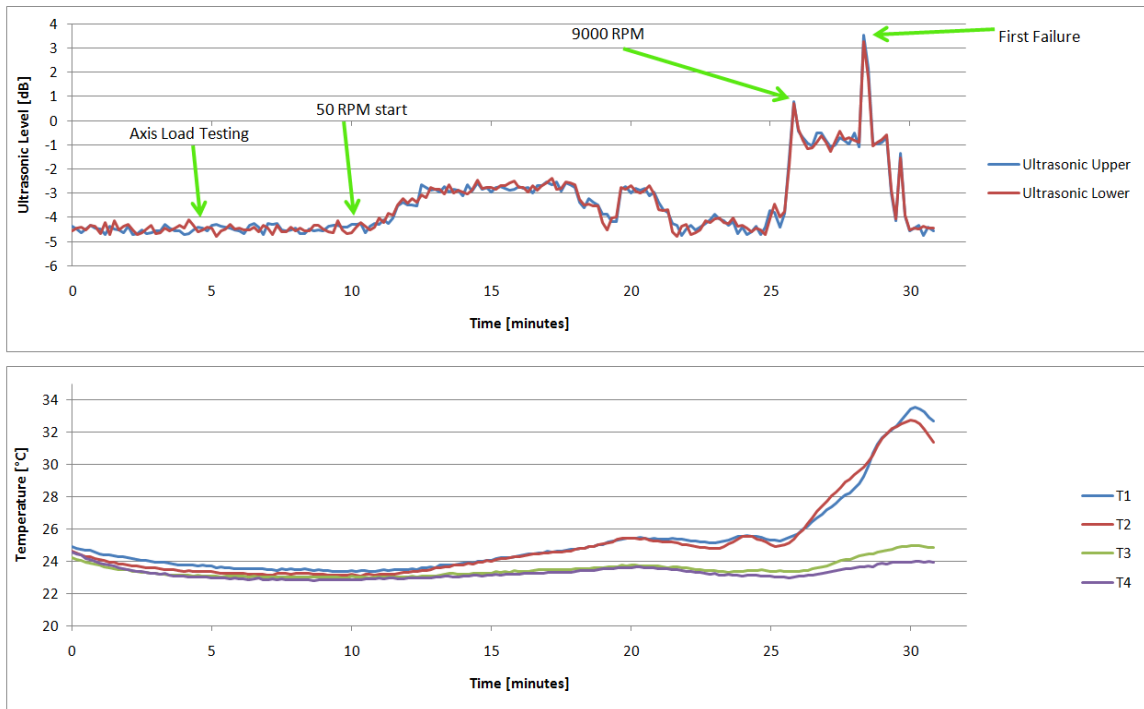
Figure 112: Spindle Loading Data up to the First Indication of Bearing Failure.

At this point the spindle still was able to rotate freely, however it is assumed that the sound heard was the initial bearing failure occurring within the spindle. This was validated by the phenomenon which occurred in the FFT spectrum before and after the sound. At this point in the testing, it was assumed the condition of the spindle bearings was still good as indicated by the temperature and ultrasonic values.

Some more testing was performed on the loading fixture to make sure that the ball stayed in place and so that ball movement could be ruled out for the cause of the screeching sound. The ball was found to have stayed in place. At this time, the lubrication system was brought back to the bearings as a concern about destroying the spindle bearings was a real possibility. The spindle was rotated at 50 RPM for

150

approximately 45 minutes to allow for the lubrication to be restored (just in case there was no oil on the bearings).

After this 45 minute relubrication period, the spindle was again slowly brought back up to 9,000 RPM, this time starting with a z-axis load of 10%. Figure 113 shows that again at 9,000 RPM, there was an initial ultrasonic spike, this time to 0 dB from this tests' baseline. This value started to decease slightly and the slowly started to increase. The ultrasonic readings appeared to have the same sort of trend that was seen when the spindle cooling unit was turned off: an increase in the reading followed by a decrease, which was seen. Then, there was a sharp spike, reaching 5 dB this time, the same screeching sound was heard, and the machine was shut off. At this point, the machine would not let the operator issue an M5 (spindle stop) command. Therefore the reset button was pushed. This stopped the spindle. The sound seemed to coincide with the machine loadings as the z-axis loading was at 95% and the spindle load was 22%, which was very similar to the previous time.

Again, both the fixture and spindle were checked, only this time, the spindle was much hotter than the fixture. Therefore, this provided the knowledge that the spindle bearings were failing. The spindle was then rotated at 50 RPM to check the spindle load. The load meter indicated an 8% load and a squeaking sound could be heard as the spindle was going around. The spindle could not be rotated by hand as one of the bearings had failed.

The temperature graph tells a different story. It was not noticed during testing, but as the machine was being relubricated, the temperature started to increase, even at the

50 RPM speed. By the time 9,000 RPM was reached, the temperature was almost at the point where it was when the screeching sound was heard. The temperature for B1 and B2 started to increase more rapidly as the ultrasonic reading decreased (just before the spike). Thirty seconds later, the maximum temperature for B1 and B2 reached 40.5°C and 38.3°C respectfully after the spindle was stopped. A dotted vertical line stretching across both graphs has been used to allow for this to be seen more easily.
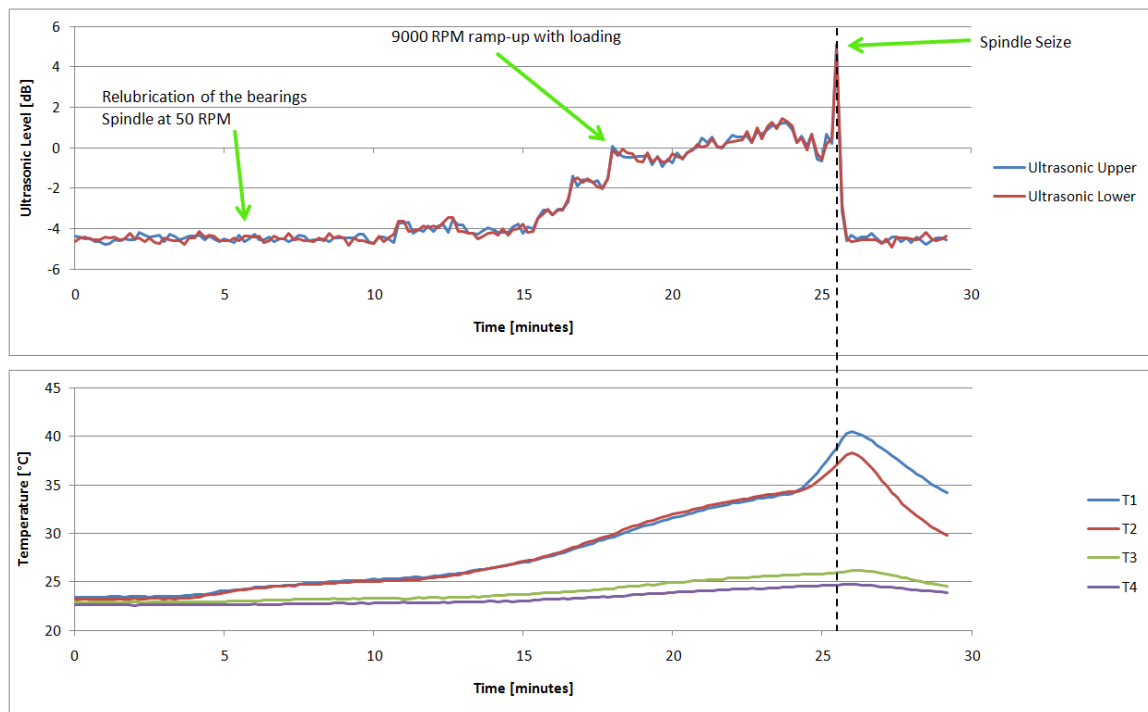
Figure 113: Spindle Bearing Failure and Seizure.

9.5 <u>Bearing Failure Analysis</u>

The reason for the spindle seize was due to a cage failure in the first bearing, B1. Upon the spindle seizure, the front cap was pulled off to reveal the failure. This can be seen in Figure 114. This was the source of the screeching sound heard during the loading test.

a) Cage Particulate in the Front Cap   b) Particulate inside the Spindle
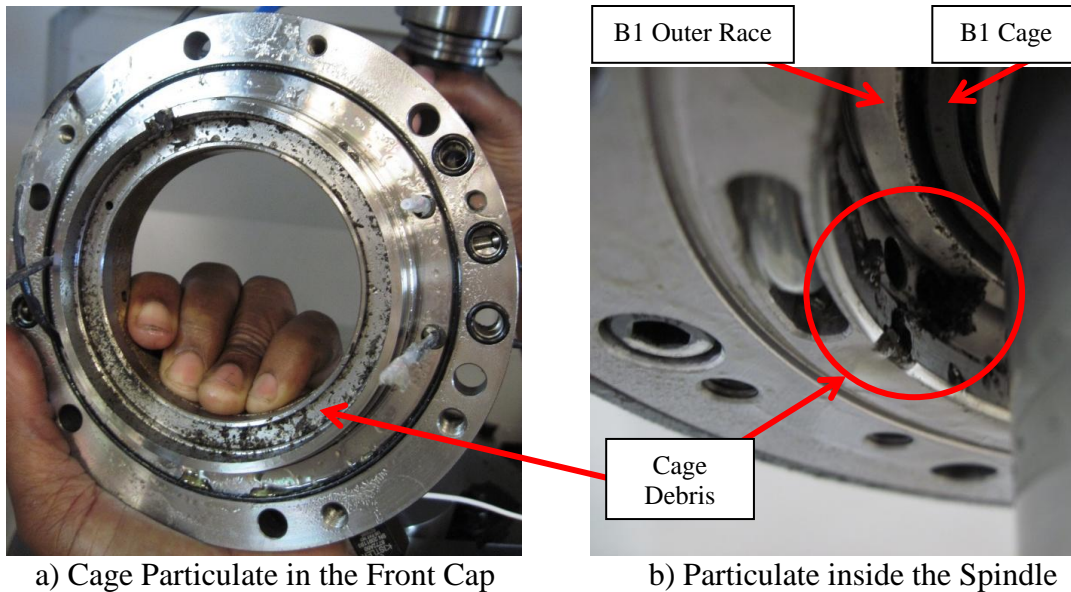
Figure 114: B1 Cage Failure.

Further bearing analysis was performed in order to identify other bearing problems, such as the BPFO frequency seen throughout this destructive test. The spindle was disassembled and all four bearings were removed. B3 and B4 did have oil in them and felt normal (no resistance) when rotated by hand. This suggested that these bearings were in good condition.

B2 was disassembled into its separate components and inspected. All components seemed to be in good condition. There were no markings on the inner or outer race.

B1 was the only bearing with damage from the testing. The cage, shown in Figure 115, was melted and broken, suggesting that it failed due to the heat. It was noticed that there was no oil in this bearing, even after relubrication. This is most likely due to the heat generated by the failure as well.

There were no markings on the inner or outer races for this bearing as well, ruling out the BPFO defect for all four bearings. The fact that there were no markings or

discolorations on the races for B1 and B2 suggests that the bearings did not get hot enough to damage the balls or the races during the spindle testing.
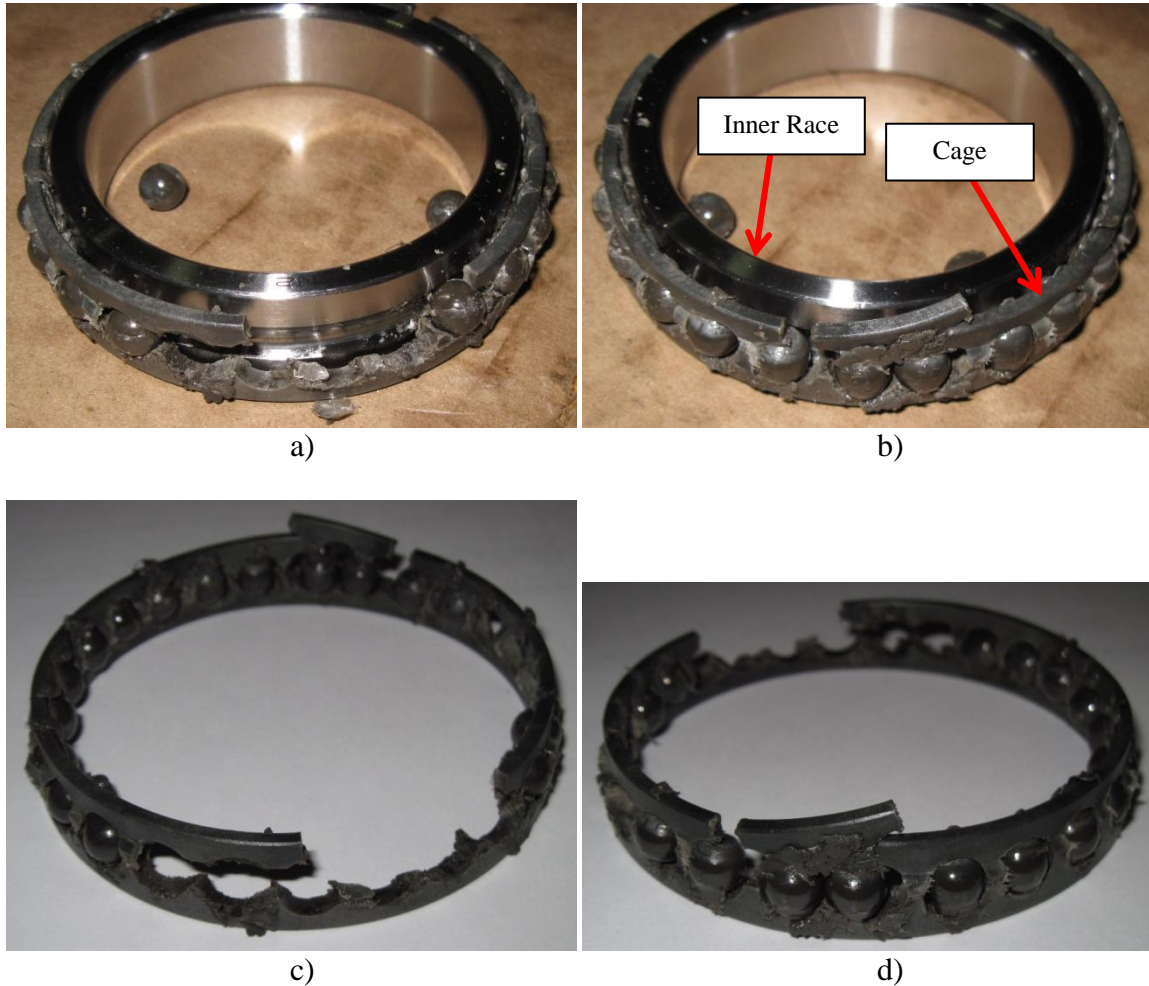
Figure 115: B1 Cage Damage.

9.6 Discussion of the Data for the Bearing Failure

The B1 bearing obviously failed due to a lack of lubrication condition and was the only bearing that showed signs of problems. Lack of lubrication tends to be the most common cause for a bearing failure to occur. Once the lubrication is gone, the other bearing failure modes will follow (wear, pitting, spalling, etc.) [70]. In this case, it was a cage failure. However, in bearing failure analysis, it is important to determine the initial

cause of the lubrication failure [70]. Obviously, the failure was due to the removal of the lubricating oil. But let's take it one step further: why did the cage fail?

The data leading up to the cage failure is somewhat inconclusive. The temperature never really got that hot and was 6°C cooler than when the spindle was running with no lubrication. However, the spindle cooling unit was running when the bearing failed. It was 22°C on one side of the temperature probe as that was the temperature of the cooling fluid. On the bearing side, it was probably just below 60°C to get an average of 40°C. This is assumed as the thermocouples where placed in the bearing housing, where the bearings are on one side and the spindle cooling fluid is on the other.

With that being said, the bearing cage is a type TYN. This designation lists the cage as a ball guided polymide resin cage with an operating temperature limit of 120°C [71]. The cage material as a whole may be able to withstand the temperatures experienced even if it actually was 60°C or greater inside the bearing, however if a hot spot in the cage formed from ball friction, a cage failure could occur. Figure 115d shows that multiple hot spots had formed by the time the spindle was stopped.

Another possible cause for the cage failure is that it was slowly degrading over time, throughout the testing. This could be a reason as to why the BFPO magnitude was getting worse for the same temperature and ultrasonic level. It was noticed that the bearing lubricating oil naturally evaporates over time at room temperature, but there is still an oil film left on the bearing surfaces. This process would only be expedited with the elevated temperatures seen when the spindle cooling unit was turned off.

The injection of alcohol in the bearing cavity is the most likely cause the bearing cage to degrade. The same cage type (TYN) was submerged in an alcohol bath and left to dry out. All of the lubricating oil was removed from the cage surfaces, leaving the cage to be very dry. This simple test showed that the alcohol had the ability to remove the oils from the rolling element surfaces as well as the cage. All of the alcohol added to all of the bearings would have eventually drained down to the lowest bearing, B1, ensuring it was washed of its oils the best. With the cage being so dry, friction started to build up at the ball/cage interface. This is why multiple there were multiple hot spots in the cage and the cause for the failure.

In addition to the cage failure analysis, there are some other items that should be mentioned. The spindle load did not increase significantly during the spindle loading operation. This can rule out failure due to extreme torque. B3 and B4 had 75% z-axis load on them during all of the Lack of Lubrication Trials 1 – 4 (for 72 hours) and did not show any signs of damage, even with being at an elevated temperature for an extended period of time.

The ultrasonic levels only came up from the original baseline by 5 dB and a total of 7 dB from the no load condition in Trail 5 before loading was applied. This is below the 8 dB microscopic damage threshold. According to the dB scale, an increase in 7 dB is only a 2.2 time sound increase, much less than the 56 time sound increase that is associated with a bearing failure at 35 dB. With this being said, the ultrasonic sensor may not be able to detect a cage failure (of this resin material) until it is too late. This is

most likely because the sounds leading up to a cage failure would be much lower than the 35-40 dB range as it was the plastic resin, as opposed to metal, that was wearing away.

However, one of the more important results that came out of this testing was that both the upper and lower ultrasonic sensors fed back the same information. Therefore, the placement on the flange of the spindle is a good place to attach the sensor for the *Okuma Spindle Monitor* system, especially since B1, the lower most bearing, failed. The sensor in the upper position (on the flange) was able to detect the failure of the lower most bearing. This provides the justification that only one ultrasonic sensor is needed on this type of spindle.

CHAPTER 10: RESEARCH CONCLUSIONS AND SUMMARY

10.1 <u>Research Conclusions</u>

The testing performed provided many good insights for how the monitoring system may react based on certain conditions as well as help guide the direction for future work. As a recap, testing was performed on two different machines, a lathe and a vertical machining center to determine the ultrasonic sensor performance in various scenarios. Through statistical analysis, it was determined that an average of at least 60 samples is needed to have an accurate ultrasonic measurement. This due to the fact that the ultrasonic sensor has a very rough RMS analog to digital converter and the output signal fluctuates.

The lathe test results provided the realization that the spindle bearings have different sound levels at different spindle speeds, with the bearings being the loudest at the spindle's natural frequency. This was seen in the mill as well. The ultrasonic sensor could not distinguish between a non-imbalance and an imbalance condition. The same results occurred for both a low mass and a high mass imbalance. However, the spindle was considered to be in "like new" condition. Therefore additional testing would have to be performed on a spindle with much more bearing degradation to determine if the imbalance causes an increase in bearing sound. Testing on this particular spindle showed that the ultrasonic sensor should not be used as a vibration detector.

The testing showed that an in-process measurement can be done, however there is much variability in the ultrasonic readings. To try to reduce the variability, a hard material should be used. Chatter may be a factor in the variability of the readings which

may cause this method to be not as accurate. Therefore, an appropriate feed and speed should be selected for the material used while the measurement is being performed. Tool wear was another factor that was found that may cause the measurement to be inaccurate.

The destructive test performed on the mill resulted in somewhat of an inconclusive test as far as the monitoring system is concerned; however valuable information was still learned. While the warm-up procedure instructs the operator to run the machine for twenty minutes at various spindle speeds, the machine may not be completely warmed up. The ultrasonic readings showed that the bearing sounds become stable after more than an hour of running the spindle at a constant RPM, while the temperature stabilizes after about 15-30 minutes. Therefore, this warm-up period may need to be extended.

The ultrasonic readings were found to both increase and decrease with a rise in temperature, however, the ultrasonic sensor was able to determine that a failure was occurring at the very instant audible sounds could be heard. The maximum temperature measurements lagged the ultrasonic sensor by 2.5 minutes for the failure experienced during the test. This validates the statement that an ultrasonic sensor can detect a bearing issue before vibration and temperature [59]. However, increasing temperatures leading up to the failure showed that a problem was occurring. Surprisingly, the spindle bearings failed rather than the bearings in the loading fixture, suggesting that the cage may have already been damaged or in the process or degrading prior to the loading test, but it can't be known for certain.

The vibration seen in the test spindle was found to be normal, based on a comparison between the machine's original spindle and the test spindle. Therefore, the test spindle did not have an initial bearing problem as originally thought. Nonetheless, Okuma is currently rethinking its spindle assembly process as the BPFO fault frequency seen in the test spindle was alarming and got them thinking about what could cause the fault during their spindle assembly process. The BPFO fault frequency also allowed for the realization that the system must be baselined on a new spindle or at least it should be assumed the bearings are in "like-new" condition. If not, the readings will be skewed, giving a false representation of the extent of the bearing damage. One may think that the bearings are in the lower dB range, when in actuality, they may be emitting sound at an elevated level. This can't be distinguished by the ultrasonic sensor as the reading is relative to what its sensitivity is set to. Therefore, vibration analysis should be employed as a follow-up to ensure the spindle condition is good, as was done in the destructive testing.

The knowledge gained from this work allows for the spindle monitoring system that is still currently under development to be improved. Spindle speed has an effect on the ultrasonic sensor's output. Therefore, care must be taken to ensure that the measurement is taken at a constant spindle speed for an accurate reading. A test mode measurement is preferred over an in-process measurement as it is more accurate. The in-process measurement depends on spindle speed, feed rate, DOC, tool type, tool wear, and the material being machined. API utilization allows for some of these parameters to be

held constant, removing some of the variability in the measurement; however, a test mode allows for all variability to be removed.

Due to the ultrasonic readings having no change in the no load condition with the lack of lubrication testing, it is possible that when measuring in a test mode, the spindle needs to have a load applied to ensure the proper bearing condition is measured. A machining center may need to have a loading fixture installed to perform this measurement. A lathe would probably be ok the way it is as the chuck allows for the spindle to experience some load. Further testing would be needed to verify this.

Based on the ultrasonic/temperature relationship, bearing problems are eminent if both parameters are increasing. Temperature via the API could be added to the system to allow for a clearer picture as to what is going on in the spindle. This would allow for the system to become greatly improved as the resin cage failure was not identified until the time of failure.

The final item that allows for the system to be improved is that the ultrasonic sensor placement in the "upper location" is sufficient to detect a B1 bearing issue. Therefore only one ultrasonic sensor is needed on a vertical machining center and can be placed on the spindle without having to modify the design of the machine, including the sheet metal covers.

10.2 Spindle Monitoring System Summary

This thesis has reviewed all aspects of the new *Okuma Spindle Monitor* system for the THINC control as well as the research that went into its creation. The total system (including accessories) costs just under $2,400, allowing for a very effective system at a

very low price. This cost can become very advantageous to the end user. A few thousand dollars towards a predictive and preventive maintenance monitoring solution can prevent tens-of-thousands of dollars in lost production and unnecessary maintenance costs if the system is utilized as intended.

The discussed system uses an ultrasonic sensor as its main sensing component and provides a singular value as to the spindle condition. This will enable the machine to flag failures at the onset of the bearing wear-out phase as well as alert engineers of operation errors (ie: turret/spindle crash). Additionally, a vibration module can be included as well that makes the system even more powerful by allowing the particular type of bearing defects to be determined. The software created for the main system allows for either a *Test Mode* or an *In Process* measurement to take place, depending on the machine tool owner's preference. Other features of the program allow for the spindle's long term history to be tracked as well as viewed remotely via Okuma Constant Care. This now allows for the spindle diagnostic work to be performed from Okuma's offices, rather than at the machine's physical location. Having the main system utilize an open source architecture provides the ability to change and modify the application at will.

Since the development of this system, it has been debuted at a major machine tool manufacturers' conference to show consumers what is now forefront of machine tool innovation when it comes to predictive and preventive maintenance. The developed system may not provide a solution for fixing all spindle problems, but is a step in the right direction when it comes to on-board maintenance systems for a machine tool. One of the goals in this work was to prevent machine breakdowns, due to spindle issues, from

occurring. Theoretically, the system can do just that by providing better information to the personnel responsible for the machine. Now, they will be more informed on how their equipment is operating, before there is a spindle failure. Spindle replacement can now be planned, allowing for machine spindle failures to be eliminated.

CHAPTER 11: FUTURE WORK

Now that a foundation of information has been laid, several directions can be pursued based on the findings in this work. The first direction that could be taken is in continuing research on spindle bearing failure. More destructive testing would be needed for this research. The most valuable test would be to establish a baseline on a good spindle, simulate a crash to Brinell the bearings, and then watch how the measurements change. The spindle tested in this work failed before a simulated crash test was able to be performed. This Brinell test would be a good time to investigate whether or not spindle loading is needed to get an accurate reading. The test would also allow one to see if the system would be able to detect that there had been a crash. This would be indicated by a severe jump in the ultrasonic readings when compared to the previous measurement.

Another route that could be taken is trying to understand more about in-process measurements and how the system can be modified to allow for the measurements to be taken accurately. It would be good to investigate the same materials investigated in this study, but change different parameters and see how that affects the readings. A design of experiments study may be able to be performed to determine these affects. Different materials should also be investigated to provide more knowledge on how the material type affects the ultrasonic readings while machining.

The third and final direction that could be taken is investigating an endurance run (what this work focused on) vs. actual machining cycle with loads. Obviously, the spindle speeds and loads will change in an actual manufacturing environment. Therefore, it would be good to pick a machine that is currently being used in a production facility.

The system could be installed on a new machine or when a spindle replacement is performed and monitor the spindle bearing degradation over time. The best option here would be to select a machine tool owner who has had many spindle failures in the past and is willing to use the system.

APPENDICES

Appendix A: Glossary

Abbreviations/Acronyms

AE...Acoustic Emissions
API..Application Programming Interface
BPFI...Ball Pass Frequency for the Inner Race
BPFO..Ball Pass Frequency for the Outer Race
CBM...Condition Based Maintenance
CNC..Computer Numerical Control
DAQ..Data Acquisition System
DFT...Discrete Fourier Transform
DOC..Depth of Cut
DTU...Data Utility Transport
FFT...Fast Fourier Transform
FMEA...Failure Mode and Effects Analysis
MTBF...Mean-Time-Between-Failure
MTTF...Mean-Time-to-Failure
NC...Numerical Control
OAC..Open Architecture Control
OEE..Overall Equipment Effectiveness
OEM..Original Equipment Manufacturer
OPC..Open Productivity and Connectivity
PHM..Prognostics and Health Management
PLC...Programmable Logic Controller
PM...Preventive Maintenance
PoF...Physics of Failure
RCM..Reliability Centered Maintenance
RMS..Root Mean Squared
RPM...Revolutions per Minute
TPM..Total Productive Maintenance
VB.NET...Visual Basic.NET

Variables

B_d...Ball Diameter
BPF..Ball Pass Frequency (aka Ball Spin Frequency)
BPFI...Ball Pass Frequency for the Inner Race
BPFO..Ball Pass Frequency for the Outer Race
FTF...Fundamental Train Frequency (aka Cage Frequency)
HP..Health Parameter
N...Number of Balls
P_d..Pitch Diameter
RPM...Running Speed
θ..Contact Angle

Appendix B: System Components and Itemized Cost Listing

The list below includes all items used in the development of the discussed monitoring system:

24 Volt Power Supply	Omron S8VS-06024	
Ethernet Bus Hub	Netgear ProSafe 8 FS108	

Beckhoff I/O Modules:
BC9050	Ethernet TCP/IP Bus Terminal Controller
KL3152	2-channel analog input terminal 4…20 mA
KL9010	End Terminal

IFM Vibration Module:
VSE002	Vibration Module
VSA001	Accelerometer
EVC002	Accelerometer Cable (straight 5m)
EC2080	Ethernet Cable
F90043	Magnet (curved surfaces)

Ultrasonic Sensor Items		Vendor
Ultra-Trak 750	Ultrasonic Sensor	UE Systems
274-678	8-pos. Euro Terminal Strip	Radio Shack
277-1008	Audio Amplifier	Radio Shack
273-355	9DCV 800mA AC adapter	Radio Shack
R12-40890	Raygo USB 7.1 Sound Card	Tiger Direct

Table B-1: Main Hardware Costs.

Part No.	Description	Unit Price	Quantity	Total
Beckhoff Hardware				
BC9050	Ethernet TCP/IP Bus Terminal	$ 277.00	1	$ 277.00
KL3022	2-channel analog input 4-20 mA	$ 258.00	1	$ 258.00
KL9010	End terminal	$ 13.00	1	$ 13.00
	Ethernet Cable	$ 17.00	1	$ 17.00
				$ 565.00
Ultrasonic Sensor				
Ultra-Trak 750	Ultrasonic Sensor	$ 266.00	2	$ 532.00
	Terminal Strip (8 position)	$ 2.79	2	$ 5.58
				$ 537.58
			System Total:	$1,102.58

Table B-2: Accessory Hardware Costs.

Part No.	Description	Unit Price	Quantity	Total
IFM Hardware				
VSE002	Vibration Module	$ 617.00	1	$ 617.00
VSA001	Accelerometer	$ 135.00	2	$ 270.00
EVC002	Accel. Cable (straight 5m)	$ 12.75	2	$ 25.50
EC2080	Ethernet Cable	$ 17.00	1	$ 17.00
F90043	Magnet (curved surface)	$ 105.00	2	$ 210.00
VES003	Software	$ 49.00	1	$ 49.00
E30114	OPC Server	$ --	1	$ --
				$1,188.50
Ultrasonic Sensor Recording (1 sensor only)				
277-1008	Audio Amplifier	$ 14.99	1	$ 14.99
273-355	9DCV 800mA AC Adapter (Type K tip)	$ 22.99	1	$ 22.99
R12-40890	Raygo USB 7.1 Sound Card	$ 12.99	1	$ 12.99
				$ 50.97
			Additional Total	$1,239.47

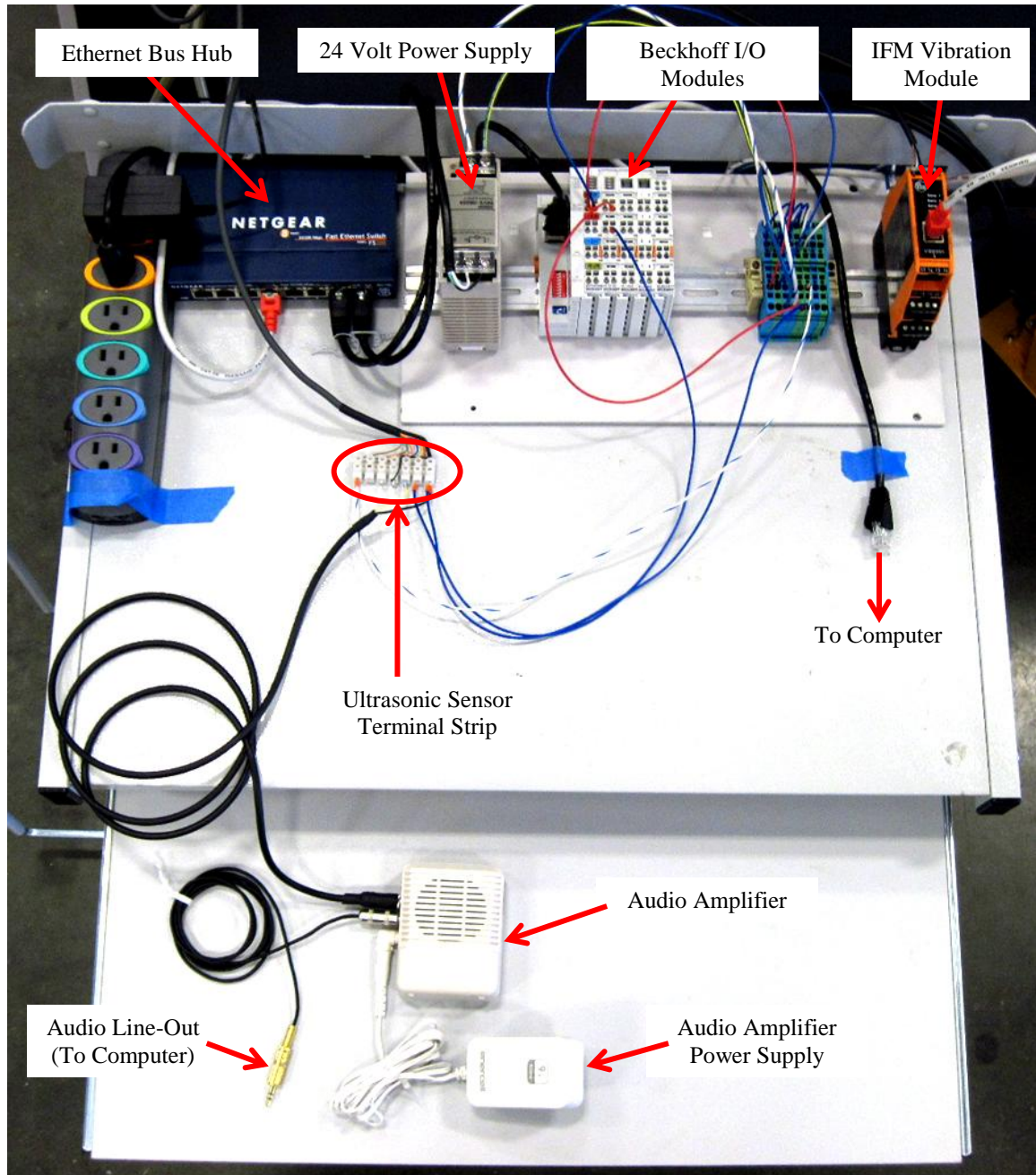Appendix C: System Setup and Wiring Diagrams
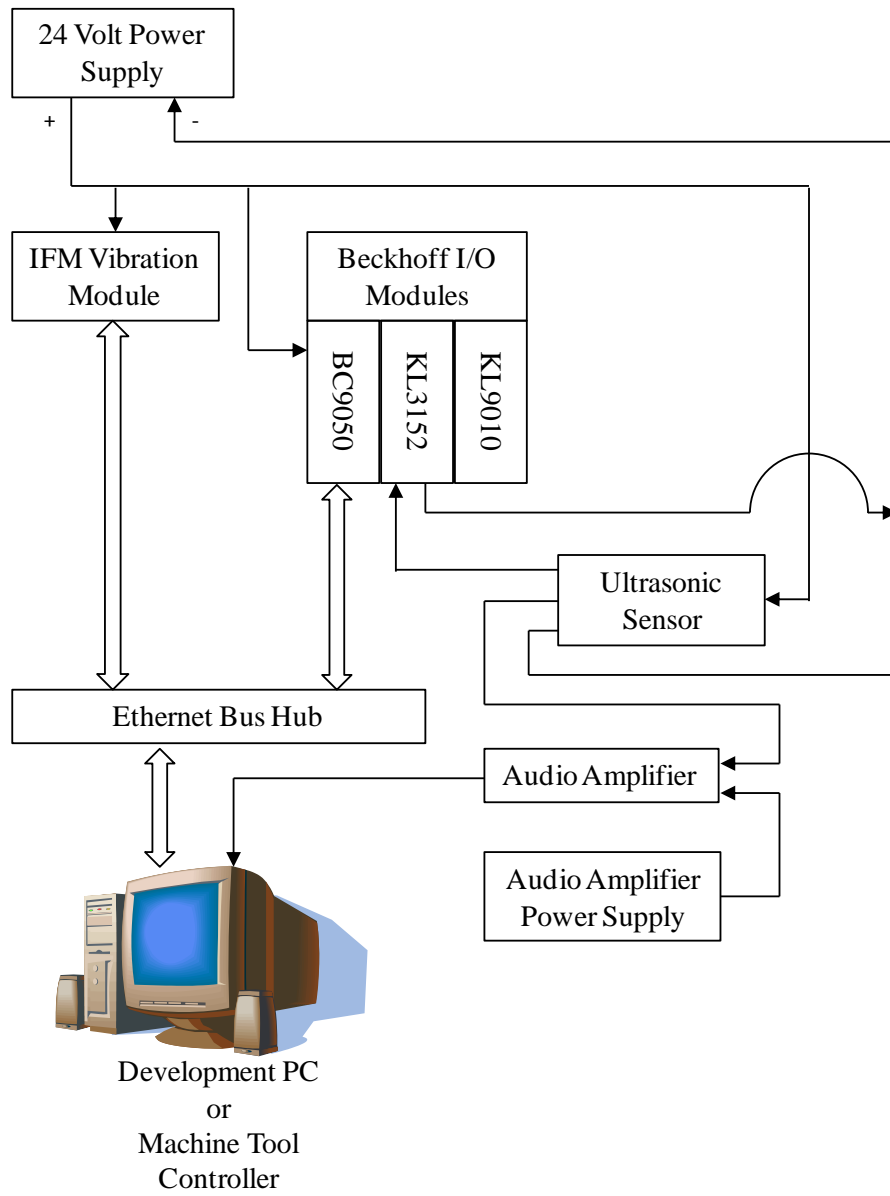

Figure C-1: Physical System Set-up.

Figure C-2: System Wiring Schematic.

Appendix D: Data Acquisition Hardware Information
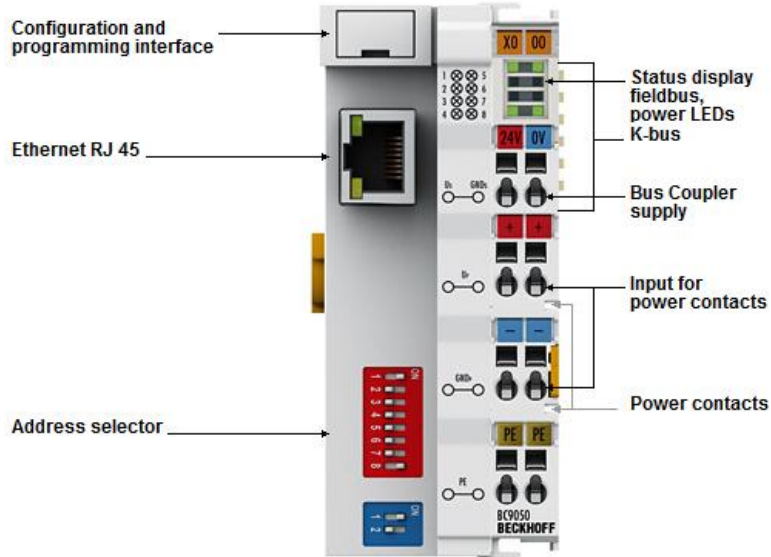
BC9050 - Ethernet TCP/IP Bus Terminal Controller [72]

Figure D-1: BC9050 PLC Controller.

Table D-1: BC9050 PLC Data.

Programming	via TwinCAT and programming interface or Ethernet
Program memory	48 kbytes
Data memory	32 kbytes
Remanent data	2 kbytes
Run-time system	1 PLC task
PLC cycle time	approx. 1.5 ms for 1,000 instructions (without I/O cycle, K-bus)
Programming languages	IEC 61131-3 (IL, LD, FBD, SFC, ST)
Online change	Yes

Table D-2: BC9050 Technical Data.

Number of Bus Terminals	64 (255 with K-bus extension)
Max. number of bytes fieldbus	512 byte input and 512 byte output
Max. number of bytes process image	2,048 byte input and 2,048 byte output
Digital peripheral signals	2,040 inputs/outputs
Analog peripheral signals	512 inputs/outputs
Protocol	TwinCAT ADS, Modbus TCP
Configuration possibility	via KS2000 or Ethernet
Data transfer rates	10/100 Mbaud, automatic recognition of the

	transmission rate
Bus interface	1 x RJ 45
Power supply	24 V DC (-15 %/+20 %)
Input current	320 mA max.
Starting current	2.5 x continuous current
Recommended fuse	≤ 10 A
Current supply K-bus	1,000 mA
Power contacts	24 V DC max./10 A max.
Electrical isolation	500 V (power contact/supply voltage/fieldbus)
Weight	approx. 100 g
Operating/storage temperature	0…+55 °C/-25…+85 °C
Protect. class/installation pos.	IP 20/variable
Approvals	CE, UL, Ex

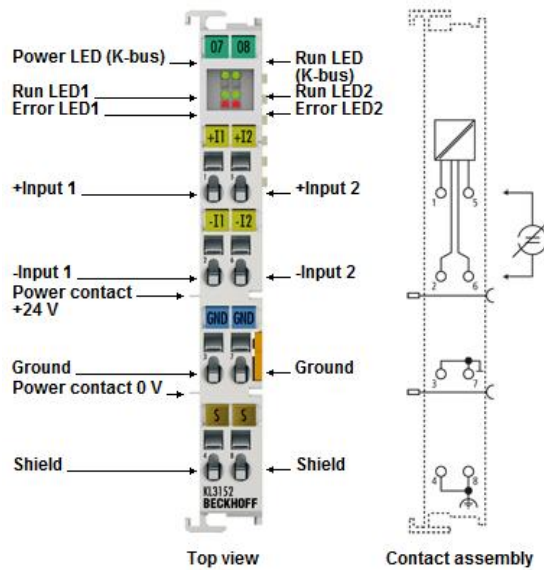**KL3152 - 2-channel analog input terminal 4…20 mA (accuracy 0.05 %) [72]**

Figure D-2: KL3152 Analog Current Input Module.

Table D-3: KL3152 Technical Data.

Number of inputs	2
Power supply	via the K-bus
Signal current	4…20 mA
Technology	differential input
Internal resistance	1 Ω typ. shunt
Common-mode voltage U_{CM}	±10 V max.
Conversion time	140 ms, configurable
Filter	50 Hz, configurable

| Resolution	16 bits
Measuring error	< ±0.05 % (relative to full scale value)
Surge voltage resistance	35 V DC
Electrical isolation	500 V (K-bus/signal voltage)
Current consumption power contacts	–
Current consumpt. K-bus	typ. 85 mA
Bit width in the process image	input: 2 x 16 bit data (2 x 8 bit control/status optional)
Special features	increased measuring accuracy
Weight	approx. 70 g
Operating/storage temperature	0…+55 °C/-25…+85 °C
Relative humidity	95 %, no condensation
Vibration/shock resistance	conforms to EN 60068-2-6/EN 60068-2-27/29
EMC immunity/emission	conforms to EN 61000-6-2/EN 61000-6-4
Protect. class/installation pos.	IP 20/variable
Pluggable wiring	for all KSxxxx Bus Terminals
Approvals	CE, UL, Ex

KL9010 - End terminal [72]

Top view   Contact assembly
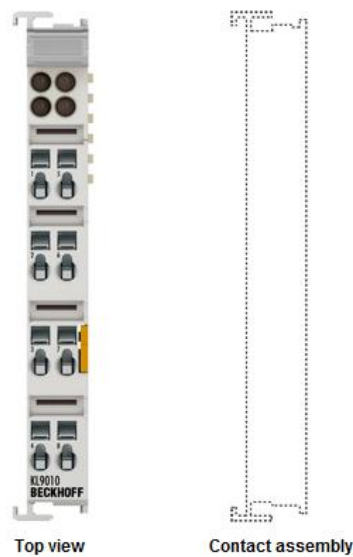
Figure D-3: KL9010 End Module.

Table D-4: KL9010 Technical Data

Nominal voltage	–
Current load	–
Integrated fine-wire fuse	–

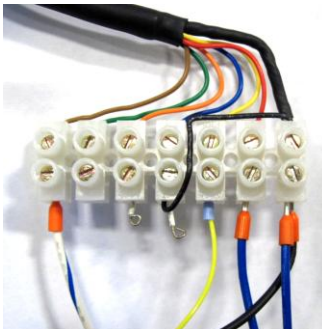|	
Diagnostics	–
Power LED	–
Defect LED	–
Reported to K-bus	–
PE contact	–
Shield connection	–
Renewed infeed	–
Connection facility to additional power contact	–
K-bus, looped through	–/yes
Bit width in the process image	0
Connection to DIN rail	–
Current consumpt. K-bus	–
Starting current	–
Electrical isolation	–
Housing width in mm	12
Special features	end terminal for bus communication
Weight	approx. 50 g
Side by side mounting on Bus Terminals with power contact	yes
Side by side mounting on Bus Terminals without power contact	yes
Operating/storage temperature	-20…+60 °C/-40…+85 °C
Approvals	CE, UL, Ex, GL

<u>Appendix E: Ultra-Trak 750 Information</u>

More information on this sensor is included with the sensor instruction manual [66].

Table E-1: Technical Specifications [73].

Power Supply:	18-30 V (30 mA max)
Current Draw:	4-20 mA (25 mA max) proportional to ultrasound signal detected
Output:	Demodulated/heterodyned
Ambient Temperature Range:	32°-122°F (0°-50°C)
Detection Frequency:	40 kHz (± 2 kHz)
Non-Volatile Sensitivity Adjustment:	Pushbutton contact closure or TTL control signal
Cable:	RF Shielded 10' (3m)
Transducer:	Piezoelectric
Method of Attachment:	10/32 thread mounting hold
Housing:	Stainless steel: water resistant & dust proof, meets NEMA 4X requirements. Exceeds IP 54 ratings

Table E-2: Ultrasonic Sensor Wiring Definitions.

Wire Color	Function	Setup
Black	Ground	
Red	Power Supply 18 to 30 VDC	
Yellow	Audio	
Blue	Sensitivity Mode Connect to +10 to +30 VDC for Max Sensitivity Connect to ground for Adjustable Sensitivity	
Orange	Sensitivity Adjustment Normally Open – Momentary Contact Closure to ground	
Green	Sensitivity Adjustment TTL Signal, 5Hz Max	Adjustable Sensitivity Shown
Brown	0 to 30 mA Output Connect to ground for loop powered operation	

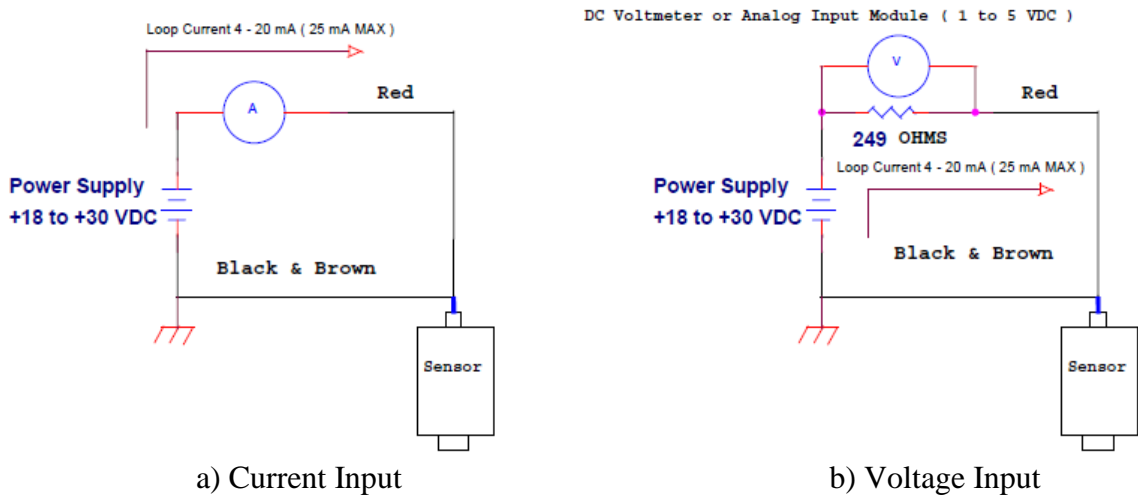a) Current Input   b) Voltage Input

Figure E-1: Sensor Wiring Schematics [66].
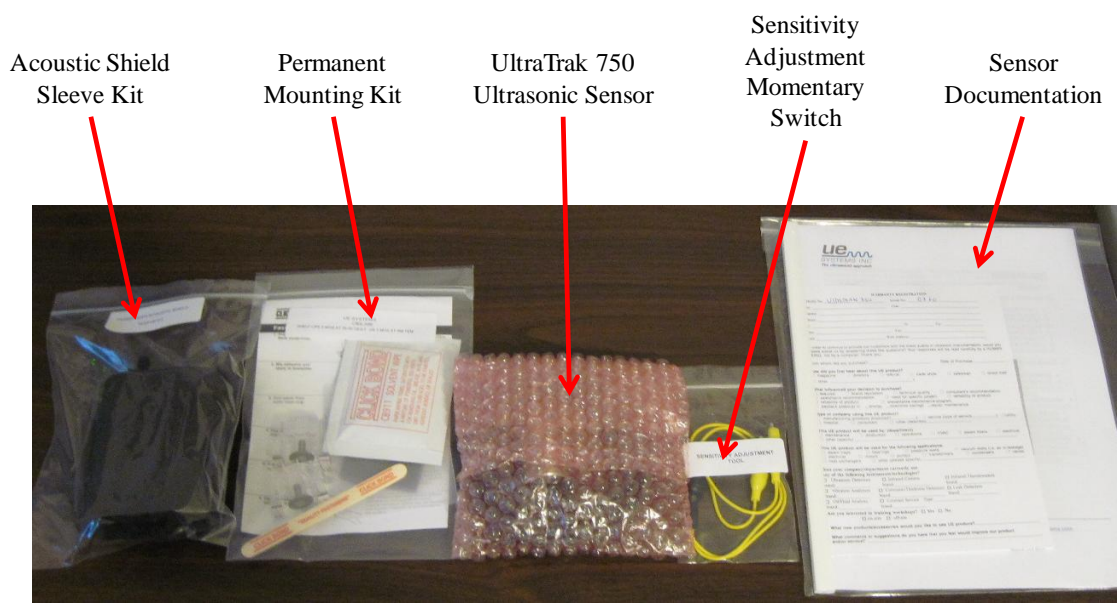

Figure E-2: Items provided with the Ultra-Trak 750

Appendix F: Ultrasonic Sensor Adapter Drawings for Magnetic Mounting

Figure F-1: Magnet Adapter Exploded Views.

Table F-1: Magnet Adapter Items.

Item No.	Part	Description	Qty.
1	Magnet	IFM FJ0043 Magnet	1
2	Adapter	Modified M8 Bolt	1
3	Set Screw	Winzer Set Screw – 10/32 in. Outer Thread	1
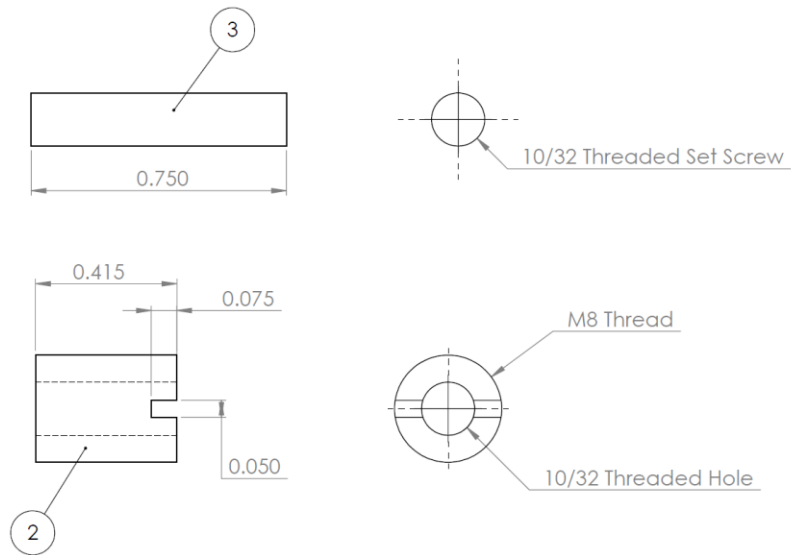
Figure F-2: Dimensioned Drawings (in inches).

Figure F-3: Assembled Adapter.

Appendix G: Machine Information

This appendix includes the physical machine information and testing parameters for both machines used.

Lathe Information:
        Serial No.:   150001
        Coolant: Houghton Hocut 795-D
        Cutting Insert: CNMG 12 04 08-PM 4225

Lathe Spindle Speeds [RPM]:
        Minimum: 42
        Maximum: 4,200 (with a B210 chuck)
        RPM Range Test: 1,000 to 4,000 RPM in increments of 100 RPM

Mill Information
        Serial No.: 147532

Mill Spindle Speeds [RPM]:
        Minimum: 50
        Maximum: 15,000
        RPM Range Test: 2,000 to 12,000 RPM in increments of 1,000 RPM
        Accelerated Lifetime Test: 9,000

Tool Holder Information:
Empty Tool Holder
        OEM: Sandvik
        Model: AA3B20-40 25 044
        Serial Number: 3180618
        Tool Length: 1 inch
        Weight: 2.12 lbs

Loading Tool
        OEM: Sandvik
        Model: A392-4025-40 25 101
        Serial Number: 28472
        Tool Length: 3.25 inches
        Weight: 3.38 lbs

Figure G-1: Tool Holders used in the Destructive Bearing Test.

Appendix H: Machine Warm Up Procedures

The following procedures occurred after the machine was switched on.

The lathe has no OEM warm up procedures, but a warm up procedure was created to ensure all spindle components were at operating temperature. The mill had an OEM warm up procedure, which was followed.

Lathe:
1. Check inside the machine to ensure that nothing is clamped into the chuck.
2. Put the machine into Manual mode and place the chuck in the clamped position.
3. Put the machine into MDI mode.
4. Issue the machine an M03S50 command.
5. Ensure the spindle is rotating properly.
6. Issue the machine a S500 command and let run for 10 minutes.
7. Issue the machine a S2000 command and let run for another 10 minutes.
8. The machine can now be considered warmed up.

Mill:
1. Check inside the machine to ensure proper tool holder is clamped into the spindle.
2. Put the machine into MDI mode.
3. Issue the machine a M03S50 command.
4. Ensure the spindle is rotating properly.
5. Issue the machine a S500 command. Let run for a few seconds.
6. Issue the machine a S1000 command. Let run for a few seconds.
7. Increase the spindle speed by 1,000 RPM, letting the spindle run for a few seconds at each speed until 4,000 RPM is reached.
8. Let the machine run for 10 minutes.
9. Increase the spindle speed by 1,000 RPM, letting the spindle run for a few seconds at each speed until 9,000 RPM is reached.
10. Let the machine run for 10 minutes.
11. The machine can now be considered warmed up.

Appendix I: Machining Procedure

1. Load a blank specimen into the chuck
2. Clamp it into the chuck
3. Face the end of the part (movement along the machine's X-axis)
4. Set Z parameter equal to 0.0000
5. Remove a small amount of material along the length of the part (uniform diameter).
6. Measure the new diameter with calipers
7. Set the tool offset to the measured diameter, noting the tool index of the tool being used.
8. Edit the part program to ensure the next pass will remove the desired volume of material (depth of cut).
9. Run the part program in single block mode.
10. When the program reaches *G01 Z-1.75 F0.0005(Cuts Desired Diameter)*, bring up the "Enlarge Actual Position" screen.
11. Press the green execute button.
12. Watch the tool position. When it gets to 0.0000, start the data recording in the Visual Basic Application for Spindle Monitoring.
13. Once the part program is finished, repeat steps 8 – 13.
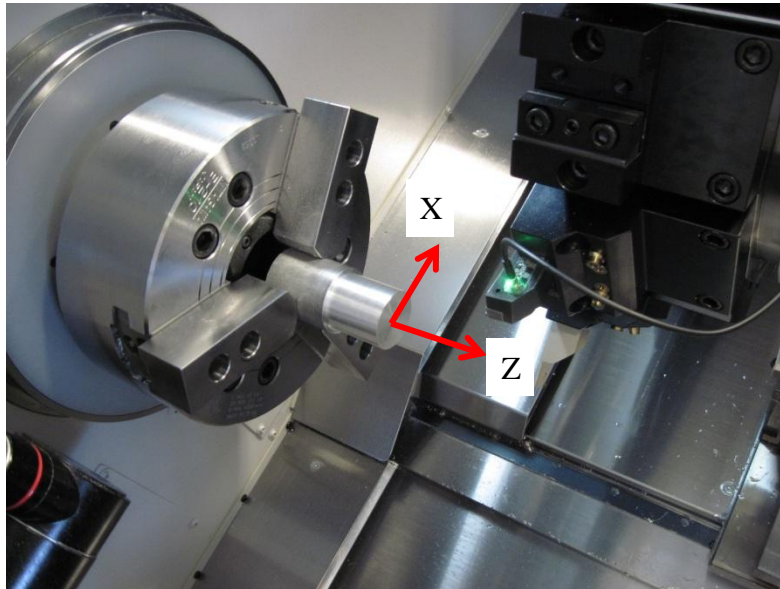
Figure I-1: Axes on the Lathe.

Appendix J: Sample Machining Program (Steel)

```
G50 S2000(Maximum Spindle Speed)
G97 S2000(Constant Cutting Off)
T0202(Tool Offset 2)
M03 S2000(Spindle ON, 2000 RPM)
G00 X1.999 Z0.25
G95(Feed Per Minute Mode in/REV)
(Make pass)
G00 X1.725
M08(Coolant ON)
G01 Z-1.75 F0.0005(Cuts Desired Diameter)
(Pull away)
G00 X2.1
M09(Coolant OFF)
G00 Z10
M05(Spindle Stop)
M02(Program End)
```
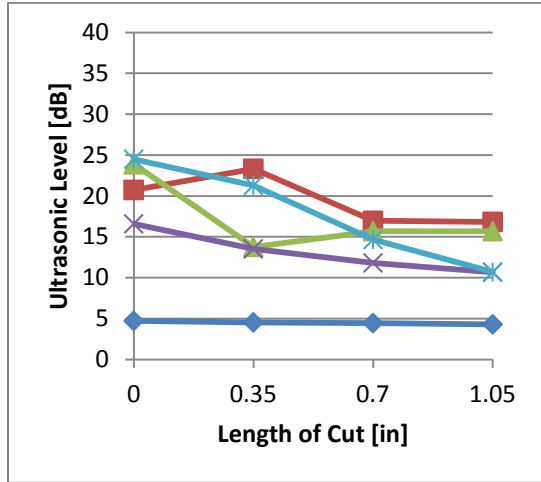

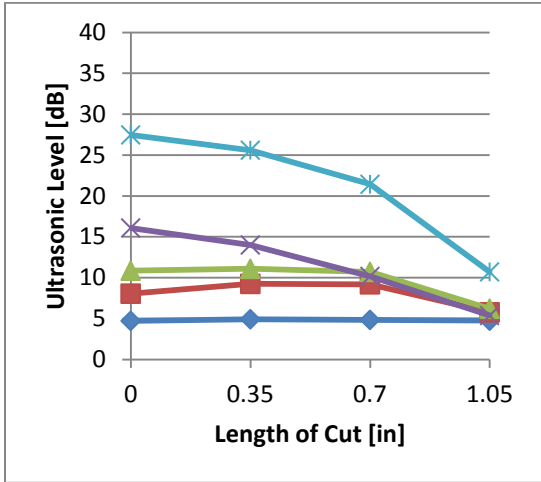**Figure J-1: Aluminum Specimens (6061 Aluminum)**
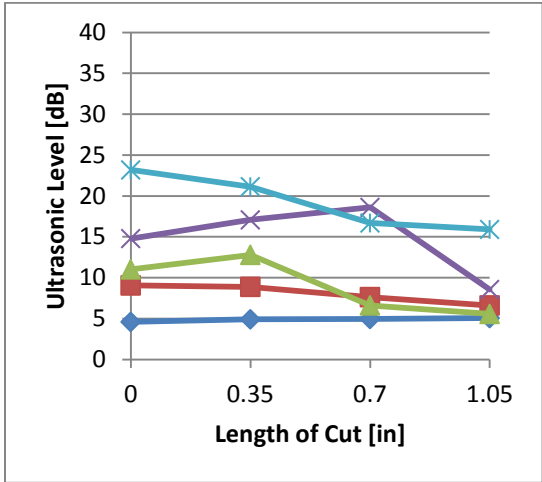

Figure J-2: Steel Specimens (Cold Roll - C-1018)

Appendix K1: Aluminum Specimens – Various DOC's
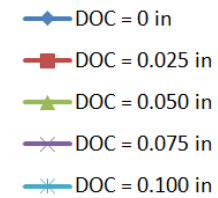

Aluminum Specimen 1
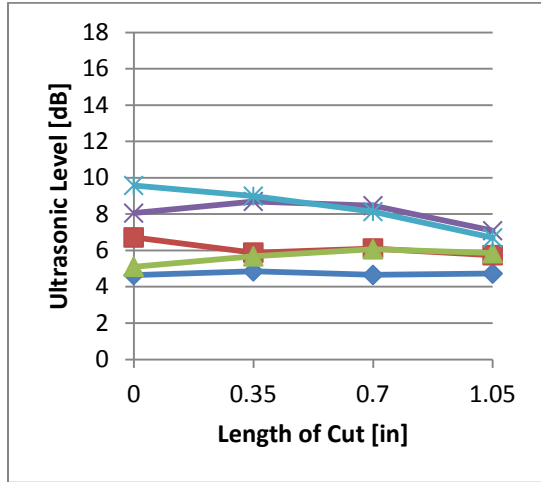
Aluminum Specimen 2

Aluminum Specimen 3
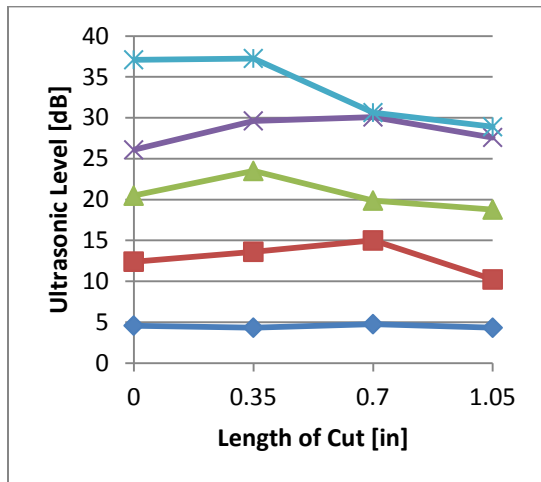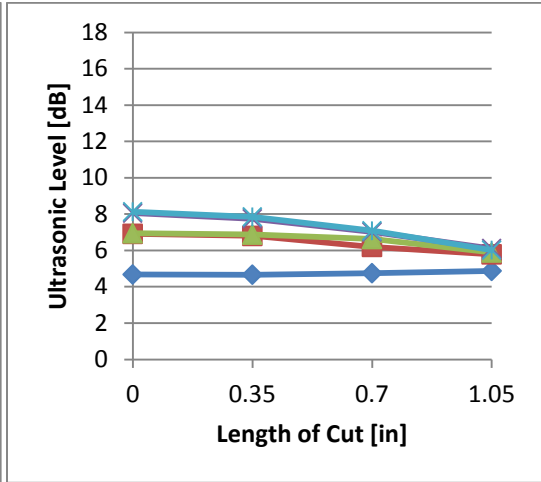
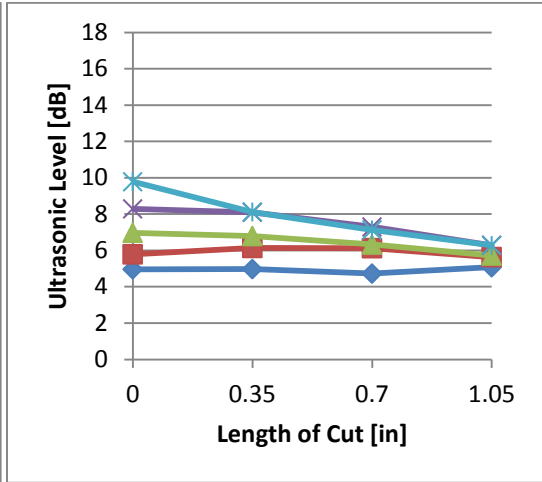Aluminum Specimen 4
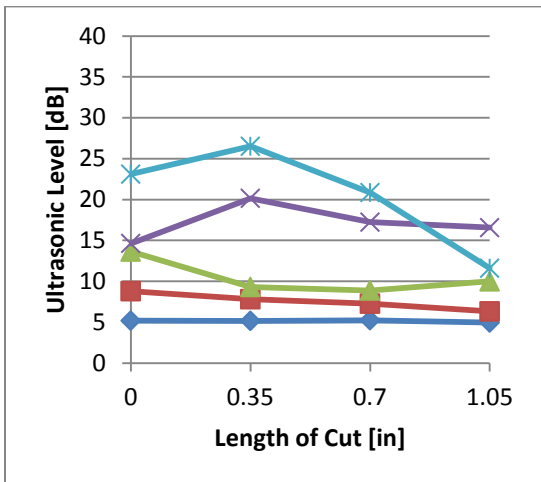
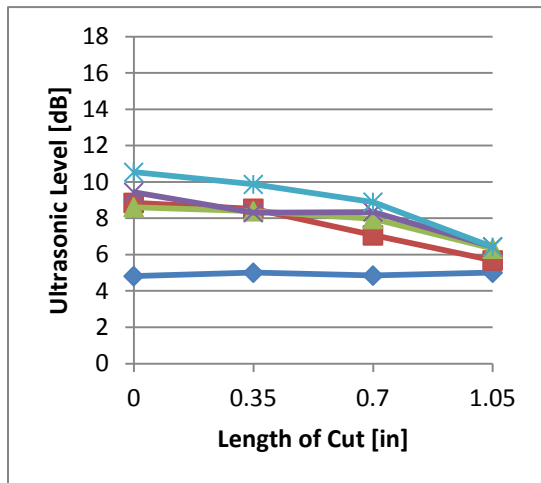Aluminum Specimen 5

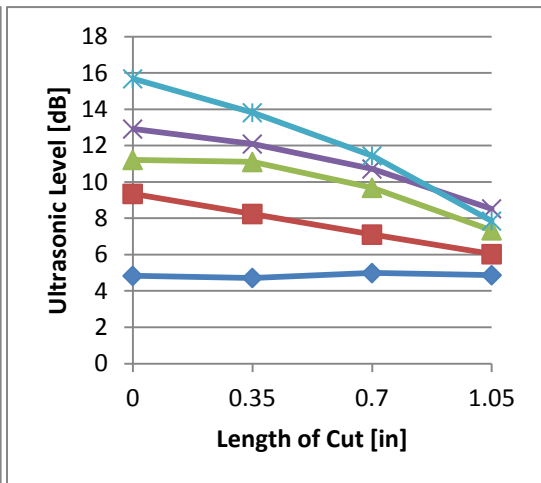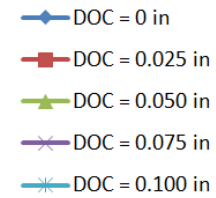Appendix K2: Steel Specimens – Various DOC's

Steel Specimen 1

Steel Specimen 2

Steel Specimen 3

Steel Specimen 4

Steel Specimen 5

Appendix K3: Aluminum Specimens – Various Specimens
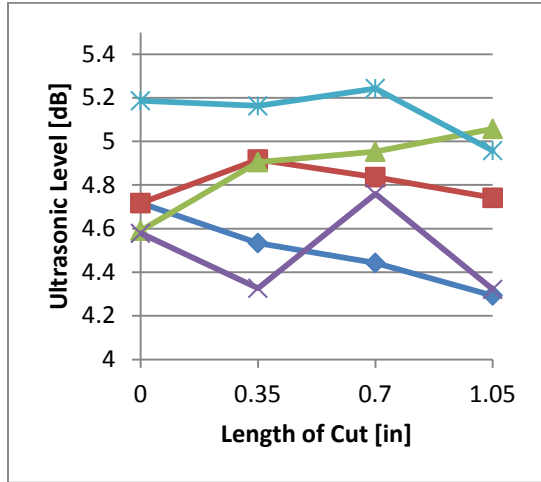
Aluminum DOC = 0.000 in.
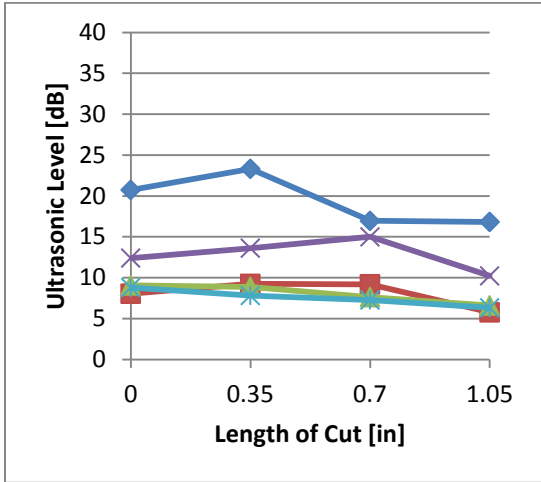
Aluminum DOC = 0.025 in.
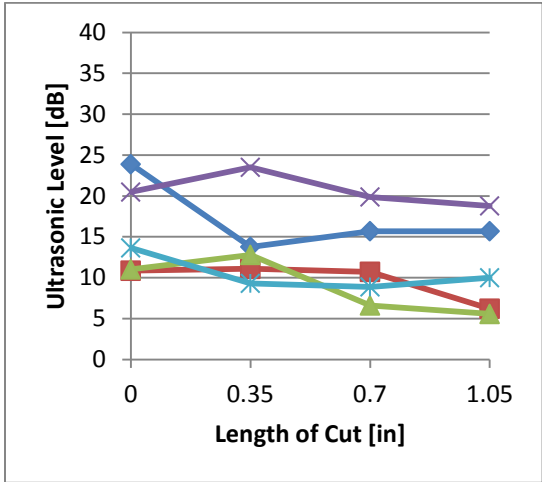
Aluminum DOC = 0.050 in.

Aluminum DOC = 0.075 in.

Aluminum DOC = 0.100 in.

Specimen 1
Specimen 2
Specimen 3
Specimen 4
Specimen 5

Appendix K4: Steel Specimens – Various Specimens

Steel DOC = 0.000 in.

Steel DOC = 0.025 in.

Steel DOC = 0.050 in.

Steel DOC = 0.075 in.

Steel DOC = 0.100 in.

Specimen 1
Specimen 2
Specimen 3
Specimen 4
Specimen 5

Purpose
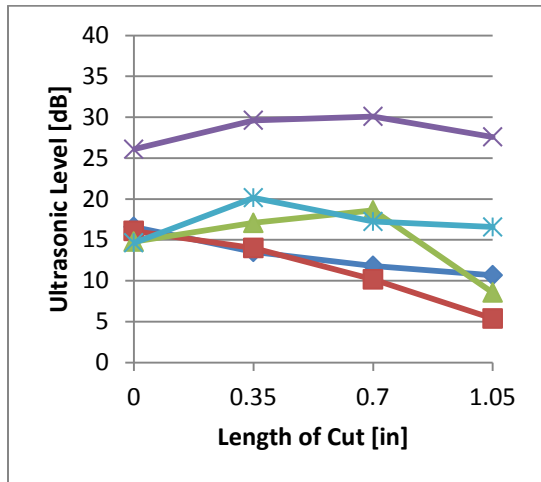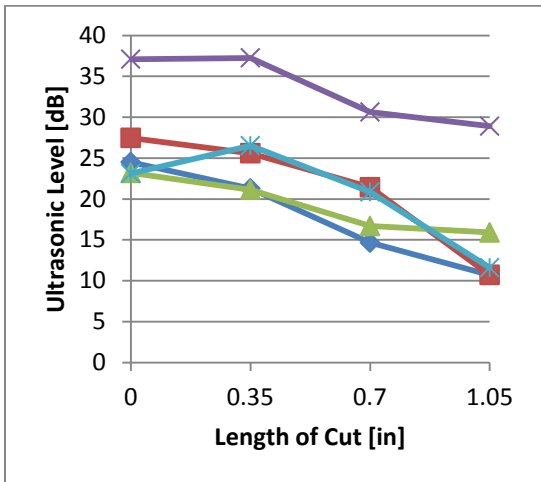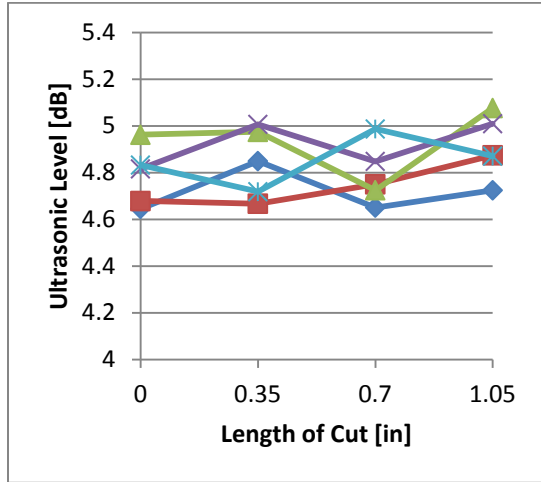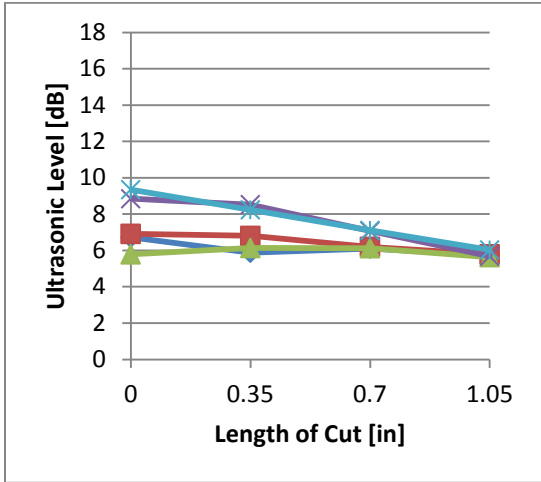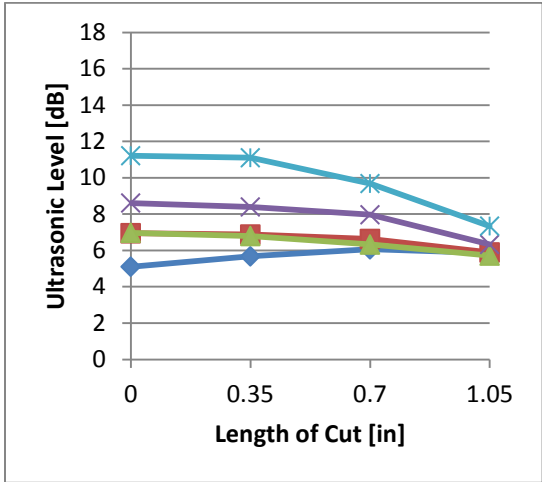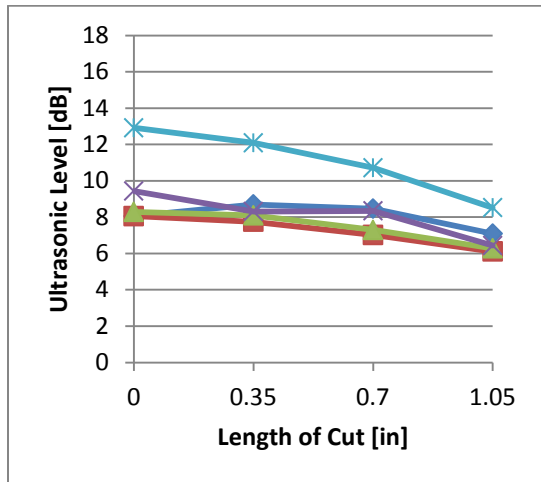The following documentation is the test protocol procedure for an accelerated life test on an Okuma MU-500VA CNC vertical milling spindle. The main goal is to gain a better understanding of Okuma spindle related failures. This will help the development of the Spindle Monitoring Program that Okuma is currently pursuing for their machines. The accelerated test will simulate possible sources for spindle failure, all of which have been common problems that are seen in the field.

Testing
The testing to be performed is listed in order of execution in Table L-1 and Table L-2, with each successive test providing a greater amount of spindle bearing damage than the last. The spindle will be taken through a variety of actions in order to gather as much data from each of the "incidents" as possible. For each test, the spindle will have only a tool holder clamped into it (with no tool at the end) and will not be under any loading conditions. The running speed chosen for this test is 9,000 RPM as this is the spindle speed with the most amount of ultrasonic sensor excitation (somewhere near the spindle's natural frequency).

Table L-1: Testing Procedure (short).

Action / Test	Description (short)	Length of Test / Event Occurrence
A	Establish a baseline	3 hours
B	Induce an improper lubrication condition	Temperature of 60°C or an 8 dB increase from baseline
C	Establish a proper lubrication condition	3 hours
D	Induce a coolant contamination condition	1 week
E	Induce powder contamination condition	TBD
F1	Light Brinelling of spindle bearings	1 week
F2	Medium Brinelling of spindle bearings	1 week
F3	Heavy Brinelling of spindle bearings	Complete bearing failure (machine shutdown)
G	Root Cause Analysis of bearing failure	N/A

Table L-2: In-Depth Testing Procedure Explanations.

Action / Test	Description (long)
A	A baseline will be established at some reference RPM. This RPM is to be determined by investigating at what RPM the spindle has the highest vibration/ultrasonic readings. Once this is known, all further tests will be performed at this rotational speed.
B	This test simulates the machine owner not refilling the oil container for the bearing air-oil mist. To induce improper lubrication, the oil line for the bearing air-oil mist will be disconnected. This will allow for the bearings to experience a lack of lubrication as the last bit of oil will evaporate out, leaving metal on ceramic contact only.
C	Proper lubrication will be brought back to the bearings by reconnecting the oil line in the air-oil mist system.
D	This test simulates coolant getting into the bearings during machine use. To induce improper lubrication, coolant will be added into the oil lines for the air-oil mist system and transported to the bearings via the lubrication system. Once this action occurs, there will be no way to remove the coolant from the bearings. This should help to accelerate complete bearing failure for the remaining tests.
E	This test simulates very small particles such as graphite getting into the spindle bearings. It serves to help accelerate the bearing failure. Unfortunately, there is no way to do this without damaging other parts of the spindle/machine. Therefore, this test will not be performed.
F1	This test simulates a small "bump" of the machine. With the spindle off, a piece of round stock will be clamped into the empty tool holder and a relatively small (subjective) impulse force will be radially applied. This will cause internal bearing deflection, which will put stress on the bearing components, slightly damaging them. A radial load was chosen over an axial load due to the fact that the spindle is more forgiving to an axial "bump". The bearings will then be monitored to see how quickly the bearing degradation occurs with a "bump" of this nature. The round stock will be removed before spindle is started again.
F2	This test simulates larger trauma to the spindle bearings. The spindle will be turned off, the round stock will be inserted and reclamped and a larger (subjective) impulse force will take place. See Figure L-1. The round stock will be removed and the bearings will then be monitored to see how quickly the bearing degradation occurs with a "bump" of this nature.
F3	This test should simulate forces experienced by the spindle during a crash. The same procedure will be used as in F1 and F2. The spindle will then be run until complete bearing failure.
G	The bearings will be sent back to NSK for a Root Cause Analysis (RCA) of each bearing.

Z

Y

Machine Axis

B4

B3

B2

B1

Tool Holder

Round Stock

Applied Impulse
Force
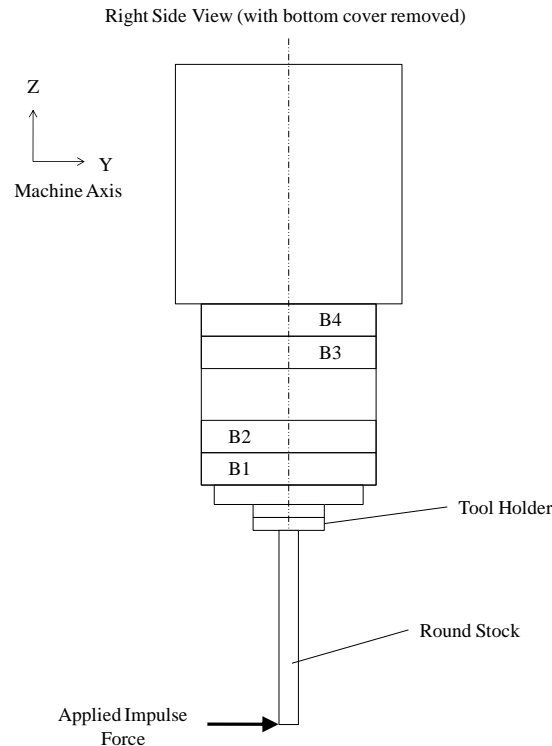
Figure L-1: Diagram explaining how Brinelling of the bearings will be performed.

Note: In all actions/tests, the spindle will be in a "warmed" condition.

Note: Difference between a bump and a crash is that a crash usually consists of the spindle locking up or getting stuck in the table / work piece.

Note: All tests will be performed with the same empty tool holder under the same conditions.

Sensors

Temperature, ultrasonic sound, and vibration will be the three parameters investigated in this study. The sensor placement chosen can be seen in Figure L-2. There are four thermocouple temperature probes, one for each bearing. These will be inserted through the nose of the spindle (the same way a rebuild spindle is tested). Two ultrasonic sensors as well as two accelerometers are on the spindle as well, as indicated by the "Upper" and "Lower" locations in Figure L-2. The reason for this is because the ultrasonic senor will need to be mounted in the *Upper Location* for the Okuma Spindle Monitoring Program, as that location provides a safe and secure place for the sensor. The *Lower Location* will serve as the location where the service representative would take a reading. One objective of this experiment is to see how much they vary from one another.
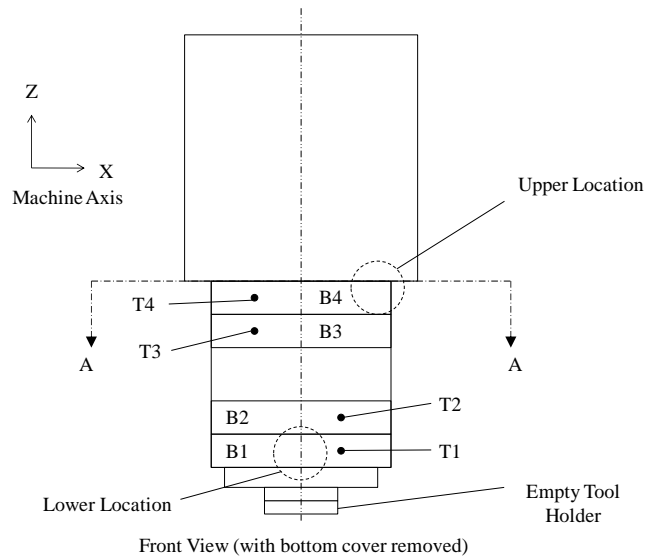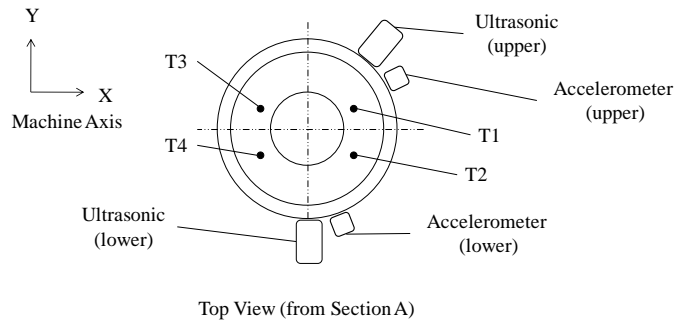
Figure L-2: Sensor Placement.

Table L-3: Sensor Information.

Part Number	Description	OEM	Quantity	Notes
NXFC-42H-O2	Type J Thermocouple	Okuma	4	Inserted through nose of spindle
Ultra-Trak 750	Ultrasonic Sensor	UE Systems	2	Magnets for attachment: IFM F90043
8772A50	50 g Accelerometer	Kistler	2	Super glued to the spindle

Data Acquisition Hardware/Software

National Instruments hardware and software will be used for the data acquisition. The hardware consists of an NI-cRIO 9073. The 9073's chassis is capable of employing eight modules, however only three will be used in the test. They are:

Thermocouple Module   NI 9211
Analog Voltage Input   NI 9201
Accelerometer Module   NI 9234

The raw signals from the sensors will be recorded through these modules via LabVIEW 2010 SP1. An acquisition algorithm was written specifically for the data recording. The data is recorded to an Excel spreadsheet, noting the time of entry. The sample rate will for the data recording is 10 S/sec.

Spindle Information

Serial Number: K7130
Orientation: Vertical
Taper: 40
Spindle Drive: Motor
Maximum Spindle Speed [RPM]:   15,000
Shaft Diameter [mm] :   + 5 as compared to nominal size
Housing Diameter [mm]:   0 as compared to nominal size
Spindle Cooling Method: Outer
Spindle Cooling Fluid: Mobile Velocite #3
Bearing Lubrication Method: Air-Oil Mist
Bearing Lubrication Oil: Mobile DTE Oil Light
Bearing Configuration: Quad set
Bearing Spacing: 18.5 mm spacers between the front and rear
                                    pairs, 63 mm spacer between both pairs

Bearing Information

Table L-4: Bearing Information.

Bearings	OEM	Part Number	Type
Bearings (B1-B4)	NSK	70BNR10XTYNDBBCA10P4YU10	Angular Contact Ball Bearings

Number of Balls: 25   Contact Angle [degrees]:   18
Ball Diameter [mm]:   8.731   Pitch Diameter [mm]:   89

Appendix M: BPFO Vibration Explanation for the MU-500VA Spindle

In Chapter 9, it was stated that initially it was thought that the test spindle may have had a damaged bearing due to the magnitude of the BPFO fault frequency. However, interestingly enough, the machine's original spindle had the same BPFO fault frequency indicator as the test spindle did, shown in Figure M-1. Therefore, this must be an inherent signature in these spindle types. The magnitude for the running frequency in the original spindle was higher than the test spindle, 66 mg compared to 37 mg. The BPFO was more than twice what the test spindle had, 760 mg versus 348 mg. This suggests that the original spindle has more vibration in it which makes sense as this spindle has been used in machining operations prior to the testing performed.
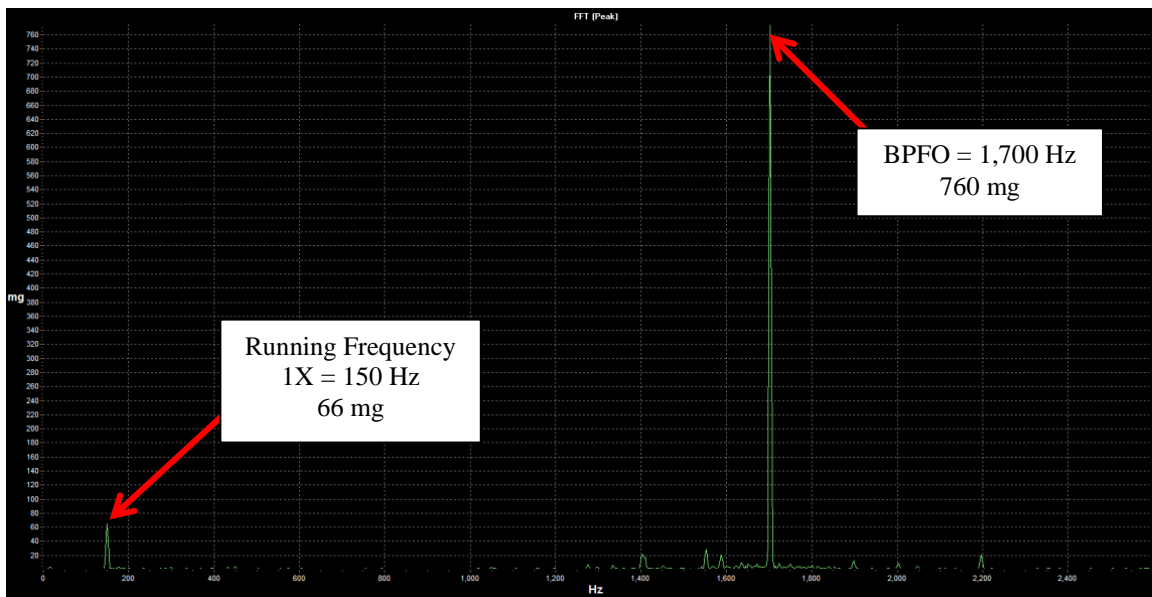
Figure M-1: Frequency Spectrum for the Original Spindle.

The reason why this signature is inherent becomes more obvious when looking at the way the bearings are configured within the spindle. Figure M-2 is a simple representation of the bearing configuration in the spindle that was tested. The diagonal lines across the balls represent the angle of contact that the inner and outer races make with the ball. This provides the direction of travel for forces to take when the bearing is loaded.

Figure M-2: Simplified Spindle Diagram.

When the spindle is in an unloaded state (as was done in most of the testing discussed in Chapter 9), the weight of the spindle assembly (shaft, motor, etc) causes the spindle to pull downward. The weight force is transferred down through the top bearings, as shown in Figure M-3a, due to the interference fit the bearings have on the spindle shaft. This causes the upper bearings to lose their play (radial clearance) as there is firm pressure being applied to the balls from the inner and outer races.

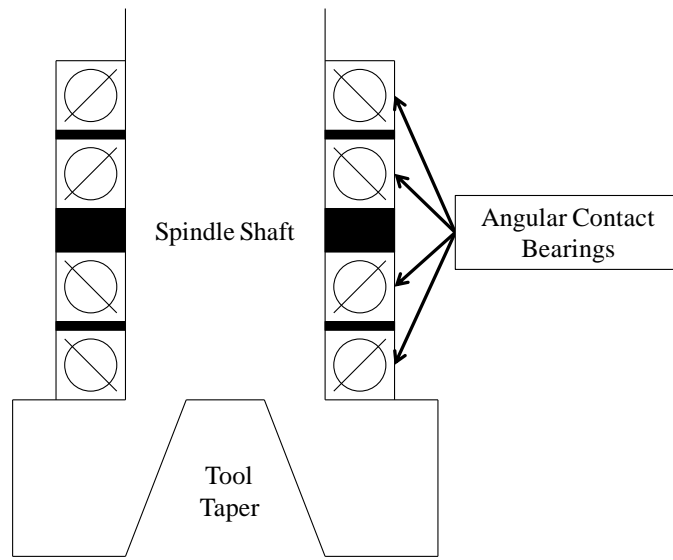In this same unloaded state, the only pressure the lower bearings are experiencing is the preload that is placed on them at the time of assembly. Therefore, they have a bit of play (microns) in them. It is this play that is being shown on the FFT spectrum. The balls have "more room" (for lack of a better term) to move around, therefore magnifying the vibration.

In a loaded state, shown in Figure M-3b, the exact opposite occurs. The lower bearings now carry the load while the upper bearings are relieved of their load. However, the tool thrust force must be greater than the weight of the spindle to allow for the upper bearings to become completely unloaded. At the point where the tool thrust is equal to the weight of the spindle, all four bearings have the same loading applied to them. The loading experienced by the bearings is the preload that was established at the time of spindle assembly.

Testing was performed on the original spindle in an unloaded state to ensure that the explanation above is accurate. The accelerometer was moved up the spindle and an FFT reading was taken at each bearing. The magnitude for the BPFO decreased with each successive move. The FFT for the research discussed in Chapter 9 was taken at the lower most bearing, therefore the bearing with the most play in it. That explains why the magnitude was so high.

194

Weight of Spindle

Tool Thrust

a) No Load   b) Load
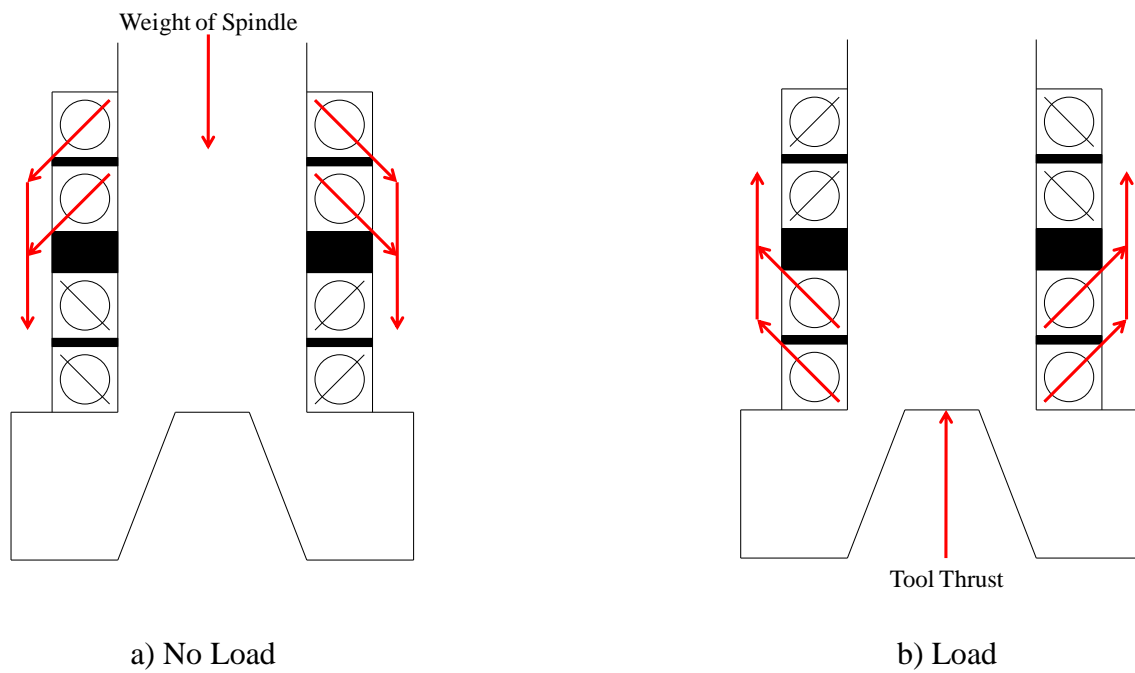
Figure M-3: Loaded and Unloaded Spindle Bearing Situations.

<u>Appendix N: Decibel Level Information</u>

A decibel is the measure of how much a value changes with respect to its input. The equation for its calculation is:

$$\text{dB Level} = 20\log\left(\frac{\text{Output}}{\text{Input}}\right) \qquad\qquad \text{(N-1)}$$

The scaling factor is determined by the ratio between the input and the output. To convert a decibel level to a scaling factor, the equation becomes:

$$\text{Scaling Factor} = 10^{\frac{\text{dB Level}}{20}} \qquad\qquad \text{(N-2)}$$

In ultrasonic monitoring, the decibel scale is a relative scale. It's all relative to the system's baseline. The dB level that the ultrasonic sensor outputs allows for a scaling factor (from baseline) to be determined. Figure N-1 and Table N-1 provide a good reference as to what the relationship between the decibel level and its respective scaling factor.
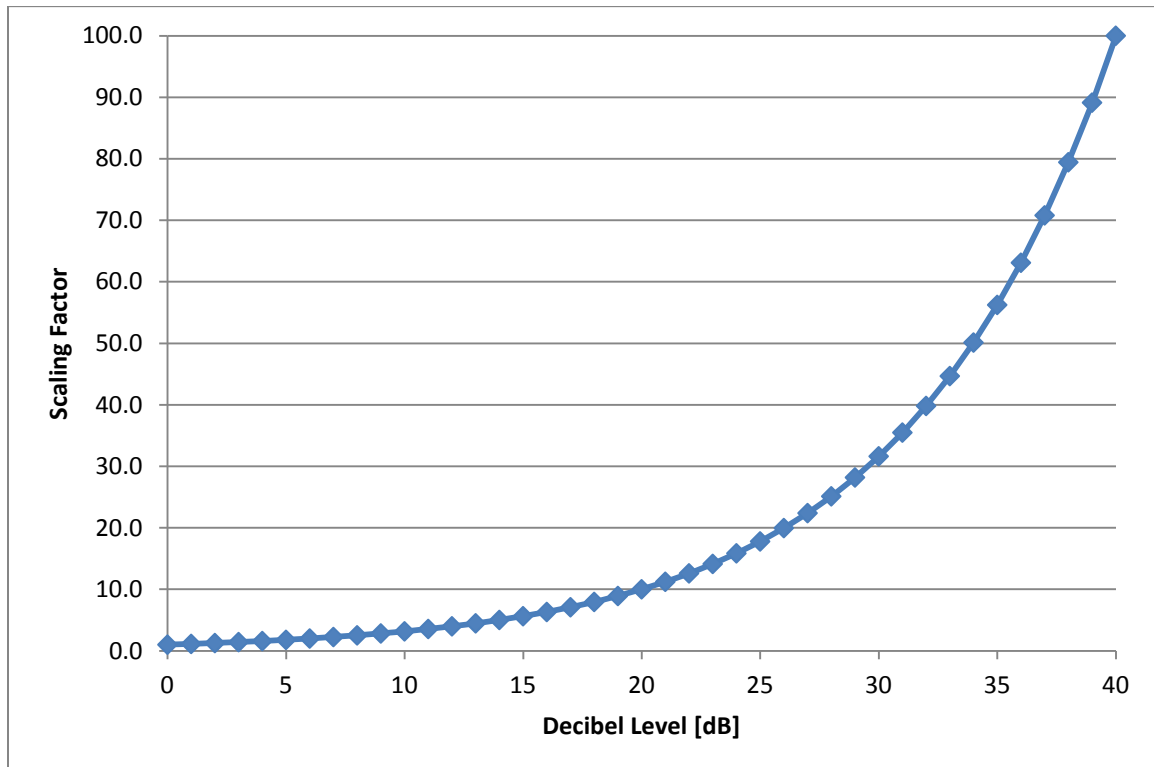
Figure N-1: Decibel Level and Scaling Factor Relationship.

Table N-1: Scaling Factor Values based on dB Levels.

dB	Factor	dB	Factor	dB	Factor	dB	Factor
0	1.0	10	3.2	20	10.0	30	31.6
1	1.1	11	3.5	21	11.2	31	35.5
2	1.3	12	4.0	22	12.6	32	39.8
3	1.4	13	4.5	23	14.1	33	44.7
4	1.6	14	5.0	24	15.8	34	50.1
5	1.8	15	5.6	25	17.8	35	56.2
6	2.0	16	6.3	26	20.0	36	63.1
7	2.2	17	7.1	27	22.4	37	70.8
8	2.5	18	7.9	28	25.1	38	79.4
9	2.8	19	8.9	29	28.2	39	89.1
						40	100.0

Appendix O: Fast Fourier Transform (FFT) Information

Every mathematical function or waveform can be approximated by a series of sine and cosine functions, known as the Fourier series. The more terms that are in the series, the better the approximation of the curve will be. The discrete Fourier transform (DFT) allows for this series to be represented in the frequency domain, with each function of the Fourier series having its own magnitude and frequency [74]. Figure O-1 allows for a visual representation of how the time and frequency domains relate to each other. The figure shows one waveform that is broken down into its sine and cosine components.
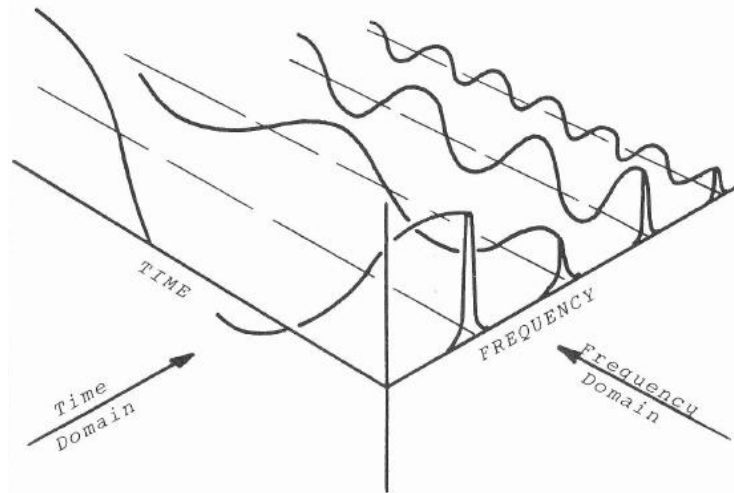

Figure O-1: Representation for both the Time and Frequency Domains [54].

The DFT comes significantly useful when trying to measure a signal with a computer. The signal being measured is analog, but becomes discretized due to the analog to digital conversion that must be performed on it. The DFT takes the sample size, along with each sample's value and estimates the magnitude and frequencies that make up that signal.

The equation for this operation can be represented as [74]:

$$X_d(k\Delta f) = \Delta t \sum_{n=0}^{N-1} x(n\Delta t)e^{-j2\pi kn\Delta f \Delta t} \tag{O-1}$$

Where:
N = number of samples being considered
Δt = the time between samples (sampling interval)
Δf = the sample interval in the frequency domain = $1/N\,\Delta t$
n = the time sample index (0, 1, 2…N-1)
k = the index for the computed set of discrete frequency components (0, 1, 2…N-1)
$x(n\,\Delta t)$ = the discrete set of time sample that defines the waveform to be transformed
$X_d(k\,\Delta f)$ = set of Fourier coefficients obtained by the DFT for all $x(n\,\Delta t)$
e = natural log base

$$j = \sqrt{-1}$$

If one lets $\Delta t = 1$ and $\Delta f = 1/N$ and the DFT equation becomes:

$$X_d(k) = \sum_{n=0}^{N-1} x(n)e^{\frac{-j2\pi kn}{N}}$$

(O-2)

Using Euler's identity:

$$e^{\pm j\theta} = \cos\theta \pm j\sin\theta$$

(O-3)

The DFT becomes:

$$X_d(k) = \sum_{n=0}^{N-1} x(n)\cos\left(\frac{2\pi kn}{N}\right) - jx(n)\sin\left(\frac{2\pi kn}{N}\right)$$

(O-4)

This form allows for computational convenience. However, computing the DFT is excessively long for large samples of data as the algorithm requires N^2 operations for N number of samples [75].

The fast Fourier transform (FFT) was introduced by Cooley and Tukey in 1965. The FFT algorithm replaces one large DFT algorithm with several smaller DFT algorithms to gain efficiency. This drastically reduced the number of calculations needed for a DFT computation. The efficiency gain allows the number of operations performed to go from N^2 operations to $N\log_2 N$ [75]. Figure O-2 allows for the efficiency gains to be realized more easily. This method has played a key role in digital signal processing when it comes to frequency analysis. For even faster algorithm execution, the FFT should be performed with an assembly level routine or firmware FFT [74]. This is how the IFM vibration module is able to quickly perform an FFT on 100,000 samples every second.
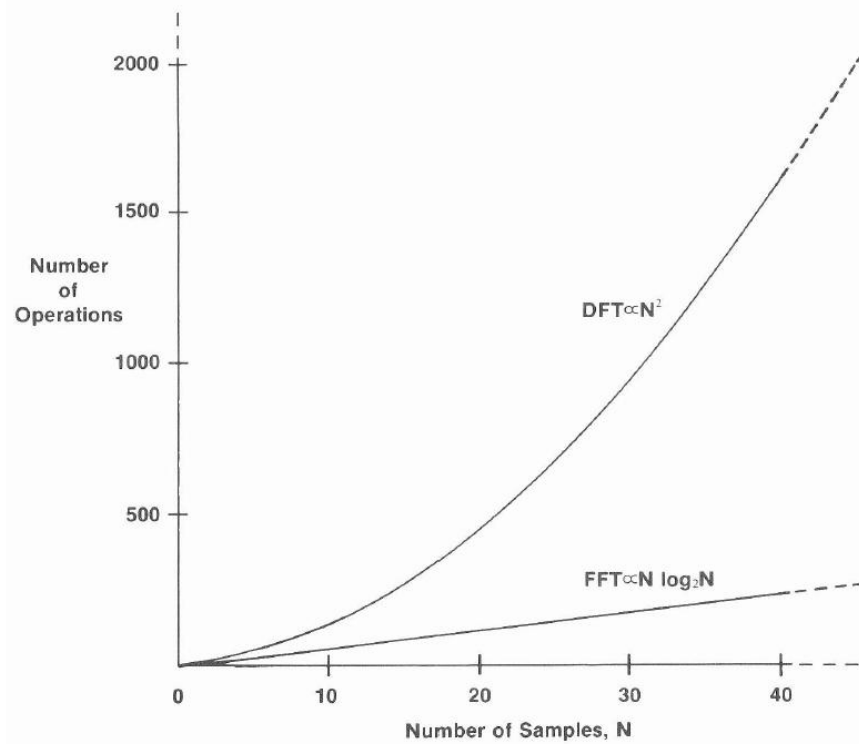
Figure O-2: Operations Comparison between DFT and FFT based on Sample Size [74].

Knowing that Equation O-2 can also be represented as:

$$X_d(k) = \frac{1}{N} \sum_{n=0}^{N-1} x(n) e^{\frac{-j2\pi kn}{N}}$$

(O-5)

The way the several smaller operations of the FFT work is looking at the number of "stages" it has, represented by M.

$$M = \log_2 N$$

(O-6)

For each stage, an additive and subtractive paired operation is required.

$$x_{m+1}(r) = x_m(r) + x_m(s)$$

(O-7)

$$x_{m+1}(s) = \left[x_m(r) - x_m(s) \right] W^{-p}$$

(O-8)

Where $r, s, p = 0 \ldots N\text{-}1$, $m = 0 \ldots M\text{-}1$, and:

$$W = e^{\frac{j2\pi}{N}}$$

(O-9)

Figure O-3 shows these paired operations. In this particular case, eight samples have been provided (indexed as 0 - 7), therefore three stages are required. The lines with the arrows on them indicate the subtractive operation being performed. At the end of the last stage, a bit reversal must be done to place the values in their proper places. For example, the value for index 4 (circled) at the end of the FFT algorithm is actually in index 1. Therefore the binary value for index 1 is 001. It gets reversed so that it becomes 100, which is binary 4.
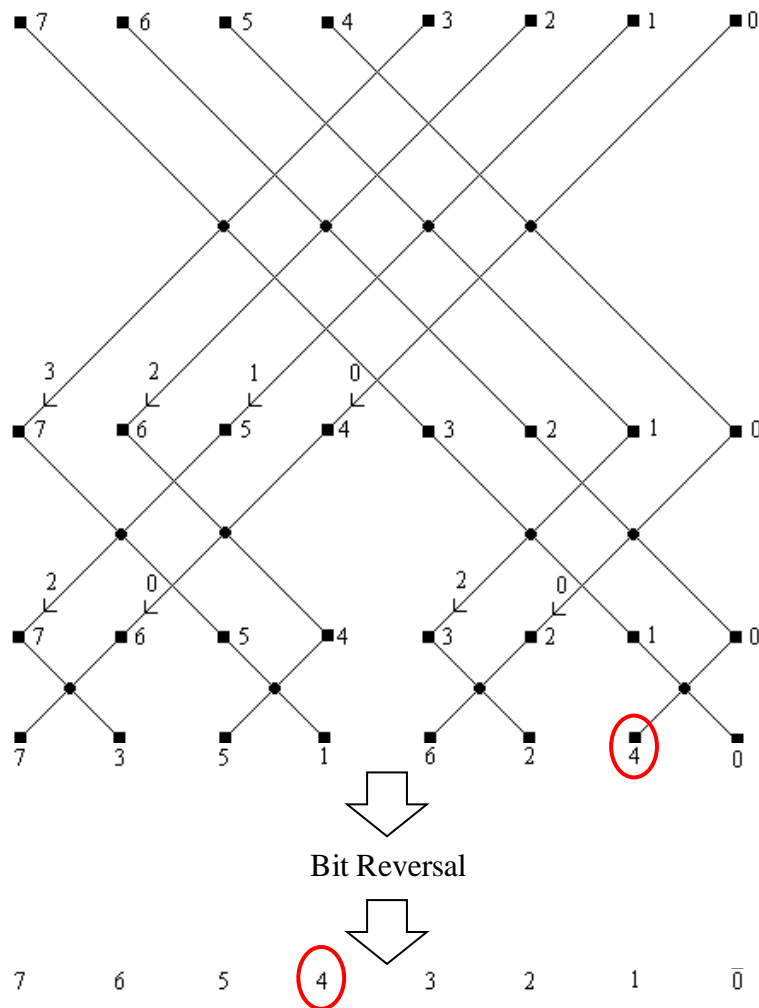

Figure O-3: FFT Algorithm (adopted from [76]).

Example:
Let's take the FFT of the waveform (in the time domain) in Figure O-4 and see how it looks with respect the frequency domain.

The waveform in Figure O-4 is the sum of two different waveforms. Therefore, each respective waveform can be extracted, both having a magnitude and frequency. These two waveforms can be seen in Figure O-5.
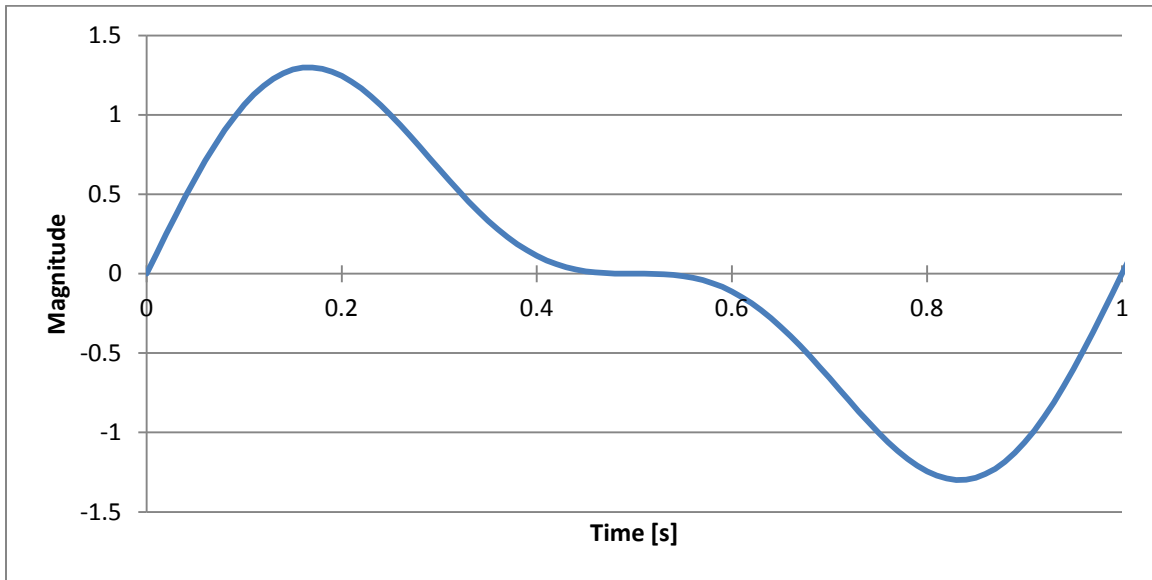
Figure O-4: Main Waveform.
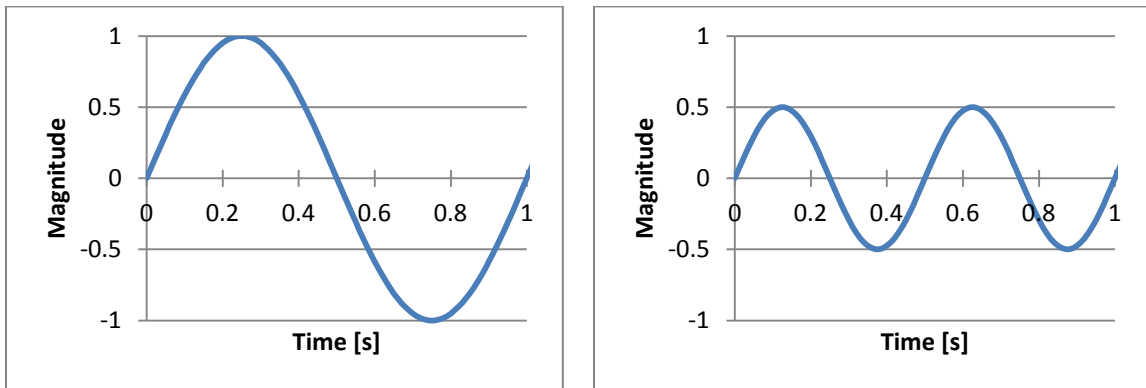
a) Part 1

b) Part 2

Figure O-5: Individual Waveforms that the Main Waveform is Comprised.

Part 1 has a magnitude of 1 and a frequency of 1 Hz. Part 2 has a magnitude that is half of Part 1 and has a frequency that is twice as fast. Therefore, the FFT will provide the frequency spectrum, shown in Figure O-6. It shows that the main waveform is actually made up of two independent waveforms with their respective magnitudes and frequencies.
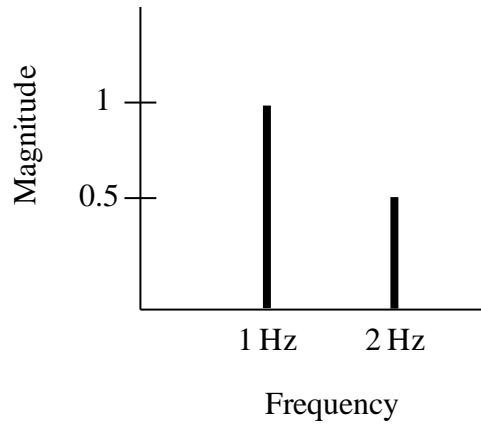
Figure O-6: Frequency Spectrum for the Main Waveform.

The sample code below shows the proper way to connect to and communicate with Okuma's THINC Control API. This particular application returns the current part program, spindle speed, and tool number that the control is currently utilizing when the *Get API Data* button is clicked.
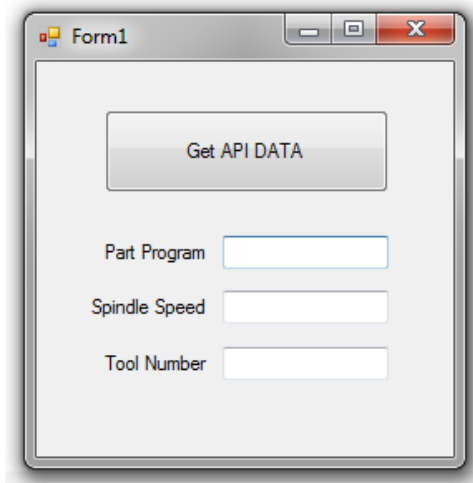
Figure P-1: API Sample Application Main Form.

Source Code:
  Form Code:

```vb
Imports Okuma.CLDATAPI

Public Class Form1
    Dim objMachine As Okuma.CLDATAPI.DataAPI.CMachine

    Private Sub Form1_Load(ByVal sender As System.Object, ByVal e As
    System.EventArgs) Handles MyBase.Load
        objMachine = New Okuma.CLDATAPI.DataAPI.CMachine
        objMachine.Init()
    End Sub

    Private Sub btnGetAPI_Click(ByVal sender As System.Object, ByVal e As
    System.EventArgs) Handles btnGetAPI.Click
        Dim API As New Get_API_Data
        txtPartProgram.Text = API.Get_Part_Program()
        txtSpindleSpeed.Text = API.Get_Spindle_Speed()
        txtTool.Text = API.Get_Current_Tool_Number()
    End Sub

    Private Sub Main_FormClosing(ByVal sender As Object, ByVal e As
    System.Windows.Forms.FormClosingEventArgs) Handles Me.FormClosing
        objMachine.Close()
    End Sub
End Class
```

Get_API_Data Class Code:

```vb
Imports Okuma.CLDATAPI

Public Class Get_API_Data
    Dim objTool As Okuma.CLDATAPI.DataAPI.CTools
    Dim objProgram As Okuma.CLDATAPI.DataAPI.CProgram
    Dim objSpindle As Okuma.CLDATAPI.DataAPI.CSpindle

    Function Get_Part_Program()
        Dim Program As String
        objProgram = New Okuma.CLDATAPI.DataAPI.CProgram
        Program = objProgram.GetActiveProgramFileName
        Get_Part_Program = Program
    End Function

    Function Get_Spindle_Speed()
        Dim Speed As Double
        objSpindle = New Okuma.CLDATAPI.DataAPI.CSpindle
        Speed = objSpindle.GetActualSpindlerate
        Get_Spindle_Speed = Speed
    End Function

    Function Get_Current_Tool_Number()
        Dim Tool As Integer
        objTool = New Okuma.CLDATAPI.DataAPI.CTools
        Tool = objTool.GetCurrentToolNumber
        Get_Current_Tool_Number = Tool
    End Function

End Class
```

WORKS CITED

[1] Mazak Corporation. (2010) Mazak - North American Customer Support. [Online]. http://www.mazakusa.com/optimumplus/op_service.htm

[2] R. K. Mobley, *An Introduction to Predictive Maintenance*. New York, USA: Van Nostrand Reinhold, 1990.

[3] P. Tse and D. Atherton, "Prediction of machine deterioration using vibration based fault trends and recurrent neural networks," *Journal of Vibration and Acoustics, Transactions of the ASME*, vol. 121, no. 3, pp. 355-362, July 1999.

[4] T. Wireman, *World Class Maintenance Management*. New York, NY: Industrial Press Inc., 1990.

[5] Merriam-Webster. (2010) Maintenance - Definition. [Online]. http://www.merriam-webster.com/dictionary/maintenance?show=0&t=1287511195

[6] P. W. Prickett, "An integrated approach to autonomous maintenance management," *Integrated Manufacturing Systems*, vol. 10, no. 4, pp. 233-243, 1999.

[7] S. Nakajima, *Introduction to TPM: Total Productive Maintenance*. Cambridge, MA: Productivity Press, 1988.

[8] M. Tajiri and F. Gotoh, *Autonomous Maintenance in Seven Steps: Implementing TPM on the Shop Floor*. Porland, OR: Productivity, Inc., 1999.

[9] R. C. M. Yam, P. W. Tse, L. Li, and P. Tu, "Intelligent Predictive Decision Support System for Condition-Based Maintenance," *The International Journal of Advanced Manufacturing Technology*, vol. 17, no. 5, pp. 383-391, 2001.

[10] Simpro Engineering. (November, 2010) Importance of Reliability and Warranty in Electrical Power Protection Relay System. White Paper.

[11] NIST/SEMATECH. (2010, June) e-Handbook of Statistical Methods. [Online]. http://www.itl.nist.gov/div898/handbook/

[12] G. P. Sullivan, R. Pugh, A. P. Melendez, and W. D. Hunt. (2010, August) Operations & Maintenance Best Practices - A Guide to Achieving Operational Efficiency. Guide.

[13] I. P. S. Ahuja and J. S. Khamba, "Total productive maintenance: literature review and directions," *International Journal of Quality & Reliability Management*, vol. 25, no. 7, pp. 709-756, April 2008.

[14] Y. Peng, M. Dong, and M. J. Zuo, "Current status of machine prognostics in condition-based maintenance: a review," *International Journal of Advanced Manufacturing Technology*, vol. 50, no. 1-4, pp. 297-313, September 2010.

[15] M. Rausand, "Reliability centered maintenance," *Reliability Engineering & System Safety*, vol. 60, no. 2, pp. 121-132, May 1998.

[16] L. R. Higgins, D. P. Brautigam, and R. K. Mobley, *Maintenance Engineering Handbook*, 5th ed. New York, NY: McGraw-Hill Inc., 1995.

[17] H. R. Steinbacher and N. L. Steinbacher, *TPM for America*. Portland, OR: Productivity Press, 1993.

[18] S. Nakajima, *TPM Development Program: Implementing Total Productive Maintenance*. Portland, OR: Productivity Press, 1989.

[19] N. M. Vichare and M. G. Pecht, "Prognostics and Health Management of Electronics," in *IEEE Transactions on Components and Packaging Technologies*, 2006, pp. 222-229.

[20] S. D. Lund, "Monitoring Machines and Processes to Improve Manufacturing Operations," in *SAE Aerospace Automated Fastening Conference and Exhibition*, Montreal, Canada, 2003.

[21] M. G. Thurston, "An Open Standard for Web-Based Condition-Based Maintenance Systems," in *IEEE Systems Readiness Technology Conference AUTOTESTCON Proceedings*, Valley Forge, 2001, pp. 401-415.

[22] D. Korn, "Taking Spindle Health Seriously," *Modern Machine Shop*, pp. 78-82, October 2010.

[23] K. Jemielniak, "Commercial Tool Condition Monitoring systems," *The International Journal of Advanced Manufacturing Technology*, vol. 15, no. 10, pp. 711-721, 1999.

[24] S. A. Elshayeb, K. Hasnan, and A. B. Nawawi, "Wireless Machine Monitoring and Control for Educational Purpose," in *2010 Second International Conference on Computer Engineering and Applications (ICCEA)*, Bali Island, 2010, pp. 401-403.

[25] A. Tiwari, F. L. Lewis, and S. S. Ge, "Wireless Sensor Network for Machine Condition Based Maintenance," in *2004 8th Internation Conference on Control, Automation, Robotics and Vision*, Kunming, 2004, pp. 461-467.

[26] National Insturments Corporation. (2011) NI USB-6259 BNC - 16-Bit, 1.25 MS/s M Series, Integrated BNC, External Power. [Online]. http://sine.ni.com/nips/cds/view/p/lang/en/nid/209150

[27] National Instruments Corporation. (2011) NI cRIO-9073 - Integrated 266 MHz Real-Time Controller and 2M Gate FPGA. [Online]. http://sine.ni.com/nips/cds/view/p/lang/en/nid/205621

[28] National Instruments Corporation. (2011) NI 9234 - 4-Channel, ±5 V, 51.2 kS/s per Channel, 24-Bit IEPE. [Online]. http://sine.ni.com/nips/cds/view/p/lang/en/nid/208802

[29] W. Hu, A. Starr, and A. Leung, "A multisensor-based system for manufacturing process monitoring," *Proceedings of the Institution of Mechanical Engineers, Part B: Journal of Engineering Manufacture*, vol. 215, no. 9, pp. 1165-1175, 2001.

[30] P. Tse, "Neural networks based robust machine fault diagnostic and life span predicting system," Univerisity of Sussex, UK, PhD thesis 1998.

[31] R. Milne, "Stratgies for diagnosis," *IEEE Transaction Systems, Man and Cybernetics*, vol. 17, no. 3, pp. 333-339, May 1989.

[32] K. Butler, "An expert system based framework for an incipient failure detection and predictive maintenance system," in *Proceedings of the International Conference on Intelligent systems Applications to Power Systems (ISAP-96)*, 1996, pp. 321-326.

[33] Montronix Company, "Signal Processing Techniques," Ann Arbor, MI, Brochure 1995.

[34] Montronix Company, "TS Series Tool Monitors," Ann Arbor, MI, Brochure 1991.

[35] J. Shao, "Application of an artificial neural network to improve short-term road ice forecasts," *Expert Systems with Applications*, vol. 14, no. 4, pp. 471-482, April 1998.

[36] D. Bansal, D. J. Evans, and B Jones, "Application of a real-time predictive maintenance system to a production machine system," *International Journal of Machine Tools & Manufacture*, vol. 45, no. 10, pp. 1210-1221, August 2005.

[37] H. Zhang, R. Kang, and M. Pecht, "A Hybrid Prognostics and Health Management Approach for Condition-Based Maintenance," in *2009 IEEE International Conference on Industrial Engineering and Engineering Management (IEEM 2009)*, Hong Kong, China, 2009, pp. 1165-1169.

[38] K. F. Martin and P. Thorpe, "Coolant System Health Monitoring and Fault Diagnosis via Health Parameters and Fault Dictionary," *International Journal of Advanced Manufacturing Technology*, vol. 5, no. 1, pp. 66-85, 1990.

[39] Predator Software Inc. (2010) Predator Software - DNC, MDC, PDM, SFC, Virtual CNC, Travelers, Tracker Tool and Gage Crib for manufacturing. [Online]. http://www.predator-software.com/index.htm

[40] General Electric Company. (2010) GE Energy - Bently Nevada, Condition Monitoring, Vibration Monitoring, Machine Diagnostic Systems & Equipment. [Online]. http://www.gepower.com/prod_serv/products/oc/en/bently_nevada.htm

[41] A. Matsubara and S. Ibaraki, "Monitoring and Control of Cutting Forces in Machining Processes: A Review," *International Journal of Automation Technology*, vol. 3, no. 4, pp. 445-456, 2009.

[42] C. Brecher, A. Verl, A. Lechler, and M. Servos, "Open control systems: State of the art," *Production Engineering Research Development*, vol. 4, pp. 247-254, April 2010.

[43] Siemens AG. (2010) Sinumerik 840 D. [Online]. http://www.automation.siemens.com/mcms/mc/en/automation-systems/cnc-sinumerik/sinumerik-controls/sinumerik-840d/Pages/sinumerik-840d.aspx

[44] Bosch Rexroth AG. (2010) Indramotion MTX. [Online]. http://www.boschrexroth.com/dcc/Vornavigation/Vornavi.cfm?&language=en&PageID=g96072

[45] Beckhoff Automation. (2010) TwinCAT CNC. [Online]. http://www.beckhoff.com/english.asp?twincat/default.htm

[46] K. F. Martin, "A review by discussion of condition monitoring and fault diagnosis in machine tools," *International Journal of Machine Tools and Manufacture*, vol. 34, no. 4, pp. 527-551, May 1994.

[47] R. Cortesi. Mini-Mill Spindle Concepts and Design. [Online].
http://rogercortesi.com/portf/spindle/spindle.html

[48] Bones Bearings. (2011) Bearing Maintenance. [Online].
http://www.bonesbearings.com/support/maintenance/

[49] C. S. Sunnersjo, "Varying compliance vibrations of rolling bearings," *Journal of Sound and Vibration*, vol. 58, no. 3, pp. 363-373, June 1978.

[50] T. E. Tallian and O. G. Gustafsson, "Progress in Rolling Bearing Vibration Research and Control," *American Society of Lubrication Engineers - Transactions*, vol. 8, no. 3, pp. 195-207, July 1965.

[51] C. S. Sunnersjo, "Rolling Bearing Vibrations - The Effects of Geometrical Imperfections and Wear," *Journal of Sound and Vibration*, vol. 98, no. 4, pp. 455-474, February 1985.

[52] N. Tandon and A. Choudhury, "A review of vibration and acoustic measurement methods for the detection of defects in rolling element bearings," *Tribology International*, vol. 32, no. 8, pp. 469-480, August 1999.

[53] SKF Condition Monitoring, Inc. (2000) Vibration Diagnostic Guide. Guide.

[54] J. S. Mitchell, *An Introduction to Machinery Analysis and Monitoring*. Tulsa, OK, USA: PennWell Publishing Co., 1981.

[55] A. Rezaei, A. Dadouche, V. Wickramasinghe, and W. Dmochowski, "A Comparison Study Between Acoustic Sensors for Bearing Fault Detection Under Different Speed and Load Using a Variety of Signal Processing Techniques," *Tribology Transactions*, vol. 54, no. 2, pp. 179-186, March 2011.

[56] Y. H. Kim, A. C. C. Tan, J. Mathew, and B. S. Yang, "Condition monitoring of low speed bearings: A comparative study of the ultrasound technique versus vibration measurements," *Australian Journal of Mechanical Engineering*, vol. 5, no. 2, pp. 177-189, 2008.

[57] N. Tandon and B. C. Nakra, "Comparison of vibration and acoustic measurement techniques for the condition monitoring of rolling element bearings," *Tribology International*, vol. 25, no. 3, pp. 205-212, June 1992.

[58] M. A. Goodman. (2005) Utilizing Ariborne/Structure Borne Ultrasound for Condition Monitoring/Predictive Mainentance Inspections. UE Systems, Inc. White Paper.

[59] National Aeronautics and Space Administration (NASA), "A System for Early Warning of Bearing Failure," Marshall Space Flight Center, Huntsville, AL, Tech Brief B72-10494, 1972.

[60] W. Kirchner, S. Southward, and M. Ahmadian, "Ultrasonic acoustic health monitoring of ball bearings using neural network pattern classification of power spectral density," in *Proceedings of the ASME Joint Rail Conference 2010, JRC2010*, Urbana, IL, USA, 2010, pp. 255-265.

[61] M. A. Goodman, "Maintenance Troubleshooting with Ultrasonic Equipment," *Plant Engineering*, vol. 34, no. 7, pp. 103-106, April 1980.

[62] A. Choudury and N. Tandon, "Application of acoustic emission technique for the detection of defects in rolling element bearings," *Tribology International*, vol. 33, no. 1, pp. 39-45, January 2000.

[63] T. Yoshioka and T. Fujiwara, "Application of Acoustic Emission Technique to Detection of Rolling Bearing Failure," in *American Society of Mechanical Engineers, Production Engineering Division (Publication) PED*, New Orleans, LA, 1984, pp. 55-76.

[64] J. Mathew and R. J. Alfredson, "The Condition Monitoring of Rolling Element Bearings Using Vibration Analysis," *Journal of Vibration, Acoustics, Stress, and Reliability in Design*, vol. 106, pp. 447-453, July 1984.

[65] J. Meacher and H. M. Chen, "Design and Fabrication of Prototype System for Early Warning of Impending Bearing Failure," National Aeronautics and Space Administration (NASA), Huntsville, Alabam, Technical Report MTI-74TR34, 1974.

[66] UE Systems Inc. (2007, July) UE ULTRA-TRAK 750. User's Manual.

[67] H. Prashad, "The Effect of Cage and Rooler Slip on the Measured Defect Frequency Response of Rolling-Element Bearings," *ASLE transactions*, vol. 30, no. 3, pp. 360-367, July 1987.

[68] P. D. McFadden and J. D. Smith, "Vibration monitoring of rolling element bearings by the high-frequency resonance technique - a review," *Tribology International*, vol. 17, no. 1, pp. 3-10, February 1984.

[69] Society of Manufacturing Engineers and American Machine Tool Distributors' Association. (2011) imX - The Interactive Manufacturing Experience. [Online]. http://www.imxevent.com/

[70] M. W Washo, "A Quick Method of Determining Root Causes and Corrective Actions of Failed Ball Bearings," *Lubrication Engineering*, vol. 52, no. 3, pp. 206-213, March 1996.

[71] NSK Ltd. (2003) Super Precision Bearings. NSK Bearing Catalog E1254.

[72] Beckhoff Automation GmbH. (2011, September) BECKHOFF New Automation Technology. [Online]. http://www.beckhoff.com/

[73] UE Systems Inc. (2010) Ultra-Trak 750 Technical Specifications. [Online]. http://www.uesystems.com/products/remote-monitoring/ultra-trak-750/technical-specs.aspx

[74] R. W. Ramirez, *The FFT - Fundamentals and Concepts*. Englewood Cliffs, NJ, USA: Prentice-Hall, Inc., 1985.

[75] H. J. Nussbaumer, *Fast Fourier Transform and Convolution Algorithms*, T. S. Huang, Ed. New York, NY, USA: Springer-Verlag, 1981.

[76] K. J. McGee. (2009) An Introduction to Signal Processing and Fast Fourier Transform (FFT). fftguru.com Tutorial.